Experimental studies of growth and heavy metal uptake in a *Lolium perenne* mapping family, with reference to elite genotype selection and possible genetic controls

Rosalind Mathews

Department of Geography and Earth Sciences

&

Institute of Biological, Environmental and Rural Sciences

Aberystwyth University

Submitted in partial fulfilment of the requirements for the degree of PhD

September 2016

ABSTRACT

The anthropogenic exploitation of heavy metals (HMs) has resulted in widespread contamination on a global scale. Nowhere is this more evident than in the Central Wales Orefield (CWO), where the historical extraction and processing of Zn-, Pb- and Cu-rich ores has led to long-lived contamination of watercourses and agriculturally valuable soils, with a concomitant decline in ecosystem health and resilience. The use of plants for the phytoremediation of polluted substrates offers a cheap alternative to costly heavy engineering solutions, but relies on the identification of species that have adopted either HM avoidance or HM tolerance strategies at a biomolecular level.

This investigation seeks to build on previous hydroponic-based HM tolerance research into the performance of genotypes selected from a *Lolium perenne* (amenity x forage) mapping family. Two experiments used a growth medium comprising sand and dominantly monometallic Zn- or Pb-rich tailings provenanced from two mines in the CWO. In each experiment, three specific treatments were applied; control, 10% and 30% by weight of tailings. In the two Zn treatments this equated to bioavailable substrate concentrations ($^{Zn}B_A$) of 1,890 µg g^{-1} and 5,670 µg g^{-1} and, in the two Pb treatments, to a $^{Pb}B_A$ of 445 µg g^{-1} and 1,335 µg g^{-1}.

A detailed analysis of the results reveals a wide variation, both within and between the two experiments, in genotype performance for traits including longevity, biomass production, tolerance index, HM uptake, tissue metal concentrations, and HM translocation. However, the phytostabilisation potential of certain genotypes in the *L. perenne* mapping family is confirmed. Individual genotypes are identified which, through poly- or pair-crossing, could provide the foundation for an elite, HM tolerant population with high potential for field-based testing on soils contaminated with Zn and Pb, as well as other HM species. MapQTL analysis facilitated the identification of numerous growth- and HM uptake-related QTL, possibly underlain by candidate genes for stress tolerance and HM transport, providing strong evidence both for pleiotropy and for the polygenetic control of these traits.

LIST OF CONTENTS

ACKNOWLEDGEMENTS

First and foremost, I would like to thank Dr. James Macduff, who originally conceived of and supervised this project. I am indebted to him for all the training and guidance he has given and for the many helpful suggestions he has made during the compilation of this thesis.

I thank my supervisors, Prof. Nick Pearce for all he has done to see me through two, and hopefully three, degrees; and Dr. Danny Thorogood for his help and for allowing me access to his *Lolium perenne* mapping population. Thanks also to Dr. Bill Perkins, who gave many suggestions on trialling digestion methods, and to Prof. John Doonan for his support.

I am very grateful to Mr. Andy Brown, without whose cheery assistance the laboratory analysis of so many samples would have been extremely daunting.

Fond thanks go to the late David Bick, for instilling me with a love for the mines in Central Wales, and for the memorable days spent with him in the field exploring them.

I am grateful to my friends and family for all their encouragement; thanks to Debbie for the sunny 'Deb Effect', and special thanks are reserved for Geoff, for taking the time to read and comment on every page.

Finally, I thank Bob, for his unwavering support at every stage of this journey, and my dogs, Brae and Archie – it was finished, despite your best efforts to sabotage its completion!


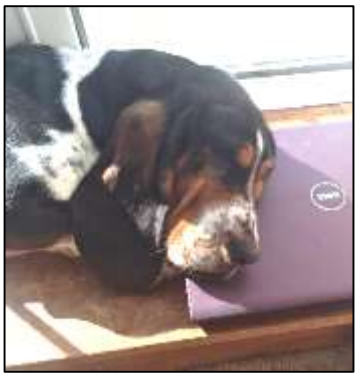


for

Joe and Ella

ꕥ

CHAPTER 1

INTRODUCTION AND RESEARCH OBJECTIVES

CHAPTER 2

REVIEW OF PREVIOUS RESEARCH

CHAPTER 3

MATERIALS AND METHODS

CHAPTER 4

RESULTS

CHAPTER 5

RELATIONSHIPS BETWEEN KEY TRAITS OF POTENTIAL PRACTICAL PLANT BREEDING VALUE

CHAPTER 6

COMPARISONS WITH SCREENING EXPERIMENTS FOR ZINC AND LEAD TOLERANCE IN FLOWING SOLUTION CULTURE

CHAPTER 7

DISCUSSION

CHAPTER 8

CONCLUSIONS AND RECOMMENDATIONS

APPENDICES

LIST OF FIGURES

LIST OF PLATES

LIST OF TABLES

LIST OF ABBREVIATIONS

AAS	Atomic absorption spectroscopy/spectrophotometer
CWO	Central Wales Orefield
DEFRA	Department for Environment, Food and Rural Affairs
DGES	Department of Geography and Earth Sciences
FSC	Flowing Solution Culture
GSH	Glutathione
HM	Heavy metal
IAA	Indole-3 acetic acid
IBERS	Institute of Biological, Environmental and Rural Sciences
LG	Linkage Group
MT	Metallothionein
NRW	Natural Resources Wales
PC	Phytochelatin
QTL	Quantitative trait loci
ROS	Reactive oxygen species
SOD	Superoxide dismutase

CHAPTER 1

INTRODUCTION AND RESEARCH OBJECTIVES

1.1 Background

Heavy metals (HMs) are naturally occurring elements that are distributed throughout the Earth's lithosphere and its thin veneer of soil. They are generally only present in trace concentrations, although with notable exceptions such as in ultramafic and granitic lithologies which, through fractionation processes, can become highly enriched in certain metals including Mg, Fe, Ca, Ni, Cr, Mo and V. During conditions of high heat flow and high geothermal gradient generated through, for example, extensional and compressional tectonism, orogenesis, plate subduction and volcanism, these metals may be mobilised and concentrated in the near-surface where they can occur in a variety of forms ranging from syngenetic sedimentary-exhalative stratabound ore deposits to epigenetic ore deposits hosted by mineral-bearing hydrothermal veins and plutonic igneous bodies (Bevins *et al*., 2010).

Certain anthropogenic activities, in particular mineral extraction and ore processing, but also other activities such as smelting, industrial manufacturing, military operations and energy production, have all contributed to the progressive release of HMs into the environment. Since many species of HM are highly toxic to organisms, even at low concentrations, and often subject to long environmental residence times, they pose a severe geohazard to ecosystem health and resilience on a global scale and their ultimate transfer to the human foodchain is now a reality that has to be faced. The cost of remediation using traditional methods such as capping, burial and chemical treatment is extremely high, as illustrated by the USA which spends $6-8 billion annually, and cannot be afforded by developing nations (Pilon-Smits, 2005; Rajakaruna *et al*., 2006). Hence, much research is currently underway to develop low-cost, more eco-friendly forms of remediation, and the use of plants is one such area of intensive investigation, with particular focus on the genetic basis of adaptive mechanisms used by plants to counter the detrimental effects of toxic HMs.

Being sessile organisms for virtually all of their life cycle, plants are constantly exposed to changing and often adverse environmental conditions that can exert a profound negative effect upon growth, development and productivity. The presence of toxic compounds in the substrate, such as HMs, is one important factor that can cause damage to plants through the alteration and interruption of critical physiological and metabolic processes (Hossain *et al*., 2011). Although

several HMs (e.g. Fe, Cu, Zn, Co and Ni) are, at certain concentrations, essential micronutrients that assist in the regulation of various biological processes in plants, such as the functionality of proteins and enzymes involved in sustaining growth and development, their presence in excess concentrations becomes toxic to plants (e.g. Nagajyoti *et al*., 2010; Dresler *et al*., 2014). These HMs, together with other non-essential species such as Pb and Cd, induce several mechanisms of plant adaptation, many of which probably became established during the earliest stages of terrestrial colonisation (e.g. Wild, 1978; Cleal and Thomas, 1995).

Depending upon their oxidation states, HMs can be highly reactive, resulting in plant cell toxicity. At the cellular and molecular level, HM toxicity is manifested by, for example, the inactivation and denaturing of critical enzymes and proteins, the blocking of metabolically important molecules, displacement or substitution of essential metal ions, the disruption of cell membrane integrity and the inhibition of photosynthesis and respiration (Hossain *et al*., 2011). Plants employ two main strategies to cope with the toxic effects of HMs, namely either 'avoidance', where plants are able to restrict metal uptake, or 'tolerance', where plants are able to detoxify metal ions that have crossed root plasma membranes or internal organelle biomembranes (Mehes-Smith, 2013). Avoidance involves extracellular detoxification of HMs through precipitation in the rhizosphere, biosorption to cell walls, reduced uptake or increased efflux (e.g. Yong and Ma, 2002). In plants adopting a tolerance strategy, HMs are intracellularly chelated and sequestered through the synthesis of various biomolecules including amino acids, organic acids, glutathione and HM-binding ligands such as metallothioneins and phytochelatins, with compartmentation and storage of metals in root and shoot vacuoles and the upregulation of antioxidant defence systems that counter the adverse effects of HM-induced reactive oxygen species (Maestri *et al*., 2010). Based on their coping strategy, three distinct classes of HM-tolerant plant have been identified (Baker and Walker, 1990): 1) metal excluders which limit translocation of HMs and maintain very low levels of HMs in their aerial tissues; 2) metal indicators which accumulate HMs in their harvestable biomass but at levels which reflect metal concentrations in the substrate; and 3) metal accumulators/hyperaccumulators which can increase the internal sequestration, translocation and accumulation of HMs in their harvestable biomass to concentrations far in excess of those in the substrate.

The identification of genes that are involved in, or control, HM tolerance and accumulation in plants is challenging as both are determined by complex multigenic systems, likely to be associated with various degrees of metal specificity (Macnair, 1993). Quantitative trait loci (QTL) mapping has proven to be a powerful tool in this area, utilising the analysis of complex

adaptive traits to determine the numbers and possible locations of candidate genes involved in a trait (e.g. Willems *et al*., 2007). QTL mapping has led to the identification of numerous candidate genes associated with HM tolerance and accumulation in a wide variety of plants (Mehes-Smith, 2013) including *Silene vulgaris* (bladder campion), *Mimulus guttatus* (Seep monkeyflower), species of the genus *Arabidopsis* (Rockcress), *Thlapsi caerulescens* (Alpine Penny-cress), *Glycine max* (soybean), species of the genus *Triticum* (wheat), *Avena sativa* (oat), *Oryza sativa* (Asian rice), *Lycopersicon esculentum* (tomato) and *Lolium perenne* (Perennial ryegrass).

Plants could play an essential role in the remediation of HM-enriched substrates through facilitating the establishment of sustainable ecosystems in areas of the world that would otherwise remain barren. One of the main goals of research in this field is the design of what may be termed 'ideal plant prototypes' that could be utilised in the remediation of HM-contaminated substrates in a variety of environments. This objective is also highly relevant on a local scale, in Wales, given the persistent HM contamination of many sites in the Central Wales Orefield (CWO) previously subject to mining activity as well as their associated water courses (e.g. Lewin *et al*., 1977, 1983). Further, the importance of gaining a better understanding of the genetic basis of HM tolerance and uptake, in general, and particularly in species belonging to the Poaceae, is underscored by the global problems associated with micronutrient deficiencies and toxicities in agriculturally important crops. These have significant detrimental consequences both in terms of human and livestock health and nutrition.

With these aims in view, the present research project focussed on investigating the genetic basis of Zn- and Pb-tolerance in a mapping family of *L. perenne*, a species that is widely acknowledged as HM-tolerant and with good potential for use in the phytoremediation of HM-polluted soils (Bidar *et al*., 2007, 2009). The main experimental component of the project involved two tolerance studies, conducted in consecutive years. Briefly, in each of these experiments tillers were extracted from 80 members of a mapping family and cultured outdoors in three different growth mediums namely, uncontaminated sand and sand contaminated with dominantly monometallic (Zn or Pb) mine tailings at concentrations of 10% and 30% by weight. Following destructive harvests after 16 weeks, the plants were analysed for a range of relevant traits, including growth, metal uptake in the roots, and root-shoot translocation indices. These traits were then examined in detail, using a variety of analytical techniques, including QTL mapping, to assess the evidence for any genetic-based control over metal tolerance and to identify any responsible candidate genes.

This project builds on previous research, commissioned by the Department for Environment, Food and Rural Affairs (DEFRA), that utilised the same *L. perenne* mapping family (DEFRA LS3648). The DEFRA study was carried out under hydroponic conditions in the Flowing Solution Culture (FSC) laboratory at the former Institute of Grassland and Environmental Research (IGER) (now part of the Institute of Biological, Environmental and Rural Sciences (IBERS) at Aberystwyth University), and aimed to provide an initial appraisal and outline genetic map for quantitative traits exploitable through 'marker assisted' precision breeding to enhance the range of 'ecosystem services' and environmental benefits provided by UK grassland. The traits surveyed included several associated with the bioremediation of HMs. Phenotypic variation was characterised within the mapping family at a range of scales from single plant to simulated swards. QTL were identified on an outline genetic map based on molecular markers produced by amplified fragment length polymorphism (AFLP) analysis. IGER's amenity x forage type *L. perenne* mapping family was specifically selected for this purpose because it includes a wide range of growth and morphological types. Phenotyping (> 150 traits) across 94 mapping family genotypes was conducted over four years and QTL were identified and mapped onto a pair of outline AFLP molecular marker-based linkage maps, constructed during the project, for a total of 43 traits. The results revealed promising variation (> two-fold across the mapping population) in the majority of the traits measured. Notable amongst these, HM-specific QTL were identified for tolerance (in terms of growth) to Fe (linkage group (LG) 1), Zn (LG4) and Pb (LG4). In addition, HM-specific QTL were identified for plant content of Fe (LG1) and Pb (LG5), together with a range of traits associated with the accumulation and partitioning of Fe, Zn and Pb between roots and shoots. However, because phenotyping of the HM-associated traits in the DEFRA study was conducted under hydroponic conditions, it is uncertain whether the findings hold true under more 'realistic' substrate conditions.

1.2 Research objectives

The research presented in this thesis was conducted at the IBERS research facility at Gogerddan (pot experiments and data analysis) and also in the Department of Geography and Earth Sciences (DGES) laboratory on Penglais campus (sample preparation and geochemical analysis). The objectives of the research presented in this thesis were as follows:

1. To conduct a literature review to include a summary of the scale of mine-related HM contamination, with special reference to the CWO, environmental HM transport pathways and

storage, current views on HM bioremediation, the molecular and genetic controls on HM uptake and tolerance in plants, and the role of FSC in the study of HM uptake and tolerance.

2. To source two geochemically appropriate (i.e. dominantly monometallic) Zn- and Pb-contaminated tailings from the CWO to be used as the primary component of the growing medium for the project's experimental work.

3. To phenotype the *L. perenne* mapping family (80 individual genotypes) with respect to a range of candidate traits associated with tolerance and physiological response to different levels of Zn and Pb in the growth medium (0, 10% and 30% contaminated mine tailings).

4. To devise a modified laboratory digestion method providing both a high level of analytical accuracy and rapid throughput of plant and mineral samples for the determination of Zn and Pb content.

5. To analyse and dissect the relationships between the measured traits, and identify those traits likely to be of most practical use in breeding programmes aimed at increasing HM tolerance and/or uptake.

6. To assess QTL arising from the trait data in the *L. perenne* mapping family, focussing on those associated with Zn and Pb tolerance and uptake, and identify, if possible, potential underlying genes.

7. To assess the agreement between the trait data and QTL arising from this project's phenotyping experiments with corresponding data generated in FSC in a previous DEFRA-commissioned study (LS3648) using the same *L. perenne* mapping family.

8. To identify specific genotypes in the *L. perenne* mapping family likely to be of use in the phytoremediation of contaminated substrates and/or in selective breeding programmes aimed at increasing HM tolerance and uptake.

1.3 Thesis structure

The work undertaken during the project is presented within the following structural framework. Chapter 2 provides a brief overview of the environmental legacy of metal mining, emphasising the impact of the CWO which, it is considered, provides a direct analogue to other exploited metallogenic provinces distributed throughout the world. Further consideration is given to the transport pathways of mine-related HMs as these provide a key to their ultimate fate in the biosphere where they become available for uptake by plants and animals. An overview of advances in phytoremediation is also presented with particular emphasis on phytoextraction and phytostabilisation for which, in the latter case, *L. perenne* has proven to be a potentially suitable candidate. A summary is provided of recent research into the molecular and genetic basis of HM tolerance in plants, with emphasis on the different adaptive and defensive strategies adopted by plants. The chapter concludes with a review of recent research, noted above, into the genetic basis of HM uptake and tolerance by the *L. perenne* mapping family, carried out under hydroponic conditions in the FSC laboratory at IGER.

Chapter 3 provides a brief geological review of the CWO and the successful search for two mines from which to provenance the appropriate monometallic Zn- and Pb-rich mine tailings. The analytical method used to assess each of the grab samples is described, concluding with the geochemical results and a justification for mine selection. A background to the origin of the *L. perenne* mapping family is followed by a detailed account of the experimental methodology, including the sampling of mine tailings, pot and plant preparation, experiment design parameters and geochemical analysis. In respect of the latter, because of the very large numbers of samples generated during the course of the two experiments, various laboratory-based digestion methods were first tested in the search for an optimal 'specific method'. These methods are described and a justification for selection of the 'specific method' is provided together with the results of an analysis of metal bioavailability and potential nitrate contamination in the selected mine tailings. A background to the methodology employed in a QTL analysis is provided, and the chapter concludes with an account of the screening methodology used to investigate Zn and Pb tolerance by the *L. perenne* mapping family in FSC.

Chapter 4 provides a comprehensive collation of the numerical data collected during the course of this research project. The chapter commences with a graphical presentation of data relating to growth, metal uptake and partitioning during Zn Experiment 1 and Pb Experiment 2. The

anomalous behaviour of the control plants, in particular with respect to plant growth, is described and an analysis undertaken of the possible factors that may have contributed to the observed variation in performance of the control plants during the two pot experiments. The chapter concludes with the results of a QTL analysis and the presentation of genetic linkage diagrams, for the *L. perenne* mapping family, showing the locations of detected trait-related QTL from the two experiments.

Chapter 5 focusses on the relationships between key traits, representative of growth, HM uptake efficiency and utilisation efficiency, which may have potential practical value for the breeding of metal-tolerant plants suitable for phytoremediation. The results of a genotype ranking analysis are presented, highlighting those genotypes that could be selected for establishing Zn- and Pb-tolerant and high uptake breeding populations. Consideration is also given to genotype selection in-common for Zn and Pb.

Chapter 6 presents details of the DEFRA-commissioned research project, carried out in FSC, into growth and metal uptake in the same *L. perenne* mapping family that was used in this Ph.D project, with a presentation of the most significant trait relationships. Consideration is given to the performance of the control plants in FSC, allowing a comparison with the variation observed in control plant performance in the two pot-based experiments discussed in Chapter 4. A comparison is made between genotype performance in FSC and in the pot experiments and a preliminary identification is made of those genotypes which, for specific traits, had performed well in FSC and also in both FSC and the pot experiments. The section concludes with the results of a QTL analysis of certain key traits based on data collected during the FSC experiment and a comparison between these QTL and those identified from the trait data gathered during the pot experiments.

Chapter 7 commences with a brief discussion of digestion methods, followed by a detailed synthesis of measurements of growth, metal uptake and translocation obtained from the two experiments. This is set out in the context of published material relating to toxicity and performance, both in *L. perenne* and other plant species. A comparative analysis of the differences in plant performance between the two experiments is discussed, with reference to possible limitations imposed by experiment design and the different physiological responses to the two HMs. This is augmented by a brief discussion of other essential and non-essential HMs and the potential use of the *L. perenne* mapping family in their bioremediation. A synthesis of the genetic basis of metal tolerance is provided within the framework of evolutionary change,

and the methods and results of a comparative QTL analysis, based on the close syntenic relationship between *L. perenne* and Brachypodium, and designed to identify any candidate tolerance-conferring genes underlying the QTL, are presented. There follows a discussion of the strategies for plant breeding using specific genotypes identified during this research, and the chapter concludes with an overview of the potential agronomic benefits of using the mapping family for the phytostabilisation of Zn- and Pb-contaminated substrates.

This work concludes with Chapter 8, which presents a summary of the background, experiment methodologies and outputs, as well as potential applications and opportunities for future investigations based around the *L. perenne* mapping family.

CHAPTER 2
REVIEW OF PREVIOUS RESEARCH

2.1 The environmental legacy of metal mining

Heavy metals (HMs) are distinguished by several metallic properties such as ductility, malleability, high electrical and heat conductivity, high light reflectivity (giving a metallic lustre), and all are characterised by a relatively high density (~ 7 – 22 g cm^{-3}), a high relative atomic weight and have an atomic number greater than 20 (Raskin *et al*., 1994; Hawkes, 1997; Nagajyoti *et al*., 2010). Some HMs (e.g. Co, Cu, Fe, Mn, Ni, V, Zn and Mo) are required in very small quantities by organisms, although excessive quantities of the same elements can prove harmful or even fatal. Other HMs and certain metalloids (e.g. Pb, Cd, Hg and As) have no beneficial effects and can therefore be regarded as 'main threats' since they are very harmful to ecosystems and their associated plants and animals. The widespread use of HMs in industrial civilisation is due partly to the properties outlined above, and also to the fact that many of the more common metals can be shaped into objects of commerce, art, high societal value and that confer high status, not only by deformation and through casting into moulds but also by alloying with other metals (as well as certain non-metals) in order to increase their strength, hardness and resistance to repeated stress.

The anthropogenic mobilisation of HMs through the extraction and processing of metal-rich ores has led to the release of these elements into the environment. This activity, in an unregulated form, has been on-going for millennia, with one of the earliest known examples of metal mining being at the 'Lion Cave' in Swaziland, where the extraction of hematite ores used for the production of red ochre pigments has been radiocarbon dated at about 43,000 years old, equating to the Palaeolithic Era (Beaumont, 1973). During the third millennium BC, the ancient Egyptians mined Cu-rich malachite at Maadi (Shaw, 2000), whilst the gold mines of Nubia, documented by the Greek author Diodorus Siculus in the first century BC, were the largest and most extensive of any in North Africa. In the Americas, copper was being mined at sites along Lake Superior at least 5,000 years ago (e.g. West, 1970), whilst in the Phillipines, mining for Ag, Au, Cu and Fe began around 1000 BC.

Mining in Europe has a long history, dating back to the Bronze Age and to the Greek and Roman empires. In the case of the Ancient Greeks, documented examples include the silver mines of Laurium which supported the city state of Athens, whilst Philip II of Macedon secured the gold

mines of Mount Pangeo in 357 BC to fund his military campaigns, as well as gold mines in Thrace for minting coinage. Subsequently, the Romans developed large-scale mining techniques, including hydraulic mining methods such as hushing, which were used in the Pb- and Sn-rich orefields of the Pennines and Cornwall in the UK and also to exploit rich alluvial gold deposits in Spain. The Romans also developed the use of adits to exploit underground ore deposits, for example at the Dolaucothi gold mine in Wales and in the copper mines at Rio Tito in Spain and, where the water table was penetrated, pioneered the use of overshot water wheels for de-watering.

In the UK and, in particular, in Central Wales, which will be discussed in this chapter as a global analogue, the history of mining dates back over 4,000 years to the Bronze Age (e.g. Timberlake, 1989; Lewis, 1990; Ixer & Budd, 1998). Many hundreds of thousands of tons of ore were extracted (Table 2.1) from several mining districts distributed across England and Wales (Figure 2.1).

Table 2.1 *Total metal concentrate output (tonnes) from selected mining districts in England and Wales (from Manning, 1959; Schnellman and Scott, 1970; Lewin and Macklin, 1987; Jenkins et al., 2000).*

Ore field	Lead (Pb)	Zinc (Zn)	Copper (Cu)
Northern Pennines-Yorkshire Dales	4,064,000	271,000	
Lake District	230,000	34,000	
Derbyshire	689,000	92,0000	60,000
West Shropshire	240,000	21,000	
Mynydd Parys			130,000
Central Wales	487,000	153,000	
Llanrwst-Harlech	48,000	33,000	
Halkyn-Minera	1,900,000	295,000	
Mendip	203,000		
Devon-Cornwall	327,000	90,000	
Isle of Man	272,000	260,000	

In addition to those shown in Figure 2.1, several other former economically important orefields occur in Wales, most notably the Lower Cambrian Mn-bearing ores of the Harlech Dome (44,000 tons of Mn ore), the pre-Acadian Dolgellau Gold Belt (over 130,000 oz of Au), the syn-volcanic Ordovician Cu-bearing veins of the Snowdon district (> 25,000 tons of Cu ore), and the Upper Palaeozoic sedimentary iron ore deposits (sideritic and hematitic) of South Wales (> 26.5 million tons of Fe ore).

Figure 2.1 Distribution of selected metalliferous orefields in England and Wales (after Dunham *et al*., 1978; Lewin and Macklin, 1987).

In the CWO, it is considered likely that HM contamination of watercourses, river sediments and floodplain soils has been on-going since late Roman times. An interesting report of environmental damage in the CWO, recorded during the reign of Henry VIII, was given by Leland in his '*Itinerary of Wales, 1536-39*', where he describes approaching Cwmystwyth Mine from the east:

'*About the middle of this Wstwith (sic.) valley that I ride in, being as I guess three miles in length, I saw on the right hand of the hill Cloth Moyne* (= Clodd Mwyn, translated as Mine of Lead Ore), *where there hath been great digging for Leade, the smelting whereof hath destroid the woodes that sometimes grew plentifully thereabout*' (Leland, 1906).

Whilst early mining methods in the CWO were primitive, simply involving the use of pick and shovel to extract ore which was crushed by hand and gravity-separated in nearby watercourses,

the Industrial Revolutions of the 18th and 19th centuries saw the introduction of more advanced techniques that led to greater efficiency both in mining techniques and the quantities of ore that could be processed. These included the construction of reservoirs, leats for conveying water, larger and more efficient water wheels for pumping and crushing, buddles for ore separation and, finally, the introduction of steam- and electromechanically-driven engines. Since most of the mines in the CWO were located close to watercourses, including several major rivers and their tributaries in mid-Wales, it was inevitable that vast quantities of metal-rich, fine-grained sediment were indiscriminately transferred into the fluvial environment. Thus, it is of no surprise that the Fifth Report of the 1868 Rivers Pollution Commission (1874) stated (p. 15) that the rivers near Aberystwyth were the most polluted:

'*All these streams are turbid, whitened by the waste of the lead mines in their course; and flood waters in the case of all of them bring down poisonous 'slimes' which, spreading over the adjoining flats, either befoul or destroy the grass, and thus injure cattle and horses grazing on the dirtied herbage, or, by killing the plants whose roots have held the land together, render the shores more liable to abrasion and destruction on the next occasion of high water. It is owing to the immense quantity of broken rock which every mine sends forth that small rivers Rheidol and Ystwyth present such surprising widths of bare and stony bed.*'

At the present-day, the phyotoxic effect of particulate HM contamination on riparian vegetation is perhaps best displayed on the Afon Ystwyth at Grogwynion, where the reach is characterised by braiding, ephemeral channels, rapid channel switching, and large areas of unvegetated stony ground. Here, overbank sediments (< 2 mm) contain Zn and Pb concentrations of 123 – 1,543 and 73 – 4,646 ppm respectively (Lewin *et al*., 1983) whilst, farther to the north, floodplain sediments (< 2 mm) along the Afon Rheidol contain Zn and Pb concentrations of 120 – 680 and 440 – 2,520 ppm respectively (Swain *et al*., 2005). The inherent dangers of particulate HM re-mobilisation during very high flows is clearly illustrated by events following the June 2012 floods in west Wales. Fine-grained overbank sediments deposited in the lower reaches of the Clarach catchment, the upper reaches of which contain several large mines, were found to be contaminated above guideline pollution thresholds by a factor of 32. Silage produced from the contaminated fields was found to contain up to 1,900 ppm Pb and, when fed to cattle in the autumn of 2012, caused illness and multiple mortality amongst calves. Blood analysis confirmed kidney Pb levels in excess of 35 µM L^{-1}, a concentration 79 times higher than levels which trigger 'exclusion from the human food chain'. Older animals due for slaughter were also tested and showed blood Pb levels in excess of 0.45 µM L^{-1} (the threshold at which animals

are not allowed to enter the food chain), a clear indication of the high level of subclinical poisoning (Foulds *et al*., 2014).

In an effort to reduce the input of contaminated fines, several mines in the CWO have been re-profiled and capped, for example at Cwmsymlog, Cwmbrwyno and Frongoch (Plate 2.1).

Plate 2.1 On-going two-phase remediation works at Frongoch Mine involving construction of surface water drains directing water to a lined pond and the re-profiling and capping of mine waste.

In the former case, work was undertaken due to the identification of high blood Pb concentrations in local inhabitants. However, disturbance of the spoil led to the release of acid mine drainage water containing high levels of dissolved Zn. In consequence of these adverse side-effects, subsequent remediation of Cwmerfin Mine, in a nearby valley, involved the encapsulation of contaminated spoil within lined pits. The cost of the works at Cwmbrwyno amounted to ~ £300,000, and the on-going works at Frongoch are likely to greatly exceed this cost (Environment Agency Wales, 2002).

In addition to particulate HM contamination, metals may also enter the fluvial environment *via* acid mine drainage in soluble forms such as metal sulphates, chlorides and carbonates. Acid mine drainage and contaminated surface water run-off presents a major problem in the CWO; indeed, from a database of 1,337 mine sites in Wales, 204 are known to cause an impact on receptor watercourses and, as a result, in 2002 Environment Agency Wales published a list of 50 priority sites requiring remediation, of which 43 are located in the CWO. The scale of the

problem is clearly visible at the Cwm Rheidol and Cwmystwyth mines (Plate 2.2) where contaminated, ochreous mine waters flow directly into the Afon Rheidol and Afon Ystwyth.

Plate 2.2 HM-rich acid mine drainage from A) Pugh's Adit at Cwmystwyth Mine, and from B) the No. 6 and No. 9 adits at Cwmrheidol Mine where discharge water has a pH of 3.0 – 3.9.

At present, discharge from Cwm Rheidol causes the river to fail European Water Framework Directive standards for 18 km to its tidal limit, and experimental remediation *via* a pilot-scale Vertical Flow Pond (VFP) is currently on-going. It is estimated that total remediation would prevent the entry of over 8 tonnes of HM into the river each year. Similarly, at Cwmystwyth Mine, which impacts on 33 km of the Ystwyth catchment, remediation would prevent the entry of over 20 tonnes of HM each year (Williams, NRW, pers comm.).

As illustrated in Figure 2.1, the problem of HM contamination in the UK is not confined to Wales. Indeed, Macklin *et al*. (2002) estimated that an area of over 12,000 km^2 of river catchments in northern England is affected by historical mining, as well as large areas of south-western England (Figure 2.2).

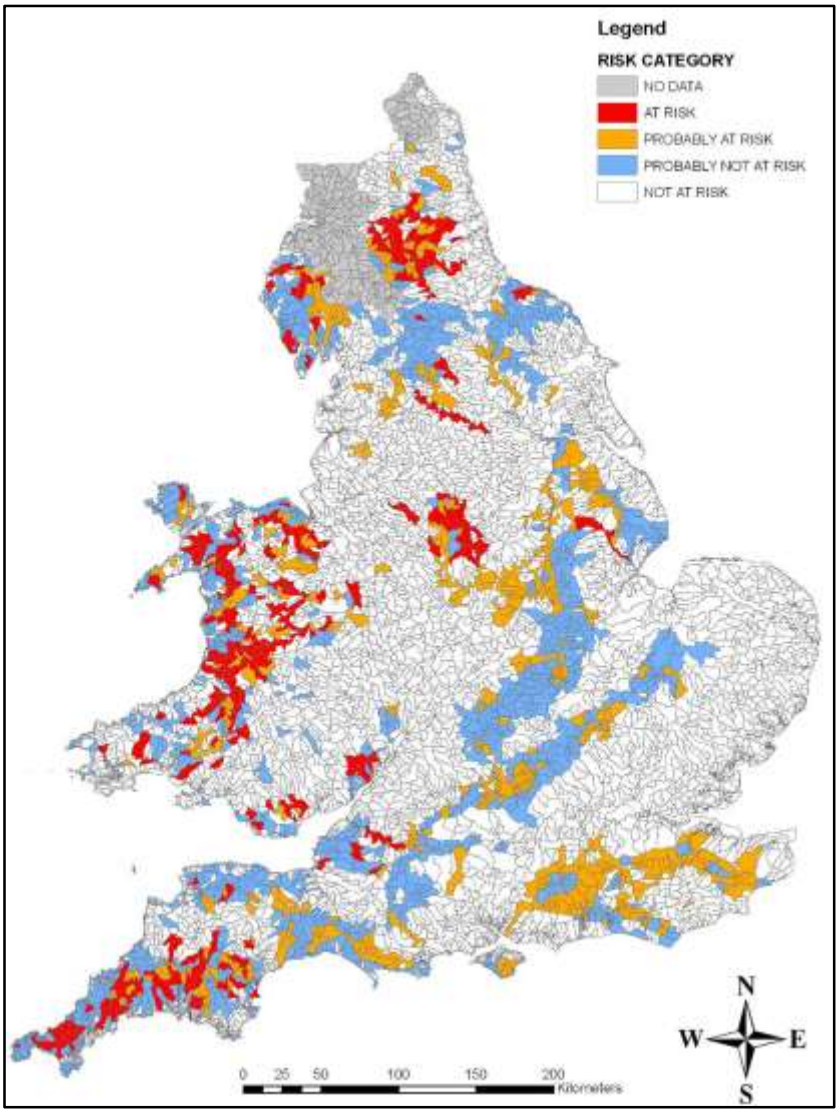

Figure 2.2 Map showing catchments of England and Wales sensitive ("at risk" and "probably at risk") to sediment-borne, mining-related metal contamination (after Environment Agency, 2008a).

On a global scale, mining on all continents, with the exception of Antarctica, has left an enormous legacy of soil, surface and groundwater contamination, with between $20 – 50 billion being spent annually on remediation (Gall and Rajakaruna, 2013). In the United States alone, for example, it is estimated by the Organisation for Economic Co-operation and Development that some 2,000 km of watercourses are affected by HM contamination and that the total cost of remediation could be up to US$34 billion. The very high costs of engineering-based HM

remediation, as alluded to above, have transformed the search for effective, low-cost, 'eco-friendly' technologies into what may now be viewed as a bioremedial 'Holy Grail'.

2.2. HM transport pathways and depositional environments

A key to predicting the ultimate fate of mine-derived HMs in the biosphere is to understand the ways in which these elements can be transported and the environmental repositories in which they may become stored and available for uptake by both plants and animals. A model for the dispersal of mine wastes is shown in Figure 2.3, which illustrates the possible transport

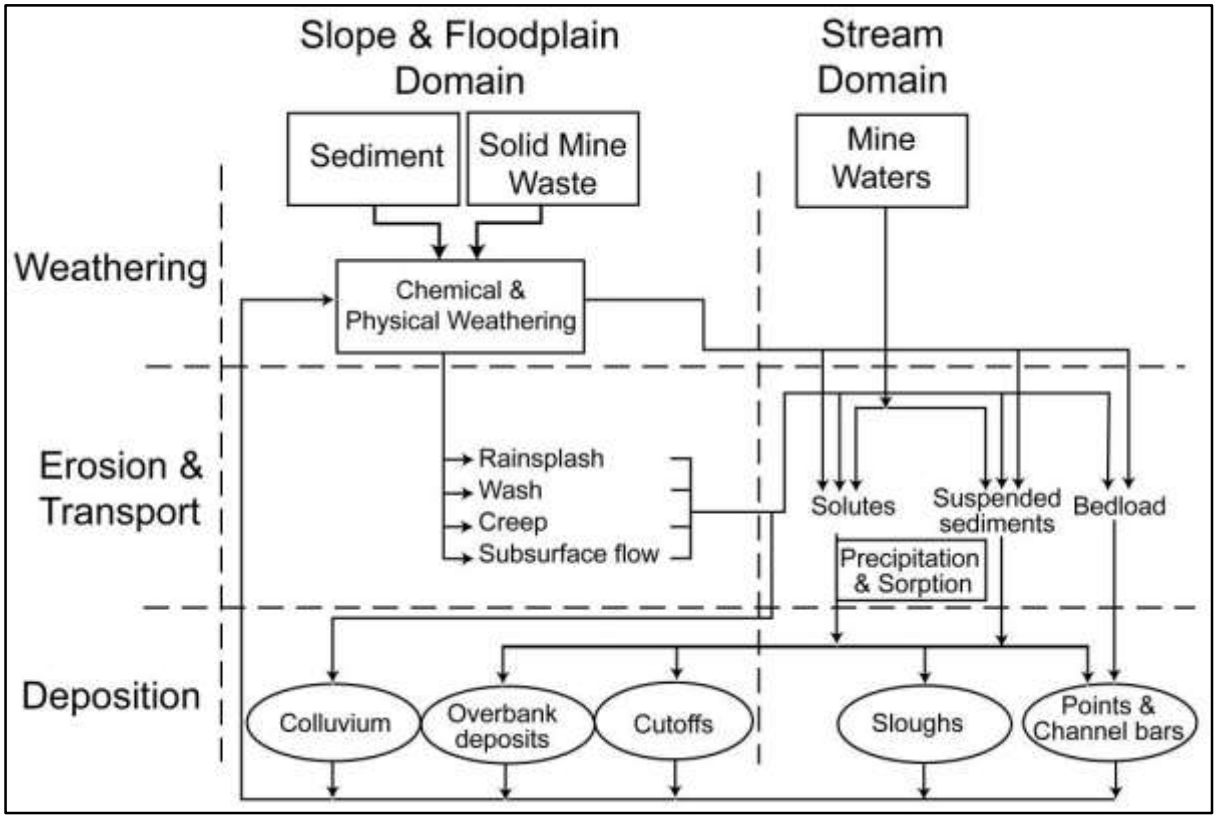

Figure 2.3 A model for the dispersal and storage of dissolved and particulate metal-rich mining wastes (Environment Agency, 2008b [after Lewin *et al*., 1977]). 'Solid Mine Waste' refers to spoil tips, tailings and other solid residues derived from ore processing.

pathways for both dissolved and particulate metal-rich wastes. In addition to the transport pathways illustrated in Figure 2.3, the role of aeolian processes should not be underestimated since these have the ability to transport fine metal-rich dusts particularly in arid zones, for example in the orefields of the western USA, the Pacific coast of South America, southern Europe and Australia, or during prolonged dry periods in the orefields of temperate zones. These processes are also at their most effective when vegetation cover is discontinuous or absent, this being a characteristic feature of HM-rich mine waste.

Figure 2.3 demonstrates that the downstream dispersal of HMs is a complex process. In regard to particulate transport in the fluvial environment, it has been shown (e.g. Lewin *et al*., 1977; Lewin and Macklin, 1987; Environment Agency, 2008b) that downstream HM concentrations decrease in patterns that can be approximated by negative linear (e.g. Afon Ystwyth), exponential (Afon Twymyn) or power functions (Afon Tywi). These decreases may be attributed to several mechanisms, which most probably will operate synchronously:

1. Dilution of contaminated sediment by uncontaminated sediment derived from watercourses upstream of contaminated point sources and sediment inputs from channel bank erosion downstream (e.g. Macklin, 1996).
2. Hydraulic sorting through size, shape and abrasion, as well as due to the differential densities (e.g. ρ PbS = 7.5 g cm^{-3}; ρ ZnS = 4.15 g cm^{-3}) of primary HM sulphide particles (e.g. Lewin *et al*., 1997; Langedal, 1997).
3. Storage of HM-rich sediments in floodplain and channel deposits, effectively isolating them from the fluvial transport system (e.g. Macklin *et al*., 1992).
4. Dissolution or chemical sorption (see below) of contaminants and HM uptake by receptor plants and animals (e.g. Lewin and Macklin, 1987; Hudson-Edwards *et al*., 1996).

A further point with regard to particulate HM transport is that the metal content in fluvial sediments increases with decreasing grain size (Figure 23.6 in Lewin *et al*., 1977). In addition, HMs are readily adsorbed by fine-grained particles, in particular those < 2 µm, and it is known that Pb is more strongly adsorbed than Zn. HMs are also readily chelated by organic molecules (see Section 2.3), Pb being more strongly chelated than Zn, and this can modify considerably their patterns of dispersal.

With regard to HM repositories, main river channels and their tributaries act as only temporary, short-term stores of metal-rich sediment. Long-term storage sites include river floodplains, riparian wetlands, reservoirs and lakes (Environment Agency, 2008b), as well as estuaries at the interface between the fluvial and marine environments (Cave *et al*., 2005). Floodplains can act as storage sinks for exceptionally long periods, with residence times varying from tens to even thousands of years (e.g. Coulthard and Macklin, 2005). However, residence times will depend on the rates of post-depositional physical, chemical and biological re-mobilisation. In reaches which are laterally mobile, storage times will be relatively short (e.g. Lewin *et al*., 1977), whereas, in stable reaches, contaminants may be stored and therefore remain available

for biotic uptake for very long periods (Bradley and Cox, 1990). In all cases, the erosion of HM-rich floodplain sediments will act as a diffuse source of metal input. Residence times will also be relatively short in fluvial systems characterised by aerially limited floodplains, such as those around the mining districts of SW England where HM contaminated waste is stored in estuarine rather than fluvial environments (Pirrie *et al*., 2002). Finally, it should also be noted that, in the floodplain environment, particulate HMs may undergo translocation *via* a number of processes including pedogenesis, groundwater percolation and fluctuations in water-table level, and sub-surface biotic activity.

The HM enrichment of mine waters and watercourses can occur through several different processes. First, unlike the common primary sulphides of, for example, Pb, Zn, Cu and Cd, their weathered products have solubility coefficients that are several magnitudes greater (Table 2.2) allowing dissolution and transport away from a contaminated area through rainsplash, surface and sub-surface flow.

Table 2.2 *Solubility coefficients (M L^{-1}) of selected salts of Pb and Zn (from Lewin et al., 1977).*

	M = Pb	**M = Zn**
MS	1.78×10^{-14}	1.26×10^{-12}
MSO_4	1.26×10^{-4}	5.37
MCO_3	2.18×10^{-7}	3.97×10^{-6}
MCl_2	1.58×10^{-2}	18.01

In the acid environment of moorland waters and especially in underground mine workings and spoil tips containing high concentrations of pyrite (FeS_2) and marcasite (FeS_2), the primary sulphide ores will oxidise to sulphates. In contrast, in mine waste where either calcite ($CaCO_3$), dolomite ($CaMg(CO_3)_2$) or Fe-rich ferroan dolomite are the dominant gangue mineral rather than quartz, carbonic acid will increase the *in situ* formation of metal carbonates. Indeed, the formation of metal salts is common in most orefields, including the CWO, leading to the development of a wide range of more soluble secondary minerals (Section 3.1) on many spoil tips.

The scale of HM solute contamination in the CWO can be clearly demonstrated by reference to geochemical analyses (Williams, NRW, pers comm.) of the discharge from Pugh's Adit at Cwmystwyth Mine and No.6 Adit at Cwmrheidol Mine (see Plates 2.2A and B). Mine water

discharge from Pugh's Adit contains a Zn concentration of 23,000 µg L^{-1} and a Pb concentration of 580 µg L^{-1}, equating to an annual load of 7,000 kg Zn and 180 kg Pb entering the Afon Ystwyth. The effect of this and other mine water discharges into the Afon Ystwyth is shown by river water concentrations of between 170 – 3,040 µg L^{-1} Zn and 92 – 121 µg L^{-1} Pb (Grimshaw *et al*., 1976; Fuge *et al*., 1991; Environment Agency, 2008b). Similarly, mine water discharge from No. 6 Adit at Cwm Rheidol Mine (see Plate 2.2B) contains a Zn concentration of 13,000 µg L^{-1} and a Pb concentration of 750 µg L^{-1}, equating to an annual load of 3,000 kg Zn and 175 kg Pb. In the Afon Rheidol, reported HM concentrations range between 14 – 285 µg L^{-1} Zn and 9.5 – 12.4 µg L^{-1} Pb (Fuge *et al*., 1991; Environment Agency, 2008b). In both rivers, HM concentrations greatly exceed the environmental quality standards (EQS), which for Zn is 8 – 125 µg L^{-1} and for Pb is 7.2 µg L^{-1} (Environment Agency, 2008b).

It is clear from the foregoing account that, in addition to the remediation of contaminated mine spoil, tailings and soils (Section 2.3) containing particulate HMs, attention must also be given to the remediation of contaminated mine water discharge. Several pilot-scale VFP treatment schemes are on-going in the CWO, for example at Cwm Rheidol Mine, where various organic substrates, such as farm manure, digested sewage sludge, woodchips, crushed whelk shells and paper waste, are being assessed. Thus far, HM extraction rates are encouraging, with the removal of up to 99% of dissolved Pb, Zn and Cd (Williams, NRW, pers comm.). In the light of these results, the implementation of full-scale VFP schemes is currently under consideration at several mines in the CWO, including Cwm Rheidol, Cwmystwyth, Abbey Consols, Esgair Mwyn and Nant y Mwyn, all of which discharge HM-rich minewaters directly into watercourses.

2.3 Bioremediation of HM contaminated substrates

Although the application of bio-based technologies for the treatment of HM contaminated substrates is a very modern field of study, there already exists a large volume of published research and critical reviews that assess the efficacy, or otherwise, of a wide range of applied methodologies. As noted in Section 2.1, some HMs are essential to organisms in very small quantities but become harmful in the presence of excessive concentrations, whilst others have no beneficial effects and are very harmful to both plants and animals (Table 2.3). Since all HMs

Table 2.3 *Toxicological impact of certain HMs on selected plants and the effects of chronic (long-term) exposure on Man (from various authors and online sources).*

HM	Organism	Toxicological effect on organism
Pb	Maize (*Zea mays*)	Reduction in germination percentage; suppressed growth; reduced plant biomass; decrease in plant protein content
	Portia Tree (*Thespesia populnea*)	Reduction in number of leaves and leaf area; reduced plant height; decrease in plant biomass
	Oat (*Avena sativa*)	Inhibition of plant enzymes which control CO_2 fixation
	Man (*Homo sapiens*)	Fatigue, nausea, loss of muscular co-ordination, short-term memory loss, anaemia, aggressive behaviour disorders
Zn	Cluster bean (*Cyamopsis tetragonoloba*)	Reduction in germination percentage; reduced plant height and biomass; decrease in chlorophyll, carotenoid, sugar, starch and amino acid content
	Pea (*Pisum sativum*)	Reduction in chlorophyll content; alteration of chloroplast structure; reduced plant growth
	Ryegrass (*Lolium perenne*)	Accumulation of Zn in plant leaves; growth reduction; decrease in plant nutrient content; reduction in efficiency of photosynthetic energy conversion
	Man (*Homo sapiens*)	Convulsions and seizures, fainting, fever, vomiting, liver and kidney derangement and disfunction, hypotension, anaemia, diarrhoea
Cu	Bean (*Phaseolus vulgaris*)	Accumulation of Cu in roots; root malformation and reduction Plant mortality; reduced biomass and seed production
	Black bindweed (*Polygonum convolvulus*)	Reduction in root growth
	Rhodes grass (*Chloris gayana*)	
	Man (*Homo sapiens*)	Vomiting, hematemesis, hypotension, coma, jaundice, gastrointestinal distress, liver and kidney damage
Cd	Wheat (*Triticum* sp.)	Reduction in seed germination; decrease in plant nutrient content; reduced shoot and root length
	Garlic (*Allium sativum*)	Reduced shoot growth; Cd accumulation
	Maize (*Zea mays*)	Reduced shoot growth; inhibition of root growth
	Man (*Homo sapiens*)	Tracheo-bronchitis, pneumonitis, kidney and liver damage, carcinoma, osteoporosis

are non-biodegradable, they accumulate in the environment and can subsequently contaminate the food chain, thereby posing significant risk to both environmental, plant and animal health, even at low concentrations (Table 2.4). Indeed, some HMs are carcinogenic, mutagenic, teratogenic and endocrine disruptors, whilst others are known to cause neurological and

behavioural problems particularly in infants. In the light of these environmental impacts and the global magnitude of industrial HM contamination, significant effort has been on-going to find practical solutions.

Table 2.4 *HM toxicity limits in ppm (after Mendez and Maier, 2008).*

Toxicity Index	Zn	Pb	Cu	Cd	Ni
Soil plant toxicity levels	400	100-500	200	3	90
Plant leaf tissue toxicity limits	100-400	30-100	2-20	5-30	10-100
Domestic animal toxicity limits	500	100	40	10	100

A wide range of engineering-based solutions have been applied to the remediation of HM contaminated substrates, including simple burial and capping (e.g. Plate 2.1), encapsulation (Randall and Chattopadhyay, 2004), solidification/stabilisation (Alpaslan and Yukselen, 2002), vitrification (Basel Convention, 2009), electrokinetics (Virkutyte *et al*., 2002) and soil washing and flushing (Abumaizar and Smith, 1999). However, all of these methods are generally very expensive and often do not subsequently yield soils that are suitable for the growth of plants. In contrast, a bio-based approach or 'bioremediation', defined here as the use of organisms (microorganisms and/or plants) for the treatment of contaminated substrates, offers what is generally perceived as an efficient, eco-friendly solar-driven solution with good public acceptance, that encourages the *in situ* re-establishment of plants and provides a cost-effective substitute for highly expensive engineering techniques. For example, it has been demonstrated that there was a cost saving of between 50 – 65% when bioremediation was used to treat 1 acre of Pb-polluted soil, rather than conventional methods involving excavation and landfill (Blaylock *et al*., 1997). In the USA, estimates of the cost of engineering-based remediation of mine tailings range from US$1.5 – 450 per m^3 (Berti and Cunningham, 2000), whilst phytoremediation can reduce this cost to US$0.4 – 26 per m^3 for re-vegetation (Mendez and Maier, 2008).

The availability of HMs for uptake by plants and microorganisms depends on a number of factors. In particular, it has long been known that pH is a major factor (Harter, 1983), with studies showing, for example, that the availability of Zn and Cd to the roots of *Thlaspi caerulescens* decreases significantly with increasing pH (Wang *et al*., 2006). In addition, the presence of organic matter and hydrous ferric oxide has been shown to immobilise these metals and thereby reduce bioavailability (Hong *et al*., 2007). Other factors controlling HM availability include soil aeration, mineral composition and microbial activity (Magnuson *et al*., 2001),

substrate moisture content and porosity (Sharma and Raju, 2013), and the degree of chelation (Norvell, 1984). In addition, the presence of one HM may affect the bioavailability of another, implying the existence of complex antagonistic and synergistic behaviours (Chibuike and Obiora, 2014). For example, Cu and Zn as well as Ni and Cd are reported to compete for the same membrane carriers in plants (Clarkson and Luttge, 1989), whilst Cu has been reported to increase the toxicity of Zn in spring barley (Luo and Rimmer, 1995). Another important feature of HMs is that they cannot be degraded during bioremediation; rather, they can be transformed from one oxidation state to another or chelated between organic complexes thereby rendering them less toxic, more water soluble (allowing removal *via* leaching) or less water soluble (allowing precipitation and subsequent removal) and therefore less bioavailable (e.g. Garbisu and Alkorta, 1997, 2003).

The use of microorganisms for the treatment of HM-contaminated substrates is well documented and will be only briefly discussed. The bacteria *Bacillus cereus and B. thuringiensis* have been shown to increase the extraction of both Zn and Cd from Cd-rich soils polluted by the metal industry (Mohideena *et al.*, 2010). *B. subtilis*, *Pseudomonas putida* and *Enterobacter cloacae* have been used to stimulate the transformation of the powerfully oxidising Cr^{6+} cation to the less toxic Cr^{3+} cation (Ishibashi *et al*., 1990; Garbisu *et al*., 1997, 1998), whilst the sulphate-reducing bacteria *Desulfovibrio desulfuricans* has been shown to convert sulphates to hydrogen sulphate, which in turn reacts with HMs such as Zn and Cd to form insoluble forms of the metal sulphides and thereby reduce bioavailability (White *et al*., 1998).

Phytoremediation is a form of bioremediation that utilises plants for the treatment of contaminated substrates (e.g. McGrath and Zao, 2003). It is a technique that is particularly suited to situations where the contamination covers a wide area and, importantly, where the contaminant lies within the root zone of plants. The remediation of HM contaminated substrates is achieved by several different forms of phytoremediation, including phyotoextraction, phytostabilisation and phytovolatilisation. The latter technique, which involves the transformation of pollutants into volatile forms that may be taken up by plants and subsequently transpired into the atmosphere, is used mainly for the remediation of soils contaminated with Hg. Although this bioremedial technique is not discussed further here, it is interesting to note that in many 19th Century gold mining districts, including the Dolgellau Gold Belt in North Wales (Hall, 1988), Hg was extensively used to extract Au through the process of

amalgamation. Phytoextraction and phytostabilisation are mechanisms that are of relevance to two central objectives of this research project, namely the uptake of Pb and Zn by a *L. perenne* mapping family and the identification of possible QTL, and they will both be discussed in further detail.

2.3.1 Phytoextraction

This mechanism involves the accumulation of HMs in the shoots and roots of the phytoremediating plants, with either the shoots or the whole plant being harvested and incinerated. Plants that are best suited to phytoextraction exhibit several important characteristics including a rapid growth rate, a high biomass, an extensive root system, and the ability to tolerate high amounts of heavy metals (Chibuike and Obiora, 2014), although it has been recognised that incorporation of high HM concentrations in shoots may pose a risk through contamination of the food chain by ingestion (Marques *et al*., 2009). There are two main approaches to phytoextraction. The first uses plants that are natural hyperaccumulators, that is plants with the ability to uptake high concentrations of metal, and this approach has been in use for over 25 years (Rascio and Navari-Izzo, 2011). The second approach uses high biomass plants whose ability to accumulate HMs in high concentrations is enhanced by the application of synthetic soil amendments (chelates) that have a HM mobilising capacity (Salt *et al*., 1998).

A plant can be classified as a hyperaccumulator if it can accumulate between 10 – 500 times more HM than an ordinary plant (Chaney *et al*., 1997). For example, hyperaccumulators of Zn accumulate > 3,000 µg g^{-1} in their dry leaf tissue, for Pb > 1,000 µg g^{-1}, for Cu > 300 µg g^{-1} and for Cd > 100 µg g^{-1} (Reeves and Baker, 2000; Van der Ent *et al*., 2012; Gall and Rajakaruna, 2013). In addition, two criteria for hyperaccumulation are, first, that the ratio of shoot to root concentration (the translocation index) must be consistently greater than 1 (McGrath and Zhao, 2003), implying the existence both of a translocation ability and a HM hypertolerance and, second, that the concentration of metal in the shoot must be higher than 0.01% for Cd, higher than 0.1% for Al, As, Co, Cr, Cu, Ni, and Se, and higher than 1.0% for Zn (Baker and Brooks, 1989). There are 582 known species of HM hyperaccumulators from over 50 families of vascular plants worldwide (Gall and Rajakaruna, 2011). Reported hyperaccumulators include *Dichapetalum gelonoides*, *Arabidopsis halleri*, *Thlaspi tatrense* and *T.* (now *Noccaea*) *caerulescens* for Zn, *Agrostis tenuis* and *Minuartia verna* for Pb, Cu and Zn (Plate 2.3), and *Aeollanthus subacaulis* for Cu (Neumann *et al*., 1997; Reeves and Baker, 2000), whilst *Sedum alfredi*, a known Zn hyperaccumulator, can also hyperaccumulate Cd (Yang *et al*., 2004). Most

hyperaccumulators are metal-specific, slow growing species with low biomass, although notable exceptions include members of the Brassicaceae, for example *B. napus*, *B. juncea* and *B. rapa* (Chibuike and Obiora, 2014), a family which accounts for approximately 25% of all known hyperaccumulators, and even certain trees (e.g. *Salix* sp., *Populous* sp. and *Alnus* sp.) which are fast-growing and have good potential as HM dendroremediators (González-Oreja *et al*., 2008).

Plate 2.3 Spring Sandwort (*Minuartia verna*), a known hyperaccumulator of Cu, Zn and Pb, seen here growing on a highly Cu-rich substrate at Turf Copper Mine, North Wales.

In order to increase bioavailability and root to shoot translocation potential, HM chelating chemicals are often used in bioremediation programmes, since these substances prevent metal precipitation in the rhizosphere. A wide range of synthetic chelates have been successfully used as soil amendments in phytoextraction (Marques *et al*., 2009). These include EDTA (ethylenediaminetetraacetic acid), EDDS (SS-ethylenediamine disuccinic acid), CDTA (1, 2-cyclohexylenedinitrilotetraacetic acid), EDDHA (ethylenediamine-di-*o*-hydroxyphenylacetic acid), DTPA (diethylenetriaminepentaacetic acid), and HEDTA (N-ydroxyethylenediaminetriacetic acid). Other compounds which have been tested include amino acids (e.g. histidine), organic acids (e.g. malic, oxalic, tartaric and citric acids), rhamnolipid biosurfactants (Gunwardana *et al*., 2010) and the biodegradable chelator nitrilotriacetic acid (NTA) (Zhao *et al*., 2013). In addition, a wide variety of inorganic ligands have also been used, sometimes in combination with organic chelates, including sulphate, lime and phosphate (e.g. Gunawardana and Singhal, 2010).

EDTA is the most widely used synthetic chelate because it is the least expensive and because it has proved highly successful in enhancing metal uptake. For example, Tanhan *et al*. (2011) reported that *Chromolaena odorata* grown in soil with 99,545 mg kg^{-1} Pb accumulated a total of 3,730 and 6,698 mg kg^{-1} Pb in the shoots and roots, respectively, representing a 17-fold increase in the shoots and an 11-fold increase in the roots relative to untreated plants. Lai *et al*. (2008) and Purakayastha *et al*. (2008) also reported that, for certain species of the genus *Brassica*, the translocation indices for Zn, Cu, Pb and Ni were greatly increased by the application of EDTA, with root length emerging as the most powerful parameter controlling the uptake of HMs. EDTA has also been used effectively in conjunction with other chelating agents. For example, Miller *et al*. (2008) reported a dramatic increase in the translocation of Pb from roots to shoots in Coffeeweed (*Sesbania exaltata*) using EDTA in combination with acetic acid, whilst Begonia *et al*. (2005) reported that the same combination of agents was effective in increasing the translocation index in Tall Fescue (*Festuca arundinacea*).

Comparisons between the effectiveness of various synthetic chelating agents have also been widely reported. For example, Santos *et al*. (2006) reported that for Signal Grass (*Brachiaria decumbens*), the use of EDTA caused a 1.77-, 1.11-, and 1.87-fold increase in the shoot concentrations of Cd, Zn and Pb, respectively, relative to controls, whereas, in contrast, the use of EDDS caused a 2.54-, 2.74-, and 4.30-fold increase, indicating that the latter agent is more effective in stimulating translocation of the HMs from roots to shoots. Luo *et al*. (2005) reported that EDTA was more efficient in solubilising Pb and Cd than EDDS, whereas the latter was more effective in solubilising Cu and Zn than EDTA.

A major issue relating to the use of synthetic chelating agents, in particular EDTA, is the concern over environmental contamination through enhanced metal solubility and leaching, as well as their environmental persistence (Meers *et al*., 2008; Tanhan *et al*., 2011). Some authors (e.g. Meers *et al*., 2009) believe that leaching poses such a hazard that there should be a move away from the use of EDTA to less aggressive strategies such as the use of more biodegradable aminopolycarboxylic acids (APCAs) or NTA (Zhao *et al*., 2013). Other authors go even further and suggest that, because an effective solution to HM leaching has not yet been found, phytoextraction has 'possibly reached a turning point and should distance itself from chelate-assisted phytoextraction and focus on alternative options' (Evangelou *et al*., 2007).

2.3.2 Phytostabilisation

This mechanism involves the use of plants to immobilise HMs and thereby reduce their bioavailability *via* erosion and leaching, and its use is most appropriate when rapid HM immobilisation is needed to prevent groundwater pollution. The stabilisation of contaminated substrates by plants is effected through a dense root system which prevents erosion by binding the substrate particles, and prevents leaching by reducing substrate permeability and water percolation, but also by isolating the contaminants from the physical environment. Plants that are best suited for phytostabilisation require several critical characteristics, including a dense rooting system, a high tolerance to the specific substrate contaminant(s) and physico-chemical conditions, a very low (<< 1) translocation index, ease of establishment and maintenance under field conditions, rapid growth rates to provide high ground surface coverage, longevity and the ability to self-propagate (e.g. Mendez and Maier, 2008; Chibuike and Obiora, 2014). In contrast to phytoextraction, the most appropriate soil amendments for phytostabilisation include agents such as phosphates, lime, and in particular compost and manure, which effectively inactivate HMs and thereby prevent their uptake by plants, provide a slow-release fertiliser and serve as a microbial inoculum.

Arienzo *et al*. (2004) cultivated *L. perenne* on soil contaminated with Cu, Pb and Zn at concentrations of 377, 366 and 679 mg kg^{-1}, respectively. The plants grew well and showed no macroscopic toxicity symptoms other than for slightly retarded growth. Shoot dry weight concentrations of Cu, Pb and Zn were recorded as ranging between 12.6 – 19.3, 0.67 – 0.98 and 88 – 99 mg kg^{-1}, respectively, and on this basis it was concluded that *L. perenne* could provide a healthy vegetative cover on contaminated soils. Similarly, Bidar *et al*. (2007, 2009) found that *L. perenne* and *Trifolium repens* formed a dense plant cover on highly contaminated Pb-, Zn- and Cd-contaminated soils, with the roots acting as preferential HM storage sites and with only limited root to shoot translocation (Tables 2.5 and 2.6). These authors concluded that both of these species were suitable for phytostabilisation programmes.

Table 2.5 *Metal concentrations (mg kg^{-1} dry weight) in the roots and shoots of T. repens and L. perenne grown in substrates containing ~25, ~1,200 and ~1,300 mg kg^{-1} Cd, Pb and Zn, respectively (from Bidar et al., 2007).*

	T. repens		***L. perenne***	
	Roots	Shoots	Roots	Shoots
Cd	126.89 ± 21.36	9.01 ± 1.57	131.84 ± 8.54	12 ± 1.6
Pb	166.98 ± 66.98	35.8 ± 7.32	269.98 ± 64.59	45.65 ± 4.03
Zn	1563.3 ± 294.4	96.70 ± 15.62	1511.18 ± 92.7	218.15 ± 20.87

Table 2.6 *Translocation indices for T. repens and L. perenne (see Table 2.5) grown in contaminated substrates (from Bidar et al., 2007).*

	T. repens	***L. perenne***
Cd	0.07 ± 0.02	0.09 ± 0.01
Pb	0.25 ± 0.11	0.18 ± 0.06
Zn	0.06 ± 0.02	0.14 ± 0.01

Qu *et al*. (2003) studied Pb uptake by the roots of four turfgrass species grown hydroponically in solutions containing up to 450 mg L^{-1} and at a pH of 4.5 and 5.5. The maximum Pb tissue concentration recorded was ~ 30 mg g^{-1} root dry weight in Tall fescue (*F. arundinacea* Schreb.). *Spartina patens* ('Common') and *F. arundinacea* survived in 450 mg Pb L^{-1} without displaying evidence of Pb toxicity, whilst Centipedegrass (*Eremochloa ophuiroides* (Munro) Hack.) and Buffalograss (*Buchlöe dactyloides* (Nutt) Engelm) deteriorated and died at this concentration level. Uptake results indicated that turfgrass plants can tolerate high Pb concentrations and absorb Pb efficiently, at least into the roots, and thus may have potential for phytostabilisation of Pb-contaminated substrates. Padmavathiamma and Li (2009) identified *L. perenne*, *F. rubra* and *Poa pratensis* as promising Zn phytostabilising species and found that maximum Zn immobilisation occurred when the plants were grown in the presence of a combination of lime, phosphate and compost soil amendments. Marquez *et al*. (2008) showed that the application of manure or compost to Zn contaminated soil on which *Solanum nigrum* was growing reduced Zn percolation through the soil by as much as 80%. Kumpiene *et al*. (2007) reported that the addition of coal fly ash and peat decreased Cu leaching by 98.2% and Pb leaching by 99.9%. This dramatic reduction led to an increase in seed germination rate, reduced HM translocation to the shoots, and decreased toxicity to plants and bacteria, thereby demonstrating that this soil amendment combination may be a very effective technique for the phytostabilisation of Cu- and Pb-contaminated substrates.

2.4 Molecular and genetic controls of HM uptake and tolerance in plants

2.4.1 Biomolecular aspects of HM tolerance

The physical manifestation of HM toxicity on plants is variable (see Table 2.3) but includes, *inter alia*, a reduction in plant growth and seed germination rate (Ernst, 2006), chlorosis, necrosis, and plant death (Plate 2.4). In addition, HMs can influence a wide range of physiological processes such as water uptake, nutrient transport and metabolism, transpiration

and the uptake of essential metal cations such as Ca, Mg, K and P, as well as a reduction in photosynthetic capability by the disruption of intra-chloroplast thylakoids and chlorophyll synthesis (Boddi *et al*., 1995; Fodor, 2002; Poschenrieder and Barceló, 2004; Hsu and Kao, 2004; Benavides *et al*., 2005).

Plate 2.4 Manifestation of Zn toxicity in a *L. perenne* mapping family grown in sand with a 30% by weight mixture of Zn-enriched mine tailings. Effects include chlorosis, reduced plant growth and plant mortality.

One of the most important reasons for HM toxicity in plants is through disturbance of redox homeostasis and the stimulated formation of free radicals and a variety of reactive oxygen species (ROS) such as singlet oxygen ($^1O_2$), superoxide radical (O^{-2}), hydroxyl radical (OH^-) and hydrogen peroxide (H_2O_2) (Salin, 1988), and methylglyoxal (MG) (Hossain *et al*., 2011). (OH^-) is extremely reactive causing extensive oxidative damage to cell membranes, photosynthetic pigments, proteins and DNA (e.g. Gechev *et al*., 2006), whilst high concentrations of H_2O_2 result in oxidative cellular damage and cell death (Figure 2.4). ROS are thought to act as signals in stress response, activating proteins and genes, and H_2O_2 in particular is probably a key molecule in triggering signal transduction, stimulating the production of glutathione (GSH), discussed further below, and higher HM sequestration in the roots (Hu *et al*., 2009). MG (2-oxopropanal) is a genotoxic mutagen, causing DNA strand breaks, that is found to increase as a result of HM stress and further amplify ROS production by interfering with vital physiological processes (e.g. Hossain and Fujita, 2010).

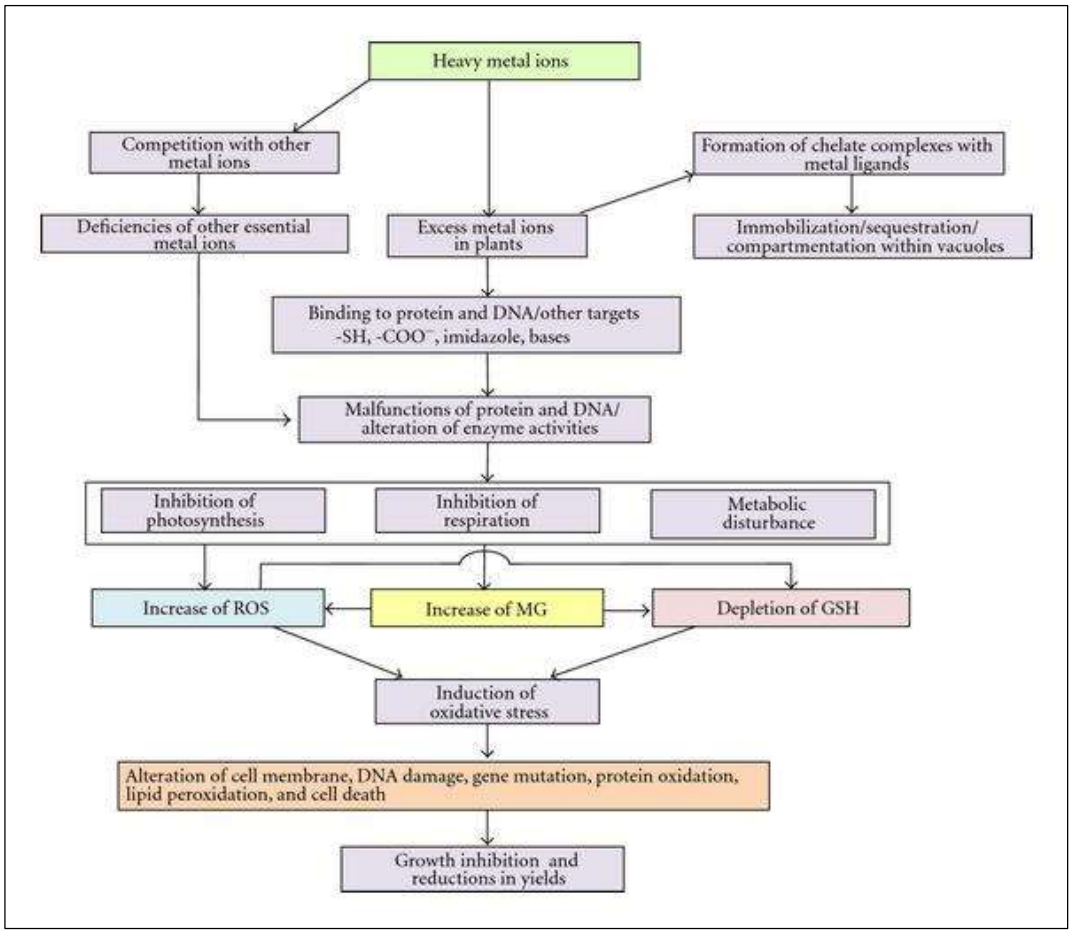

Figure 2.4 Possible biochemical and molecular mechanisms of HM-mediated reactive oxygen species (ROS) induction and their potential for damage to the development of higher plants (from Hossain *et al*., 2011).

In order to minimise the potential biotoxic effects of HM-induced stress, plants that live on HM contaminated substrates have evolved a range of different strategies at a molecular level. In broad terms, there is a class of plants which have developed an avoidance strategy, involving mechanisms such as: 1) extracellular precipitation of root exudates (e.g. organic acids) which precipitate or chelate metals in the rhizosphere and prevent their entry into the root cell (e.g. Yong and Ma, 2002; Pinto *et al*., 2008; Colzi *et al*., 2011); and 2) biosorption to cell walls, in particular by binding to functional groups such as -COOH, -OH and -SH and to polysaccharides such as pectins (Mehes *et al*., 2013). In contrast, another class of plants have developed a tolerance strategy involving the synthesis of a wide range of chelating agents and the storage of HMs by intracellular sequestration and vacuolar compartmentation (Liu *et al*., 2007). Within the class of HM tolerant plants, Baker and Walker (1990) differentiated three sub-classes, namely metal excluders, metal indicators and metal accumulators/hyperaccumulators. Metal excluders limit the amounts of metal translocated from roots to shoots, thereby maintaining a low HM concentration in their aerial biomass. Metal indicators accumulate HMs in their aerial tissue at concentrations in proportion to those in the substrate, whilst

accumulators/hyperaccumulators can accumulate higher levels of one or more HMs (Mganga *et al*., 2011) in their shoots than in their roots (see Section 2.3.1).

When the roots of a metal-tolerant plant come into contact with bioavailable HMs, the latter may either migrate passively in the free diffusional space outside the plasma membrane (i.e. the apoplast) or cross the plasma membrane into the symplast where cytoplasm-cytoplasm transport may occur. The latter is mediated *via* a range of ion transporter proteins such as HM (CPX-type) ATPases, natural resistance-associated macrophage proteins (NRAMPs), cation-diffusion facilitator (CDF) proteins, cation exchangers (CAXs), Zn-Fe permeases (ZIPs) and copper transporters (COPTs) (e.g. Salt *et al*., 1995; Hall and Williams, 2003; Jabeen *et al*., 2009; Chaffai and Koyama, 2011; Mehes *et al*., 2013).

Once within the symplast of a root cell, HMs are either sequestered into root vacuoles or transported *via* the xylem to the shoots. To prevent internal damage, in both cases the HMs are bound to a variety of organic chelators, including organic acids (e.g. citrate, malate, malonate, oxalate, succinate and aconitate), amino acids (e.g. nicotianamine (NA) and histidine), glutathione (GSH), metallothioneins (MTs) and phytochelatins (PCs) (Maestri *et al*., 2010). Studies indicate that GSH, a non-enzymatic low molecular weight thiol, plays a pivotal role in HM tolerance by controlling a wide range of physiological processes which, in addition to chelation, include HM uptake, translocation, compartmentation and, crucially, the detoxification of ROS and MG. GSH therefore forms a key component of a plant's antioxidant defence mechanism (Hossain *et al*., 2012). PCs are a class of sulphur donor ligand, derived from GSH, which are induced by many HMs including Cu, Pb, Zn, As, Hg and, particularly, Cd, as in the case of *Sedum alfredii* (Pal and Rai, 2010), and that have also been reported to restrict HMs to the roots (Zenk, 1996). MTs, another class of sulphur donor ligand, play certain essential roles in HM tolerance including Cu, Cd and Hg detoxification, Zn homeostasis and scavenging ROS (e.g. Palmiter, 1998; Wong *et al*., 2004). Amino acids are nitrogen donor ligands that play an important role in chelation. For example, Salt *et al*. (1999) reported that the majority of Zn in the roots of the Zn hyperaccumulator *Thlaspi caerulescens* was complexed with histidine, whilst Verbruggen *et al*. (2009) noted that much of the Zn in the shoots of *A. halleri* was associated with malic acid, an important member of the class of oxygen donor ligands that can form highly stable complexes with certain HMs.

For HMs to finally reach the leaves of a hyperaccumulator, they must be transported to the vacuoles of leaf cells *via* the xylem, a process which requires transport across three plasma

membranes, namely the root cell membrane, the plasma membrane of the leaf cell and the tonoplast of the leaf vacuole. Rates of HM movement are proportional to the HM concentration in the roots and, in this respect, ATPases and NRAMP type transporters are particularly effective for HM loading into the xylem (Gall and Rajakaruna, 2013). Once in the xylem, HM ions are bound to PCs, amino acid and organic acid chelators and pulled *via* transpiration to the leaves, where they undergo compartmentation to leaf vacuoles and/or re-distribution *via* the phloem (e.g. Broadhurst *et al*., 2004). For example, the chelation of Ni by histidine facilitates the long distance translocation in *Alyssum lesbiacum*, with a 36-fold increase in histidine levels reported on exposure to the HM (Solanki and Dhankhar, 2011). On translocation to the leaf cytosol, ATPase and PCs transfer the HMs to the cell vacuole, where they are bound to organic acids and stored until senescence (Chaffai and Koyama, 2011). Zn-malate complexes are reported to play an important role in the transfer of Zn to the leaf vacuole. Once in the vacuole, Zn is released from the malate to a terminal receptor, the malate returning to the cytosol where the process is repeated (Yong and Ma, 2002).

2.4.2 Genetic aspects of HM tolerance

It seems highly probable that genetic adaptations to HM tolerance in plants appeared at a very early stage in their colonisation of the terrestrial environment. Support for such a hypothesis comes from studies of the internationally famous *Lagerstätte*, first discovered in the early 20th Century, at Rhynie in the Grampian Region of Scotland. Volcanogenic hydrothermal deposits (the Rhynie Chert) generated from fault-controlled hot springs and geysers have been dated as early Devonian (*c*. 410 Ma) in age, and these preserve in exquisite detail an entire microecosystem that has yielded the oldest known vascular land plants in Britain as well as a diverse range of arthropods ranging from collembolans to predatory trigonotarbid arachnids (Cleal and Thomas, 1995; Jarzembowski *et al*., 2010). Survival in such a metal-enriched environment would have most probably required a level of HM tolerance, which was possibly also developed in the herbivorous arthropods that formed a key component of the associated terrestrial biota. Such genetic-based adaptations would, through geological time, have aided the progressive colonisation, by so-called edaphic endemics, of other HM-enriched substrates such as those developed, for example, in mafic and ultramafic igneous terrains (Kruckeberg and Rabinowitz, 1985; Macnair, 1993).

Numerous hypotheses have been advocated to explain the ecological basis for HM tolerance in accumulators and hyperaccumulator plant species. These include: 1) the *metal tolerance hypothesis* (Kruckberg and Reeves, 1995), which advocates that plants sequester HMs into their

cell walls and vacuoles, thereby isolating metals from physiologically active sites in the plant and avoiding toxicity; 2) the *disposal hypothesis* (Farago and Cole, 1988), which advocates that HMs are stored in those tissues about to be shed by the plant, or in the leaf epidermis where rainfall could wash out the metals; 3) the *elemental allelopathy hypothesis* (Boyd and Jaffre, 2001), which suggests that hyperaccumulators shed metal-rich tissue to increase metal concentrations in the local substrate and thereby reduce competition from metal-intolerant species; 4) the *drought resistance hypothesis* (Baker and Walker, 1990), which advocates that plants uptake metal ions into their roots, thereby generating a negative water potential that induces water uptake; 5) the *inadvertent uptake hypothesis* (Boyd and Martens, 1992), which suggests that hyperaccumulation is a by-product of another adaptive function; 6) the *defensive enhancement hypothesis* (e.g. Strauss and Boyd, 2011; Boyd 2012), perhaps the most experimentally tested and commonly accepted hypothesis, which suggests that HM sequestration in the leaf tissues provides a defence against insect predation and pathogen infection; and finally 7) the *joint effects hypothesis* (Boyd, 2012), an extension to the *defensive enhancement hypothesis*, which suggests that additive or synergistic effects between element-based defences, or between toxic element and organic defences, may have contributed to the evolution of hyperaccumulation.

Whichever hypothesis is correct, it is clear from Section 2.4.1 that, to pursue either an HM avoidance or HM tolerance strategy, plants have undergone major adaptations at a genetic level to encode for a wide range of organic molecules. Although the identification of genes involved in HM tolerance and accumulation is challenging, of the rapidly developing genetic technologies, the identification of genetic markers and genetic mapping is considered most likely to have the greatest impact on the breeding of HM-tolerant plants. In an effort to understand the genetic architecture of quantitative trait loci (QTL), discussed below, and single genes that control a wide range of important agronomic traits such as yield, size, disease and HM tolerance, genetic marker-based maps have been constructed for many different plant species, including *L. perenne*. The fundamental basis of these genetic maps has been the recognition of molecular markers which reveal, at the DNA sequence level, 'neutral' sites of nucleotide variation which are not visible in the phenotype (e.g. Jones *et al*., 1997). In turn, these genetic markers can be used to test for the presence or absence of specific nucleotide sequences in the genome of individual plants.

In the case of *L. perenne*, several classes of molecular marker have been utilised, such as restriction fragment length polymorphisms (RFLPs), random amplified polymorphic DNA

(RAPDs), amplified fragment length polymorphisms (AFLPs), microsatellites/simple sequence repeats (SSRs) and single nucleotide polymorphisms (SNPs) (e.g. Jones *et al*., 2002; Armstead *et al*., 2002, 2008; Dumsday *et al*., 2003; Blackmore *et al*., 2015, 2016; see Sections 2.5.5 and 4.6). Genetic framework maps for *L. perenne*, created from the markers mentioned above, have recently been significantly augmented with Diversity Array Technology (DArT) markers (King *et al*., 2013), which now give an overall map length of 683 cM defined by 1,316 markers (Figure 2.5). QTL mapping has proved a powerful tool in the identification of candidate genes controlling HM tolerance (e.g. Willems *et al*., 2007), and provides a means of 'dissecting' complex traits and improving understanding of their control (Humphreys and Macduff, 2000). A QTL is a section of DNA (i.e. the locus) that correlates with variation in a phenotype (i.e. the quantitative trait), and the QTL typically is linked to, or contains, the genes that control that phenotype. QTL cannot be mapped in the standard way as for molecular markers. Rather, the basis of QTL mapping, which is a statistical procedure, is to associate the QTL with the molecular markers in their inheritance and thereby to identify them on the basis of their specific map locations.

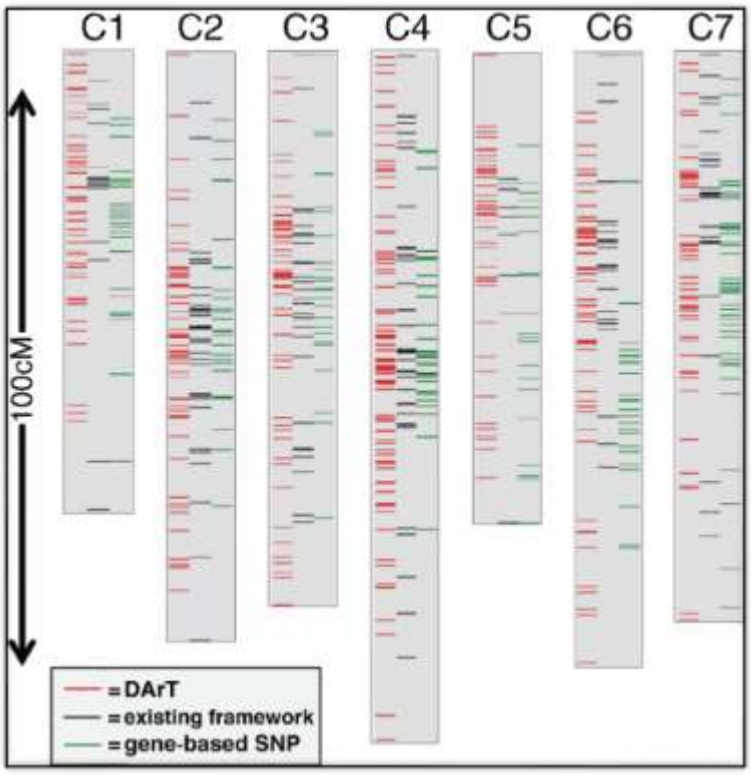

Figure 2.5 Genetic map of a *L. perenne* F2 mapping population illustrating the relative distributions of marker types over the 7 LGs (C1-C7). For each LG, column 1 contains the DArT marker positions, column 2 framework marker positions excluding gene-based single nucleotide polymorphisms (SNPs), and column 3 the gene-based SNP marker positions (from King *et al*., 2013).

Studies attempting to identify associations between molecular markers and HM tolerance/accumulation traits have been performed using both interspecific and intraspecific crosses. For example, two major QTL were found to be involved in the increased accumulation of Zn in a cross between high and low Zn accumulating *Thlaspi caerulescens* parents (Assunçãno *et al*., 2006). QTL mapping for the hyperaccumulation of Zn and Cd in *T. caerulescens* revealed two QTL responsible for Cd and two for Zn accumulation in the roots, as well as one QTL for Cd and three for Zn accumulation in the shoots (Deniau *et al*., 2006).

Courbot *et al*. (2007) identified three QTL involved in Cd tolerance in progeny from an interspecific cross between *Arabidopsis halleri* and *A. lyarata*, and a major QTL region, found to be common to both Cd and Zn tolerance, was co-localised to the HMA4 gene which encodes a P-type ATPase protein transporter involved in the xylem loading of Cd and Zn (Mehes-Smith *et al*., 2013). Further studies of backcross progeny from an interspecific cross between *A. halleri* and *A. lyrata* identified three major QTL involved in Zn tolerance in *A. halleri* and these were mapped to three different chromosomes (3, 4 and 6) and co-localised to HMA4 and MTP1-A and MTP-2, the latter encoding for vacuolar transporters (e.g. Gustin *et al*., 2009; Krämer, 2005). In *A. thaliana*, a total of 15 genes have been identified to code for the transport of various metals (Chaffai and Koyama, 2011), including ZIP 1-12 (Zn), IRT (Fe), MTP1 (Zn), HMA3 (Co, Zn, Cd, Pb), COPT1 (Cu) and YLS2 (Fe, Cu). In addition, genes have also been identified that encode for PCs, including the AtPCS1 and CAD1 genes that encode PC synthase, whilst CAD encodes GSH synthesis (Cobbett and Goldsbrough, 2002), vital for the detoxification of ROS and MG (Section 2.4.1).

In addition to the aforementioned studies of species of the Brassicaceae family, QTL mapping of Cu tolerance and accumulation in wheat (*Triticum aestivum*) has characterised loci on chromosomes 4D, 5A, 7A, 7B and 7D (Mayowa and Miller, 1991), chromosomes 1A, 1D, 3A, 3B, 4A and 7D Ganeva *et al*., 2003), and chromosomes 3D, 5A, 5B, 5D, 6B and 7D (Bálint *et al*., 2003). These results clearly indicate that Cu tolerance in *T. aestivum* is of polygenetic character. Similar studies on rice (*Oryza sativa* L.) have led to the identification of four possible QTL on chromosomes 3, 6, 7 and 8 involved in Cd accumulation (Ueno *et al*., 2009; Ishikawa *et al*., 2010), whilst Tezuka *et al*. (2010) identified a major QTL (qCdT7) on chromosome 7 which controlled the translocation of Cd from roots to shoots. Finally, in studies of a *L. perenne* mapping family grown in FSC, HM-specific QTL were identified for tolerance (in terms of

growth) to Pb, Zn and Fe, together with a range of traits associated with HM accumulation and partitioning between roots and shoots. The methodology and derived data are discussed further in Section 2.5.

2.5 The role of FSC in studies of HM uptake and tolerance in plants

2.5.1 System schematics and operation

The FSC system, located on the IBERS campus at Plas Gogerddan, Aberystwyth, is an internationally renowned, automated hydroponics research facility. Originally designed and constructed in the 1970s, it provides non-destructive continuous measurement of a range of different ions, at the whole plant level, from defined and rhizosphere pH, under controlled environmental conditions in an air conditioned pressurised greenhouse. The system enables the phenotyping and characterisation of nutrient uptake/remediation and assimilation under conditions of: 1) constant external nutrient concentrations; 2) constant relative addition rates (where performance under limiting nutrient supply is of interest); and 3) controlled episodic regimes of supply. Resolution of uptake rates is between 10 minutes and 10 weeks, and the system may be used for short- (i.e. < 24 hours) or long-term (12 weeks) studies or screens.

The FCS system consists of 8 'plant culture units', which supply the plants growing within them with a flowing nutrient solution of controlled composition, together with an extra culture unit without plants for control purposes. The units are linked to nutrient monitoring and control equipment in an adjacent laboratory, which facilitate automatic measurement of nutrient uptake over periods ranging between 6 minutes and 3 months. Each plant culture unit, with a growing area of 0.8 m^2, contains up to 300 litres of continuously re-circulating nutrient solution passing through 24 vessels in which the plants are grown. The units are temperature-controlled within the air-conditioned greenhouse and lighting may be either natural or artificially supplied *via* overhead high pressure sodium and mercury halide growth-lamps, which provide up to 600 µmol m^{-2} s^{-1} PAR over a variable photoperiod. Samples of nutrient solution are taken automatically *via* a by-pass loop from each culture unit in turn and analysed by ion-selective electrodes and flame photometry. During a three minute cycle, a unit is measured for pH, nitrate, ammonium, potassium and a possible further two nutrients. If the measured concentrations fall below pre-set levels, the appropriate nutrients are automatically pumped into the culture unit. Plant nutrient uptakes are then calculated from the rates at which nutrients are re-supplied to the units. The cycle of nutrient measurement and re-supply is controlled and

monitored by a computer linked to an industrial process controller (Figure 2.6). System downtime is minimised by the use of appropriate technology, thereby enabling 'on the spot' diagnosis and repair to be effected in almost all situations. A smaller scale 'mini tank' culture unit, particularly suited to small plants, is also available in the facility and this can also be linked to automatic control of nutrient concentrations.

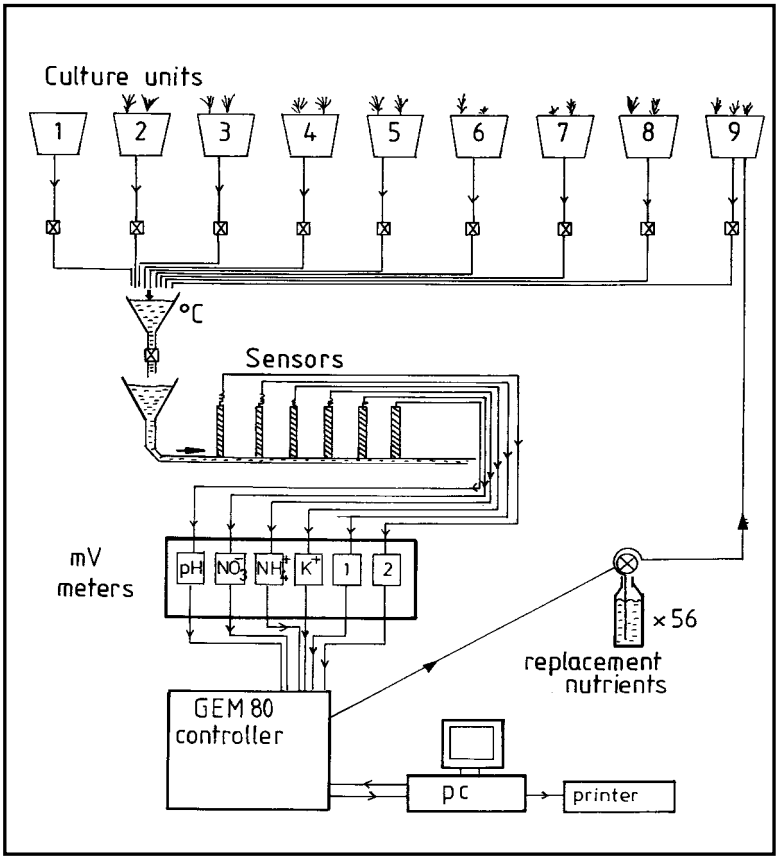

Figure 2.6 Diagram showing the linkage between plant culture units and control-ware in the FSC system.

Research performed in the FSC facility has produced over 80 refereed publications in international scientific journals and numerous contributions to conference proceedings and books. Research has focussed on a wide range of topics, including system development, plant nitrogen relationships, K and P uptake, acidity/pH, plant morphology, as well as studies of the uptake and transport of several HM species, including Pb, Cu, Cd, Zn, Fe and Mn.

2.5.2 HM tolerance research in the IBERS FSC facility

A DEFRA-commissioned research project (DEFRA LS3648), entitled 'Identification, genetic control and evaluation of traits enhancing environmental quality and bioremediation in multifunctional grassland', was carried out in the FSC facility at IGER/IBERS between 2003

and 2007. That part of the project addressing HM tolerance (Fe, Zn, Pb) is noted here because it informed both the approach and research objectives of the work reported in this thesis. A series of 7 screening experiments were performed in FSC to investigate the tolerance of a *L. perenne* mapping family to Fe, Zn and Pb as follows:

Experiment 1:23:51 Characterisation of the mapping family under optimal conditions of macro- and micro-element nutrition.

Experiment 1:23:59 Trial to identify concentration range of Fe in flowing nutrient solution eliciting toxicity symptoms in selected genotypes.

Experiment 1:23:60 Characterisation of the mapping family under conditions of supra-optimal Fe supply.

Experiment 1:23:62 Trial to identify concentration range of Zn in flowing nutrient solution eliciting toxicity symptoms in selected genotypes.

Experiment 1:23:64 Characterisation of the mapping family under conditions of supra-optimal Zn supply.

Experiment 1:23:65 Trial to identify concentration range of Pb in flowing nutrient solution eliciting toxicity symptoms in selected genotypes.

Experiment 1:23:66 Characterisation of the mapping family under conditions of toxic Pb supply.

The results of growth and Zn/Pb uptake in Experiments 1:23:64 and 1:23:66 are presented in Chapter 6, together with a comparative analysis of variation between FSC results and data acquired during the course of the research addressed by this thesis.

2.5.3 QTL analysis and genetic mapping of FSC data

A final phase of the DEFRA-commissioned research programme was molecular characterisation of the *L. perenne* mapping family, based on amplified fragment length polymorphism (AFLP) analysis, and an outline genetic map was produced using JoinMap Version 3.0. Associations between markers and traits were analysed using MapQTL Version 4.0 (Van Ooijen *et* al., 2002).

QTL (threshold LOD > 2.0) were detected for 9 HM-specific traits on the amenity allele map (Table 2.7) and 14 HM-specific traits on the forage allele map (Table 2.8). Data were also mapped onto a pre-existing SSR-based map for the population, revealing QTL for a total of 38

traits (data not presented). QTL, frequently overlapping, were detected for traits associated with most of the 'ecosystem services' addressed in the project. The majority of LOD scores ranged between 2 – 3, with 'the percentage of variance accounted for' ranging between 10 –15%. The locations of the QTL are shown on the outline linkage maps for the forage alleles (Figure 2.7) and the amenity alleles (Figure 2.8).

HM-specific QTL were identified firstly for tolerance (in terms of growth) for Zn (LG4) and Pb (LG4), and secondly for plant content (i.e. potential hyperaccumulation) of Pb (LG5), together with a range of traits associated with the accumulation and partitioning of Zn and Pb between roots and shoots.

Table 2.7 *HM-specific QTL with LOD > 2.0 detected on the project amenity x forage map (amenity alleles). The recorded QTL position is that of the peak LOD score given by interval mapping. The significance level of the Kruscal-Wallis test statistic associated with each of the QTL is also given. % variance explained = percentage phenotypic variation explained by the QTL. Trait number refers to the project's referencing system.*

Category	Trait No	Description	Linkage group	Position (cM)	Marker / locus	LOD score	% variance explained	Kruscal-Wallis Significance (P)
Zn toxicity	145	Relative growth rate (f.wts)	4	34.8	a_ACTCTC.210	2.5	11.5	*0.001*
	155	Shoot:root ratio relative to control plants	3	7.5	a_ACA-CAC.27	2.3	10.7	*0.005*
Pb toxicity	175	Relative growth rate (f.wts)	4	0	a_ACA-CAC.35	2.11	9.8	*0.005*
	181	Shoot d.wt	5	73.6	a_ACT-CAA.159	2.2	10.2	*0.005*
	188	Total Pb content of plant	5	73.6	a_ACT-CAA.159	3.03	13.8	*0.001*
	190	Shoot Pb content	5	73.6	a_ACT-CAA.159	2.48	11.4	*0.001*

Table 2.8 *HM-specific QTL with LOD > 2.0 detected on the project amenity x forage map (forage alleles). The recorded QTL position is that of the peak LOD score given by interval mapping. The significance level of the Kruscal-Wallis test statistic associated with each of the QTL is also given. % variance explained = percentage phenotypic variation explained by the QTL. Trait number refers to the project's internal referencing system.*

Category (Table 4.)	Trait No.	Description	Linkage group	Position (cM)	Locus	LOD score	% variance explained	Kruscal-Wallis Significance (P)
Zn toxicity	145	Relative growth rate (f.wts)	4	24.4	f_ACC-CCT.103	1.99	9.3	0.005
	148	Tiller number	1	26	f_ACC-CAC.82	2.23	10.3	0.005
	154	Shoot:root ratio	1	22.9	f_ACC-CAC.84	2.32	10.8	0.005
	154		1	26	f_ACC-CAC.82	2.32	10.8	0.005
	160	[Zn] in roots	1	26	f_ACC-CAC.82	2.4	11.1	0.005
	160		6	8.3	f_ACA-CTA.39	2.51	11.6	0.0005
	160		6	20.7	f_ACG-CTG.145	2.75	12.6	0.0005
	160		6	24.3	f_ACC-CCC.97	3.32	15	0.0001
	160		6	26.1	f_ACTCTC.202	3.21	14.5	0.0001
	160		6	28.7	f_ACT-CAA.151	2.59	11.9	0.0005
	161	[Zn] in roots relative to control plants	7	20	f_ACC-CAA.70	2.43	11.2	0.0005
	161		7	32.2	f_ACC-CCC.96	2.18	10.1	0.005
	166	Proportional Zn content of shoot	6	8.3	f_ACA-CTA.39	3.5	15.8	0.0001
	166		6	20.7	f_ACG-CTG.145	5.15	22.3	0.0001
	166		6	24.3	f_ACC-CCC.97	6.16	26	0.0001
	166		6	26.1	f_ACTCTC.202	5.39	23.2	0.0001
	166		6	28.7	f_ACT-CAA.151	3.44	15.5	0.0001
	166		6	37	f_ACG-CTG.138	2.38	11	0.001
	167	Proportional Zn content of shoot relative to controls	6	8.3	f_ACA-CTA.39	2.76	12.6	0.0005
	167		6	20.7	f_ACG-CTG.145	3.29	14.9	0.0001
	167		6	24.3	f_ACC-CCC.97	4.17	18.5	0.0001
	167		6	26.1	f_ACTCTC.202	3.68	16.5	0.0001
Pb toxicity	186	[Pb] in shoot	1	0	f_ACT-CTA.187	2.51	11.6	0.001
	186		1	6	f_ACG-CTA.129	3.07	14	0.0005
	186		1	9.7	f_ACC-CAA.64	2.63	12.1	0.001
	186		1	12	f_ACA-CAC.37	2.55	11.7	0.005
	186		1	14.4	f_ACC-CCC.91	2.83	12.9	0.001
	186		2	0	f_ACC-CCT.104	3.16	14.4	0.005
	188	Plant Pb content	1	0	f_ACT-CTA.187	2.41	11.1	0.001
	188		1	14.4	f_ACC-CCC.91	2.3	10.7	0.005
	190	Shoot Pb content	1	0	f_ACT-CTA.187	2.32	10.7	0.0005
	190		1	9.7	f_ACC-CAA.64	2.12	9.9	0.005
	190		1	14.4	f_ACC-CCC.91	2.48	11.4	0.001

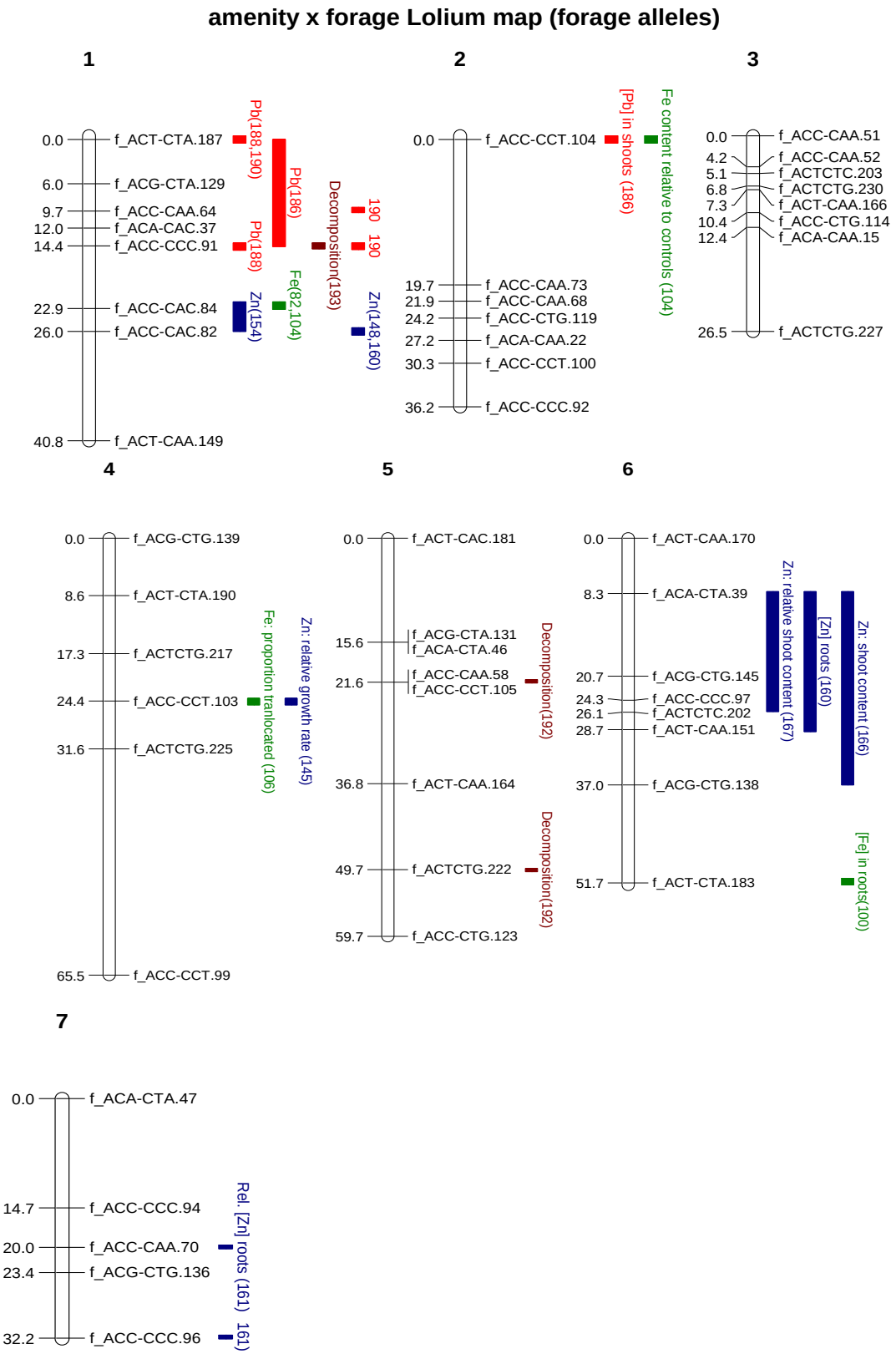

Figure 2.7 Linkage map (forage alleles) showing QTL (LOD > 2.0) for traits associated with heavy metal tolerance and rhizosphere decomposition of organic matter. Different colours are used to denote each metal/process. The trait identification number given in parenthesis refers to the listing in Table 2.8.

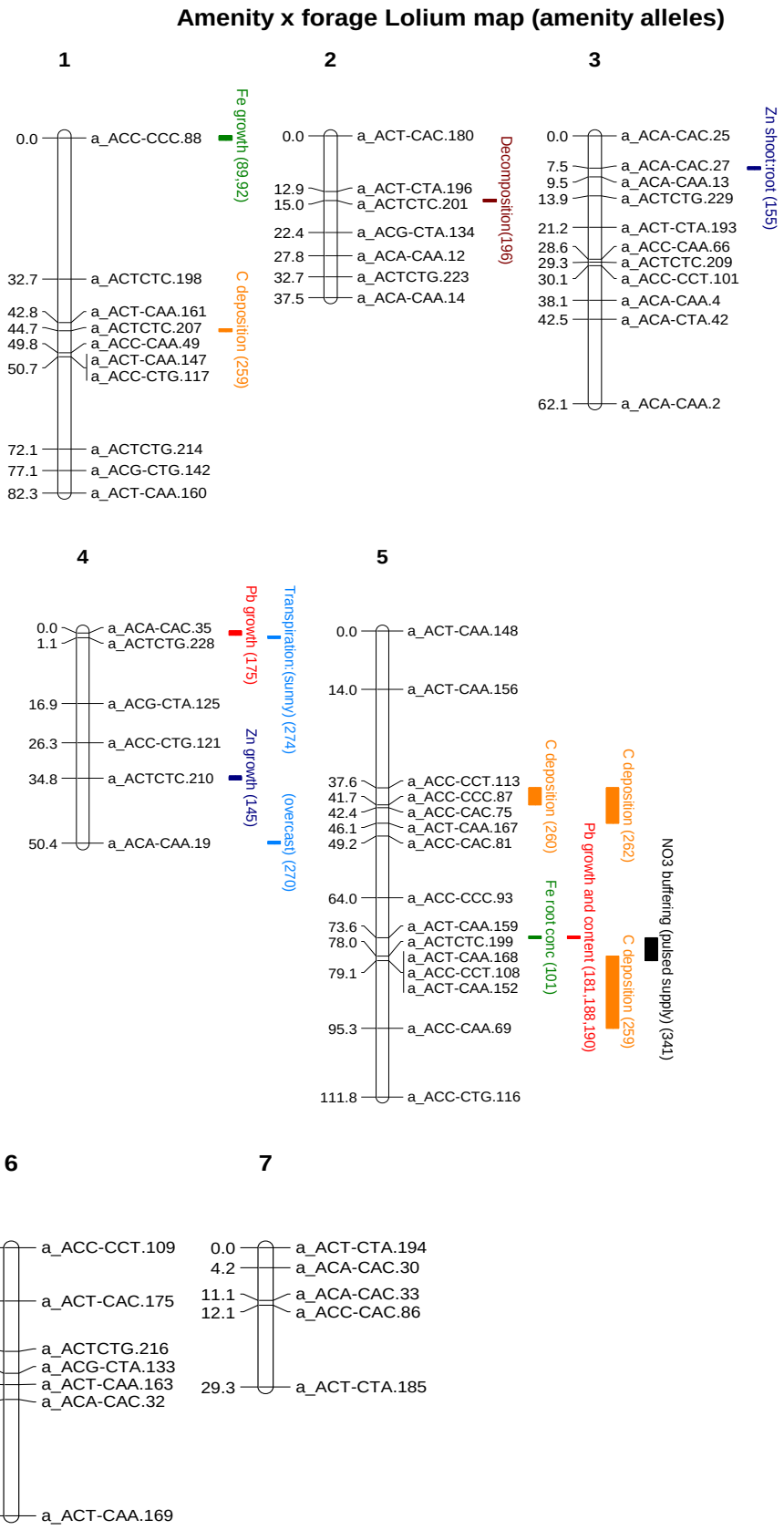

Figure 2.8 Linkage map (amenity alleles) showing HM-specific QTL (LOD > 2.0) for traits associated with heavy metal tolerance (also shown are QTL for rhizosphere decomposition of organic matter, aspects of plant water relations, C deposition and nitrate buffering capacity, not discussed here). Different colours are used to denote each metal. The trait identification number given in parenthesis refers to the listing in Table 2.7.

2.6 Summary

- Anthropogenic exploitation of minerals over many millennia has resulted in widespread contamination of global ecosystems. In the UK, the CWO analogue has contributed to Pb, Zn, Cu and Cd contamination derived *via* HM emissions from mine drainage systems and tailings, and with complex dispersal and storage mechanisms.
- Engineering-based solutions to the remediation of HM contaminated substrates is costly whilst, in contrast, plant-based bioremediation (phytoextraction or phytostabilisation) offers a low cost, eco-friendly alternative.
- Phytostabilisation involves the use of plants that are characterised, *inter alia*, by a dense rooting system, high tolerance to specific HM contaminants, very low translocation indices and rapid growth rates. Published experimental data indicate that *L. perenne* is highly suited for phytostabilisation programmes.
- HM toxicity in plants is manifested by the disturbance of internal homeostasis and, for example, the production of ROS. Many plant species have adapted, at genetic, biomolecular and physiological levels, to cope with HM-related stress, with the development of specific strategies such as HM avoidance, exclusion and tolerance.
- The automated FSC hydroponics research facility at IBERS has previously been used to investigate growth and Zn/Pb uptake in the same *L. perenne* mapping family used in this research project. The hydroponics-based research, which also identified potential growth- and metal uptake-related QTL, informed both the approach and objectives of the work reported in this thesis.

CHAPTER 3
MATERIALS AND METHODS

3.1 The Central Wales Orefield as a source of mine tailings

Contaminated mine tailings, which formed a key component of the pot experiment growth medium, were sourced from abandoned workings within the CWO. Covering an area of over 2,500 km^2 centred on a regional-scale anticline known as the Plynlimon Dome (Figure 3.1), this orefield extends from the Machynlleth-Dylife districts in the north to Llandovery in the south. Archaeological evidence indicates that mining activity may have commenced as early as Bronze Age times (Timberlake, 1989), with sporadic activity during the Roman occupation and later in the Middle Ages. Whilst a documented boom in activity occurred during the 16th Century, in particular focussed on a group of mines between Talybont and Goginan where silver-rich tetrahedrite ($(CuFeAgZn)_{12}Sb_4S_{13}$) was the primary target, the orefield reached its maximum output during the second half of the 19th Century, followed by a slow decline with closure of the last remaining mines during the Second World War (Hughes, 1988). Metal production in the CWO was dominated by ores of argentiferous galena (PbS), sphalerite (ZnS) and chalcopyrite ($CuFeS_2$), and mineral concentrate returns, only recorded compulsorily in the UK since 1845, indicate that over 450,000 tonnes of lead, 140,000 tonnes of zinc, 8,000 tonnes of copper and 2.5 million ounces of silver were raised (Burt *et al*., 1986, 1990; Bevins *et al*., 2010).

The ores of the CWO occur in mineralised veins and breccia cements hosted by dominantly ENE-striking oblique normal faults (lodes), inclined either to the NNW or SSE, that seldom exceed 20 m in width but vary greatly in length between 1 – 10 km and with downthrows of up to 200 m (Jones, 1922; Bevins *et al*., 2010). The lodes transect the regional, NNE-trending folds and cleavage that were generated during the late Caledonian (Acadian) inversion of the Lower Palaeozoic Welsh Basin in early to mid-Devonian times. In addition to the primary minerals noted above, dimorphous pyrite and marcasite (FeS_2) are also present, but neither mineral was workable as an ore. The principal gangue mineral is typically quartz (SiO_2), with less common ankerite ($Ca(Fe^{2+}MgMn)(CO_3)_2$), dolomite and calcite. Early studies of the regional mineral paragenesis (Raybould, 1973, 1974) have been superseded following later investigations by Mason (1994, 1997), who recognised that the mineralisation in the orefield is in fact polyphase, with two discrete mineral groups, referred to as the A1 ('Early Complex') and A2 ('Late

Simple') assemblages, that are differentiated by several factors including mineral diversity, internal vein morphology and grain size (Bevins *et al*., 2010).

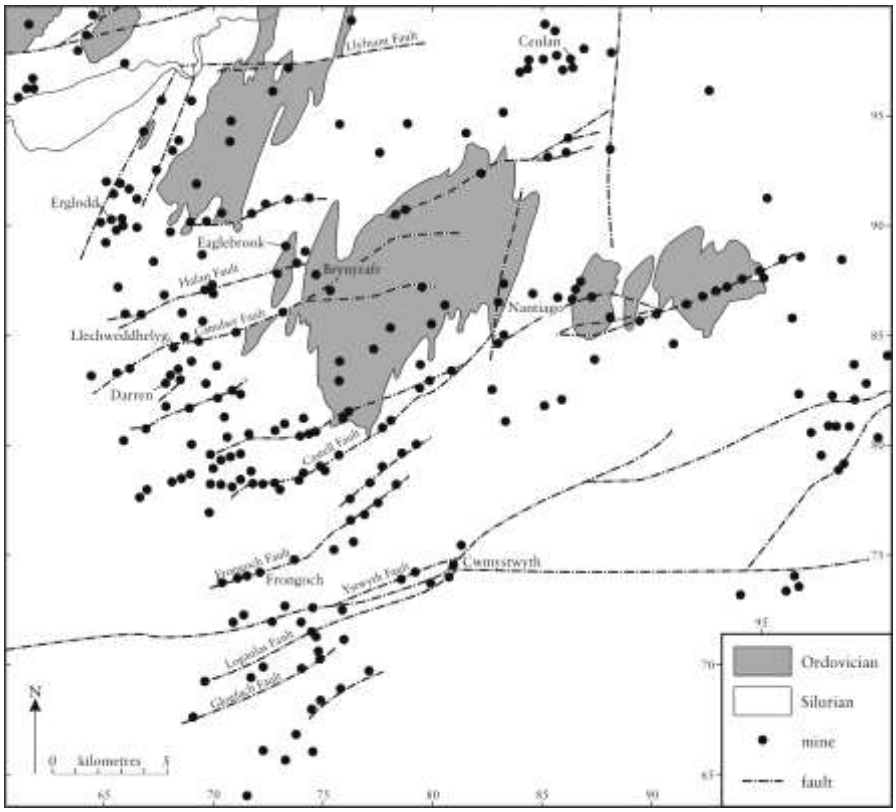

Figure 3.1 Map of the CWO showing the distribution of mines and lodes around the Ordovician inlier (centre of the map) known as the Plynlimon Dome (Ball and Nutt, 1976). The map grid refers to the 1:50,000 OS Sheet 135 Aberystwyth and Machynlleth.

The age and origin of the hydrothermal fluids that formed the mineral veins of the orefield have been the subject of considerable debate. Fitches (1972, 1992) demonstrated that mineralisation post-dated the upright F_1 fold-forming phase of the Acadian Orogeny, since veinlets of quartz, carbonate and sulphide minerals occur in the hinge zones of flat-lying F_2 chevron folds. Lead-isotopic dating of galena samples (Swainbank, *et al*., 1992; Fletcher *et al*., 1993) indicates two main phases of mineralisation, at about 390 Ma during the mid Devonian and later between 330 – 360 Ma during the Lower Carboniferous (Mississippian), followed by a possible third phase between 270 – 240 Ma during Permian-early Triassic times. These model age data are, therefore, broadly consistent with the paragenetic sequences identified by Mason (1994, 1997). Whilst the origin and morphology of the lodes has previously been attributed to hydraulic fracturing (Phillips, 1972; Raybould 1974), later studies (James, 2011) have highlighted the close spatial relationship between the lodes and underlying massive turbidite sandstone bodies of late Ordovician-early Silurian age. It was argued that under a high fluid pressure gradient, these bodies acted as preferential sites of lode nucleation which, during the A1 phase, captured

and transmitted mineralizing fluids generated by Acadian metamorphic dehydration reactions. In contrast, the A2 phase fluids probably originated either as seawater derived from supradjacent Permo-Carboniferous basins or from a now eroded lagoonal basin sited directly above the pervasively fractured Welsh Massif that facilitated density-driven convection and lode reactivation (James, 2011).

3.2 Mine selection for tailings sampling

In order to collect tailings carrying a high concentration of either Zn or Pb but with low concentrations of Cu and Cd, specific mines were targeted which, through analysis of mineral return records (e.g. Jones, 1922; Burt *et al*., 1986) and mineralogical investigations (Mason, pers comm.), were known to have exploited lodes that were rich in either sphalerite or galena. Six mines were selected, namely Castell, Bwlchglas, Cwmystwyth, Darren, Esgairfraith and Eaglebrook (Figure 3.2), all of which had utilised on-site mineral processing methods (Bick, 1976, 1992) that generated substantial quantities of discarded tailings and, importantly, were accessible by vehicle for ease of bulk sample collection.

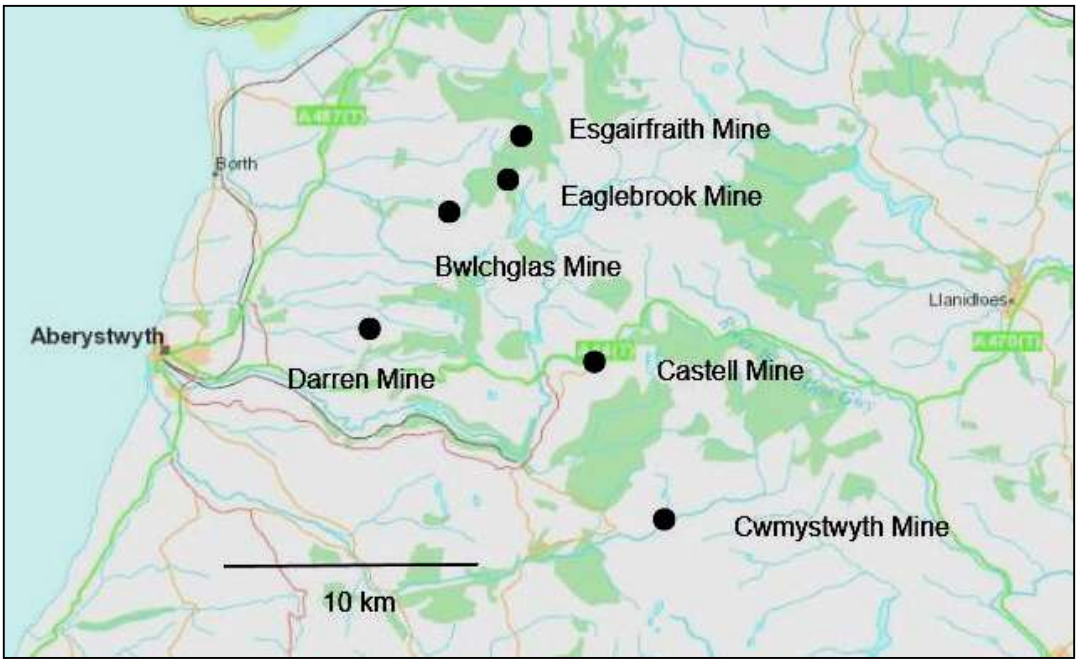

Figure 3.2 Map showing the mine site locations for tailings sampling (Source: Natural Resources Wales).

3.2.1 Castell Mine (SN 775813)

Castell Mine (Plate 3.1), also known as West Esgairlle, is located approximately 2.5 km east of Ponterwyd, and immediately south of the main A44 road from Aberystwyth to Llangurig,

Plate 3.1 View of Castell Mine looking north. Note the large tips above the crusher house with tailings occupying the floor of Dyffryn Castell beyond.

and was operated sporadically between 1785 and 1913, during which time recorded returns indicate a total production of 5,365 tons of Zn ore, 139 tons of Pb ore, 25 tons of Cu ore and 435 ozs of Ag (Burt *et al*., 1985). The mine is located on the ENE-striking Castell Lode (Cave and Haines, 1986), which dips steeply to the south and downthrows the Devil's Bridge Formation (Upper Llandovery) against the Cwmere Formation (Lower Llandovery). Inspection of the spoil tips and a spectacular *in situ* lode exposure (Plate 3.2) indicates abundant A1 mineralisation represented by quartz, sphalerite, chalcopyrite and ferroan dolomite, and later A2 mineralisation represented by quartz and galena. Hydrozincite ($Zn_5(CO_3)_2(OH)_6$) is an abundant secondary mineral phase, testifying to the large quantities of sphalerite in the tips (Westgate, 2000).

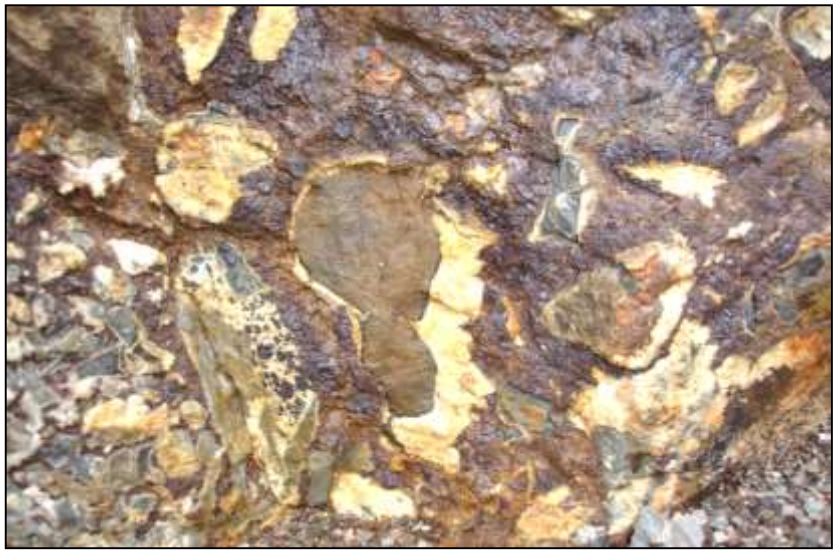

Plate 3.2 *In situ* exposure of the Castell Lode showing fragments of country rock (grey) with rims of quartz (white), all enclosed within a matrix of massive sphalerite (brown).

Remaining mine infrastructure, including a fine crusher house, constructed in 1898, and buddles, confirms that ore was processed on-site. Large volumes of tailings, covering several thousand square metres, lie beneath the crusher house on the floodplain of the Afon Castell and it was in this area, at grid reference SN 77274 81365 (Plate 3.3), that a 5 kg sample was collected for geochemical analysis.

Plate 3.3 Laminated tailings with thin horizons of Fe/Mn oxides on the floor of Dyffryn Castell.

3.2.2 Bwlchglas Mine (SN 710876)

Bwlchglas Mine is situated in the Maesmawr Valley, approximately 6 km east-south-east of the village of Talybont and was operated in two phases, between 1892 and 1913 and again between 1914 and 1923 (Bick, 1976; Hughes, 1989), with recorded returns for the earlier phase amounting to over 466 tons of Pb ore and 85 tons of Zn ore. The mine is located adjacent to the ENE-striking Hafan Lode which extends for a distance of 10 km from Penycefn Mine in the west to Brynyrafr Mine, on the north bank of Nant-y-Moch Reservoir, in the east. However, the Hafan Lode at Bwlchglas Mine was not productive; rather the mine apparently exploited two parallel veins, Evan's Lode and Main Lode, which are thought to be strike-parallel splays from the Hafan Lode (Jones, 1922), 10 – 15 m apart and with a combined southerly downthrow of between 65 – 85 m. The veins are emplaced within siltstones and mudstones of the Lower Silurian (Llandovery Series) Devil's Bridge Formation (Cave and Haines, 1986). A1 mineralisation comprises sphalerite and quartz, veined by galena and quartz, whilst A2 mineralisation comprises coarsely crystalline quartz overgrowing minor galena and calcite. A wide range of secondary minerals occurs on the spoil tips, including species such as crystalline pyromorphite ($Pb_5(PO_4)_3Cl$), for which the mine is famous, cerussite ($PbCO_3$), anglesite ($PbSO_4$) and caledonite ($Pb_5Cu_2(CO_3)(SO_4)_3(OH)_6$) (Bevins and Mason, 1997). Remaining mine infrastructure (Plate 3.4) includes the concrete foundations of a crusher house with adjacent buddles, and a nearby wheelpit, whilst a large volume of unvegetated tailings occupies the floor of the valley on the left bank of the Afon Maesmawr. It was in this area, at grid reference SN 71019 87841, that a 5 kg sample was collected for geochemical analysis.

Plate 3.4 General view of Bwlchglas Mine, looking south-west, showing the remains of mine buildings and spoil tips. A large area of unvegetated tailings is located on the floor of the valley in the right of view.

3.2.3 Cwmystwyth Mine (SN 802746)

Cwmystwyth Mine is located on the north flank of the Ystwyth valley (Plate 3.5), approximately 2 km north-east of Cwmystwyth. Radiocarbon dating of deer antler implements, charcoal and wood indicate that mining here took place as early as Bronze Age times (Timberlake, 1989). Although there is as yet no definitive proof of Roman mining activity, there is evidence for 13th Century operations administered by Cistercian monks from the nearby Strata Florida abbey, whilst three centuries later, during the reign of Henry VIII, Leland noted that the site was heavily polluted by smelting (see Section 2.1), observations which testify to the scale of these pre-industrial operations. The mine achieved its economic heyday from the mid-18th to mid-19th centuries, with both underground and surface mining continuing until 1941, when all operations finally ceased (Hughes, 1979). Recorded production between 1848 and 1916 amounted to 39,912 tons of Pb ore, 33,509 oz of Ag and 18,913 tons of Zn ore, although these returns certainly represent only a fraction of total output, with Hughes (1981) suggesting an historical output closer to 250,000 tons.

Plate 3.5 Cwmystwyth Mine, looking east. Note the very large volume of coarse spoil and tailings which are located both above and below the mountain road.

The mine exploited a series of three anastomising ENE-striking mineralised veins which transect a synclinal fold developed within Llyn Teifi Member of the Lower Silurian (Llandovery Series) Cwmystwyth Grits Group (Davies *et al.*, 1997). Two of these veins, namely the Kingside and Comet lodes, generally dip south at 50 – 60º, and both are cut by north-dipping Mitchell's Lode. In the vicinity of Graig Fawr, the Kingside and Comet lodes intersect and it was here that very large quantities of ore were recovered. In the western sector of the mine, the

Kingside Lode flattened out at depth creating an area known as 'The Great Flat'. Jones (1922) reported that 'for an area of 150 sq.yds. a mass of galena, lying almost horizontally with a constant thickness of 6ft 2in. between its floor and its roof, was worked'. The mineral paragenesis at Cwmystwyth is complex (Mason, 1994, 1997; Bevins and Mason, 1997), with various elements of A1 mineralisation dominated by quartz-, sphalerite-, galena- and chalcopyrite-bearing breccias with abundant ferroan dolomite. A2 mineralisation is more abundant than the earlier phase, being represented by quartz, galena and sphalerite, and a final phase dominated by pyrite and marcasite. Secondary mineralisation is widespread, including species such as pyromorphite, cerussite, hydrozincite hemimorphite ($Zn_4Si_2O_7(OH)_2$), brochantite ($Cu_4(SO_4)(OH)_6$), malachite ($Cu_2(CO_3)(OH)_2$) and linarite ($PbCu(SO_4)(OH)_2$) (Bevins and Mason, 2010).

Presently a wide range of mining infrastructure remains, including wheelpits, crusher houses and leats. A huge volume of spoil and unvegetated tailings lies along the right bank of the Afon Ystwyth below the crushers (see Plate 3.5) and it was in this area, at grid reference SN 80342 74544, that a 5 kg sample was collected for geochemical analysis.

3.2.4 Darren Mine (SN 680832)

Darren Mine is situated approximately 10 km east of Aberystwyth and located on an ENE-striking mineralised vein, the 'Darren Lode', which transects a hill overlooking the village of Pen-bont Rhydybeddau (Plate 3.6). Although there is circumstantial evidence that the mine may have been worked during Iron Age times, it is perhaps most famous for its operation during the 17th and 18th centuries when miners were attracted by the very high grade (~ 30 oz per ton) of Ag in the recovered ores (Hughes, 1990). Recorded returns between 1849 and closure in 1879 total 1,650 tons of Pb concentrates, 21,000 oz of Ag and 50 tons of Cu concentrates (Jones, 1922), although these figures certainly represent only a fraction of total output (Bick, 1976). The Darren Lode cuts mudstones and sandstones of the Lower Silurian (Llandovery Series), Rhayader Mudstones and Devil's Bridge formations (Cave and Haines, 1986). Primary mineralisation in the lode, which is in excess of 5 m wide, is dominated by an A1 assemblage comprising quartz, chalcopyrite, galena, and richly argentiferous tetrahedrite. A2 mineralisation is represented only by minor calcite and marcasite. Secondary mineralisation is

widespread, although generally microcrystalline, with a variety of recorded species including cerussite, malachite, anglesite, leadhillite ($Pb_4(SO_4)(CO_3)_2(OH)_2$) and wulfenite ($PbMoO_4$) (Bevins *et al*., 2010).

Plate 3.6 View of Darren Mine looking north. The excavated lode occupied a narrow notch, visible near the summit of the hill, adjacent to an Iron Age fort.

None of the once extensive mining infrastructure remains at the present-day, although extensive spoil tips exist on the north-facing hillside below the Iron Age settlement (Plate 3.6). Additionally, a large volume of mixed spoil and tailings was located a short distance to the south adjacent to Darren Farm where, at grid reference SN 67517 82800 (Plate 3.7), a 5 kg sample was collected for geochemical analysis.

Plate 3.7 An admixture of coarse spoil and tailings adjacent to Darren Farm.

3.2.5 Esgairfraith Mine (SN 742912)

Esgairfraith Mine is situated approximately 8 km ENE of Talybont and is located on a WNW-striking lode hosted by sedimentary formation of the Lower Silurian (Llandovery Series) Cwmere and Devil's Bridge formations (Cave and Haines, 1986). The lode at Esgairfraith was first exploited, in close association with the adjacent Esgairhir Mine to the west, during the late 17th Century, when they were collectively known as the 'Welsh Potosi', in allusion to the fabulous silver mines of Peru (Borrow, 1862; Bick, 1976). Despite the vast sums of capital invested in both mines over a period of nearly 200 years, Esgairfraith recorded returns of only 144 tons of Pb ore and 2,690 tons of Cu ore, the latter rendering it probably the only true copper mine in the CWO. It should be noted that mining records indicate that much of lead ore from Esgairhir Mine, possibly amounting to more than 4,000 tons, was processed in the crusher at Esgairfraith Mine (Bick, 1976). Primary A1 mineralisation is represented by several mineral assemblages including siegenite ($(NiCo)_3S_4$), cobalt pentlandite (Co_9S_8), millerite (NiS), chalcopyrite, galena and quartz, and a late A1 influx of ferroan dolomite which is well represented on the spoil tips. A2 mineralisation is only minor but comprises galena-sphalerite-quartz and calcite-pyrite-marcasite-quartz assemblages (Bevins and Mason, 1997). A wide range of secondary minerals occur on the spoil tips, including species such as malachite, linarite, pyromorphite, chrysocolla ($(CuAl)_2H_2Si_2O_5(OH)_4.nH_2O$) and hemimorphite ($Zn_4Si_2O_7(OH)_2.H_2O$).

Two impressive wheelpits and a leat complex are the only remaining mining infrastructure at Esgairfraith, although the large volume of unvegetated tailings close to the site of the crusher house, on the left bank of the Afon Lluestgota (Plate 3.8), testifies to large-scale on-site ore processing. It was in this area, at grid reference SN 74084 91143, that a 5 kg sample was collected for geochemical analysis.

Plate 3.8 Esgairfraith Mine looking east, showing an extensive area of unvegetated tailings located on the left bank of the Afon Lluestgota below the wheelpit and the remains of the crusher house.

3.2.6 Eaglebrook Mine (SN 735892)

Eaglebrook Mine (also known as either Dolrhuddlan or Nantycagl) is located close to the north-western margin of Nant-y-Moch Reservoir, approximately 8 km east of Tal-y-bont. The mineralisation is located on an E-striking fracture that transects the axis of the Carn Owen Pericline, the core of which exposes sedimentary rocks of the late Ordovician (Ashgill Series) Drosgol and Bryn-glâs formations (Cave and Haines, 1986). The mine was initially exploited by the so-called 'Company of Mine Adventurers' prior to 1708, although their lease was relinquished in 1722 (Bick, 1976). During the mid-19th Century renewed interest in the mine culminated in returns of 598 tons of Pb ore and 71 tons of Cu ore (Jones, 1922), although true production figures, prior to final closure in 1874, are likely to be much larger.

Elements of both the A1 and A2 mineral parageneses are well represented at this mine. The A1 assemblage accounted for most of the Pb and Cu ores, in association with a variety of other primary minerals including pyrite, millerite, cobalt pentlandite, electrum (AuAg) and tucekite

($Ni_9Sb_2S_8$) (Bevins *et al.*, 2010). A late A1 phase of ferroan dolomite influx is well represented on the spoil tips. A2 mineralisation, although less abundant, comprises calcite, galena and sphalerite, together with later marcasite and pyrite. Secondary mineralisation shows spectacular development at Eaglebrook Mine, falling into two distinct genetic groups, namely a pre- and post-mining phase. The former is represented by species that include cerussite, pyromorphite and wulfenite, as well as a range of Cu-bearing minerals such as malachite, chalcocite (Cu_2S), covellite (CuS) and cuprite (Cu_2O). Post-mining mineralisation also includes Cu-bearing species such as linarite, serpierite ($Ca(CuZn)_4(SO_4)_2(OH)_6.3H_2O$), brochantite ($Cu_4(SO_4)(OH)_6$), and langite ($Cu_4(SO_4)(OH)_6.2H_2O$) (Bevins *et al*., 2010).

At the present-day, little remains of the former mining infrastructure other than the 40 ft wheelpit, four infilled shafts distributed on either side of the mountain road and a recently excavated cut-and-cover adit. A large volume of unvegetated tailings is located below the wheelpit (Plate 3.9), and it was in this area, adjacent to the adit, at grid reference SN 73519 89255, that a 5 kg sample was collected for geochemical analysis.

Plate 3.9 Eaglebrook Mine, looking east, showing an extensive area of tailings beyond the wheelpit.

3.3. Geochemical analysis of samples of mine tailings

3.3.1 Sample preparation

The 5 kg samples of tailings collected from the six mines described in Section 3.2 were spread onto separate polythene sheets and dried in the FSC facility at IBERS for approximately four weeks. Each sample was then sieved through a 5 mm gardeners' mesh and 500 g sub-samples were extracted and placed into minigrip bags to await digestion and analysis at DGES.

Following labelling of all glassware, a 5 g sample of each 500 g sub-sample was weighed to 4 decimal places and placed in a 100 ml conical flask. A 50 ml quantity of 50% HNO_3 was added using a measuring cylinder, and each conical flask was covered and placed overnight on a hotplate at 60 ^oC and then allowed to cool for 24 hours. The samples were then filtered through 150 mm diameter Whatman No. 1 filter paper into 250 ml volumetric flasks. Each conical flask was rinsed 10 times with MQ ultradistilled water to ensure that all the sample was washed through the filter and into the volumetric flask. Finally, each sample was stored in a 125 ml low density polythene (LDPE) sample bottle with screw lid, pre-contaminated with the sample, to await analysis.

3.3.2 Sample analysis

Each sample was analysed for Zn, Pb, Cu and Cd in the DGES laboratory using a Perkin Elmer Analyst 400 atomic absorption spectrophotometer (AAS). The standard in-house start-up, analysis and shut down protocols were adopted. Each sample was replicated three times, blanks were included and standards for the relevant element were run before, during and at the end of each analytical run.

3.3.3 Analytical results and mine selection

The results obtained through AAS analysis of the six mine spoil samples are presented in Table 3.1 and the data for each element are the mean of three replicate samples.

Table 3.1 *Concentrations of metals, presented as parts per million (ppm), and inter-element ratios obtained through AAS analysis of mine tailing samples.*

MINE	Zn	Pb	Cu	Cd	Zn/Pb	Pb/Zn	Zn/Cu	Pb/Cu
Darren	57	16916	32	0	0.0034	296.78	1.78	528.62
Bwlchglas	1907	12938	35	5	0.15	6.78	54.49	369.66
Cwmystwyth	20554	7323	208	44	2.81	0.36	98.82	35.21
Esgairfraith	896	6783	176	2	0.13	7.57	5.09	38.54
Eaglebrook	16753	38817	4101	24	0.43	2.32	4.08	9.47
Castell	29676	95	158	33	312.38	0.0032	187.82	0.60

It is clear from these analytical data that Castell Mine, displaying very high absolute concentrations of Zn and very high Zn/Pb and Zn/Cu ratios, would provide a suitable source of Zn-rich tailings for the first pot experiment. Similarly, Darren Mine, displaying very high absolute concentrations of Pb and very high Pb/Zn and Pb/Cu ratios, would provide a suitable source of Pb-rich tailings for the second pot experiment. Indeed, both mines display closely comparable ratios of Zn/Pb and Pb/Zn, respectively, in the order of $3x10^2$. The remaining four mines, although containing relatively high concentrations of either Pb or Zn and, in the case of Eaglebrook Mine, relatively high concentrations of Cu, were rejected as a potential source of pot experiment growth medium on the grounds that inter-element ratios were unsatisfactory relative to those obtained from the Castell and Darren tailings samples.

3.4 Mine tailings sampling and analysis

The Zn (Experiment 1) and Pb (Experiment 2) pot experiments were carried out in consecutive years over the summer months of 2009 and 2010 and the methodologies were identical for both. With relevant landowner permissions, the initial phase entailed the collection of approximately 150 kg of fine-grained tailings from Castell and Darren mines.

The tailings were sieved through a 5 mm gardeners' mesh and the finer fraction reserved and spread across polythene sheets to dry thoroughly at the FSC facility at IBERS. Once dry, the tailings were transferred outside and spread upon a large polythene sheet where they were mixed to ensure homogeneity. The tailings were mixed for approximately 20 minutes with a large shovel, whilst wearing safety clothing and a mask, as for mixing sand and cement (Plate 3.10). The tailings were then transferred into 10 kg polythene bags for storage.

Plate 3.10 Hand-mixing the tailings.

Four sub-samples of the tailings were taken for analysis at DGES to assess sample homogeneity. The samples were digested following the same method described in Section 3.3.1 and analysed by AAS. The results are displayed in Table 3.2 and confirmed the suitability of these two tailings for the proposed experiments, in terms both of concentrations and Zn/Pb ratios.

Table 3.2 *Concentrations of Pb and Zn (ppm) in tailings used for the pot experiments*

CASTELL MINE		**DARREN MINE**	
Zn	**Pb**	**Zn**	**Pb**
29604.83	71.88	54.48	17490.10
30630.06	69.43	47.88	18939.87
31768.86	63.48	62.17	21605.92
30205.38	51.74	61.69	17628.08
Average	Average	Average	Average
30552.28	64.13	56.56	18915.99
Standard deviation	Standard deviation	Standard deviation	Standard deviation
913.62	8.99	6.77	1908.59
% Error	% Error	% Error	% Error
2.99	14.01	11.96	10.08

3.5 Sand as the main rooting medium

Sand is considered the ideal rooting medium for use in any experimental work in artificial culture (Hewitt, 1966). It is preferred to other forms of rooting medium, for example vermiculite, perlite or clay granules, both for its purity and for the ease with which the roots can be washed out prior to subsequent analyses.

The sand component of the growing medium used in this study was recommended by the company Construction Materials Ltd (CML, pers comm.), who are leading suppliers to the turfgrass industry, as it is of uniform grain size, is pre-washed and therefore clean and dust-free and is widely used as a top dressing on sports pitches as it promotes good rooting. Analysis of the physico-chemical properties of the sand CML LB40 is shown below in Table 3.3.

Table 3.3 *Physico-chemical properties of the sand component of the growth medium. Note that the condition of the sand at the time of purchase was moist and loose, but bagged.*

Typical Analysis

Particle Size Distribution

Category	Diameter (mm)	% retained	% passing
Fine gravel	4.0 – 2.0	0.0	100.0
Very Coarse Sand	2.0 – 1.0	1.4	98.6
Coarse Sand	1.0 – 0.5	15.9	82.7
Medium Sand	0.5 – 0.25	63.9	18.8
Fine Sand	0.25 – 0.15	17.6	1.2
Very Fine sand	0.15 – 0.053	1.2	0.0
Silt and Clay	< 0.053	0.0	0.0

Physical Properties

Particle density (g/cm^3)	2.65
Colour	White/Pale Yellow
pH (1:1 water)	7.4

Particle Shape

Angularity	Sub-rounded
Sphericity	Medium

3.6 Pot preparation

A total of 480 15 cm diameter pots and saucers was required for each pot experiment. Each pot base was lined with a 13 cm diameter circle of 'ground cover mesh'. The latter comprises a black plastic woven sheet, which was known to be suitable for this pot experiment as the material had already been tested for drainage characteristics and the prevention of sand loss in previous studies with plants grown in sandboxes. Each pot was weighed during the filling process to ensure that exactly the same amounts of growing media were used across all treatments.

Following 'ground proofing' trials at IBERS using different spoil mixtures, and also based on methodologies applied in two M.Sc. theses (Macro, 2005; Warrender, 2005), three treatment levels of tailings were imposed in each experiment: zero (control), 10% and 30% mixes by weight of tailings/sand. Higher levels of tailings application were not used as it was anticipated they would exert an immediately toxic effect on the plants.

A total of 160 pots were filled with 2 kg of LB40 CML sand as the control treatment, 160 pots were filled with 200 g tailings and 1800 g sand, which had been mixed thoroughly by tumbling in a large vessel, to provide a 10% by weight substrate of tailings, and finally 160 pots were filled with 600 g tailings and 1400 g sand, mixed thoroughly, to provide a 30% by weight substrate of tailings. Once weighed, each pot was watered to field capacity with 500 ml tap water and then a further 500 ml tap water was flushed through to remove any fines present. All pots were then moved from the laboratory to an outside standing area in readiness for planting with mapping population genotypes.

3.7 Background to the *L. perenne* mapping family

The plant material used in the two pot experiments consisted of a back-cross mapping family derived from an initial cross between contrasting amenity-type and forage-type genotypes of *L. perenne*. The amenity-type parent was selected from the cultivar AberSprite (accession number Ba11972), characterised by low shoot height, high shoot density, small leaves and a low relative growth rate. In contrast, the forage-type parent was selected from a wild ecotype collected from Cardigan Island (accession number Ba12142), characterised by low tiller number, large tall leaves and a high relative growth rate.

From this original cross, a single F_1 plant was crossed to an AberSprite plant related to, but not the same as, the original AberSprite parent to produce the mapping family used in this study. The mapping population is therefore a backcross-type in that one of the F_1 plants was backcrossed to an individual plant genetically related to, and with similar characteristics to, the original AberSprite parent. The population can be defined as a Common Pedigree (CP) cross where the two parent plants are heterogeneously heterozygous and homozygous. The population consisted of 80 genotypes chosen at random for inclusion in this study so that the full range of morphological variation was incorporated and parallel experiments in FSC could be feasibly managed.

This mapping family has been used extensively in DEFRA-funded studies of 'Enhanced Environmental Quality' (EEQ) traits at IBERS (Section 2.5.2). These studies have included investigations into carbon sequestration in soil, aspects of soil microbial diversity, bioremediation of HMs, buffer zone removal of nitrate and potential for flood mitigation. In this regard, the mapping family is very well documented for its phenotype and genotype and was therefore deemed the best choice for the present research project. Another important advantage of this family was the wide range of growth and morphological phenotypes (amenity and forage types), some of which might display enhanced performance with respect to survival on HM-contaminated mine tailings. A fully replicated set of the mapping family genotypes was maintained throughout the project in pots containing potting compost and renewed and renovated biannually. The plants were watered daily, fed every other week and cut back every month.

Plate 3.11 Mother plants maintained in greenhouse.

3.8 Preparation of plant material

Tillers were taken from a set of mother plants of the amenity x forage mapping family (Section 3.7) growing in 1 m sward sand trays. These plants were used, rather than the mother plant set maintained in potting compost, as they were already acclimatised to sand and therefore pre-conditioned to the sand component of the growth medium chosen for the pot experiments.

A total of 40 tillers per genotype were washed out of the sand substrate, their roots cut to 1 cm and shoots to 10 cm to give uniformity at the start of the experiment. These were stored in tap water overnight prior to sowing up (Plate 3.12).

Plate 3.12 Tillers stored in tap water prior to sowing.

Each pot was sown with 5 tillers, with fresh weights recorded prior to sowing (Plate 3.13).

Plate 3.13 The sowing-up procedure.

Tillers from 80 genotypes were transplanted into pots, with two replicates per treatment and three treatments in each experiment. The procedure took two days to complete, in the following order: 80 x 2 replicate control pots, 80 x 2 replicate 10% tailings pots and 80 x 2 replicates 30% tailings pots (Plate 3.14).

Plate 3.14 The completed set of pots on an irrigated standing area.

3.9 Fertiliser application rate

The rate of fertiliser application in the two pot experiments was based on sand box grass sward experiments previously conducted for DEFRA (LS3648) at IBERS. The optimum rate was 100 kg N/ha of soluble fertiliser Phostrogen ® 14-10-27 (N-P-K% plus trace elements).

The calculations for the required fertiliser application rate are detailed below.

Each pot used was 6″ in diameter which ~ 15cm.

∴ surface area of pot $A = \pi r^2$ = $\pi.7.5^2$ = 176.7cm^2

100 kg N/ha = 10 g N/m^2

∴ per pot require $\frac{177}{10{,}000}$ x 10 = 0.177 g N

∴ for 14-10-27 fertiliser require *x* g fertiliser per pot

N = 14% ∴ $\frac{14}{100} = \frac{0.177}{x}$

$$\therefore \quad x = \frac{0.177 \times 100}{14} = \frac{17.7}{14} = 1.264 \text{ g Phostrogen ® per pot}$$

Each pot was given 1.264 g fertiliser each week using a calibrated scoop and the plants were watered twice daily by an automatic irrigation system.

3.10 Experiment design

The two pot experiments were carried out in 2009 and 2010 and each ran from June until the end of September. It was critical for the experiments to run at the same time of year to ensure the plants would be at the same growth and vegetative state; plants at different stages of floral development may have resulted in different behavioural responses. The design for each experiment was identical.

Eighty mapping family genotypes were grown over a 16 week period in pots containing three different tailings/sand ratios (0, 10% and 30% tailings by weight). Duplicate pots containing 5 tillers of each genotype per tailings treatment were grown outside on an irrigated standing area and fertiliser was applied as detailed in Section 3.9. There was no variation across the standing area with respect to aspect, shading or watering. Consequently, rearrangement of blocks and internal randomisation of pots within blocks was not performed during the experiments.

Eight weeks after transplanting into the treatment pots, the shoots were cut back to 2 cm height and fresh weights of the clippings recorded (Plate 3.15). The clippings were then freeze dried, dry weights recorded and milled for analysis to 2 mm with a Glen Creston ® mill (model number DFH48). After a further 8 weeks, all plants were destructively harvested over a period of 5 days. The number of plants per pot surviving from the original 5 tillers was recorded, as were tiller numbers per pot. The shoot and root fractions were separated and the roots thoroughly washed to remove as much of the growth medium as possible. Fresh weights were recorded and the samples freeze dried prior to measuring dry weights and subsequent milling with a Glen Creston ® mill through a 2 mm mesh.

Plate 3.15 Control plants following the 8 week cut.

Following final harvest and freeze drying of the roots in Zn Experiment 1, it was noted that some of the growth medium was still adhering as particles to the sample. In order to remove these contaminants, prior to digestion, each sample was blown through a gradient tube to separate the lighter sample from the heavier contaminant material. This method utilised a plastic tube, 30 cm long and with a diameter of 2 cm, inclined at 30º to the horizontal. Samples were introduced *via* a vertical tube, connected to the inclined tube approximately 10 cm from its base, whilst a gentle, but steady stream of compressed air was pumped into the tube. The effect was to blow the lighter root sample to the end of the tube, while any heavier, high density growth medium accumulated at the base of the tube. It was found that only a small fraction (< 1%) of root material was lost during the process. To avoid requiring this method in Pb Experiment 2, growth medium adhering to the root sample after freeze drying was removed prior to milling by rubbing the sample between two pieces of corrugated rubber, a process known in-house as 'rubbling' (Macduff, pers comm.). All ground samples were stored in sealed mini-grip bags prior to analysis. Cut 1 produced 480 shoot samples, and the final harvest produced a further 480 shoot samples and 480 root samples for each experiment (assuming a 100% rate of survival), giving an anticipated total of 2,880 samples for both experiments.

3.11 Preparation of in-house reference materials

Due to the large number of samples requiring analysis and the expensive nature of certified reference materials, two 'in-house' reference samples were created and characterised, from: a) contaminated samples from the first pot experiment; and b) a large field sample of grass harvested from contaminated land, as follows:

a) From each of the 10% and 30% shoot samples from the final harvest ~ 0.5 – 1 g was removed and combined together to create a 'pot standard'. This bulk sample was milled with a Glen Creston ® mill through a 0.5 mm mesh to ensure homogeneity.
b) Approximately 3 kg of grasses were collected from Castell Mine at grid reference SN 77289 81366. These were identified as a mixture of tussock grass (*Deschampsia cespitosa*), cotton grass (*Eriophorum*) and red fescue (*Festuca rubra*) (Thorogood, pers comm.). This bulk field sample was freeze dried and milled with a Glen Creston ® mill, initially to 1 mm and then re-milled to 0.5 mm, to ensure homogeneity.

These in-house standards were digested and analysed by AAS to check for homogeneity and the results are shown in Table 3.4.

Table 3.4 *Zn and Pb concentrations (ppm) in reference materials created*.

Reference material	Zn	Pb
Pot reference material A	2119.5	135.0
	2171.0	141.0
	2218.9	137.0
	2095.2	132.0
	2175.3	129.0
Average	2156.0	134.8
Standard deviation	48.9	4.6
% Error	2.26	3.4
Field reference material B	659.6	Not detected
	665.3	
	658.9	
	673.0	
	661.2	
Average	663.6	
Standard deviation	5.8	
% Error	0.87	

3.12 Development of analytical protocols

Given the anticipated large number of samples (~ 2,880) generated across the two pot experiments, it was necessary to use a digestion method allowing firstly, large numbers of samples to be digested in a single batch, and secondly, providing a reliable, accurate and repeatable method of recovery in order to assess variation between the samples; the exact concentration was not important, providing the results were internally consistent and repeatable. Established methods for plant digestion are often very lengthy and it is generally possible to digest only a few samples at a time. For example, procedures using the IBERS standard method and the DGES standard method described below, whereby samples are digested in batches of ~ 20, can take up to a week. Therefore, a number of different methods were evaluated in the laboratory, together with several modifications to protocols (Test Methods 1 – 9) aimed at optimising the procedure for the current project. In each case, four replicate field standards, four replicate pot standards and one IAEA Reference Material V-10 Hay were digested and analysed. Blanks were also included. Analar grade reagents were used throughout the analyses. The following procedures were compared:

IBERS standard method for determination of trace elements in plant material

- Weigh 0.5 g plant material into an acid washed beaker
- Place beakers in a muffle furnace and ash at 450ºC overnight
- Once cool, slowly add 10 ml 25% HCl
- Filter the solutions through Whatman No. 1 filter paper into 50 ml volumetric flasks, washing out the beaker and rinsing the filter paper twice
- Allow to filter completely and make up to volume with MQ ultradistilled water

DGES standard wet oxidation method

- Weigh 0.5 g sample into a 100 ml conical flask
- Add 5 ml MQ water
- Add 50 ml 50% HNO_3 swirl, cover with a watchglass and leave cold overnight
- Place on a hotplate at 60ºC and reflux overnight
- Increase heat to 110ºC and reflux through the day
- Remove from heat, cool and add 5 ml concentrated HNO_3
- Replace on hotplate at 110ºC and reflux overnight
- Cool, then add 1 ml of 30% w/v H_2O_2

- Wait for 1 hr then replace on hotplate at 150ºC
- When samples stop effervescing, the digestion is complete
- Remove from heat and cool
- Filter sample through Whatman No.1 filter paper into a 200 ml volumetric flask
- Store in pre-contaminated 125 ml plastic bottles

Test Method 1

- Weigh 0.5 g sample into 40 ml boiling tubes
- Add 5 ml 10% HNO_3 and Whirlimix for ~ 5 seconds
- Leave cold for 1 hr
- Place in a digestion block on a hotplate and gradually heat to 50ºC and leave overnight
- Some loss was observed overnight and so it was decided to evaporate to dryness, then scrape material from sides with glass rod and wash to base with MQ water
- Place on a digestion block on a hotplate and heat at 80ºC for ~ 3 hrs
- Add 5 ml concentrated HNO_3 and leave cold overnight
- Place on a digestion block and evaporate to dryness then make up to 20 ml with 5% HNO_3
- Pipette out 2 ml sample into small test tube and make up to 10 ml with MQ water for analysis (x5 dilution)

Test Method 2

- Weigh 0.5 g sample into 40 ml boiling tubes
- Add 2 ml concentrated HNO_3 and Whirlimix for ~ 5 seconds
- Leave cold for 1 hr then add 2 ml MQ water
- Place in a digestion block on a hotplate at 55ºC for 2 hrs
- Remove from hotplate and make up to 10 ml by adding 6 ml MQ water
- Whirlimix and allow to settle

Test Method 3

- Follow procedure exactly as for Test Method 1 but substitute HNO_3 with HCl in all relevant steps

Test Method 4

- Follow procedure exactly as for Test Method 2 but substitute HNO_3 with HCl in all relevant steps

Test Method 5

- Weigh 0.5 g sample into 40 ml boiling tubes
- Add 4 ml 50% HNO_3 and leave cold for 1 hr
- Place in a digestion block on hotplate set at 55ºC for 2 hrs
- Remove from hotplate and make up to 10 ml by adding 6 ml MQ water.
- Whirlimix for ~ 10 seconds
- Cover with film and allow to settle overnight
- Spin down half of the samples in a centrifuge and decant off the resulting clear liquid for analysis

Test Method 6

- Follow procedure exactly as for Test Method 5 but substitute HNO_3 with HCl in all relevant steps

Test Method 7

- Weigh 0.25 g sample into 40 ml boiling tubes
- Add 10 ml 10% HNO_3 and swirl by hand (a Whirlimixer is too vigorous at this volume). Add a further 10 ml to wash the residue from the sides to the base of the tube
- Place in a digestion block on a hotplate at 55ºC overnight
- Increase heat to 95ºC and evaporate until ~ 1 ml solution left
- Remove from hotplate and cool
- Scrape the tube sides with a glass rod and wash down with 5 ml concentrated HNO_3
- Return to hotplate at 80ºC overnight until dry
- Add 20 ml 5% HNO_3 and pipette out 2 ml sample into small test tube and make up to 10 ml with MQ water for analysis (x5 dilution)

Test Method 8

- Weigh 0.25 g sample into 40 ml boiling tubes
- Add 10 ml 50% HNO_3 and swirl by hand, then a further 10 ml to wash the residue from the sides to the base of the tube
- Leave cold overnight covered in film
- Place in a digestion block on a hotplate at 55ºC and gradually increase heat through the day to 80ºC overnight and evaporate to dryness
- Add 20 ml 50% HNO_3
- Pipette out 2 ml sample into small test tube and make up to 10 ml with MQ water for analysis (x5 dilution)

Test Method 9 (adapted from Husted *et al*., 2004)

- Weigh 0.25 g sample into 40 ml boiling tubes
- Add 5 ml 50% HNO_3 and swirl gently to mix
- Place in a digestion block on a hotplate at ~ 180 – 190ºC and boil vigorously for 10 minutes (Plate 3.16)

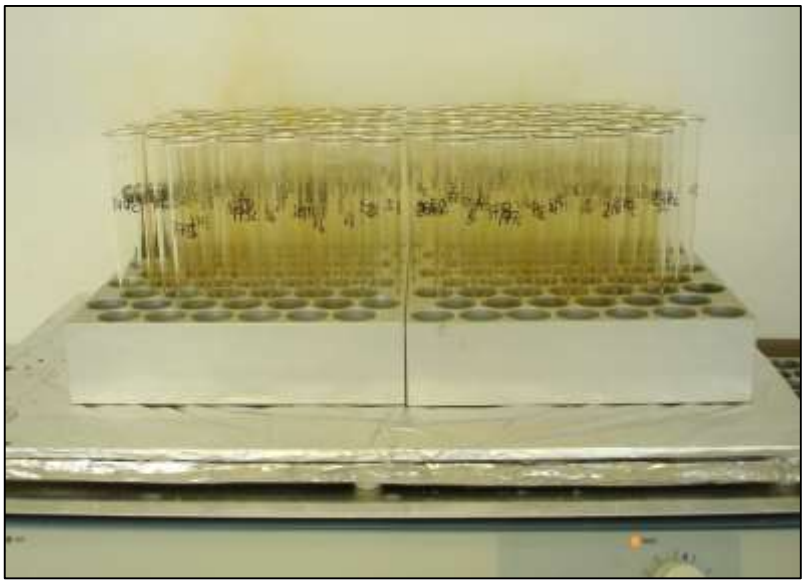

Plate 3.16 Initial heating phase on digestion block. Note the liberation of a brown nitrous oxide vapour.

- Remove from hotplate and cool for 5 minutes
- Add 2.5 ml concentrated HNO_3
- Return to hotplate at 100ºC, cover with cling (pierce above each tube with a small hole to allow some fumes to escape) and reflux for 1 hr (Plates 3.17 and 3.18)

Plate 3.17 Second heating and reflux phase on digestion block.

Plate 3.18 Piercing of film cover to allow venting but no cross-contamination.

- Remove from hotplate and cool
- Make up to 40 ml with MQ water
- Cover each tube and invert to mix thoroughly
- Leave to settle overnight prior to analysis

Results of method comparisons

Both the IBERS and the DGES methods gave clean digestions and satisfactory results in terms of accuracy and repeatability, although the IBERS method gave lower recoveries compared with the DGES method (possibly due to the ashing phase, as Zn is fairly volatile and the low recovery could be thus explained). However, both these methods were regarded as unsuitable for the project due to the length of time required to complete the digestion and the low number of samples (20 – 40) that could be digested at one time over a matter of several days.

All the methods using HCl (Test Methods 2, 4, 5 and 6) were rejected due to the presence of a black viscous deposit in the samples making them too impure for AAS analysis. In addition, methods involving whirlimixing or centrifugation (Test Methods 1 – 6) were also rejected on the grounds of time requirements and limited sample number throughput.

Table 3.5 *Analytical results of the test method trials (IAEA V-10 certified value Zn = 24ppm)*

METHOD	**Zn (ppm)**		
	Pot standard A	**Field standard B**	**IAEA V-10 hay**
IBERS Method	1638.50	472.90	17.86
	1420.40	460.80	
	1483.40	465.80	
	1650.40	442.40	
Average	1548.18	460.48	
Standard deviation	114.21	13.03	
% Error	7.38	2.83	
DGES Method	2099.29	598.19	22.8
	2215.08	605.70	
	2098.59	599.80	
	2110.80	598.07	
Average	2130.94	600.44	
Standard deviation	56.37	3.59	
% Error	2.65	0.60	
Test Method 1	1895.60	685.23	20.14
	1811.60	695.88	
	2193.50	684.62	
	1744.20	677.76	
Average	1911.23	685.87	
Standard deviation	198.11	7.48	
% Error	10.37	1.09	
Test Method 2	not analysed	not analysed	not analysed

Table 3.5 *Continued*

Test Method 3	1432.00	602.37	19.5
	1707.99	661.37	
	1608.65	591.84	
	2059.11	608.82	
Average	1701.94	616.10	
Standard deviation	264.06	30.98	
% Error	15.52	5.03	
Test Method 4	not analysed	not analysed	not analysed
Test Method 5	not analysed	not analysed	not analysed
Test Method 6	not analysed	not analysed	not analysed
Test Method 7	1719.62	633.35	15.49
	1616.77	716.85	
	1529.84	629.98	
	1470.24	636.76	
Average	1584.12	654.24	
Standard deviation	108.54	41.84	
% Error	6.85	6.39	
Test Method 8	1418.97	524.09	14.38
	1288.00	635.12	
	1502.20	571.20	
	1767.05	614.34	
Average	1494.06	586.19	
Standard deviation	202.23	49.22	
% Error	13.54	8.40	
Test Method 9	2133.55	652.35	23.5
	2205.08	637.70	
	2144.78	647.32	
	2110.89	631.24	
Average	2148.58	642.15	
Standard deviation	40.22	9.48	
% Error	1.87	1.48	

The method selected for routine use in the project was Test Method 9. This method was adapted from Husted *et al*. (2004) with modifications to minimise both digestion and dilution steps.

Method from Husted *et al.* (2004)

- Weigh 0.25 g sample into 70 ml boiling tubes
- Add 5 ml 35% HNO_3
- Place uncovered on a digestion block at 95°C for 15 minutes
- Cool then add 2.5 ml 70% HNO_3
- Place uncovered on digestion block for 25 minutes
- Cool, then add 1.5 ml H_2O_2
- Wait for peroxide reaction to cease then add a further 1 ml H_2O_2
- Cover and place on a digestion block for 40 minutes
- Cool samples overnight then dilute to 50 ml with ultra-pure water

The method described by Husted *et al*. (2004) involved digesting samples in batches of up to 50 at one time. Test Method 9, described above, was based similarly on a rapid HNO_3 digest, firstly uncovered and then with a second and longer covered reflux phase. It was decided to trial the method without the intermediate H_2O_2 step and determine if the recovery was good enough to proceed without these steps in order to minimise digestion time.

With this method it was possible to digest up to 160 samples in one day and to produce clean samples for analysis. Furthermore, when sample volumes were made up to 40 ml, the dilution was such that it was usually possible to analyse the sample directly from the boiling tube; no further dilution steps were required for the sample to be within the analytical range of the instrument. A two tailed t-test comparison between the results of the DGES Standard Method and Test Method 9 showed no significant difference. Subsequently, Test Method 9 has become a standard procedure in the DGES laboratory for the rapid, multi-sample digestion of plant material.

3.13 Analysis of plant material

All samples generated from the two pot experiments were digested using Test Method 9 described above. Samples were digested in batches of eighty, which included two replicate samples to check repeatability, four replicate reference materials and four blanks per run. It was possible to digest two batches of eighty per day.

Each sample was then analysed by AAS. Within each analytical run, standards were included at the beginning, after every twenty samples and at the end, in order to check the calibration of the instrument and to confirm the absence of drift.

3.14 Bioavailable HM and nitrate concentrations in the tailings

Tailings collected from Castell Mine and Darren Mine were tested for Zn and Pb bioavailability using the standard DGES, single-extraction, acetic acid digestion method (Swain *et al*., 2005). A 50 ml volume of 5% acetic acid was used to extract the available metals from ~ 2 g of tailings. The acid was added to the tailings in an extraction bottle with a screw cap. The bottles were then clamped tightly into a reciprocating shaker and shaken for 30 minutes. The contents were then filtered using Whatman No. 1 filter papers. The first 10 drops passing through the filter paper were discarded, whilst the remaining filtered volume was stored for analysis by AAS. The results of the analyses are displayed in Table 3.6.

Table 3.6 *Concentrations of bioavailable Zn and Pb, from Castell and Darren mines, presented as parts per million (ppm), obtained through AAS analysis of tailing samples.*

Mine	Zn	Pb
Castell	19572	Not detected
	19539	Not detected
	17919	Not detected
	18574	Not detected
Average	**18901**	-
Standard deviation	**801**	-
Darren	7.62	4124
	7.03	3977
	8.07	4495
	10.44	5201
Average	**8.29**	**4449**
Standard deviation	**1.49**	**546.2**

The analytical data indicate a significant difference in bioavailability index (B_I), that is, the ratio between the bioavailable metal concentration and absolute metal concentration in the Zn- and Pb-rich tailings. With an absolute bioavailability ($^{Zn}B_A$) of 18,901 µg g^{-1}, the $^{Zn}B_I$ for Castell Mine tailings is ~ 0.619, whereas, with a $^{Pb}B_A$ of only 4,449 µg g^{-1} for the Darren Mine tailings, the $^{Pb}B_I$ is ~ 0.235. This represents a significant bioavailability differential ($^{Zn}B_A : {}^{Zn}B_A$) of ~ 2.63. It should also be noted that episodes of heavy rainfall followed by periods of high temperatures will greatly increase the bioavailability (Westgate, 2000).

In addition to testing for HMs, the samples from the bioavailability extraction from Castell Mine and Darren Mine were also analysed for possible nitrate contamination. This analysis was undertaken because both mines are located on farmland that is actively used for stock grazing (sheep and cattle). Merckoquant^{TM} NO_3^- colorimetric test strips (product number 110020) were immersed in each sample for 1 second. The excess liquid was then shaken off the strip, and

after 1 minute the colour was determined by comparison with the standard colour field provided. In all samples the levels of NO_3^- were below detection.

3.15 Background to QTL methodology

The use of molecular markers to construct genetic maps and the application of quantitative trait loci (QTL) analysis to establish genetic architecture and identify potential trait-controlling candidate genes has previously been introduced in Section 2.4.2. Specific reference was made to ongoing research to generate increasingly marker-saturated genetic framework maps for *L. perenne* based, for example, on the recent augmentation of existing genetic maps with DArT markers (King *et al*., 2013) and array-based SNP genotyping (Blackmore *et al*., 2015).

The genetic framework map utilised in this study is based on the publicly available custom Illumina Infinium SNP genotyping array for *L. perenne*. The construction of the microarray, as described by Blackmore *et al*. (2015), was based on the sequencing of 5 diverse genotypes of *L. perenne*, namely an IBERS synthetic forage variety known as AberMagic, a Chromosome 3 substitution line with *Festuca pratensis*, a mother plant from IBERS' late-heading recurrent breeding population, a 'stay-green' amenity variety and an early-flowering ecotypic sample from France. Across the five genotypes, a total of 53,149 putative single nucleotide polymorphisms (SNPs) were identified, within 11,892 unique contigs (i.e. series of overlapping DNA sequences used to make a physical map that reconstructs the original DNA sequence of a chromosome or a region of a chromosome). Subsequent validation steps reduced the final marker set to 2,185 SNPs, spanning 1,606 unique contigs.

In order to generate a robust consensus linkage map, Blackmore *et al*. (2016) described the genotyping of *L. perenne* cultivars (n = 249), ecotypes (n = 716) and three of IBERS' mapping populations (n = 450), including the forage x amenity population used in this research project, utilising the custom Illumina Infinium array across 3,425 SNPs. Following the application of various exclusion parameters, a final validated set of 2,199 SNPs, spanning 1,615 contigs, was used for analysis, of which a total of 1,161 SNPs were derived from the amenity x forage mapping family used in this research project. LOD thresholds of between 5.0 and 8.0 were able to separate seven distinctive groups representing the seven chromosomes of *L. perenne*. Map order was determined by applying a weighted least squares linear regression using marker linkages with a recombination frequency of 0.4 and a LOD threshold of 1.0. Map distances were calculated from recombination frequencies using Haldane's mapping function. From the

genotyping of the three mapping populations, linkage maps were generated using JoinMap v4.0 (Figure 3.3).

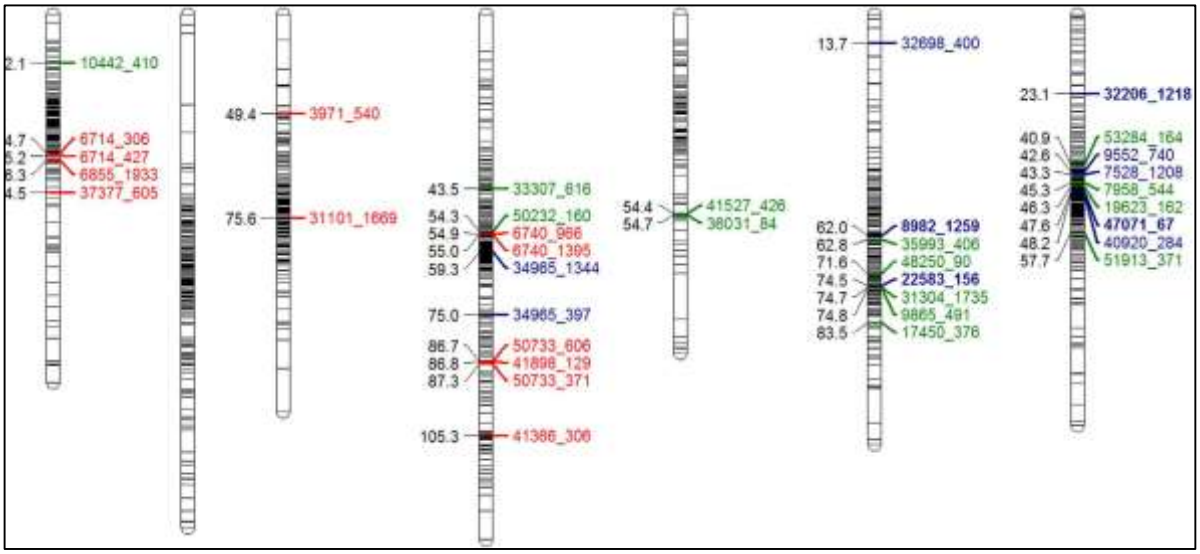

Figure 3.3 Consensus *L. perenne* genetic linkage map, constructed from 3 mapping populations, including the amenity x forage mapping family used in this research project, showing 1,386 of the 2,199 validated SNP markers (from Blackmore *et al*., 2015).

One of the primary objectives of this research project was to identify QTL arising from the trait data derived from the *L. perenne* mapping family, in particular those specifically associated with growth and HM uptake, and to identify, where possible, potential underlying genes and any evidence of polygeny (i.e. where multiple genes contribute to a particular phenotypic characteristic) or pleiotropy (i.e. where a single gene affects one or more phenotypic characteristics).

In order to achieve this objective, the harvest data (Appendices 1 and 2) and analytical data for the control, 10% and 30% metal treatments for each of the two experiments were collated into 45 individual traits (Appendices 3 and 4). It should be noted, however, that some traits were derivative (e.g. final harvest tiller numbers per plant, final harvest tiller numbers per m^2) and that therefore not all detected QTL and their associated traits are shown on the linkage maps presented hereafter. In order to identify any QTL, the trait data were assessed in MapQTL v.5 (Van Ooijen, 2004) in a 3-step process using three statistical parameters. Firstly, the Kruskal-Wallis test statistic (K*) was applied, whereby the data for each individual trait were sorted and ranked according to the number of associated K*. All K* of ≥ K***** were classified as 'significant' and their map positions and contigs were recorded. In the second step, the traits were assessed *via* interval mapping, whereby a 'QTL likelihood map' is calculated, and the

likelihood ratio statistic, or LOD score, was generated for each map position. The resultant dataset was very large and, in order to match and combine the data from step 1 with those of step 2, a computer algorithm was provided by IBERS' Phenomics Centre (A. Gay pers comm.). In the final step, the MapQTL permutation test relative cumulative count generated a LOD threshold score for each trait, and the LOD threshold score must be less than the peak LOD score from step 2 in order for the trait in question to remain 'significant'. The relative cumulative count number and associated threshold score taken was the first above 0.95, and individual thresholds for each LG were used throughout.

3.16 Screening methodology for HM metal tolerance in FSC

The FSC system at IBERS was described in Section 2.5. As part of the DEFRA project, it was intended to identify QTL in *L. perenne* for 'physiological' tolerance to Zn and Pb. Two screening experiments (Experiments 1:23:64 and 1:23:66) were performed in the FSC system, whilst incorporating automatic control of the concentrations of NO_3^-, NH_4^+, K^+ and H^+ in solution (Clement *et al*., 1974; Hatch *et al*., 1986). These experiments screened 96 genotypes from the amenity x forage *L. perenne* mapping family, including the 77 genotypes used in the current project. The chronology common to both screening experiments consisted of an establishment period of 40 days followed by a screening period of 28 days. In the absence of unequivocal evidence from the literature regarding critical concentrations of heavy metal ions in FSC eliciting toxicity in *L. perenne* (e.g. Qu *et al.*, 2003), preliminary trials were conducted to determine appropriate supra-optimal concentrations of Zn and toxic concentrations of Pb for the main screening experiments. These trials compared the growth and metal tolerance of six contrasting genotypes to the same parameters under optimal conditions. Plants were grown in FSC using customised 'mini-culture units' (Soussana *et al.,* 2002), and exposed to three or four different concentrations of the metal in question over 43 days prior to harvesting. Initial concentrations trialled were as follows: zero, 0.15, 1.5 and 15 μM Zn, and zero, 10, 100 μM Pb. The results informed the concentrations of Zn and Pb used in the main screens. The methodology for these is described in detail in the following sections, as the approach differed significantly from that taken in the pot experiments performed in the current project.

Main screen plant establishment and culture

For each of the two screening experiments in FSC, 12 tillers, visually uniform in size, were removed from each of the 96 genotypes belonging to a set of 'mother plants' maintained in FSC. The tillers were trimmed to a standard shoot length of 10 cm and root length of 2 cm, then

divided into two similar groups of 6 tillers on the basis of fresh weight. Each tiller group was transplanted into one of 24 culture vessels within each of the 8 plant culture units containing 200 dm^3 of re-circulating nutrient solution. The design of the culture vessels enabled measurement of shoot attributes on individual plants, but only root measurement per vessel (i.e. bulked across the six plants) because of the entanglement of the individual plant root systems within a given culture vessel.

The eight plant culture units were treated as two replicate blocks of four units, each block containing one culture vessel (i.e. six plants) of each genotype. The grouping of genotypes within each culture unit was common across the two blocks, although the position of each genotype within a given culture unit was random. The plants were grown on for 40 days prior to a screening period which lasted 28 days.

The initial composition of the nutrient solution in each culture unit was (μM): NO_3^-, 250; K^+, 250; Ca^{2+}, 344; SO_4^{2-}, 424; Mg^{2+}, 100; $H_2PO_4^-$, 50; Fe^{2+}, 5.4, with appropriate micronutrients (Clement *et al.*, 1978), and solution pH 6.0 ± 0.5. All culture units were drained and refilled on day 35 of the establishment period with 300 dm^3 of nutrient solution of the same initial composition, except for NO_3^- (50 μM). Natural light was supplemented by a single 400W HPI-T lamp (Philips) suspended 1.5 m above the surface of each culture unit from day 10 onwards, producing 250 ± 50 μmol m^{-2} s^{-1} PAR at top of plant canopy over a 12 h photoperiod (0600 – 1800 h). From day 34 onwards, light was supplied solely by a 400 W HPI-T and 400 W SON-T (Philips) lamp suspended 1.5 m above the surface of each culture unit, producing 550 ± 50 μmol m^{-2} s^{-1} PAR at the top of the plant canopy. This lighting regime was maintained throughout the 28 day treatment period of the Pb screen (1:23:66), but natural lighting was used throughout the treatment period of the Zn screen (1:23:64), as this was performed during April and May. Air temperature was 20/15ºC (± 2ºC) day/night and solution temperature was 18–20ºC throughout both experiments.

Nutritional control during the screening period

From day 40 onwards, nutrient concentrations were controlled automatically with reference to the NO_3^- concentration in each culture unit. This was measured every 28 minutes (Orion Nitrate Electrode Mod. 93-07, Boston, USA) and a 'set-point' concentration of 50 ± 5 μM NO_3^- was maintained by automatic addition of $Ca(NO_3)_2$ stock solution (containing 15 mg N/g), together with all other nutrients, barring the HM under test, supplied in proportion. Solution pH 6.0 ± 0.1 was maintained by automatic titration of $Ca(OH)_2/H_2SO_4$. Net uptake of NO_3^- per culture unit (i.e.

24 genotypes) was recorded on a daily basis by the amount of NO_3^- required to maintain the set-point concentration. Experiment-specific conditions were as follows:

Experiment 1:23:64 (Zn toxicity): Four culture units received a 'high Zn' treatment in the form of 100 μM Zn (as $ZnSO_4.7H_2O$) at the start of the screening period. The remaining four units were designated 'controls' and received an initial 0.076 μM Zn (Plates 3.19A and 3.19B).

Plate 3.19 Genotypes of the *L. perenne* mapping family growing in FSC during the DEFRA-commissioned research project (LS3648). A) General view of the eight culture units in the glasshouse, and B) a pair of culture units with plants growing under control and supra-optimal Zn treatments. Note the difference in performance with regard to biomass production between control and supra-optimal Zn treatments, a feature not seen in the toxic Pb treatment.

Thereafter, additional Zn was supplied to both high Zn and control culture units as a component of a standard 'complete' nutrient stock-solution containing, amongst other nutrients, 15 mg NO_3-N g^{-1} and 15 μg Zn g^{-1}. This stock solution was supplied automatically to maintain the 'set point' concentration of 50 ± 5 μM NO_3^-. Hence, Zn was supplied according to the aggregate plant demand for NO_3^- within the unit. Analysis of Zn in culture solutions on day 21 by ICP-AES gave a mean of 76.6 μM Zn across the four 'high' Zn units, compared with 0.07 μM Zn across the control units.

Experiment 1:23:66 (Pb toxicity): Four culture units received a 'high' Pb treatment in the form of 25 μM Pb (as $Pb(NO_3)_2$) at the beginning of the screening period, equivalent to a total addition of 1.554 g Pb per culture unit. The remaining four units were designated 'controls' and contained zero Pb throughout the experiment. No further Pb was added to the high Pb units until day 15, when 1.037 g Pb (as $Pb(NO_3)_2$) was added to the 200 dm^3 of culture solution remaining in each unit, equivalent to a 25 μM increment in the concentration of Pb. Analysis of Pb in culture solutions on day 27 by ICP-AES gave a mean of 0.58 μM Pb across the four 'high' Pb units compared with 0.0074 μM Pb across the control units. This suggests that significant precipitation of added Pb had occurred, a view supported by the observation of a cloudy white precipitate dispersing from the surface of the roots of plants under the 'high' Pb treatment when agitated in the nutrient solutions.

Plant harvests and analyses

Total plant fresh weights per culture vessel (i.e. bulked for six plants) were recorded non-destructively on days 0, 7, 14, 21 and 28 of the screen, for calculation of fresh weight relative growth rates. All plants were harvested on day 28 and separated into shoot and root fractions (per vessel). Tiller numbers, fresh weights and total leaf area (Licor Model 3100 Area Meter) were recorded. All fractions were freeze-dried prior to re-weighing and milling (< 0.5 mm mesh, Glencreston Model DFH48). Total Zn and Pb in plant fractions were determined by standard ICP-AES procedures in IGER's Analytical Chemistry Section, with results expressed on a dry weight basis.

3.17 Summary

- Predominantly monometallic Zn- and Pb-rich tailings were provenanced, respectively, from Castell Mine and Darren Mine in the CWO. Analysis by AAS revealed Zn concentrations of 29,676 ppm and Pb concentrations of 16,919 ppm, whilst an acetic acid digestion indicated a $^{Zn}B_A$ of 18,901 µg g^{-1} and $^{Pb}B_A$ of 4,449 µg g^{-1}.
- Two pot experiments were carried out in consecutive years using tillers taken from 80 genotypes of an amenity x forage *L. perenne* mapping family. Three different treatments were trialled namely zero (control), 10% and 30% mixes by weight of tailings and sand, and with two replicate pots for each genotype. The plants were grown over a 16 week period with an intermediate 8 week cut and a destructive final harvest.
- A total of 11 different digestion methods were evaluated in order to identify a procedure that was both accurate and reproducible and that would facilitate a high volume of sample throughput.
- Samples of both root and shoot were freeze dried, milled, digested and analysed by AAS, whilst 'in-house' reference materials were prepared from contaminated samples from the first pot experiment and also from a large field sample of grasses collected from Castell Mine.
- QTL data from both experiments were derived through a Kruskal-Wallis test statistic, the generation of a LOD score and application of a permutation test. QTL were then transposed onto the Illumina Infinium SNP genotyping array for *L. perenne*.
- The same mapping family used in the pot experiments were previously grown, over a 28 day period, in FSC under 'supra-optimal' Zn concentrations of 100 µM and 'toxic' Pb concentrations of 25 µM.

CHAPTER 4

RESULTS

4.1 Zn Experiment 1

Experiment 1 was conducted between June and September 2009 and used Zn-rich tailings collected from Castell Mine (Section 3.2.1). The background and methodology of the experiment has been detailed in Chapter 3.

All the plants in the control treatment survived for the full 16 weeks, whilst in the 10% and 30% Zn treatments many of the plants showed increasing levels of chlorosis and ultimately died (Plates 4.1 and 4.2). Within the 10% Zn treatment there was a mortality rate of ~ 15% recorded, and in the 30% Zn treatment this rate was seen to increase to ~ 40%. Those genotypes which did not survive in the 10% and 30% treatments are listed in Table 4.1 and their time of death is also recorded in Figure 4.1, which indicates survival for between 60 – 90 days in the 10% Zn treatment (average of 77.75 days) and 65 – 100 days in the 30% Zn treatment (average of 79.8 days). Genotype 48 was anomalous in that it died during the 10% Zn treatment and yet survived the full term of the 30% Zn treatment.

All samples were digested using the newly-developed rapid HNO_3 method, described in Section 3.12, and the samples were analysed by AAS at DGES. The results for plant growth, Zn uptake and metal partitioning are variously displayed in this section as a series of bar charts, scatter plots and tables. All results are the mean of two replicate pots (all orginal data are presented in Appendix 1), with standard deviations given as an average for each treatment in the legend of each bar chart (the full dataset is presented in Appendix 3). In 2012, following completion of the pot experiments, the IBERS-maintained *L. perenne* mapping population was re-genotyped and it was found that 3 of the 80 plants used in this project (Genotypes 27, 126 and 202 F1) were contaminants. Hence all harvest and analytical data relating to these individuals were removed.

Plate 4.1 Plants growing in the 10% Zn treatment showing early signs of chlorosis prior to the 8 week cut.

Plate 4.2 Plants growing in the 30% Zn treatment following the 8 week cut showing chlorosis and mortality in many genotypes.

Table 4.1 *List of genotypes which did not survive the full length of the Zn experiment.*

10% treatment Genotype no.	30% treatment Genotype no.		
15	2	41	90
17	3	44	145
48	5	45	148
55	7	54	169
58	15	55	178
61	16	58	179
62	17	61	201 A
73	18	62	
75	25	72	
90	33	73	
145	38	75	
169	40	77	

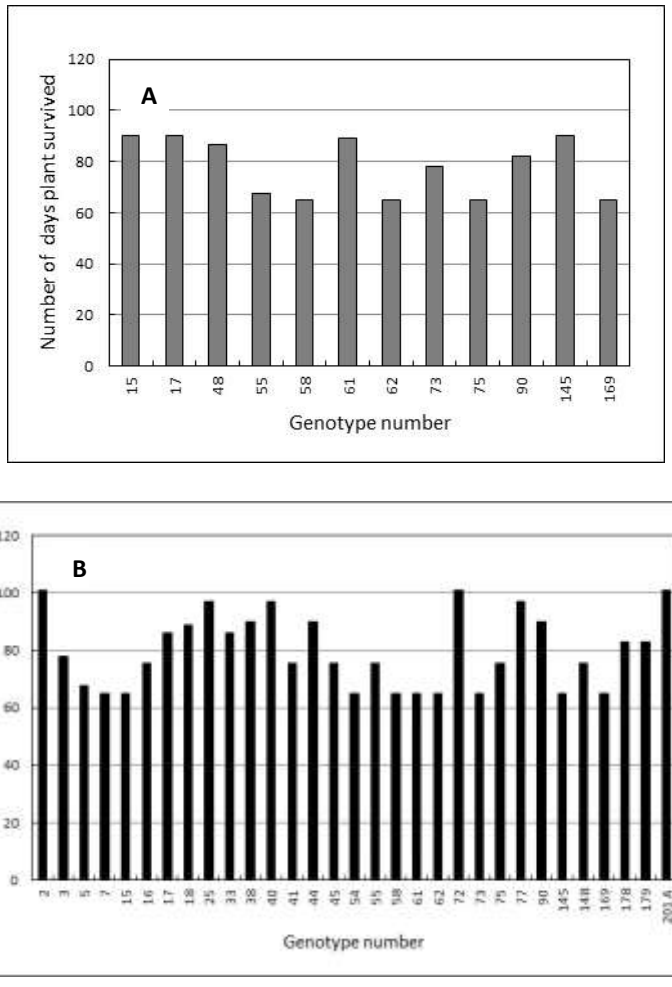

Figure 4.1 Duration of survival for those genotypes that died before the full 16 week term of the Zn experiment in A) the 10% Zn treatment, and B) the 30% Zn treatment.

4.1.1 Growth

For clarity, and in order to display all growth results precisely for each genotype, it was necessary to split some of the datasets and display them across two bar charts. Figure 4.2 shows that after the 8 week cut, the general trend across most genotypes was that shoot dry weight decreased as the Zn content of the growth medium increased. The mean shoot dry weight for

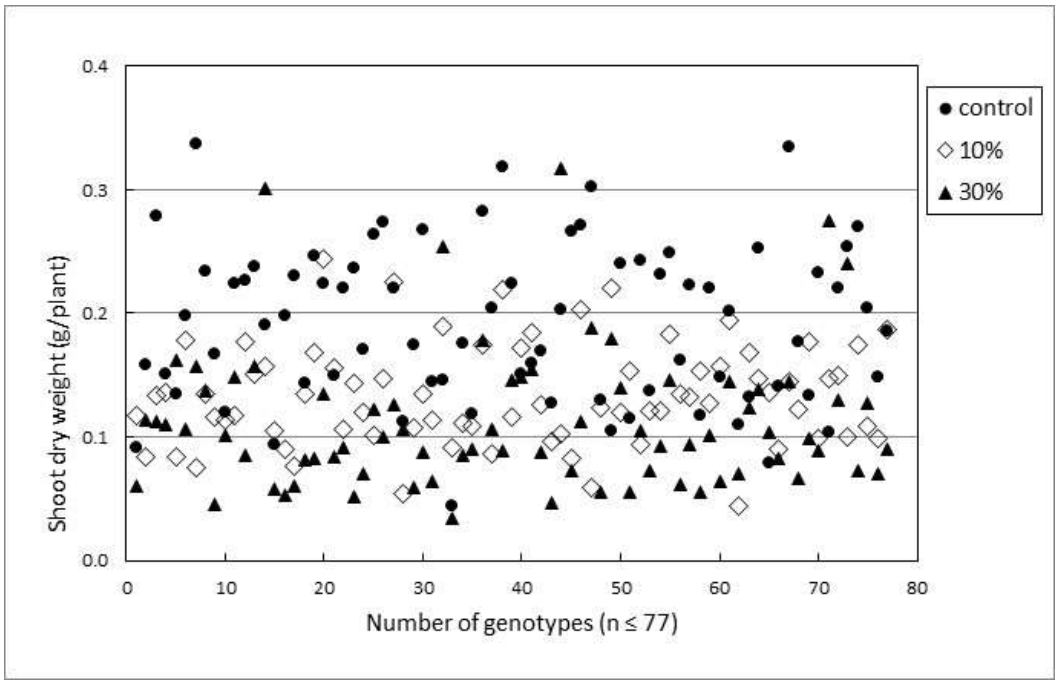

Figure 4.2 Shoot dry weights of 77 genotypes harvested at Cut 1, after 8 weeks of growth, under control, 10% or 30% Zn treatments.

each treatment was 0.192 g, 0.133 g and 0.122 g, respectively, for controls, 10% and 30% Zn-contaminated tailings, with corresponding standard deviations (SD) of 0.064, 0.041 and 0.057. Exceptions to this trend were genotypes 5, 16, 39, 55 and 157, shown in Figure 4.3, whose shoot dry weights in the 30% treatment were greater than those in the control treatment.

This trend was maintained until the final harvest, after 16 weeks of growth (Fig. 4.4), with shoot dry weight decreasing as toxicity levels increased. The mean shoot dry weights at final harvest were 2.102 g, 1.339 g and 0.966 g, respectively, for the controls, 10% and 30% Zn treatments, with corresponding SDs of 0.435, 0.508 and 0.506.

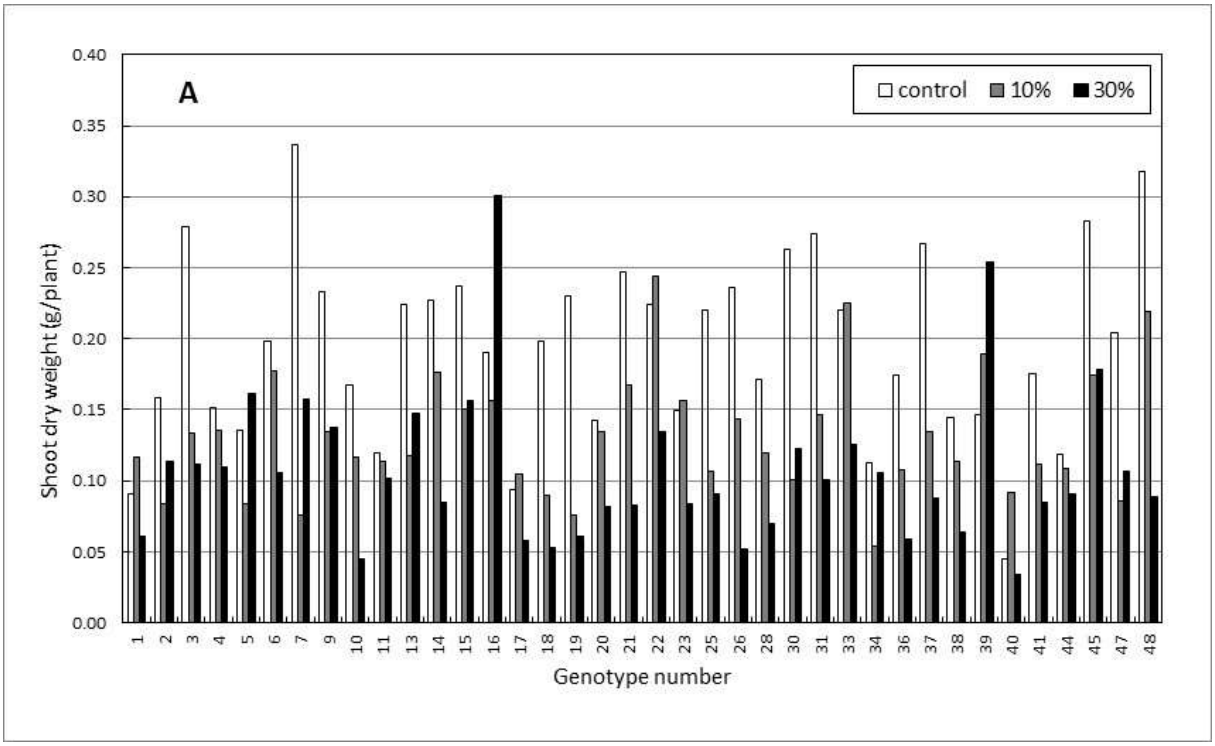

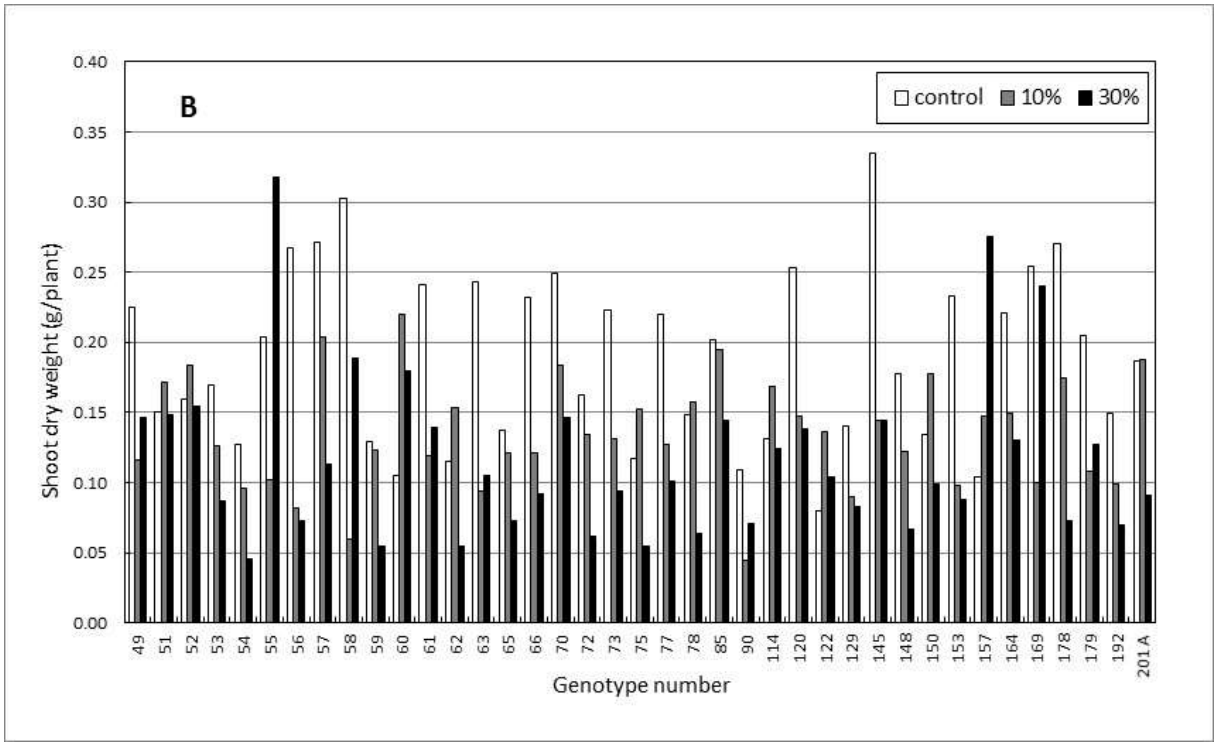

Figure 4.3 Shoot dry weights of 77 genotypes harvested at Cut 1, after 8 weeks of growth, under control, 10% or 30% Zn treatments. Data are split for clarity into A) Genotypes 1 – 48, and B) Genotypes 49 – 201A. Mean standard deviations are 0.08, 0.03 and 0.05 for control, 10% and 30% Zn treatments, respectively.

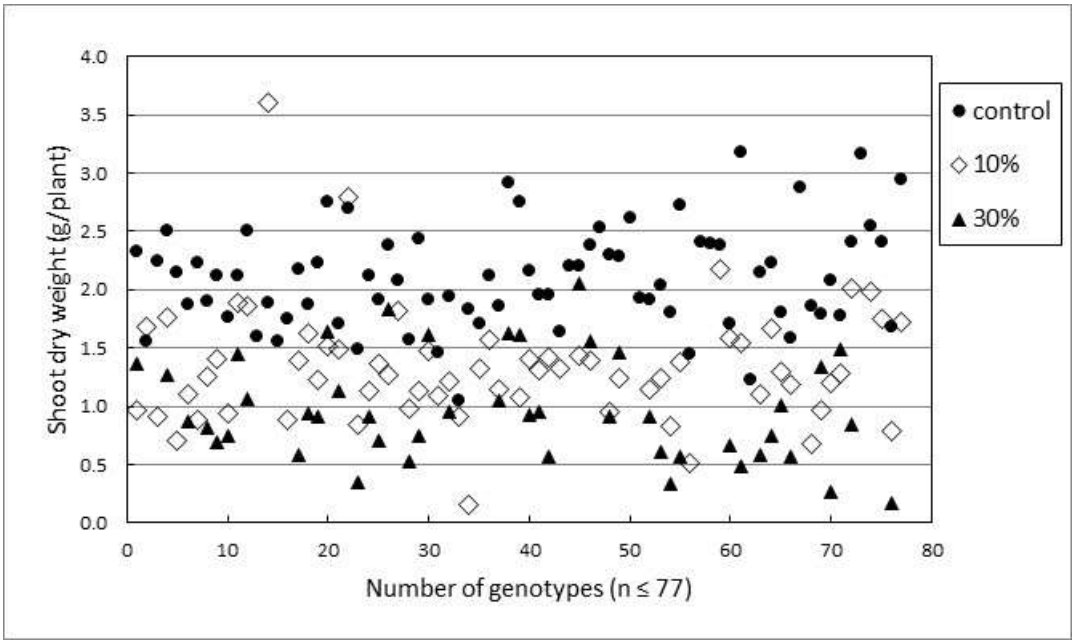

Figure 4.4 Shoot dry weights of ≤ 77 genotypes harvested after 16 weeks of growth, under control, 10% or 30% Zn treatments.

Figure 4.5 highlights the variation in performance across the range of genotypes in the experiment at final harvest. For example, Genotype 16, which had performed well up to Cut 1 and exceptionally well in the control and 10% Zn treatments to final harvest (1.88 g and 3.60 g shoot dry weight respectively), died under the 30% Zn treatment before the final harvest. Genotypes 25, 77 and 178 also performed well in both the control and 10% Zn treatments to final harvest but died under the 30% Zn treatment. In contrast, Genotypes 15, 17, 55, 58, 61, 62, 73, 75, 90, 145 and 169, many of which performed well during the early phase (Cut 1) of both treatments, subsequently all died in both treatments before final harvest. Genotypes 55 and 169 were of particular note in this group, as they performed very well in both treatments until Cut 1, after 8 weeks of growth.

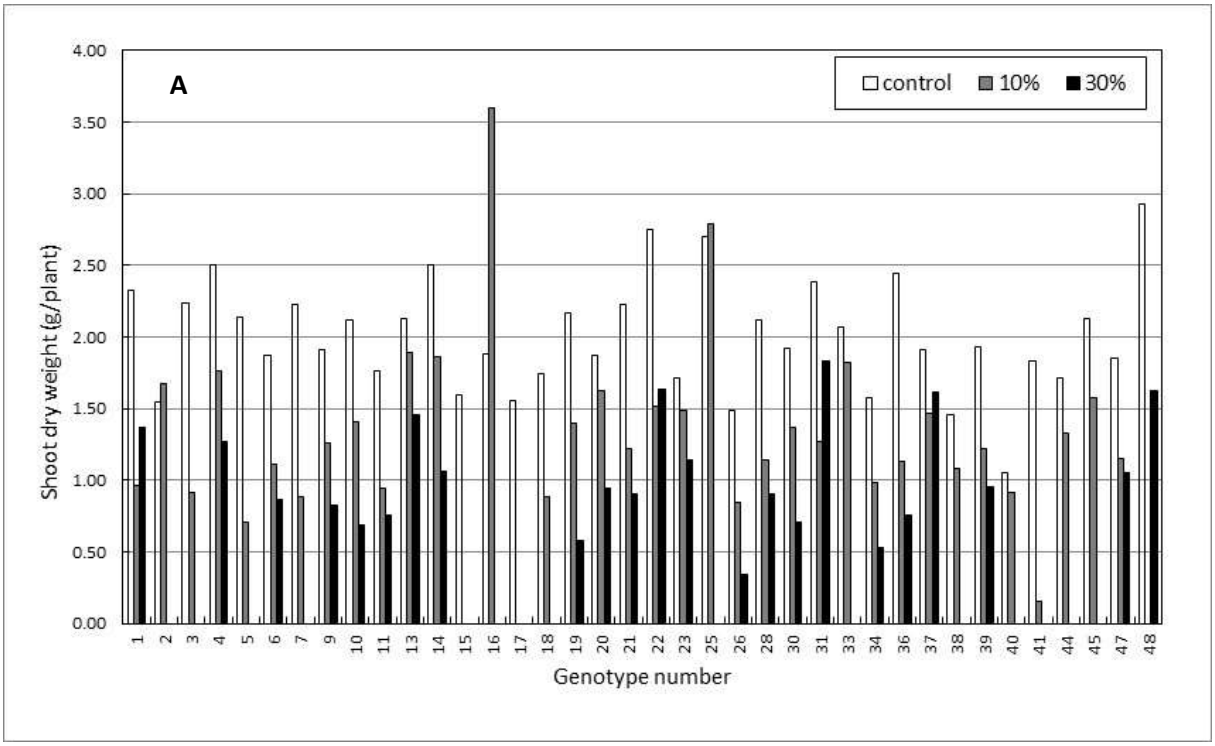

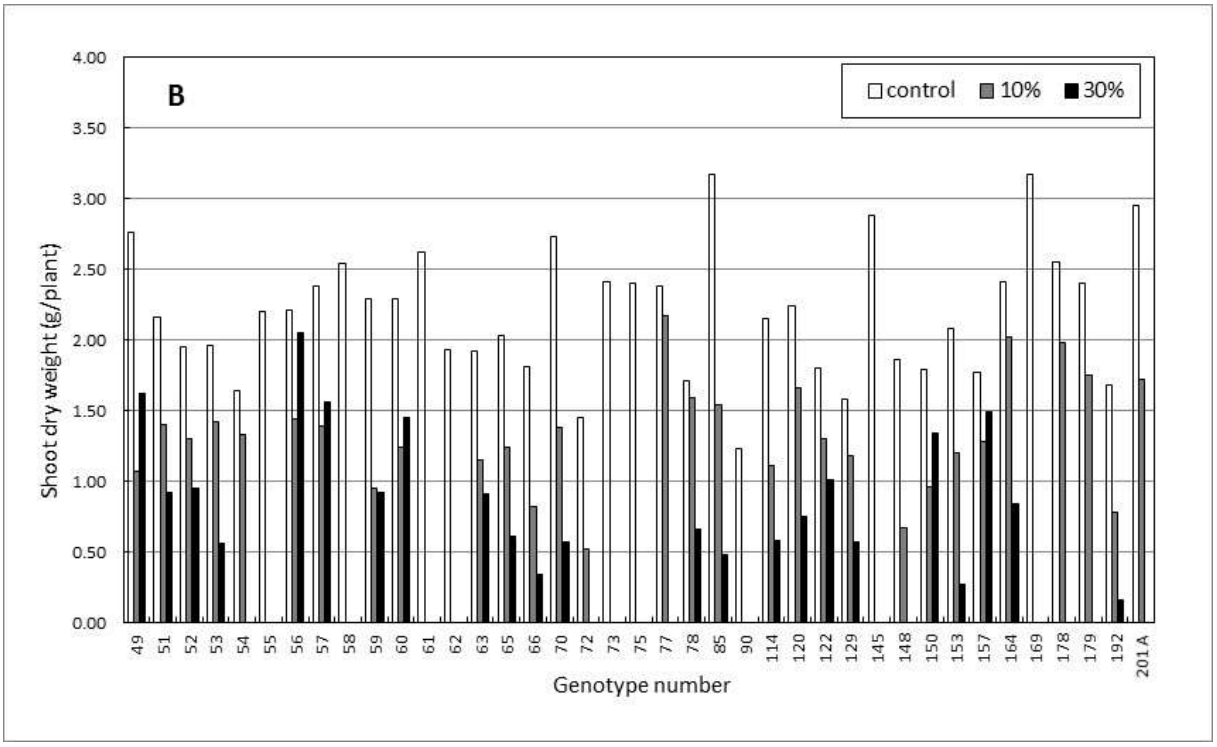

Figure 4.5 Shoot dry weights of ≤ 77 genotypes harvested after 16 weeks of growth, under control, 10% or 30% Zn treatments. Data are split for clarity into A) Genotypes 1 – 48, and B) Genotypes 49 – 201A. Mean standard deviations are 0.33, 0.39 and 0.39 for control, 10% and 30% Zn treatments, respectively.

The responses to treatments displayed by shoot dry weights were generally mirrored by those for root dry weights (Figure 4.6). Mean root dry weights at final harvest were 2.449 g, 1.069 g and 0.549 g, respectively, for the control, 10% and 30% Zn treatments, respectively, with corresponding SDs of 1.261, 0.445 and 0.293, However, there was considerable variability in root dry weight within treatments and particularly in the control group (Figure 4.6).

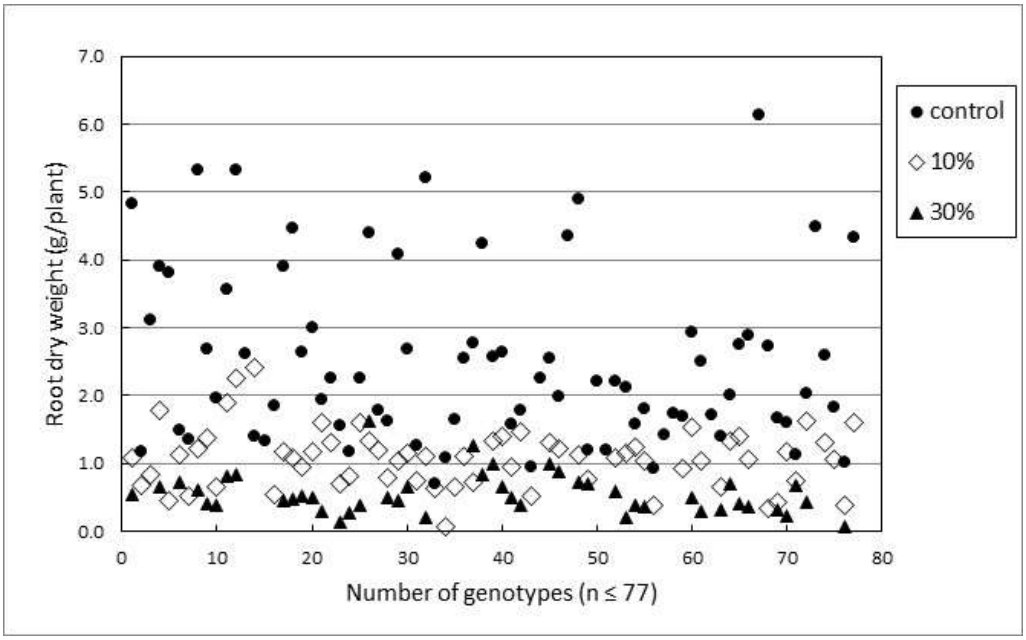

Figure 4.6 Root dry weights of ≤ 77 genotypes at final harvest, after 16 weeks of growth, under control, 10% or 30% Zn treatments.

Figure 4.7 highlights more clearly the variability in root growth across the genotypes and shows that, in most cases, root dry weight decreased as Zn concentration in the growth medium increased. This is shown, for example, by Genotype 9 with final root dry weights of 5.315 g, 1.223 g and 0.617 g, respectively, for control, 10% and 30% Zn treatments. There were two notable exceptions to this trend, namely Genotypes 31 and 47. Both these genotypes had slightly higher final root dry weights in the 30% Zn than in the 10% Zn treatment.

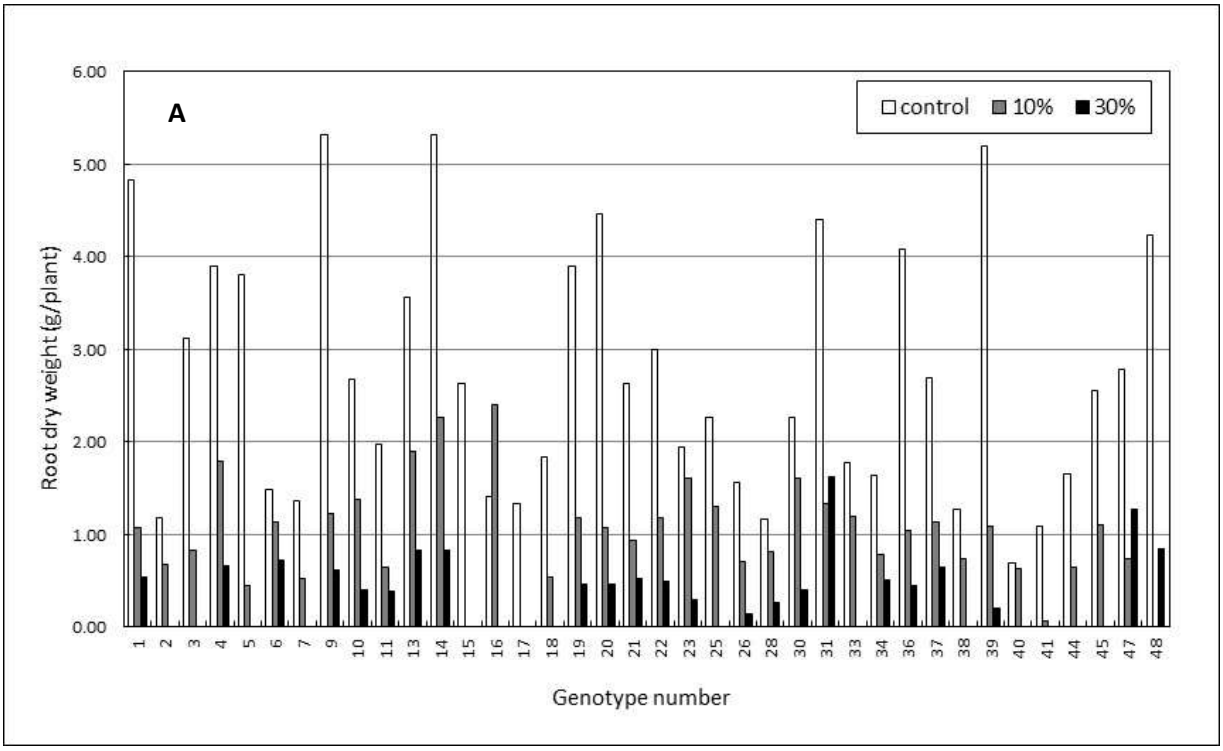

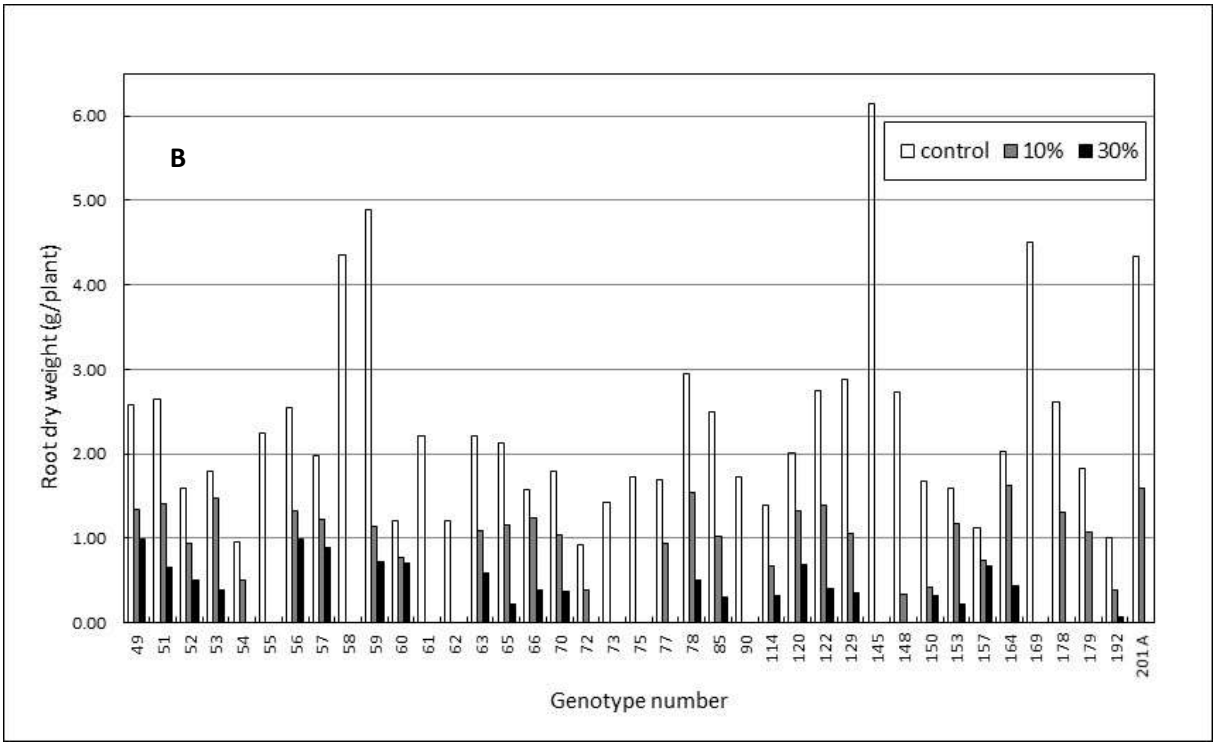

Figure 4.7 Root dry weights of ≤ 77 genotypes harvested after 16 weeks of growth, under control, 10% or 30% Zn treatments. Data are split for clarity into A) Genotypes 1 – 48, and B) Genotypes 49 – 201A. Mean standard deviations are 0.67, 0.38 and 0.22 for control, 10% and 30% Zn treatments, respectively.

Plots of total plant dry weight (i.e. roots plus shoots) in the Zn treatments at final harvest against those of the control plants (Figures 4.8 and 4.9), an important index of tolerance (*sensu* Macnair, 1993), show that the growth of nearly all genotypes was inhibited by Zn treatment, and more so in the 30% Zn treatment. However, linear regressions fitted to the datasets showed weak correlations between growth of the control plants and those under Zn treatments ($R^2 < 0.15$). Hence, total dry weights of genotypes under Zn treatments were not accurately predictable on the basis of the corresponding weights under the control regime. Similarly, very weak correlations ($R^2 = 0.076$) were determined between total plant dry weight in the 10% Zn treatment and total plant dry weight in the 30% Zn treatment.

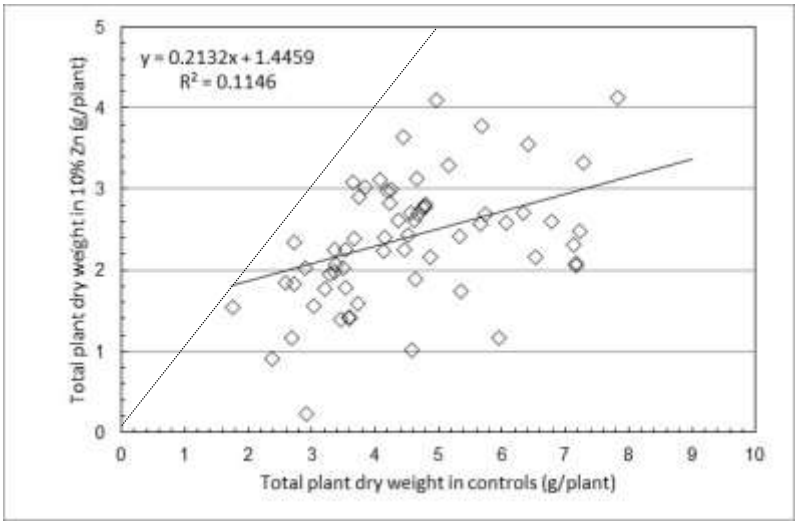

Figure 4.8 Relationship between total plant dry weights (roots and shoots) of the surviving genotypes in the 10% Zn treatment and under control conditions. The straight line is the linear regression for the data, whilst the dotted line is the 1:1 line (i.e. gradient = 1).

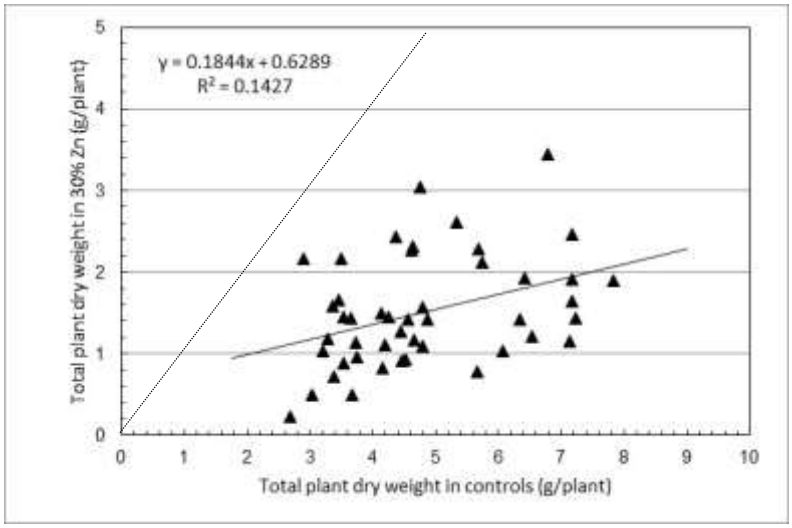

Figure 4.9 Relationship between total plant dry weights (roots and shoots) of the surviving genotypes in the 30% Zn treatment and under control conditions. The straight line is the linear regression for the data, whilst the dotted line is the 1:1 line (i.e. gradient = 1).

An ability to tiller profusely is useful in establishing effective ground cover for soil stabilisation. The results for tillering contrast with those for dry matter production, in so far as the Zn treatments had inconsistent effects on the number of tillers produced by many of the genotypes at final harvest (Figure 4.10). The mean tiller numbers at final harvest were 25.8, 28.6 and 24.7, respectively, in control, 10% and 30% Zn treatments. However, there was considerable variation between the surviving genotypes in terms of response under the 10% and 30% Zn treatments (Figure 4.11). For example, Genotypes 1, 4, 6, 13, 22, 31, 37, 49, 52, 59, 60 and 157 produced more tillers under the 30% Zn treatment compared with both the control and 10% Zn treatments. Genotype 13, in particular, showed by far the highest rate of tiller production, with 69 and 75 tillers produced per plant, respectively, in the 10% and 30% Zn treatments. Furthermore, within the group of genotypes that died under the 30% Zn treatment, tiller production by Genotypes 2, 16, 25, 33, 44, 54, 77, 178 and 201A was greater under 10% Zn treatment than the control treatment. Amongst the genotypes which survived under all treatments, the expected trend of decreasing tiller production with increasing Zn concentration was only observed in Genotypes 9, 10, 11, 21, 36, 51, 56, 63, 65, 66, 114, 122 and 192.

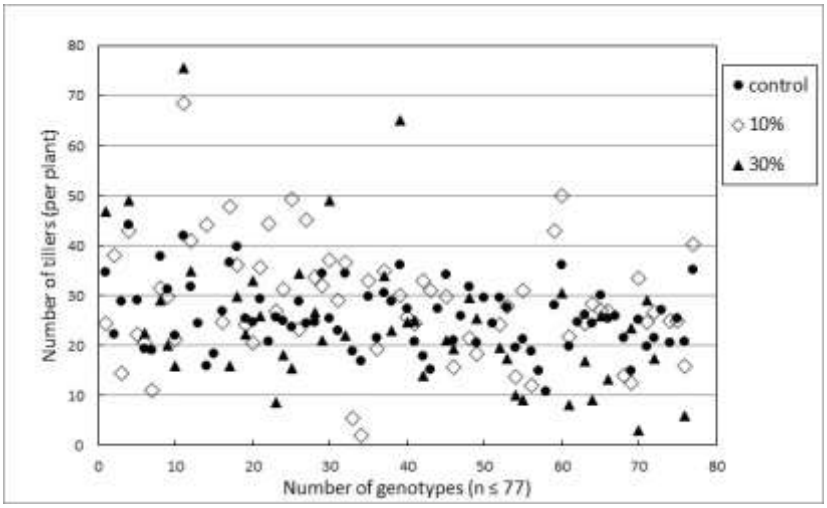

Figure 4.10 Tiller numbers of ≤ 77 genotypes at final harvest, after 16 weeks of growth, under control, 10% or 30% Zn treatments.

The relationship between tiller numbers and shoot dry weights varied with treatment (Figure 4.12). Linear regressions fitted to the data showed little or no correlation (R^2 = 0.04) in the control treatment (Figure 4.12A) group, but modest positive correlations between tiller numbers and shoot dry weights in both the 10% Zn (Figure 4.12B, R^2 = 0.39) and 30% Zn (Figure 4.12C, R^2 = 0.41) treatments. The steeper gradient to the best fit line for the 30% Zn data (20.6), compared with the 10% Zn data (14.3), reflects the impact of the reduction in shoot dry weights with increasing Zn concentration in the growth medium.

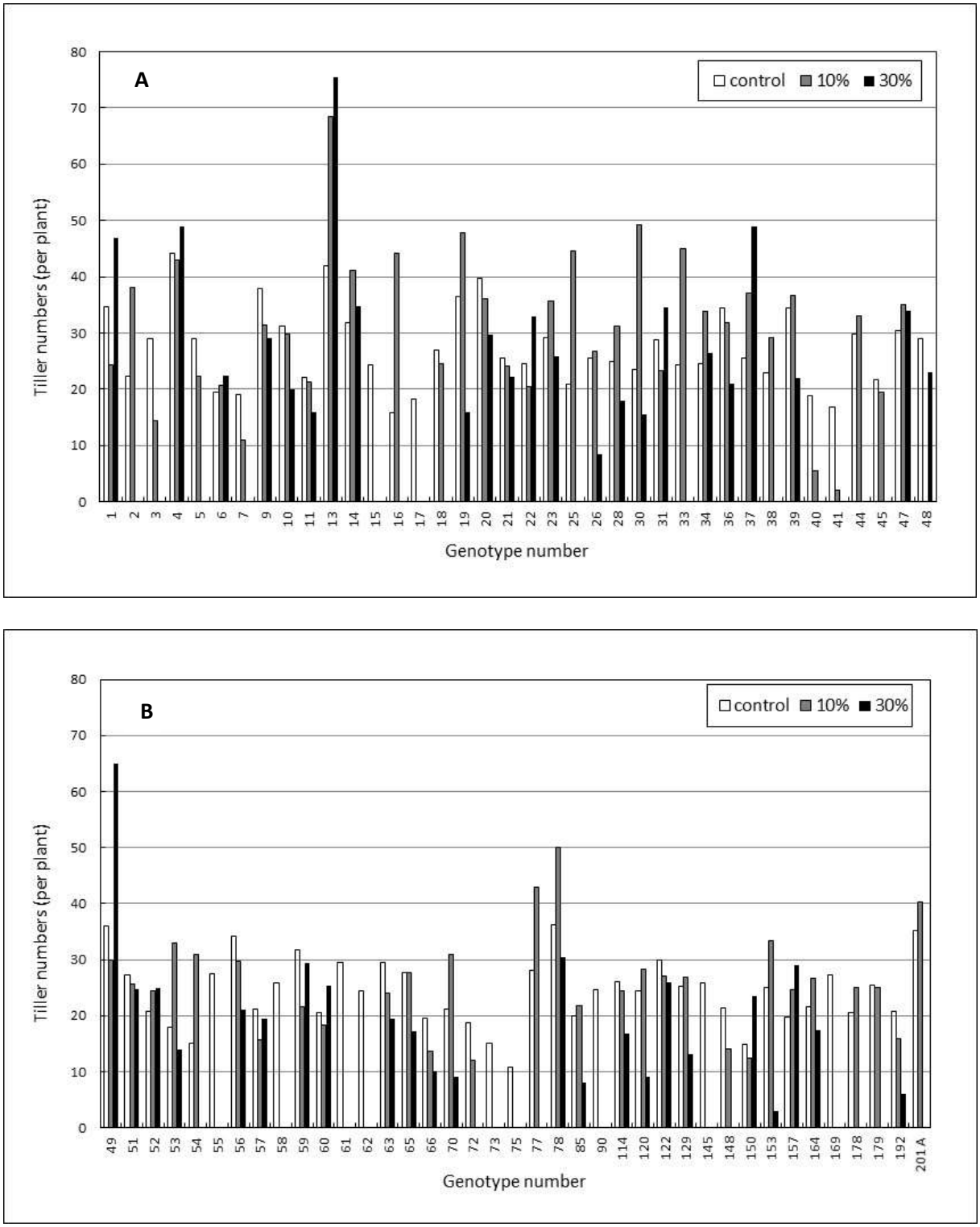

Figure 4.11 Comparison of tiller numbers of ≤ 77 genotypes harvested after 16 weeks of growth, under control, 10% or 30% Zn treatments. Data are split for clarity into A) Genotypes 1 – 48, and B) Genotypes 49 – 201A. Mean standard deviations are 2.6, 7.8 and 8.9 for control, 10% and 30% Zn treatments, respectively.

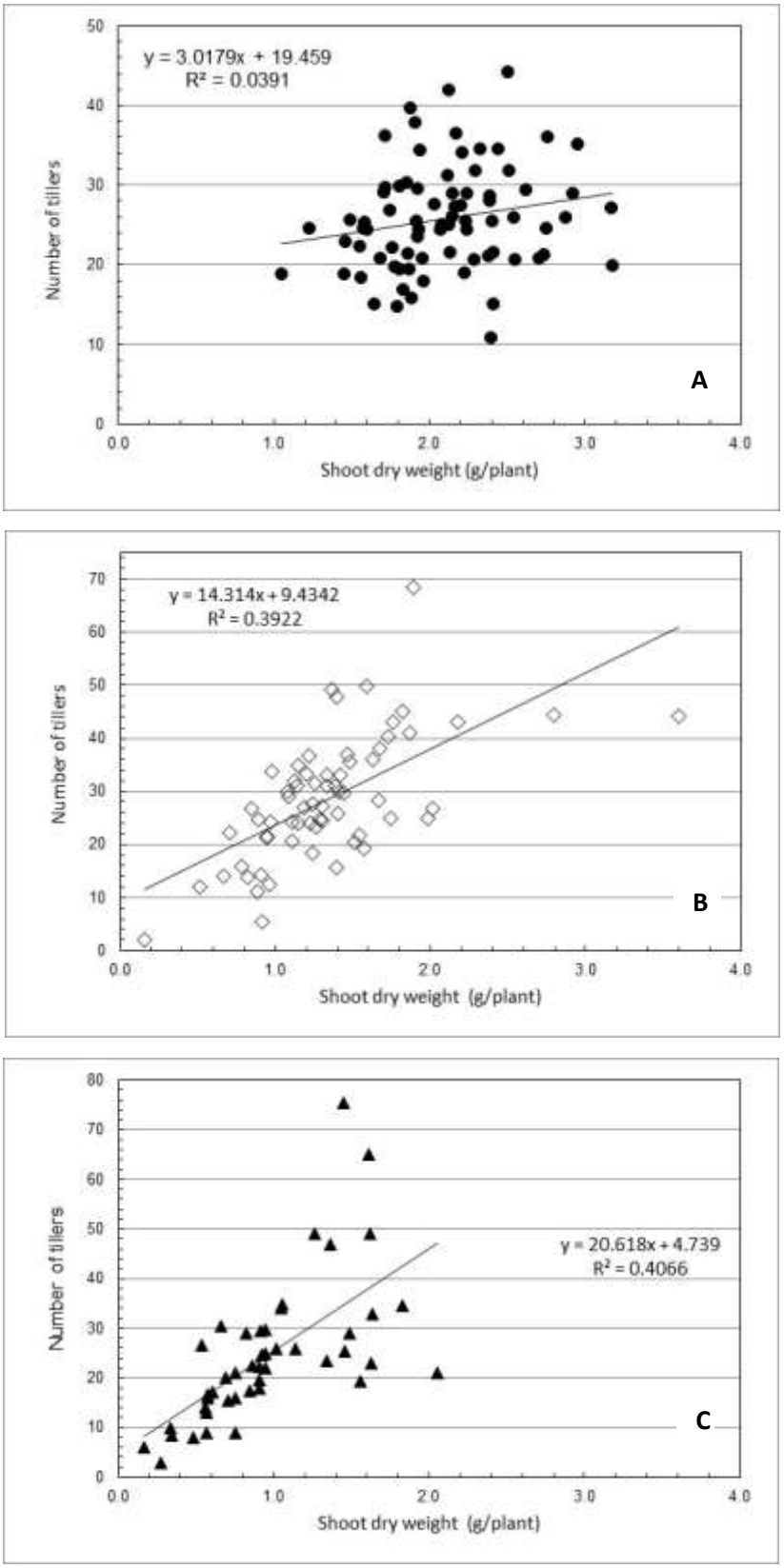

Figure 4.12 Scatter plots showing the relationship between shoot dry weights and numbers of tillers produced by the ≤ 77 genotypes at final harvest in A) the control, B) 10% Zn treatment, and C) the 30% Zn treatments. Straight lines are the linear regressions for the data.

4.1.2 Zn uptake and partitioning

The inclusion of the intermediate 'Cut 1' harvest after 8 weeks of growth provided a way of assessing the short-term responses to the Zn treatments in terms of Zn uptake, albeit not on the basis of total uptake of Zn by the plant. The variation in Zn content of the harvested shoot fraction after 8 weeks of growth is shown in Figure 4.13. The mean Zn content of this fraction across all genotypes was 211 µg Zn/plant in the 10% Zn treatment and 314 µg Zn/plant in the 30% Zn treatment. The trend of increasing Zn content and, by implication, uptake of Zn, with increasing Zn concentration in the growth medium, was shown by 45 of the genotypes, with 14 of these having > 500 µg Zn/plant. Four genotypes, namely 4, 5, 58 and 169, contained > 800 µg Zn/plant. Several genotypes in the 10% and 30% Zn treatments, namely 17, 41, 56, 153 and 178, showed very similar levels of Zn uptake in the shoots, ranging from 150 – 250 µg Zn/plant. The mean Zn content of the shoot fraction of the control plants was 2.59 µg Zn/plant, and is a measure of Zn availability as a micronutrient in the fertiliser application.

The Zn content of the shoots at final harvest, after 16 weeks of growth, is shown in Figure 4.14. Twenty-seven genotypes contained more Zn in their shoots in the 30% Zn treatment compared with the 10% Zn treatment. In contrast, 18 genotypes contained more Zn in their shoots under the 10% Zn treatment compared with the 30% Zn treatment. The highest shoot content of Zn was observed in Genotypes 48 and 56, which contained 8,500 and 9,700 µg Zn/plant, respectively. A further 21 genotypes had > 3,000 µg Zn/plant. As might be expected, there was a strong positive linear correlation between Zn content of the shoot and shoot dry weight (Figure 4.15), in both the 10% ($R^2 = 0.79$) and 30% ($R^2 = 0.77$) Zn treatments.

The Zn contents of the roots at final harvest are shown in Figure 4.16. Only seven genotypes, namely 31, 47, 48, 56, 59, 60 and 150, contained more Zn in the roots under the 30% Zn treatment compared with the 10% Zn treatment. Of these, the roots of Genotypes 31 and 56 contained the most Zn with levels > 16,000 and > 14,000 µg Zn/plant, respectively. In the 10% Zn treatment, five individuals contained over 15,000 µg Zn/plant, namely Genotypes 4, 14, 16, 78 and 201A, with the highest root content of Zn observed in Genotype 14, at 29,000 µg Zn/plant. As in the case of the shoots, there was also a strong positive linear correlation between the Zn content of the roots and root dry weight (Figure 4.17) in both the 10% ($R^2 = 0.70$) and 30% ($R^2 = 0.82$) Zn treatments.

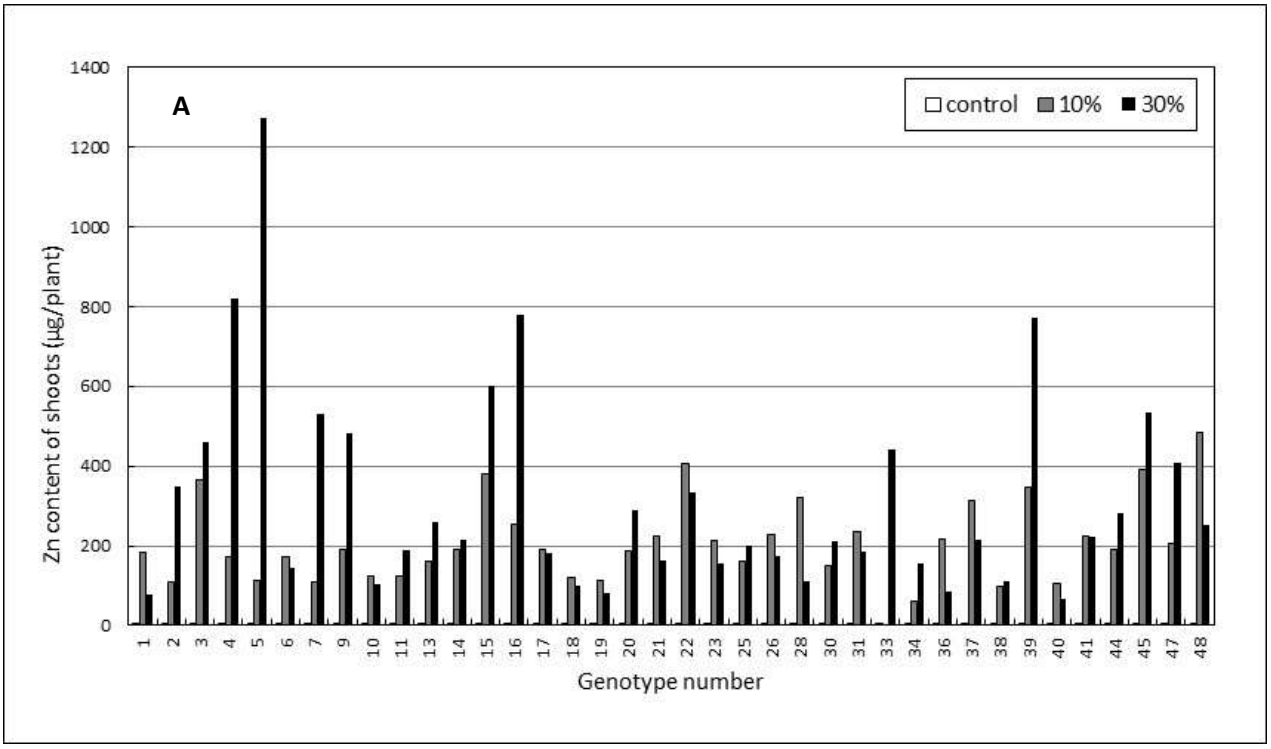

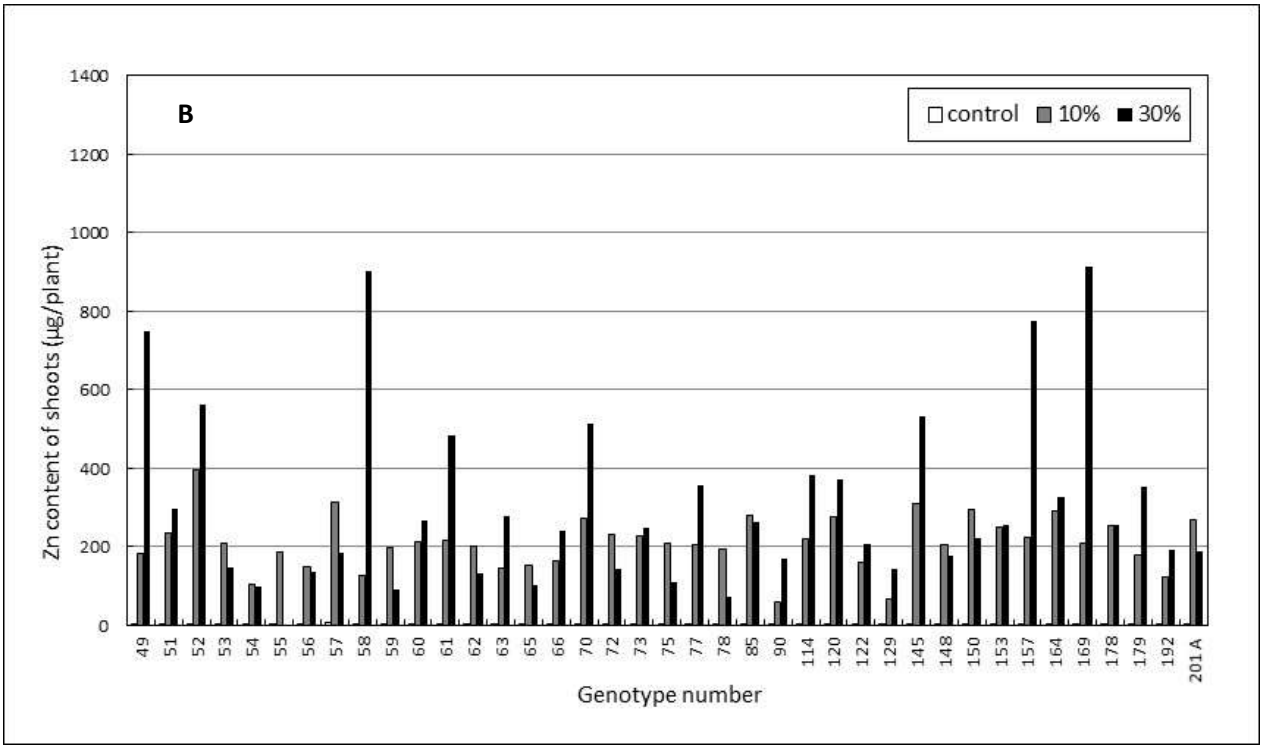

Figure 4.13 Comparison of the Zn content of the shoots, expressed as µg/plant, for ≤ 77 genotypes, harvested after 8 weeks of growth under control, 10% or 30% Zn treatments. Data are split for clarity into A) Genotypes 1 – 48, and B) Genotypes 49 – 201A. Mean standard deviations are 1.8, 68.1 and 212.1 for control, 10% and 30% Zn treatments, respectively.

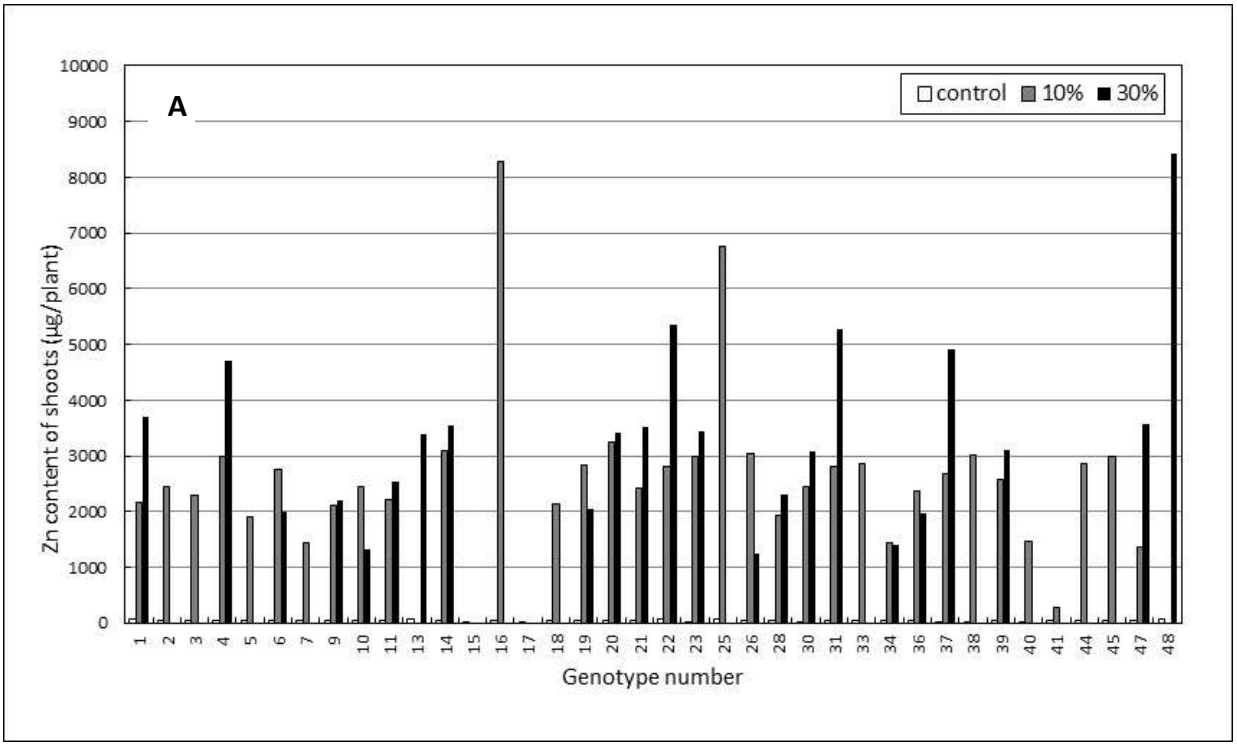

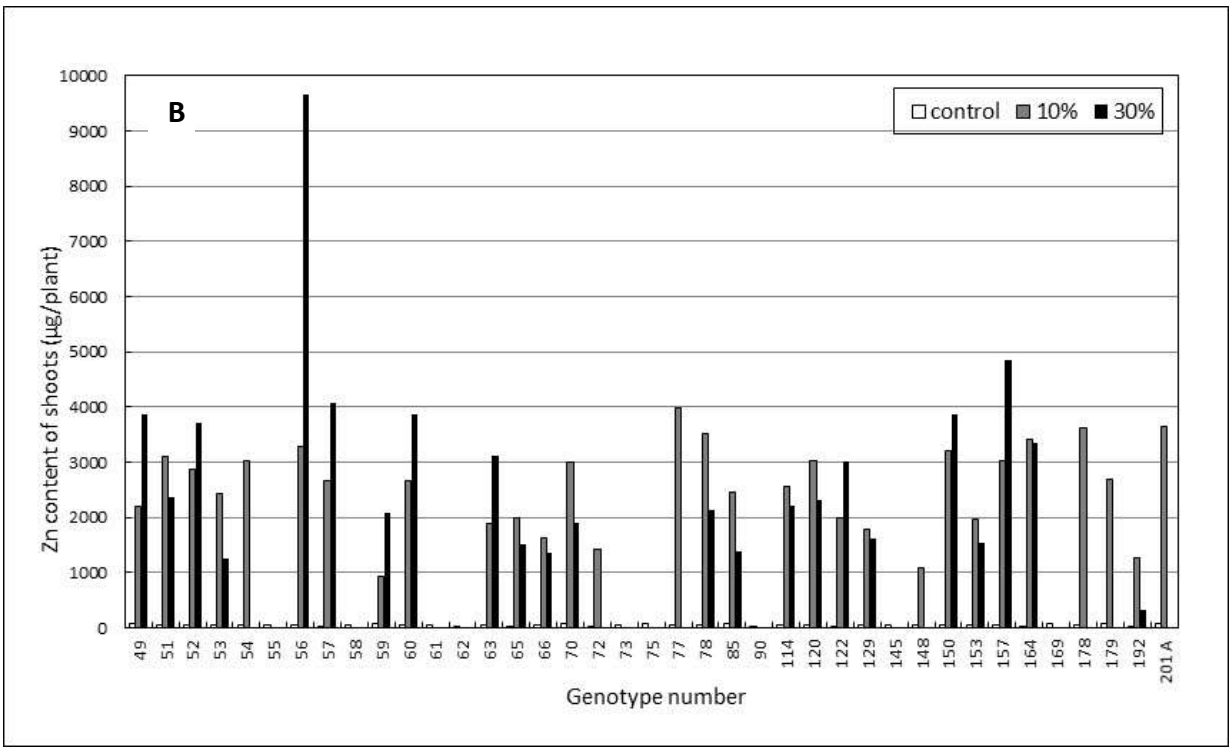

Figure 4.14 Comparison of the Zn content of the shoots, expressed as µg/plant, for ≤ 77 genotypes, harvested after 16 weeks of growth under control, 10% or 30% Zn treatments. Data are split for clarity into A) Genotypes 1 – 48, and B) Genotypes 49 – 201A. Mean standard deviations are 14.7, 997.3 and 1201.1 for control, 10% and 30% Zn treatments, respectively.

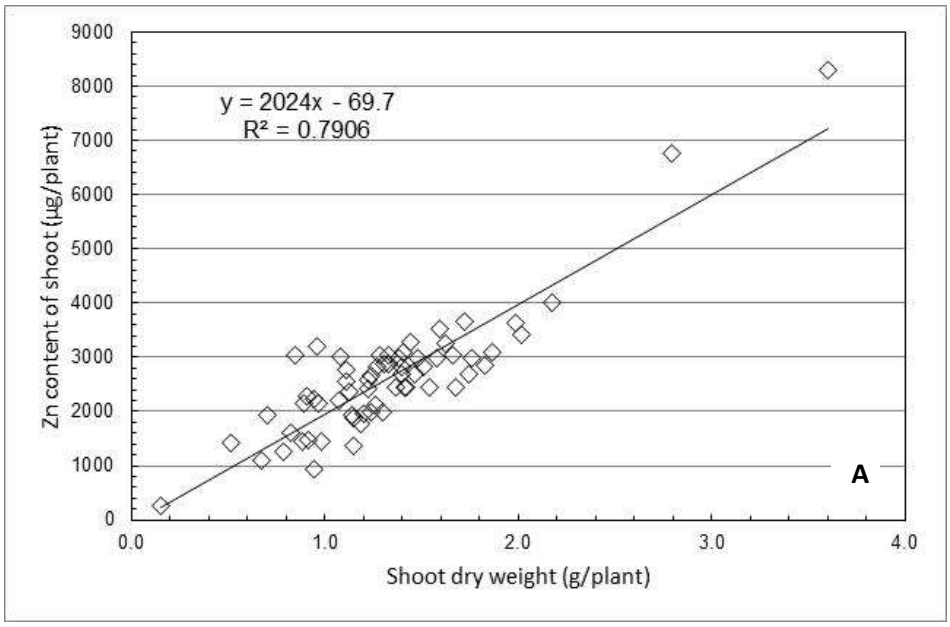

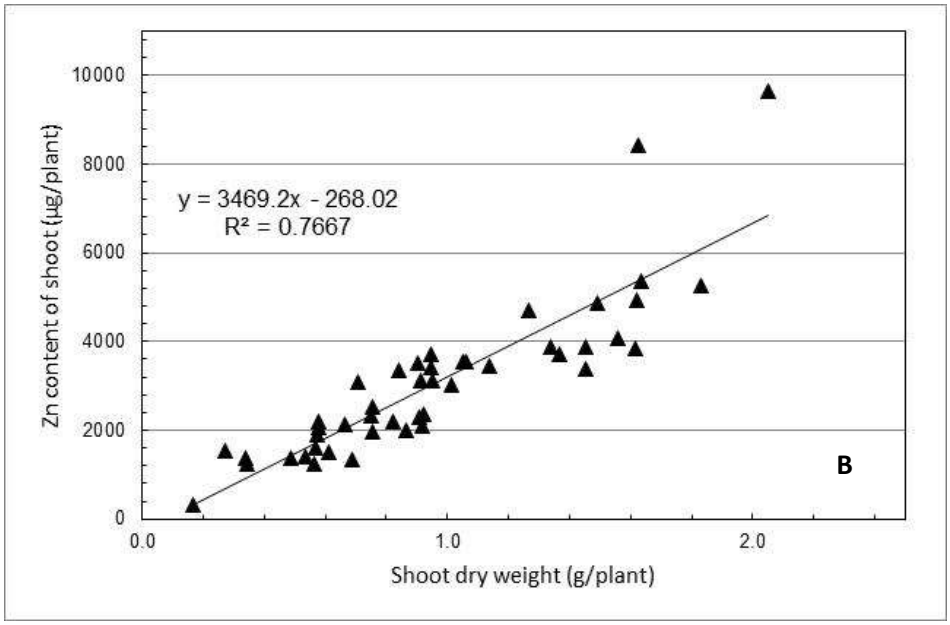

Figure 4.15 Relationship between the Zn content of the shoots and shoot dry weight at final harvest for the surviving genotypes in A) the 10% Zn treatment, and B) the 30% Zn treatment. The straight lines are the linear regressions for the data.

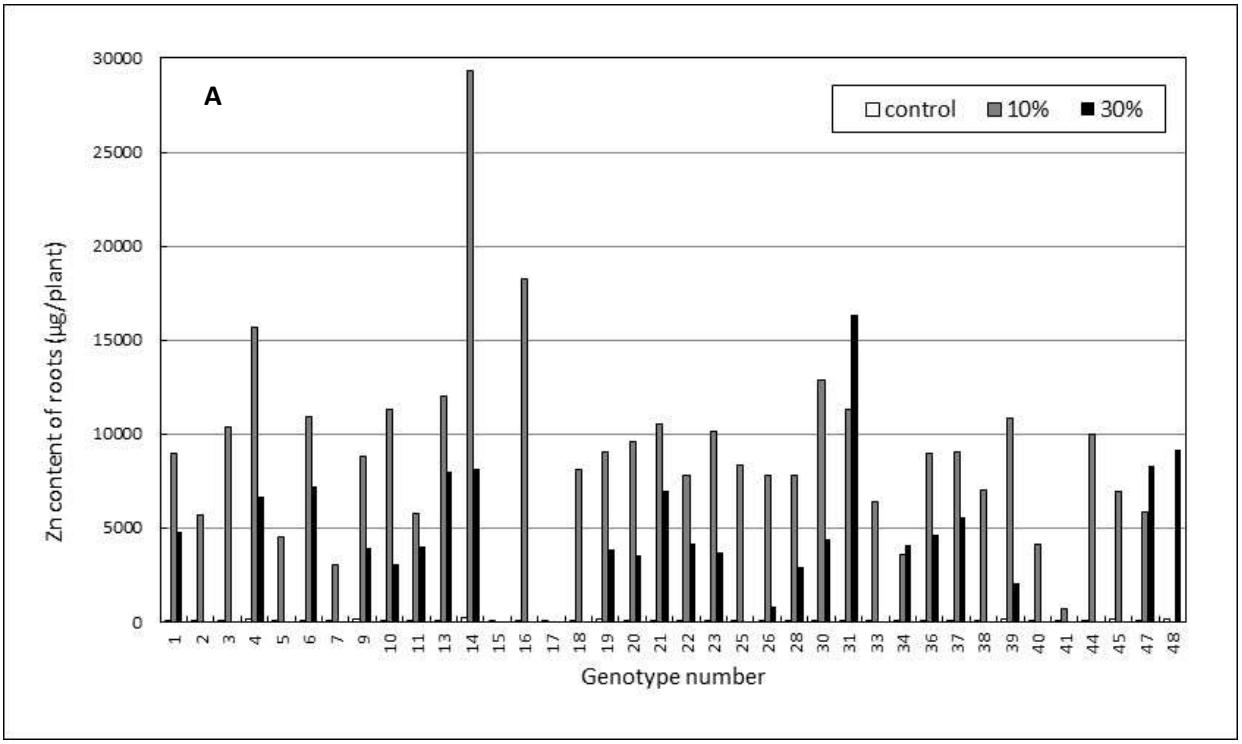

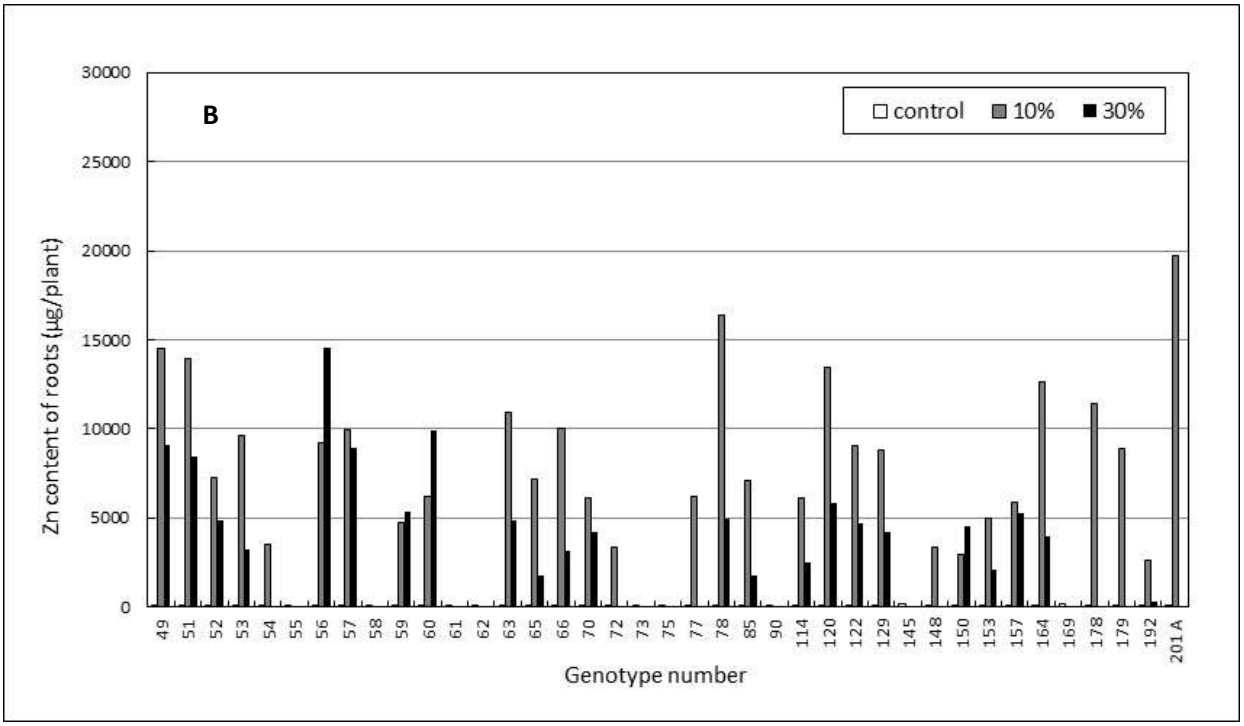

Figure 4.16 Comparison of the Zn content of the roots, expressed as µg/plant, for ≤ 77 genotypes, harvested after 16 weeks of growth under control, 10% or 30% Zn treatments. Data are split for clarity into A) Genotypes 1 – 48, and B) Genotypes 49 – 201A. Mean standard deviations are 25.6, 3355.6 and 2641.2 for control, 10% and 30% Zn treatments, respectively.

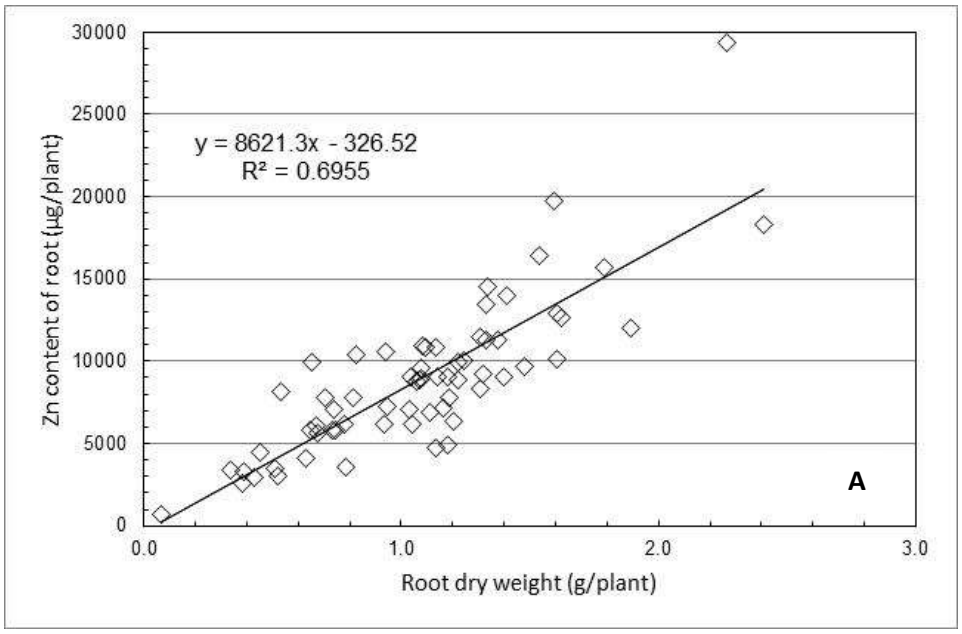

Figure 4.17 Relationship between the Zn content of the roots and root dry weight at final harvest for the surviving genotypes in A) the 10% Zn treatment, and B) the 30% Zn treatment. Straight lines are the linear regressions for the data.

The total amount of Zn absorbed by the plants over the course of the entire experiment (i.e. Zn content of shoots at Cut 1 and in the shoot and root fractions at final harvest, combined) are shown in Figure 4.18A for the 10% Zn treatment and Figure 4.18B for the 30% Zn treatment. The data reveal a strong positive correlation between Zn content and total plant dry weight, as evidenced by high R^2 values of ~ 0.8 in the 10% Zn treatment and ~ 0.94 in the 30% Zn treatment. In the 10% Zn treatment, Genotypes 4, 16, 25, 164 and 201A were the best five performers, having the highest Zn content and total plant dry weight, whilst the poorest performers (of those individuals that survived to final harvest) were Genotypes 5, 7, 72, 148 and 192. In the 30% Zn treatment, Genotypes 31, 48, 49, 56 and 57 were the best five performers, having the highest Zn content and total plant dry weight, whilst the poorest performers (of those individuals that survived to final harvest) were Genotypes 26, 65, 66, 85 and 153.

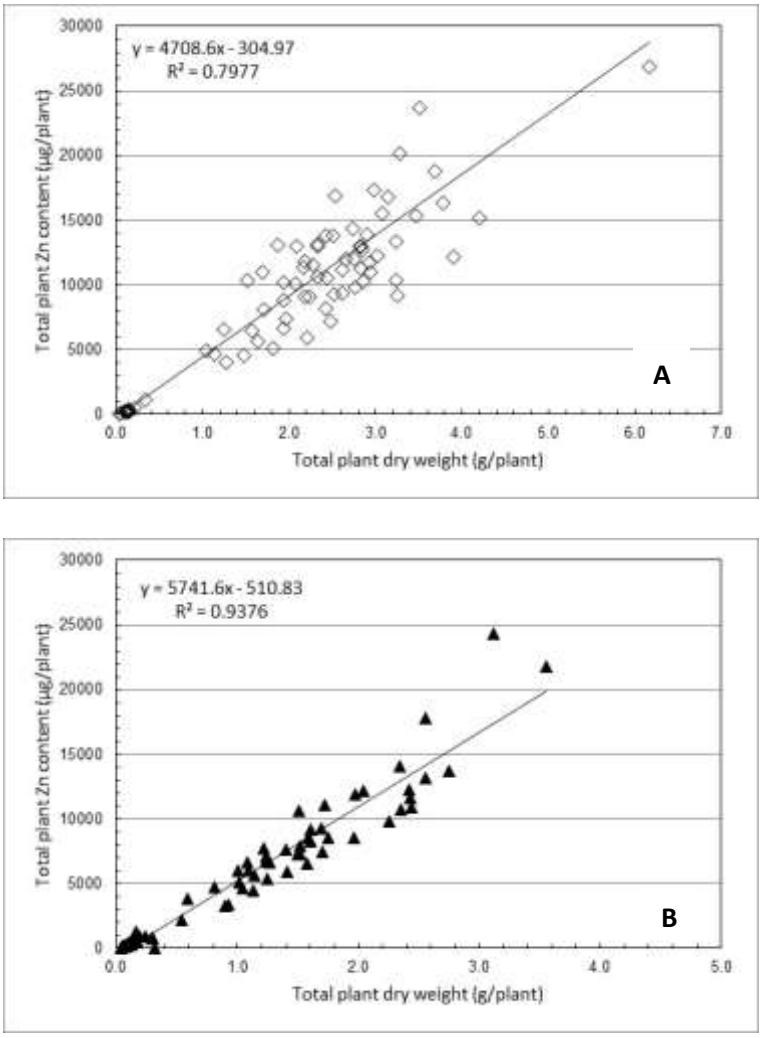

Figure 4.18 Relationship between total plant Zn content and total plant dry weight in A) the 10% Zn treatment, and B) the 30% Zn treatment. Straight lines are the linear regressions for the data.

Scatter plots of the relationship between tissue concentrations of Zn in the shoots and the total Zn content of the shoots at Cut 1, after 8 weeks of growth (Figure 4.19), showed a stronger linear relationship under the 30% Zn treatment ($R^2 = 0.66$) compared with the 10% Zn treatment ($R^2 = 0.44$). However, the relationship was much weaker by the final harvest (Figure 4.20) in both treatments. Although total shoot Zn contents had increased by a factor of > 10 in both Zn treatments during the intervening period, tissue concentrations had remained relatively stable, as shown by the clustering of the data in Figure 4.20.

The corresponding relationships between total Zn content of the roots and the mean concentrations of Zn in root tissue at final harvest (Figure 4.21) also showed weak correlations under 10% Zn ($R^2 = 0.18$) and 30% Zn ($R^2 = 0.23$) treatments.

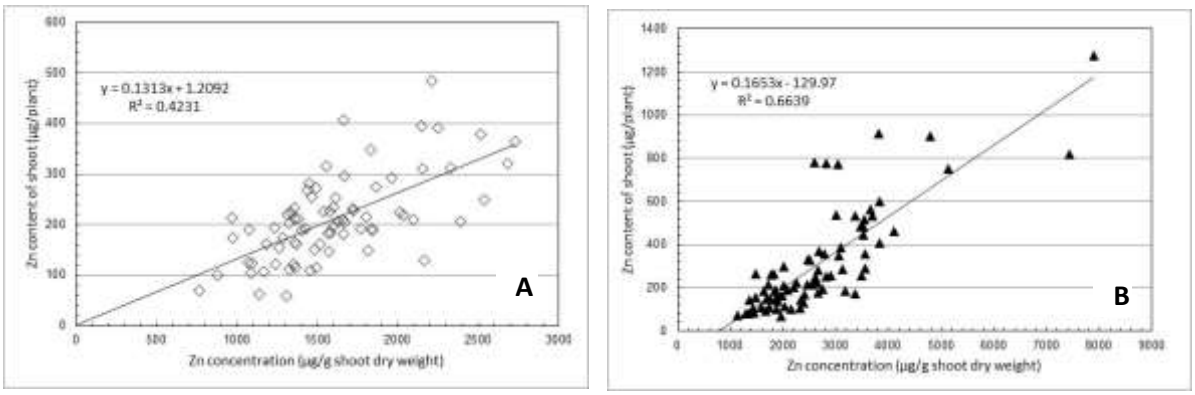

Figure 4.19 Relationship between total Zn content of the shoots and the concentration of Zn in shoot tissue of the 77 genotypes at Cut 1 after 8 weeks of growth under A) the10% Zn treatment, and B) the 30% Zn treatment. Straight lines are the linear regressions for the data.

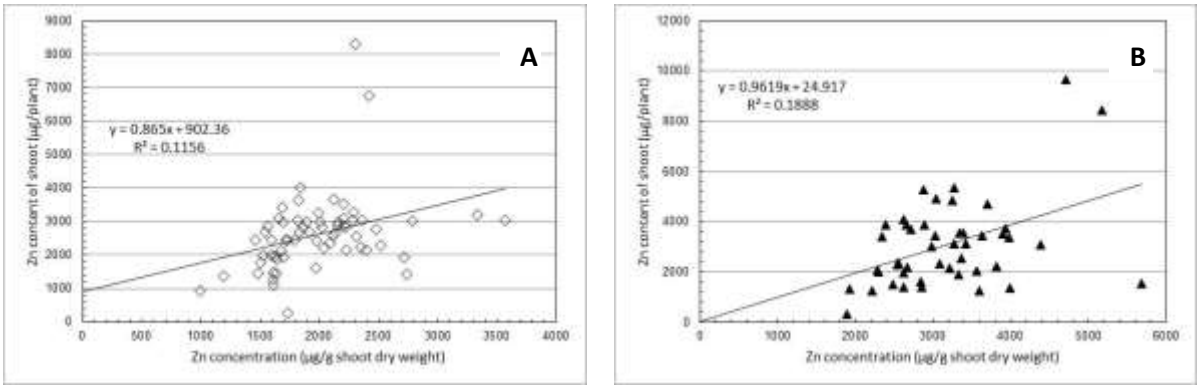

Figure 4.20 Relationship between total Zn content of the shoots and the concentration of Zn in shoot tissue of the surviving genotypes at final harvest after 16 weeks of growth under A) the 10% Zn treatment, and B) the 30% Zn treatment. Straight lines are the linear regressions for the data.

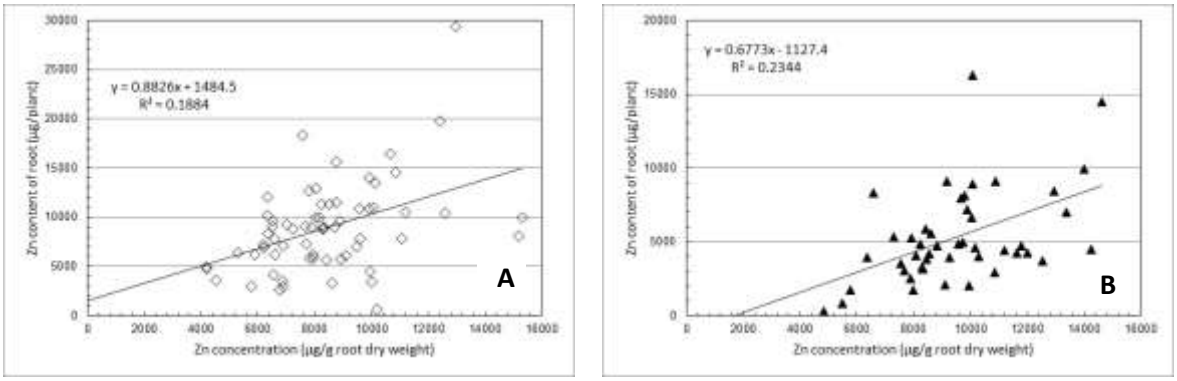

Figure 4.21 Relationship between total Zn content of the roots and mean concentrations of Zn in root tissue of the surviving genotypes at final harvest after 16 weeks of growth under A) the 10% Zn treatment, and B) the 30% Zn treatment. Straight lines are the linear regressions for the data.

The majority of the Zn absorbed by the plants during the 16 week experimental period was recovered in the roots rather than the shoots in all but one genotype under the 10% Zn treatment (Figure 4.22), and all but four genotypes under the 30% Zn treatment (Figure 4.23). The bar charts show substantial variation between genotypes in the proportion of the total uptake of Zn recovered in the roots and shoots of genotypes. The proportion of total Zn content recovered in the roots, relative to the shoots, ranged between 44% and 90% under the 10% Zn treatment and between 40% and 80% under the 30% Zn treatment.

In terms of the 'translocation index' (i.e. TI_{Zn} = shoot Zn content/root Zn content), only Genotype 150 had an index > 1 (TI_{Zn} ~ 1.1) under the 10% Zn treatment. However, all genotypes had higher translocation indices when grown under the 30% Zn treatment compared with the 10% Zn treatment. The four individuals with translocation indices ≥ 1 under the 30% Zn treatment were Genotypes 22 (TI_{Zn} ~ 1.3), 26 (TI_{Zn} ~ 1.5), 39 (TI_{Zn} ~ 1.5) and 192 (TI_{Zn} = 1). With regard to the lowest translocation indices, seven individuals in the 10% Zn treatment, namely Genotypes 4, 14, 30, 49, 63, 66 and 201A, had a translocation index < 0.2, with the lowest index observed in Genotype 14 (TI_{Zn} ~ 0.11). In the 30% Zn treatment, five individuals, namely Genotypes 6, 34, 51, 53 and 129, had a translocation index of < 0.4, with the lowest indices observed in Genotypes 6 and 51(TI_{Zn} ~ 0.28). Interestingly, the translocation index for Genotype 150 under the 30% Zn treatment was only ~ 0.85, compared with ~ 1.1 in the 10% treatment, indicating a differential response by this genotype to the two treatments.

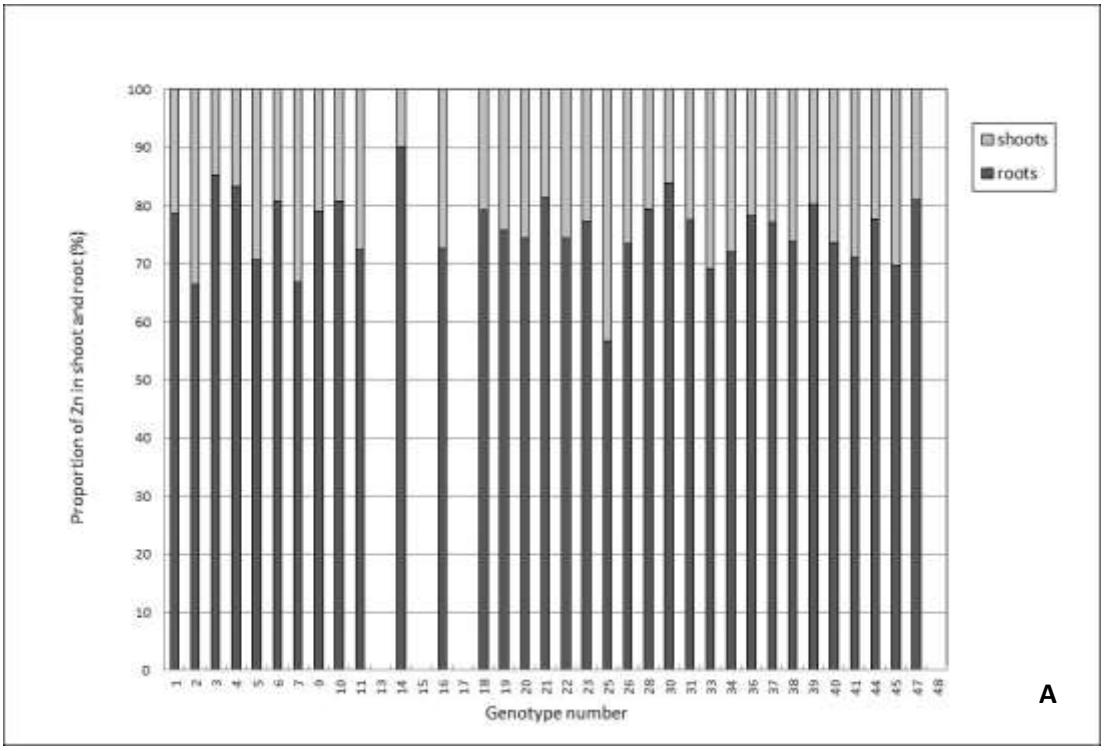

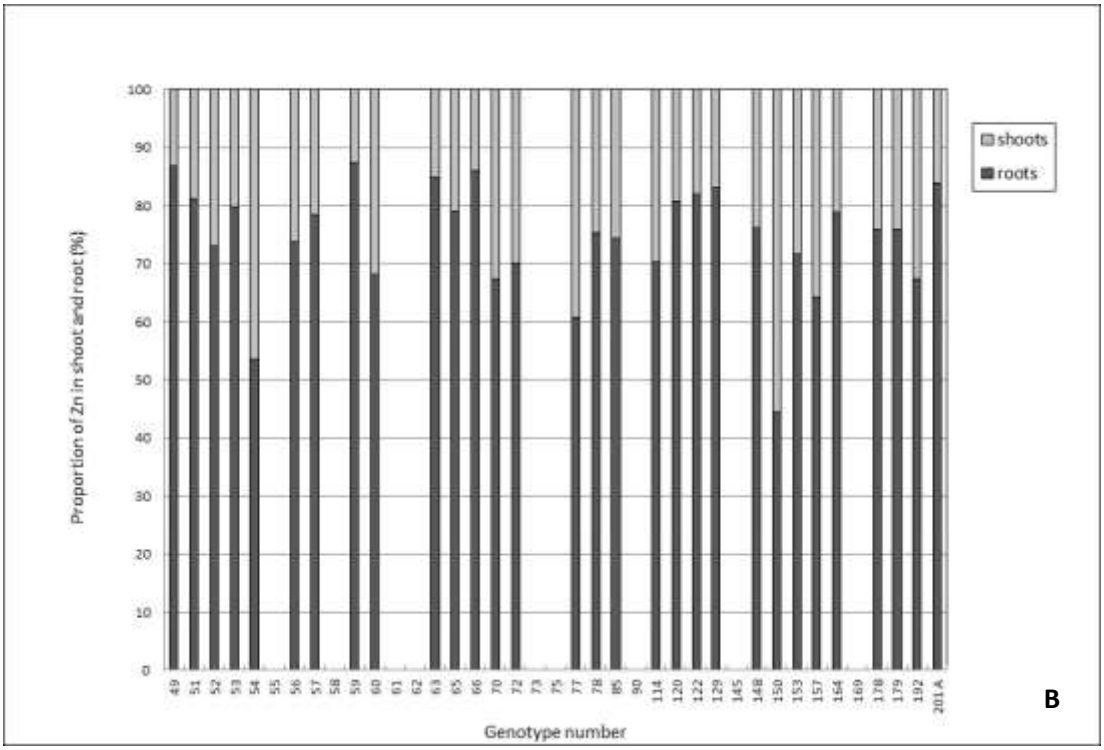

Figure 4.22 Relative partitioning of Zn between the roots and shoots of the surviving genotypes, after 16 weeks of growth under the 10% Zn treatment at final harvest. Data are split for clarity into A) Genotypes 1 – 48, and B) Genotypes 49 – 201A.

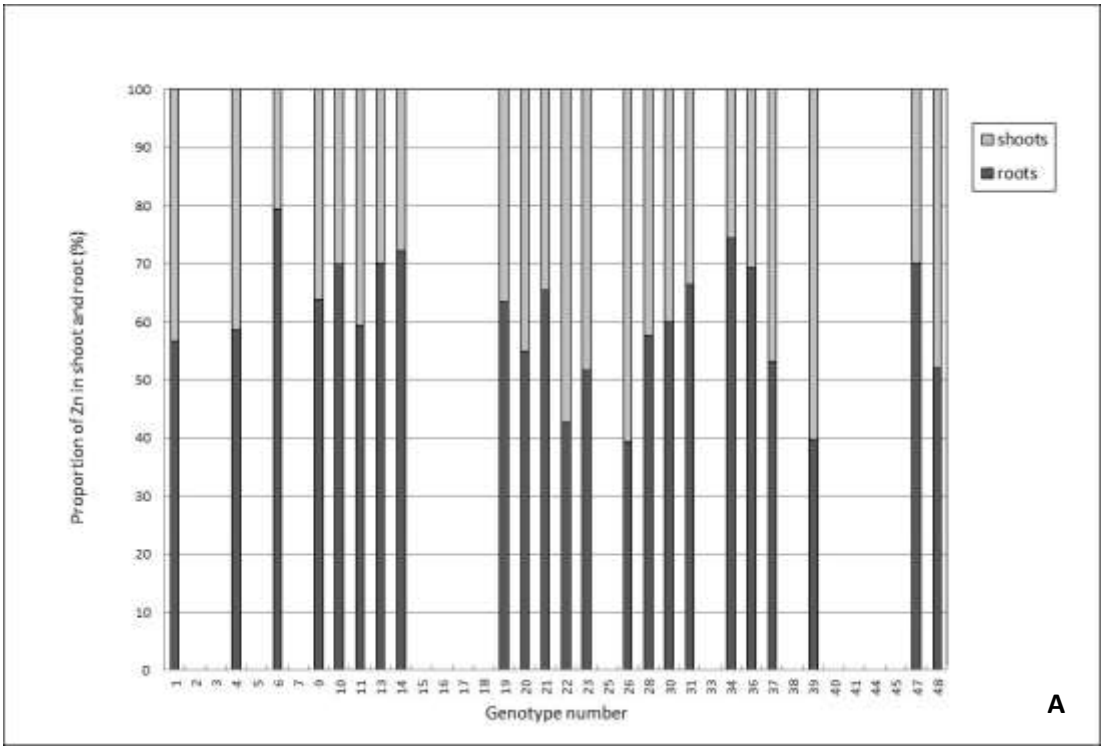

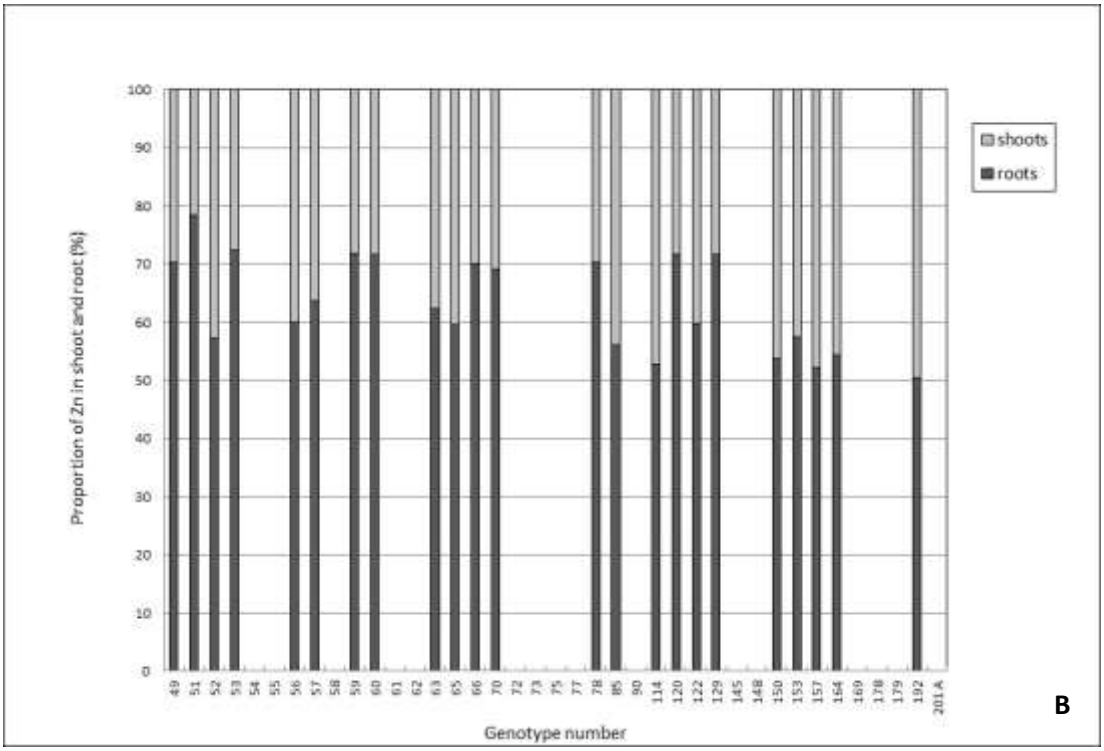

Figure 4.23 Relative partitioning of Zn between the roots and shoots of the surviving genotypes, after 16 weeks of growth under the 30% Zn treatment at final harvest. Data are split for clarity into A) Genotypes 1 – 48, and B) Genotypes 49 – 201A.

4.2 Pb Experiment 2

Experiment 2 was conducted between June and September 2010, using Pb-rich tailings collected from Darren Mine, and the background and methodology has been detailed in Chapter 3.

All of the plants survived in the control, 10% and 30% Pb treatments for the full 120 days' duration of the experiment. Inspection of the plants showed no visible signs of Pb toxicity such as chlorosis, stunted growth or die-back, even in the 30% Pb treatment (Plate 4.3), and all genotypes appeared to be very vigorous and healthy.

All samples were digested using the newly-developed rapid HNO_3 method described in Section 3.12 and analysed by AAS at DGES. The results for plant growth, Pb uptake and metal partitioning are variously displayed in this section as a series of bar charts and scatter plots, following the same framework used in Section 4.1. All results are the mean of two replicate pots (all original data are presented in Appendix 2), with standard deviations given as an average for each treatment in the legend of each bar chart (the full dataset is presented in Appendix 4). As for the Zn results, the 3 contaminant genotypes identified in 2012 (Section 4.1) have been removed from all datasets.

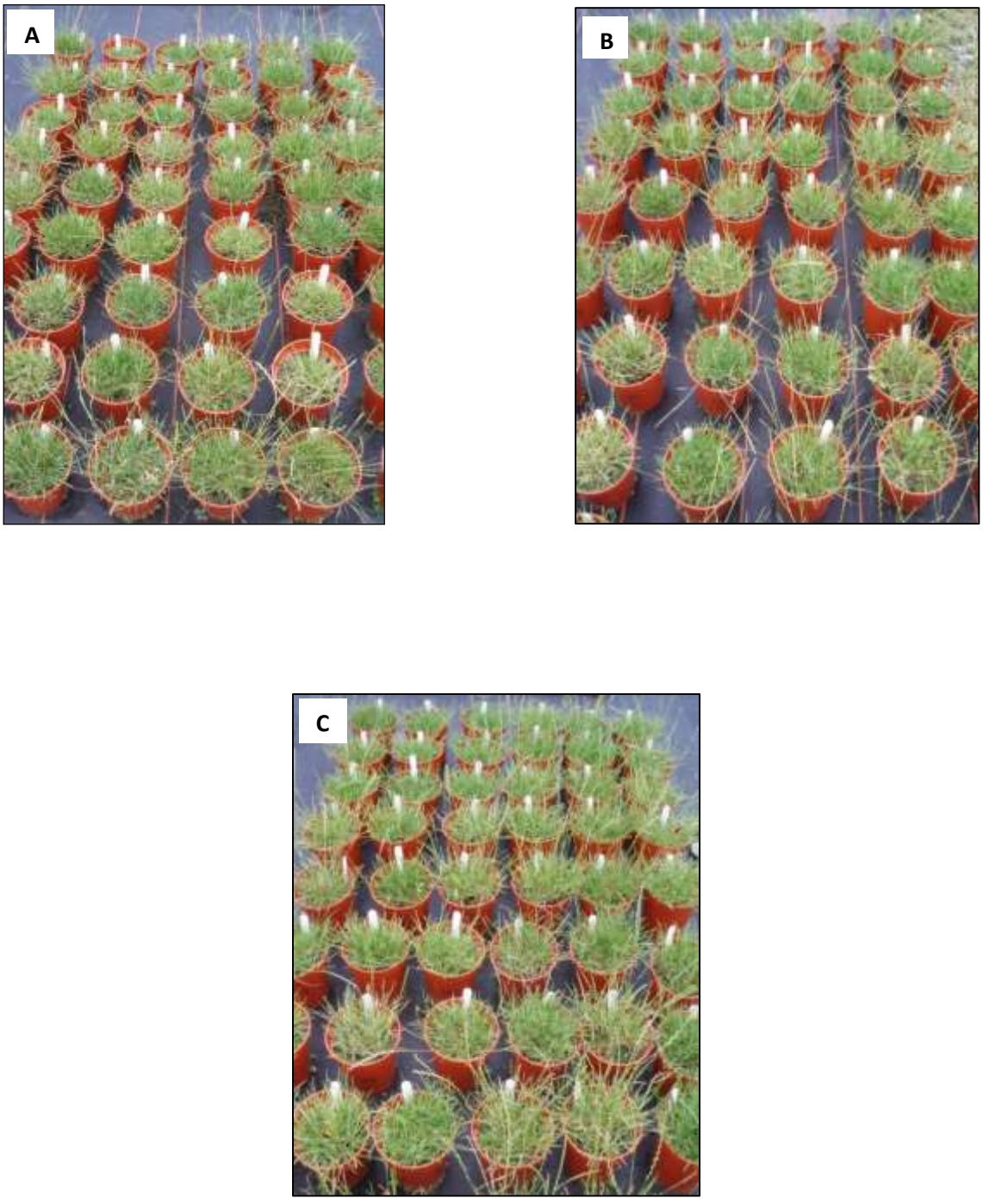

Plate 4.3 Plants growing in A) the control treatment, B) the 10% Pb treatment, and C) the 30% Pb treatment at final harvest. Note that all appear healthy and vigorous and none show any visible evidence of Pb toxicity.

4.2.1 Growth

After eight weeks of growth (Cut 1), the general trend across most genotypes was that shoot dry weight increased markedly as the Pb content in the growth medium increased (Figures 4.24 and 4.25). This trend is reflected by the mean shoot dry weights across the 77 genotypes, which were 0.172 g, 0.232 g and 0.316 g, respectively, for the controls, 10% and 30% Pb-contaminated treatments, with corresponding standard deviations (SDs) of 0.05, 0.05 and 0.06.

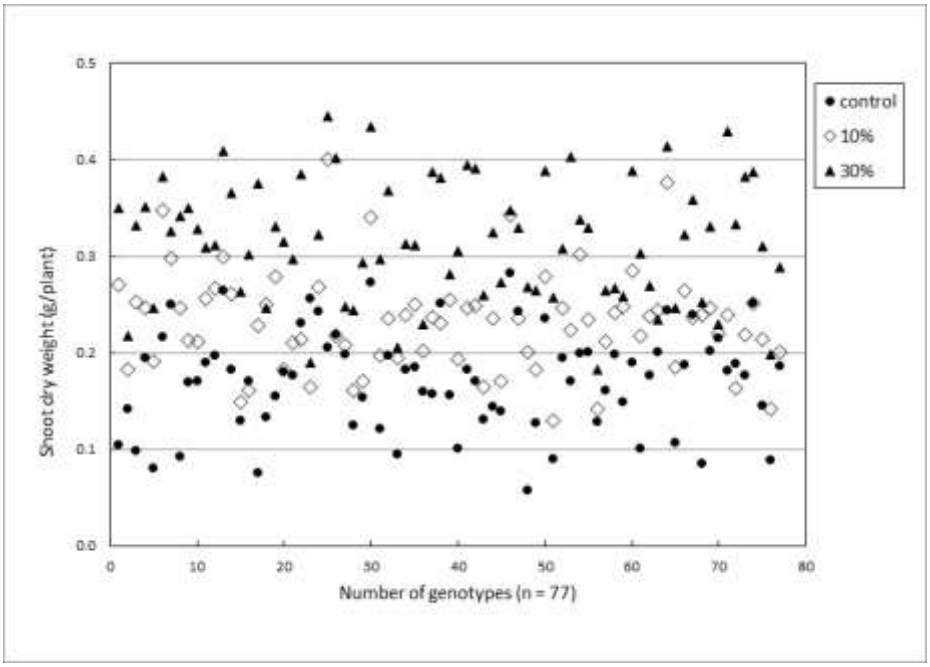

Figure 4.24 Shoot dry weights of 77 genotypes harvested at Cut 1, after 8 weeks of growth, under control, 10% or 30% Pb treatments.

Genotype 26 was the only exception to this trend (Figure 4.25), with a shoot dry weight in the 30% Pb treatment that was lower (0.19 g) than in the control treatment (0.25 g). Only two genotypes, namely 20 and 114, showed a greater shoot dry weight in the 10% Pb treatment than in the 30% treatment. Several individuals, including Genotypes 1, 3, 9, 19 51, 59 and 85, showed more than a three-fold increase in shoot dry weight in the 30% Pb treatment compared with the control treatment. Many others, for example Genotypes 11, 16, 21, 40, 47, 52, 53, 56, 65, 122, 148, 179 and 192, showed more than a two-fold increase in dry weight in the 30% Pb treatment, compared with the control treatment.

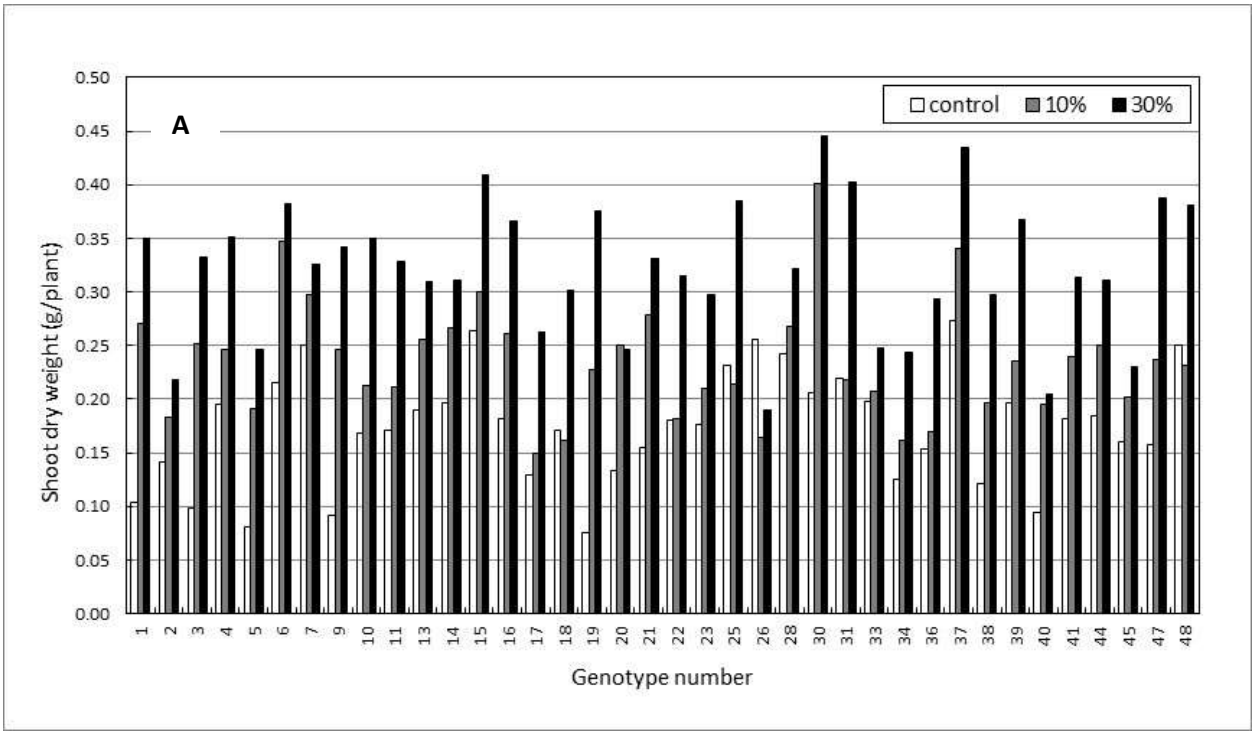

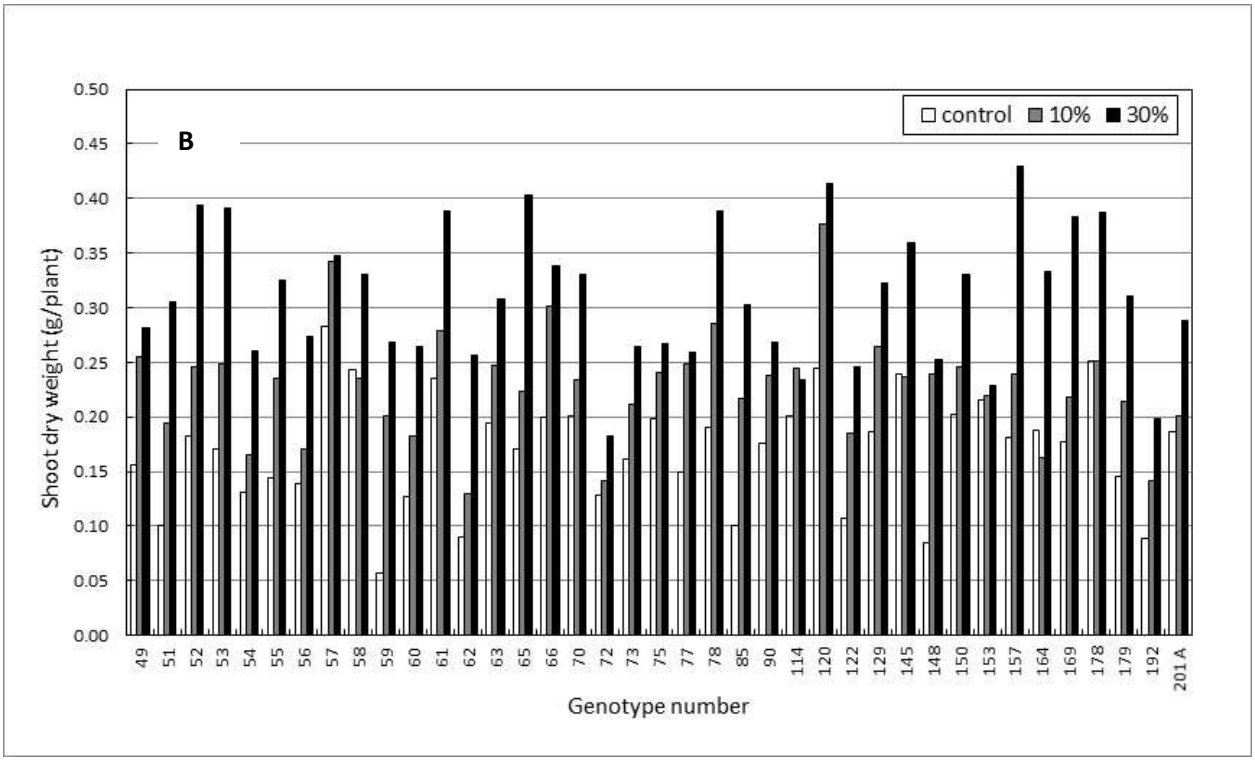

Figure 4.25 Shoot dry weights of 77 genotypes harvested at Cut 1, after 8 weeks of growth, under control, 10% or 30% Pb treatments. Data are split for clarity into A) Genotypes 1 – 48, and B) Genotypes 49 – 201A. Mean standard deviations are 0.04, 0.05 and 0.06 for control, 10% and 30% Pb treatments, respectively.

The general trend for shoot dry weights to increase with increasing Pb content of the growing medium continued to the final harvest, after 16 weeks of growth (Figure 4.26). Mean shoot dry weights across the 77 genotypes at final harvest were 1.11 g, 1.25 g and 1.41 g, respectively, for the control, 10% and 30% Pb treatments, with corresponding SDs of 0.31, 0.24 and 0.20.

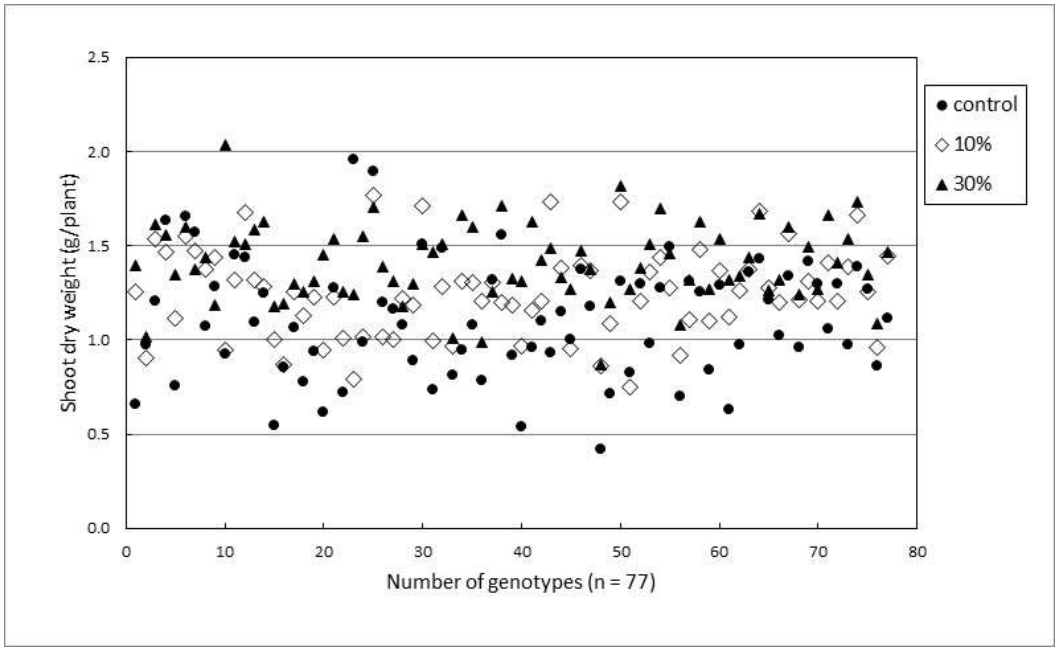

Figure 4.26 Shoot dry weights of 77 genotypes harvested after 16 weeks of growth, under control, 10% or 30% Pb treatments.

The wide variation in final shoot dry weight across the genotypes, together with the inconsistencies in this variation between the treatments, are illustrated in Figure 4.27. Shoot dry weights of Genotypes 11, 17, 22 and 77 at final harvest were twice those of the control plants, with Genotype 11 having the greatest shoot dry weight at > 2.0 g/plant. Several genotypes, namely 7, 10, 14, 30, 34, 37, 45, 47, 54, 55, 120 and 122, had greater shoot dry weights in the 10% Pb treatment at final harvest compared with the 30% Pb treatment. In contrast, six genotypes, namely 4, 6, 7, 26, 30 and 70, had greater shoot dry weights in the control treatment at final harvest compared with either the 10% or 30% Pb treatments. Of these, only Genotype 26 had a higher shoot dry weight in the control treatment at Cut 1 (Figure 4.25), the remaining five having their highest shoot dry weights in the 30% Pb treatment at Cut 1. Genotype 30 is also notable for having the greatest shoot dry weight of all the genotypes under the 30% Pb treatment after 8 weeks of growth, although this was not the case after 16 weeks of growth.

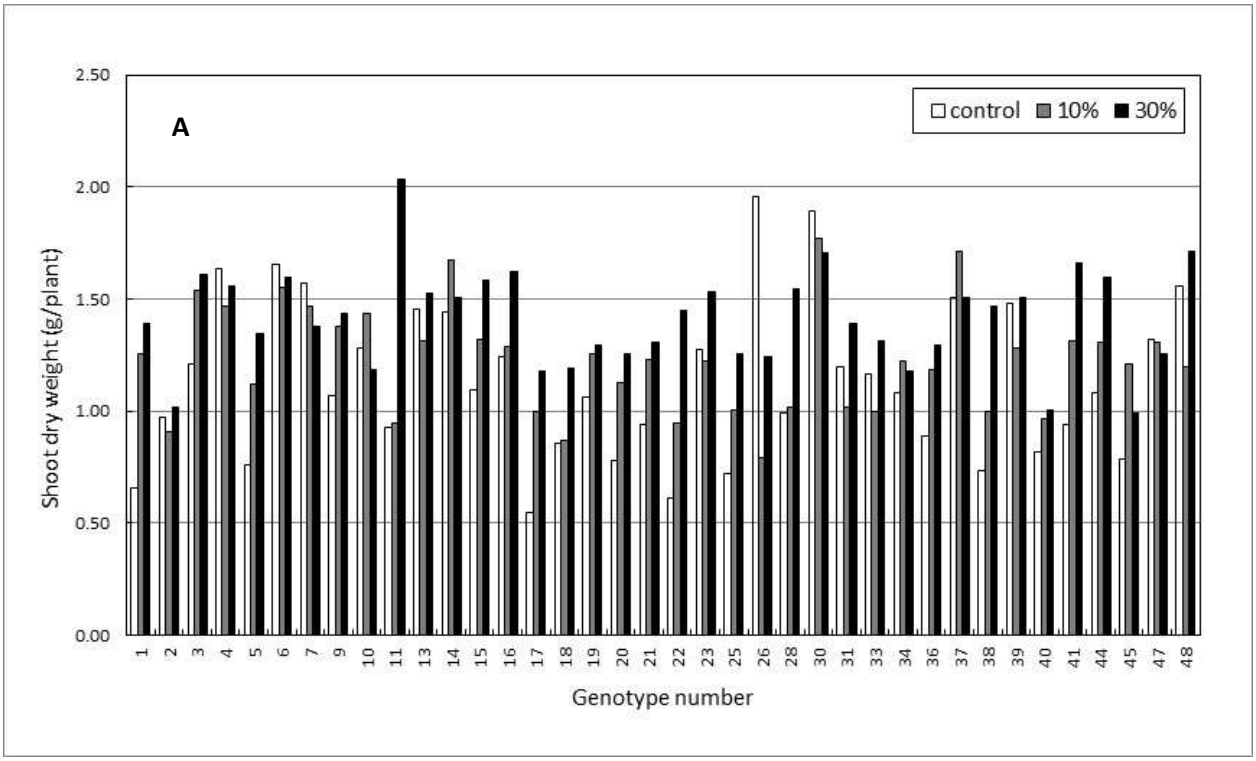

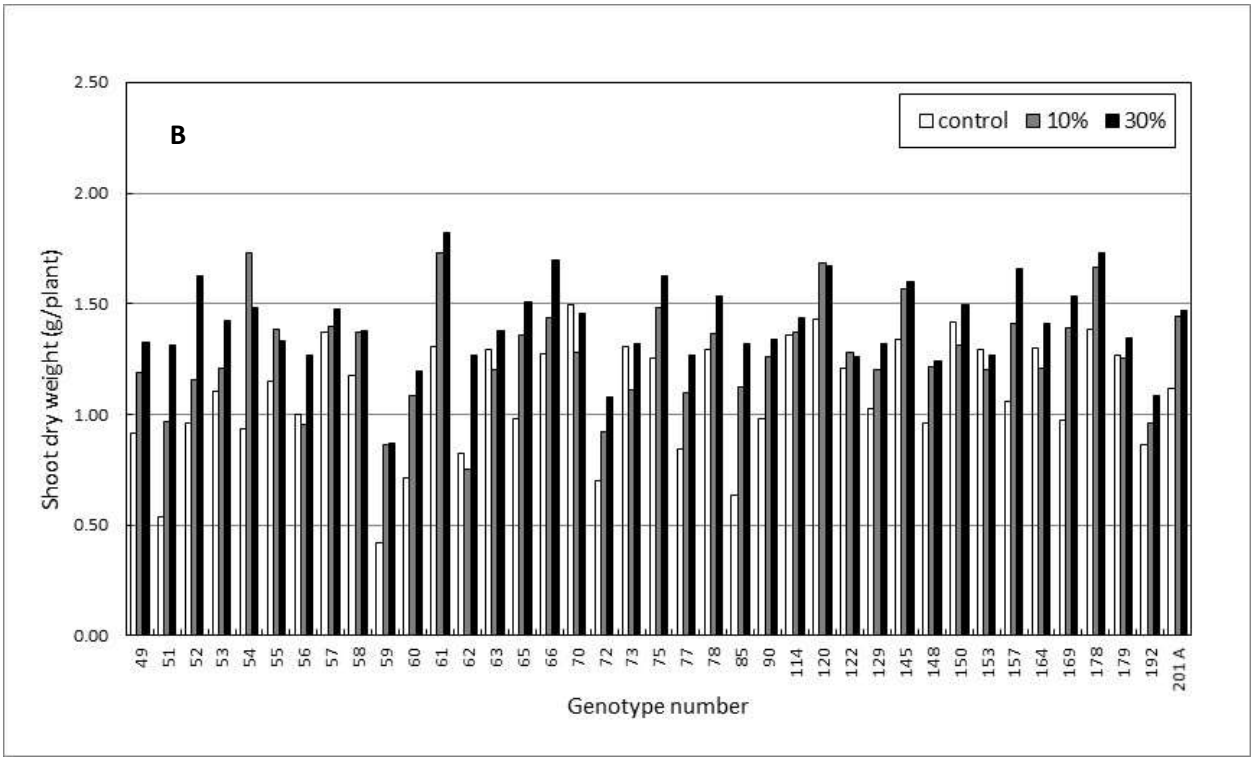

Figure 4.27 Shoot dry weights of 77 genotypes harvested after 16 weeks of growth, under control, 10% or 30% Pb treatments. Data are split for clarity into A) Genotypes 1 – 48, and B) Genotypes 49 – 201A. Mean standard deviations are 0.24, 0.17 and 0.17 for control, 10% and 30% Pb treatments, respectively.

The general trend for root dry weight to increase as Pb content of the growing medium increased was similar to that observed for shoot dry weight (Figure 4.28). Mean root dry weights across the 77 genotypes at final harvest, after 16 weeks of growth, were 0.69 g, 0.93 g and 1.07 g, respectively, under control, 10% and 30% Pb treatments, with corresponding SDs of 0.27, 0.22, and 0.25. However, root dry weight showed wide variation across the genotypes within each treatment, displaying more than a two-fold variation in the case of the 10% and 30% Pb treatments.

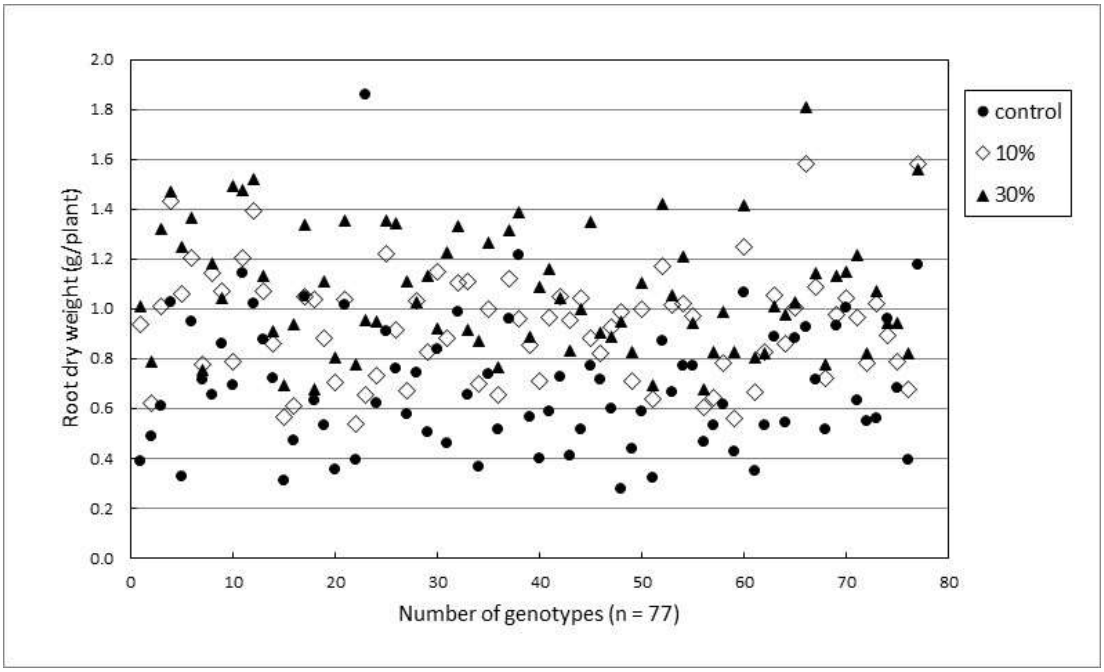

Figure 4.28 Root dry weights of 77 genotypes at final harvest, after 16 weeks of growth, under control, 10% or 30% Pb treatments.

Figure 4.29 highlights the variability in root growth across the range of genotypes and confirms that, in the majority of cases, root dry weight increased as Pb concentration in the growth medium increased. Genotype 26 was a notable exception, with a root dry weight of 1.90 g/plant in the control treatment, but only 0.95 g/plant in the 30% Pb treatment. This genotype also had a greater shoot dry weight in the control treatment than in the 30% Pb treatment (Figure 4.27). Several genotypes, namely 7, 10, 20, 34, 37, 40, 53, 54, 55, 58, 59, 70, 90, 114 and 201A, had higher root dry weights under the 10% treatment compared with the 30% Pb treatment.

However, in all these cases, other than Genotype 20, the differences in root dry weights between treatments were small.

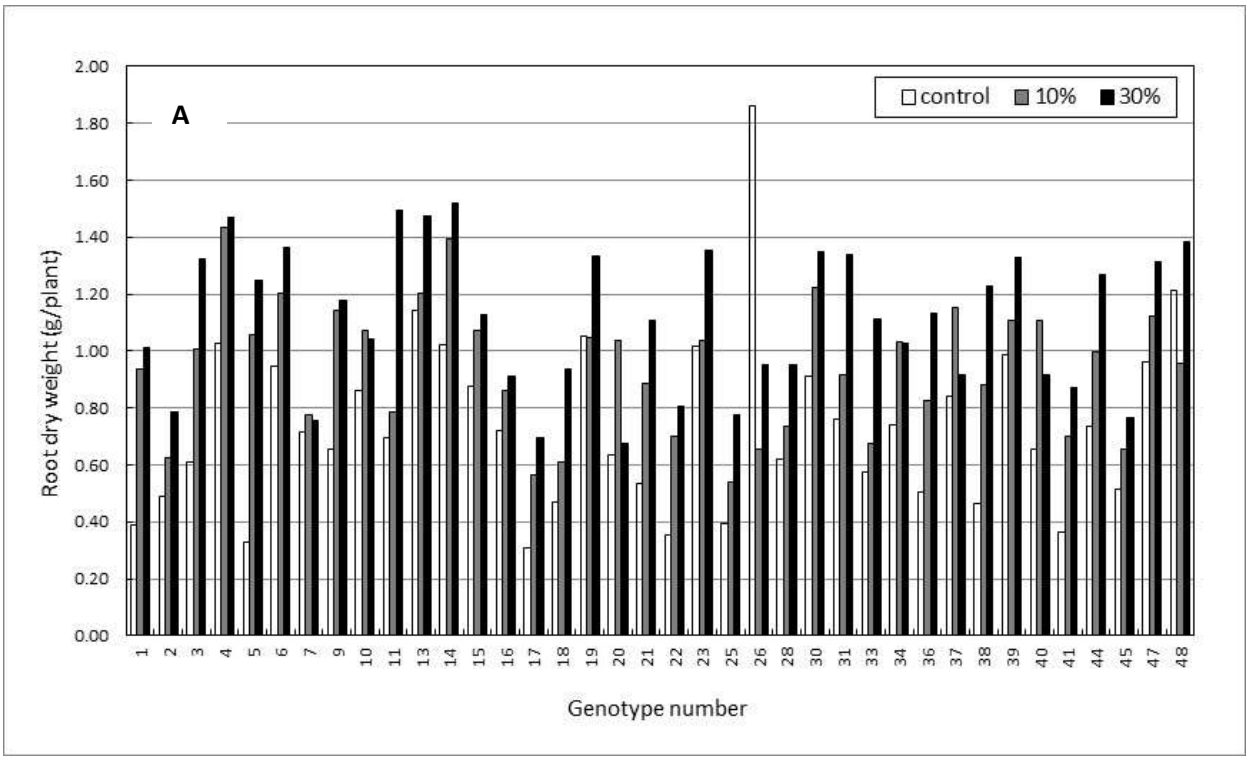

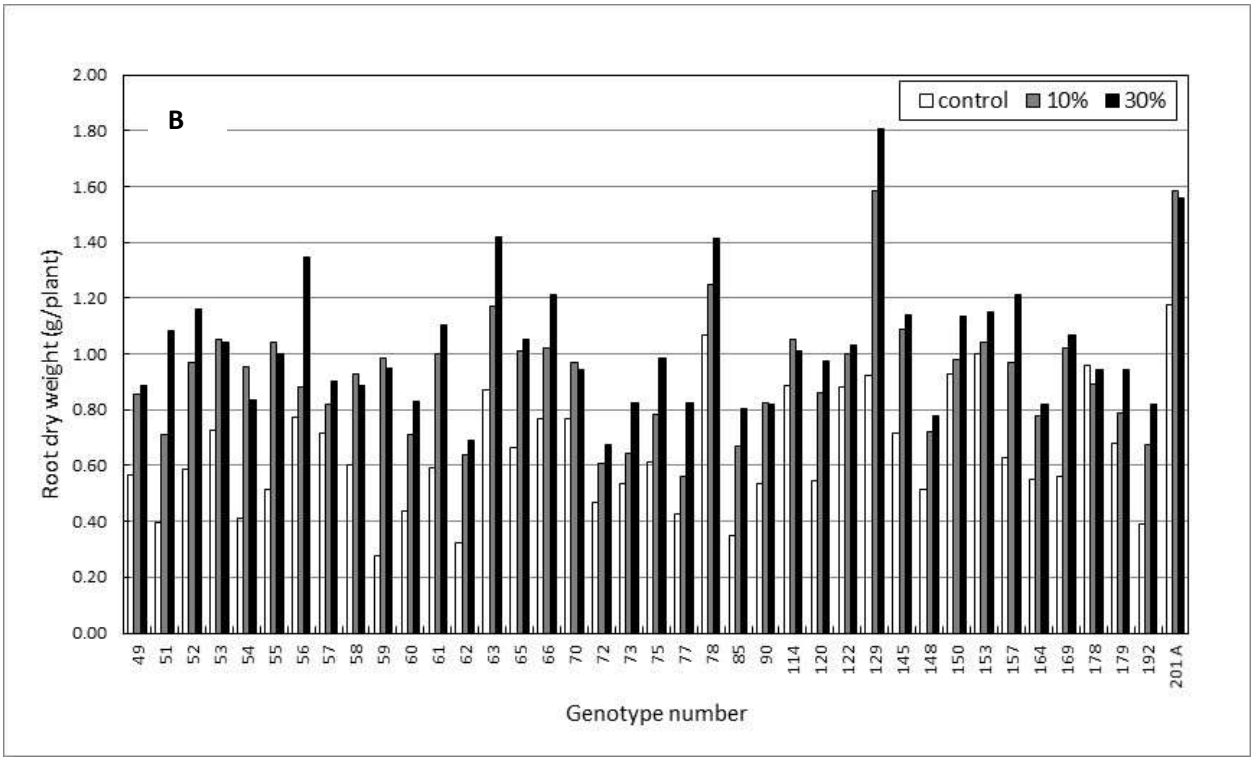

Figure 4.29 Root dry weights of 77 genotypes harvested after 16 weeks of growth, under control, 10% or 30% Pb treatments. Data are split for clarity into A) Genotypes 1 – 48, and B) Genotypes 49 – 201A. Mean standard deviations are 0.16, 0.15 and 0.11 for control, 10% and 30% Pb treatments, respectively.

Regression plots of total plant dry weight (i.e. roots plus shoots) at final harvest under the 10% (Figure 4.30) and 30% Pb (Figure 4.31) treatments against plant dry weights in the control treatment, an important index of tolerance (*sensu* Macnair, 1993), show the range of performance and Pb tolerance across the genotypes. Nearly all genotypes produced more dry matter in the 10% Pb treatment compared with the control plants. However, there was only a weak positive correlation between total plant dry weights at 10% Pb and those of the control plants ($R^2 \sim 0.29$). The relationship between total plant dry weights at 30% Pb and those of the control plants (Figure 4.31) was similar ($R^2 \sim 0.28$) but slightly more acute.

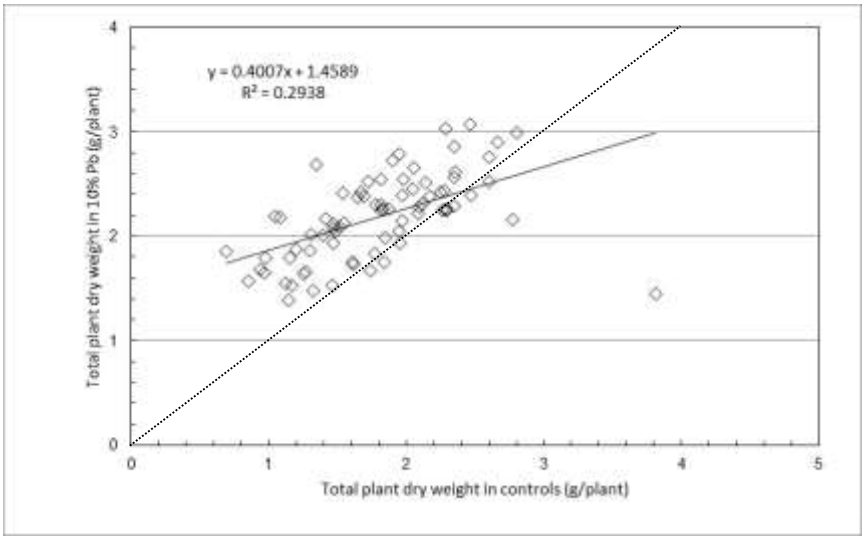

Figure 4.30 Relationship between total plant dry weights of the 77 genotypes in the 10% Pb treatment and under control conditions, at final harvest after 16 weeks of growth. The straight line is the linear regression for the data, whilst the dotted line is the 1:1 line (i.e. gradient = 1).

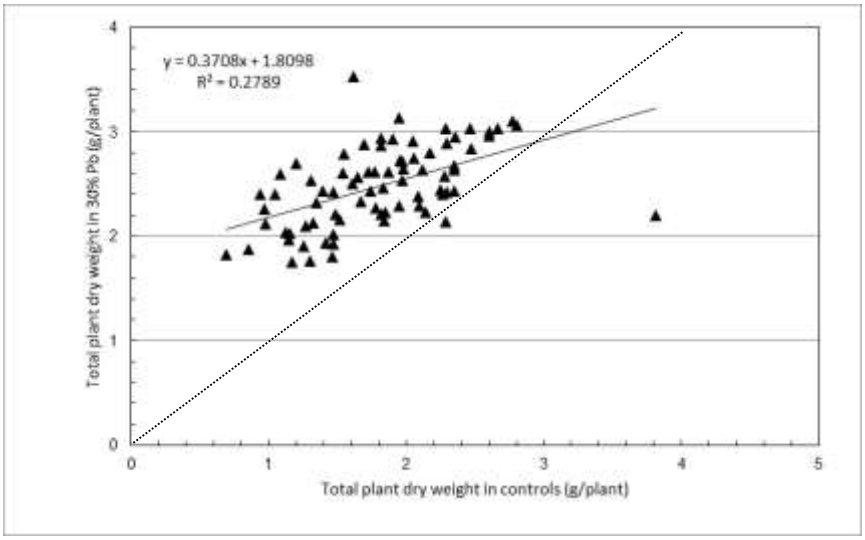

Figure 4.31 Relationship between total plant dry weights of the 77 genotypes in the 30% Pb treatment and under control conditions, at final harvest after 16 weeks of growth. The straight line is the linear regression for the data, whilst the dotted line is the 1:1 line (i.e. gradient = 1).

Figure 4.32 shows a moderate correlation between total plant dry weights in the in the 10% and 30% Pb treatments, as evidenced by an R^2 value of ~ 0.4. The plot clearly reveals that most genotypes in the 30% Pb treatment produced more biomass than in the 10% Pb treatment, with the majority plotting above the 1:1 gradient line.

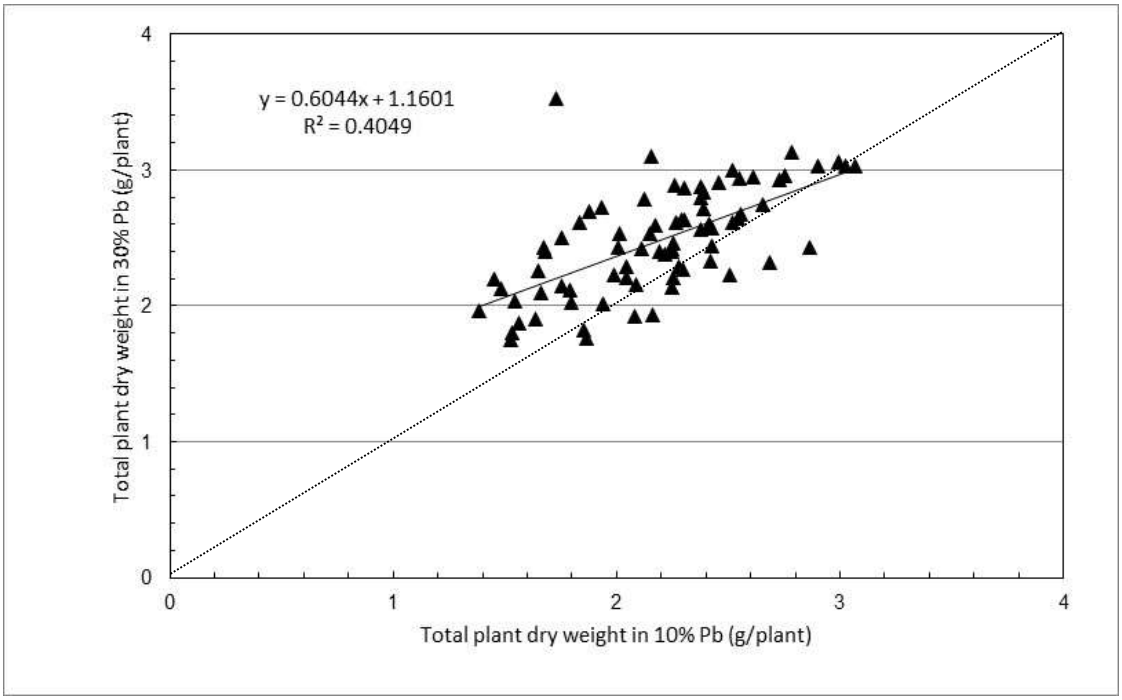

Figure 4.32 Relationship between total plant dry weights of the 77 genotypes in the 30% Pb treatment and under the 10% Pb treatment, at final harvest after 16 weeks of growth. The straight line is the linear regression for the data, whilst the dotted line is the 1:1 line (i.e. gradient = 1).

The results for tiller production contrast with those for dry matter production, in so far as the effect of the Pb treatments on the final number of tillers produced after 16 weeks of growth was inconsistent (Figure 4.33). Mean tiller numbers across the 77 genotypes at final harvest were 30.3, 31 and 35, respectively, in the control, 10% and 30% Pb treatments. However, these values mask wide variation in response amongst the genotypes, as shown in Figure 4.34.

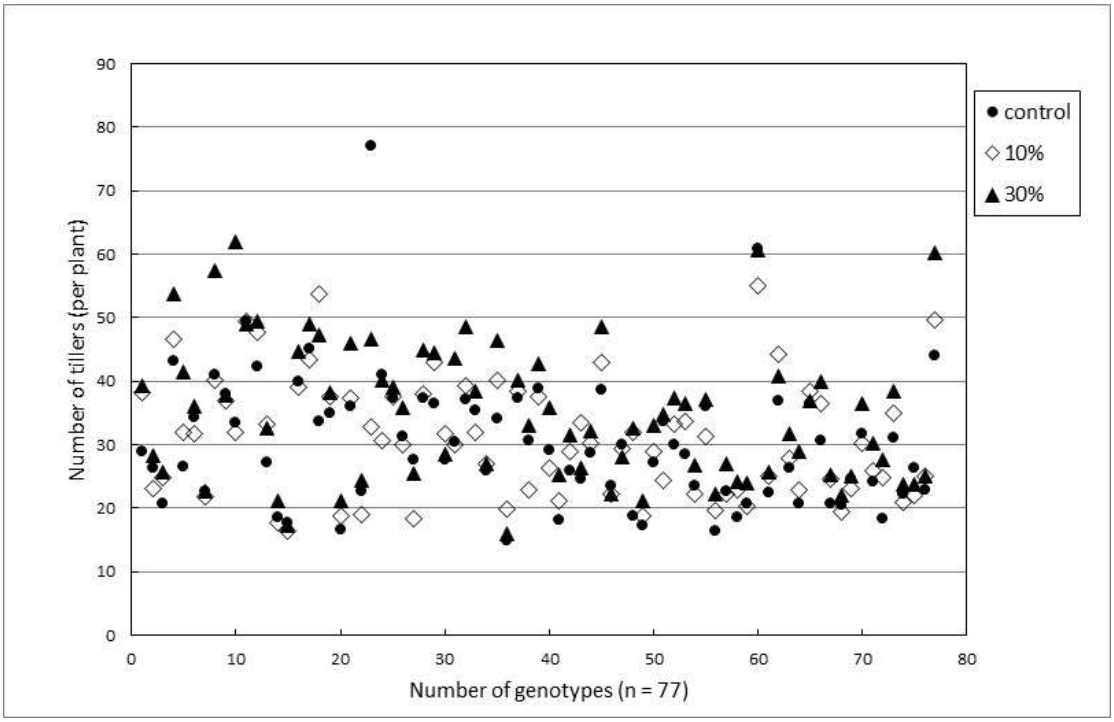

Figure 4.33 Tiller numbers for 77 genotypes at final harvest, after 16 weeks of growth under control, 10% Pb or 30% Pb treatments.

Three genotypes, namely 11, 78 and 201A, produced ≥ 60 tillers in the 30% Pb treatment, whilst a further 18 genotypes produced ≥ 40 tillers (Figure 4.34). In general, higher numbers of tillers were produced under the 30% Pb treatment compared with the 10% Pb treatment. However, Genotypes 15, 20, 37, 41, 45, 54, 58, 90 and 122 were exceptions to this rule, although in each case the differences were small. Genotype 26 was unusual, having produced the highest number of tillers (77) in the control treatment, whilst only 33 and 47 tillers, respectively, under the 10% and 30% Pb treatments. Figure 4.35 shows a strong linear relationship between tiller numbers in the 10% and 30% Pb treatments, as evidenced by a moderately high R^2 value of ~ 0.76, with most genotypes plotting either on or close to the 1:1 gradient line.

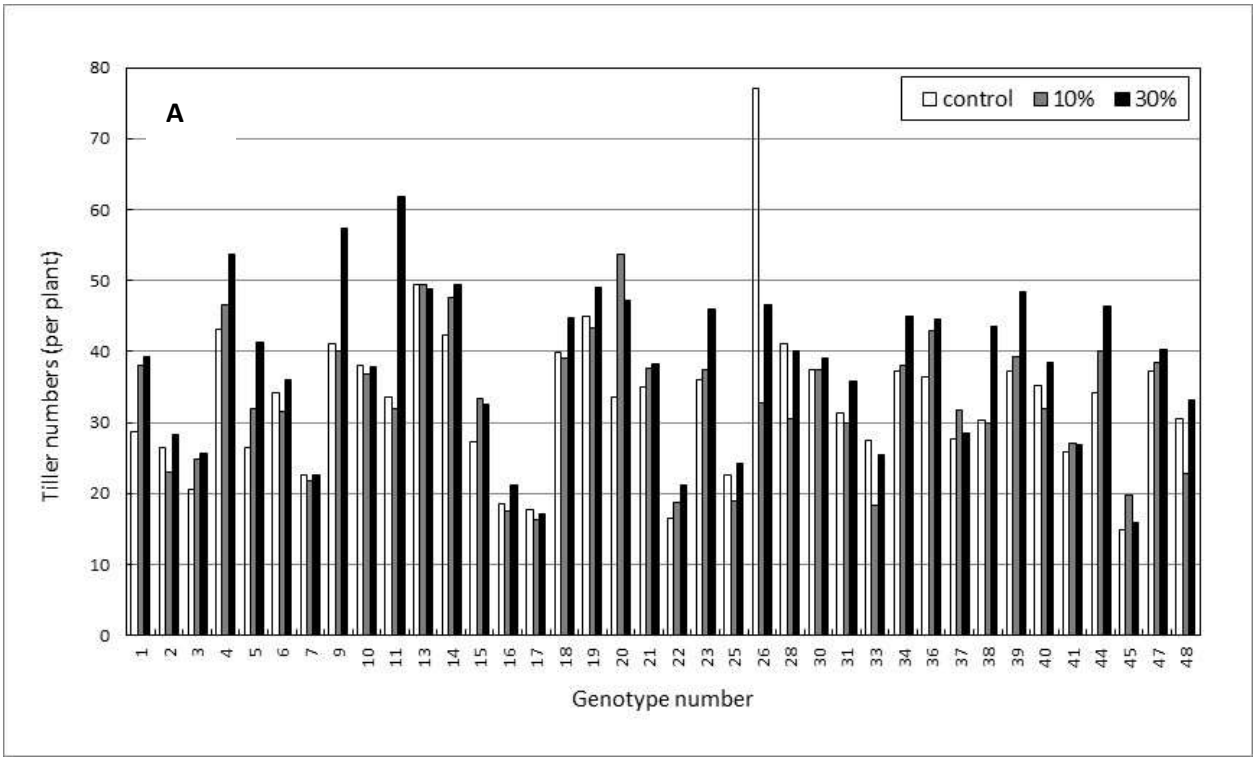

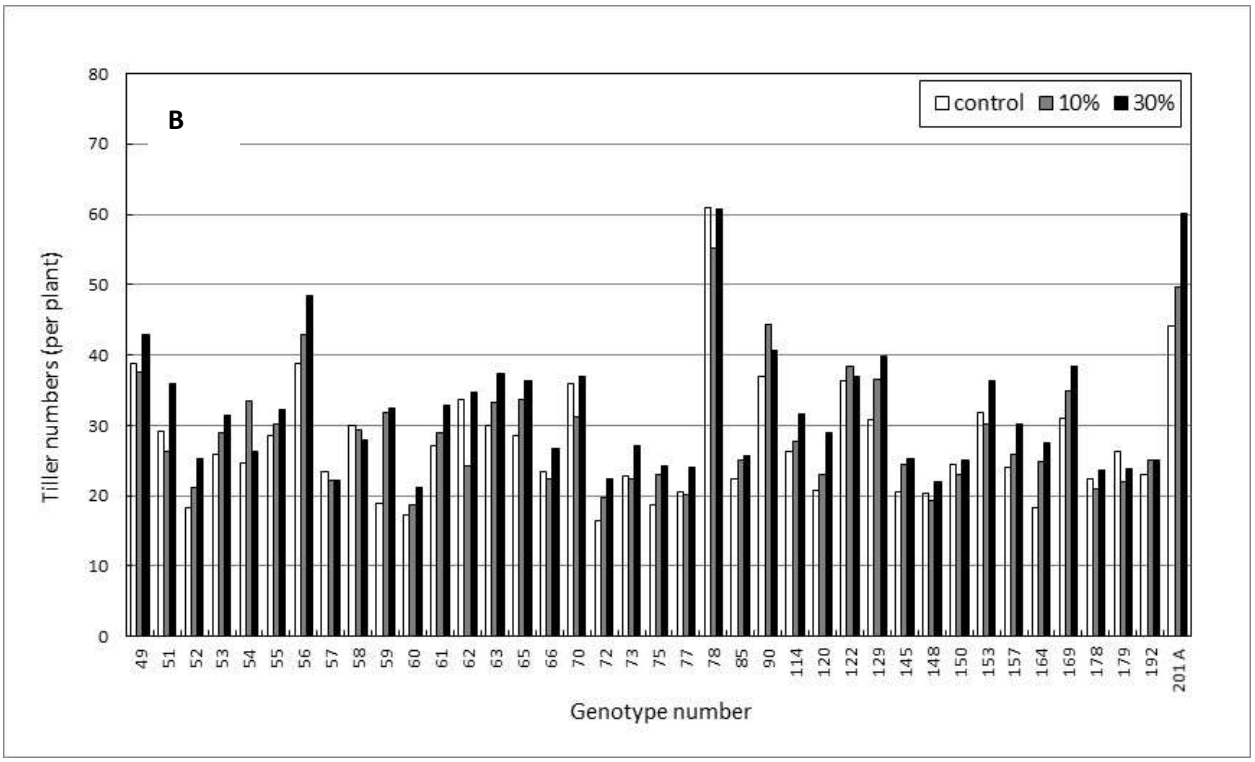

Figure 4.34 Comparison of tiller numbers of 77 genotypes harvested after 16 weeks of growth, under control, 10% or 30% Pb treatments. Data are split for clarity into A) Genotypes 1 – 48, and B) Genotypes 49 – 201A. Mean standard deviations are 3.6, 3.7 and 3.9 for control, 10% and 30% Pb treatments, respectively.

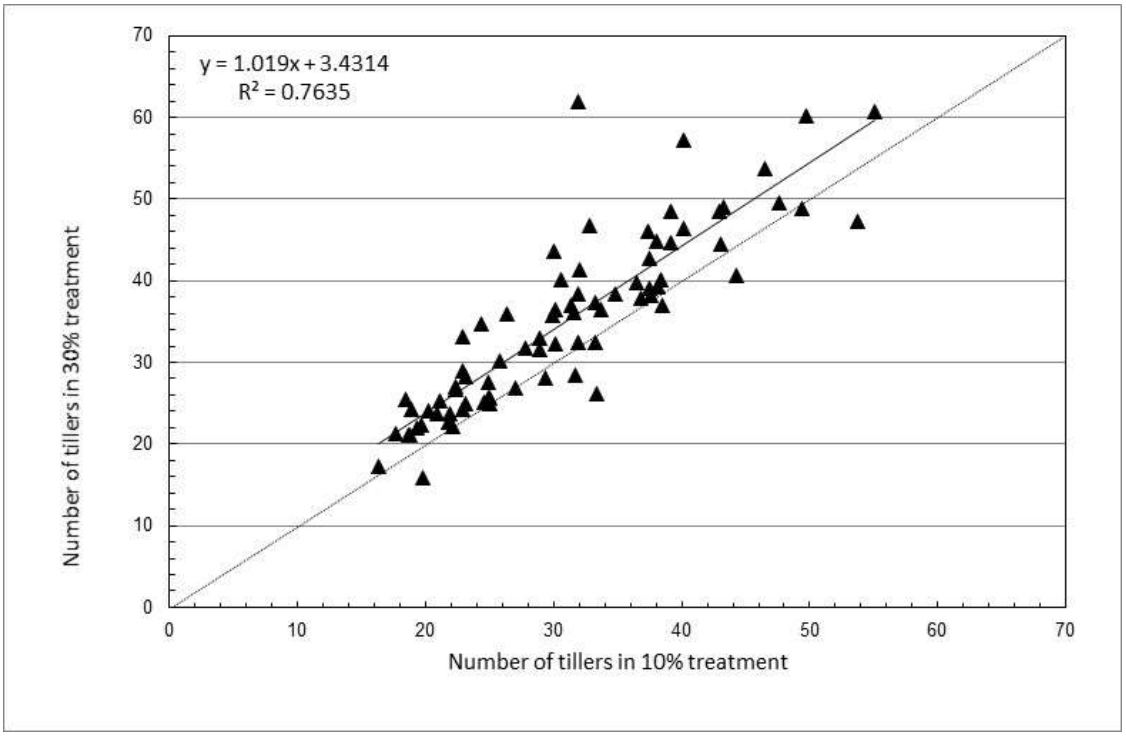

Figure 4.35 Relationship between tiller numbers in the 10% and 30% Pb treatments. The straight line is the linear regression for the data, whilst the dotted line is the 1:1 line (i.e. gradient = 1).

The relationship between tiller numbers and shoot dry weights at final harvest was surprisingly weak across the 77 genotypes (Figure 4.36). Linear regressions fitted to the data showed little or no correlation, with R^2 values of only ~ 0.15, 0.02 and 0.02, respectively, in the control, 10% Pb and 30% Pb treatments. Inspection of the data for the 10% and 30% Pb treatments shows that for any given shoot dry weight in the range 1.0 – 1.6 g/plant, there was as much as a three-fold variation in the number of tillers produced.

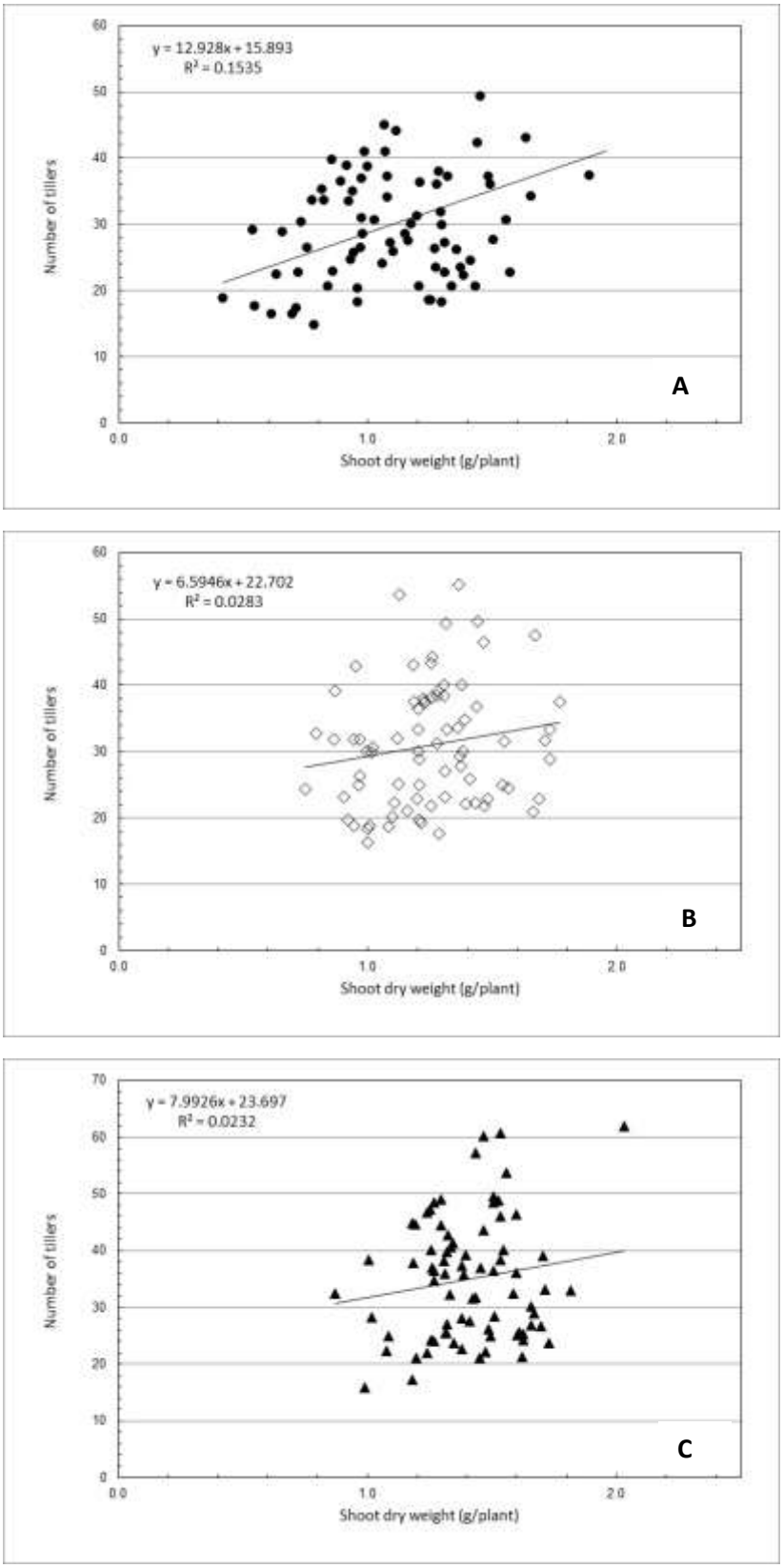

Figure 4.36 Scatter plots showing the relationship between shoot dry weights and numbers of tillers produced by the 77 genotypes at final harvest in A) the control, B) 10% Pb treatment, and C) the 30% Pb treatments. Straight lines are the linear regressions for the data.

4.2.2 Pb uptake and partitioning

As in the experiment with Zn-rich tailings, the inclusion of the intermediate Cut 1 harvest after 8 weeks of growth provided a way of assessing the intermediate responses to the treatments in terms of Pb uptake, albeit not on the basis of total uptake of Pb by the plant. The variation in the Pb content of the harvested shoot fraction at 8 weeks is shown in Figure 4.37. The mean Pb content of this fraction across all genotypes was 50.1 µg Pb/plant in the 10% Pb treatment and 138.8 µg Pb/plant in the 30% Pb treatment. Pb was undetectable in the harvested shoot fraction of the control plants. At this stage all genotypes had higher shoot contents of Pb in the 30% Pb treatment compared with the 10% Pb treatment. The difference was more than seven-fold for Genotypes 1, 3, 4, 9, 25, 31, 47, 48, 52, 53, 54, 56, 65 and 164. Genotypes 1 and 31 had the highest shoot contents of Pb, in the 30% Pb treatment, at > 60 µg/plant, whilst a further 11 genotypes, namely 4, 10, 16, 30, 47, 48, 53, 65, 150, 178 and 201A, had Pb contents of ≥ 50 µg/plant.

The Pb content of the shoots at final harvest, after 16 weeks of growth, is shown in Figure 4.38. As expected, all genotypes had a higher Pb content at final harvest compared with Cut 1. Likewise, shoot Pb content was higher under the 30% Pb treatment compared with the 10% Pb treatment, by a factor of between two- and six-fold (Figure 4.39). Genotype 38 showed the greatest proportional increase in Pb content with increasing level of Pb treatment, and had the highest shoot content of Pb (> 260 µg/plant) under the 30% Pb treatment. Genotypes 30, 66, and 157 contained ~ 200 µg/plant and a further 25 genotypes had a shoot Pb content ≥ 150 µg/plant. Figure 4.40 demonstrates that shoot Pb content at final harvest was poorly correlated with shoot dry weights across the 77 genotypes, in both the 10% (R^2 ~ 0.34) and 30% (R^2 ~ 0.28) Pb treatments.

The Pb content of the roots of all genotypes was much higher under the 30% Pb treatment compared with the 10% Pb treatment at final harvest (Figure 4.41). The highest recovery of Pb in the roots was recorded in Genotype 30, at 5,000 µg/plant, whilst the roots of four other genotypes, namely 4, 39, 78 and 129, contained > 3,000 µg/plant. Genotype 30 also displayed the highest differential between the 10% and 30% Pb treatments, with a 10-fold increase in root content of Pb. There was a reasonable positive linear correlation between the Pb content of the roots and root dry weight across the 77 genotypes (Figure 4.42) in both the 10% (R^2 ~ 0.58) and 30% (R^2 ~ 0.52) Pb treatments. In both cases the correlation was closer than observed for

shoot content of Pb (Figure 4.40), but not as close as observed for root Zn content in Zn Experiment 1 (see Figure 4.17).

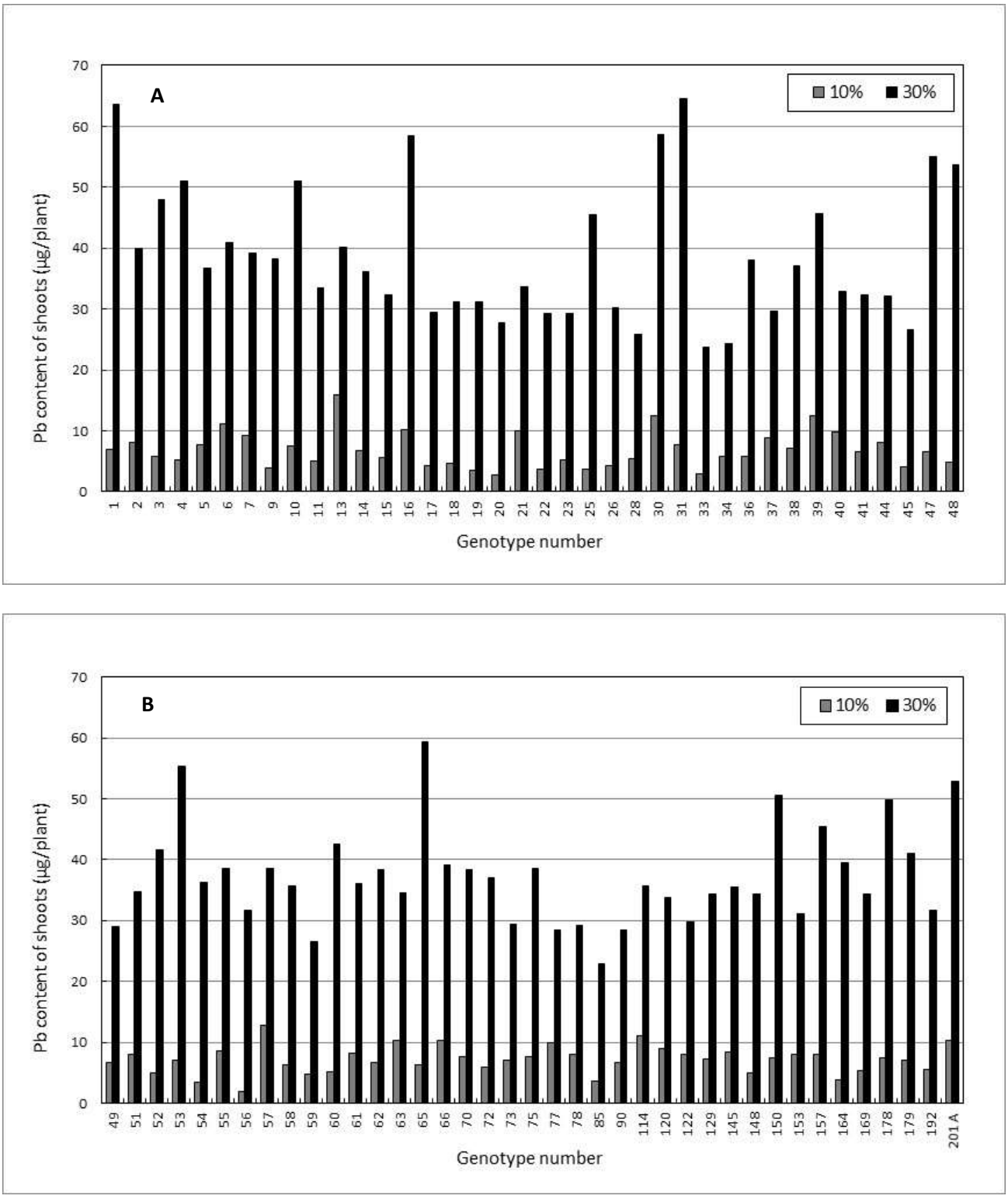

Figure 4.37 Comparison of the Pb content of the shoots, expressed as µg/plant, for 77 genotypes, harvested after 8 weeks of growth under 10% or 30% Pb treatments. Data are split for clarity into A) Genotypes 1 – 48, and B) Genotypes 49 – 201A. Mean standard deviations are 2.3 and 10.8 for the 10% and 30% Pb treatments, respectively.

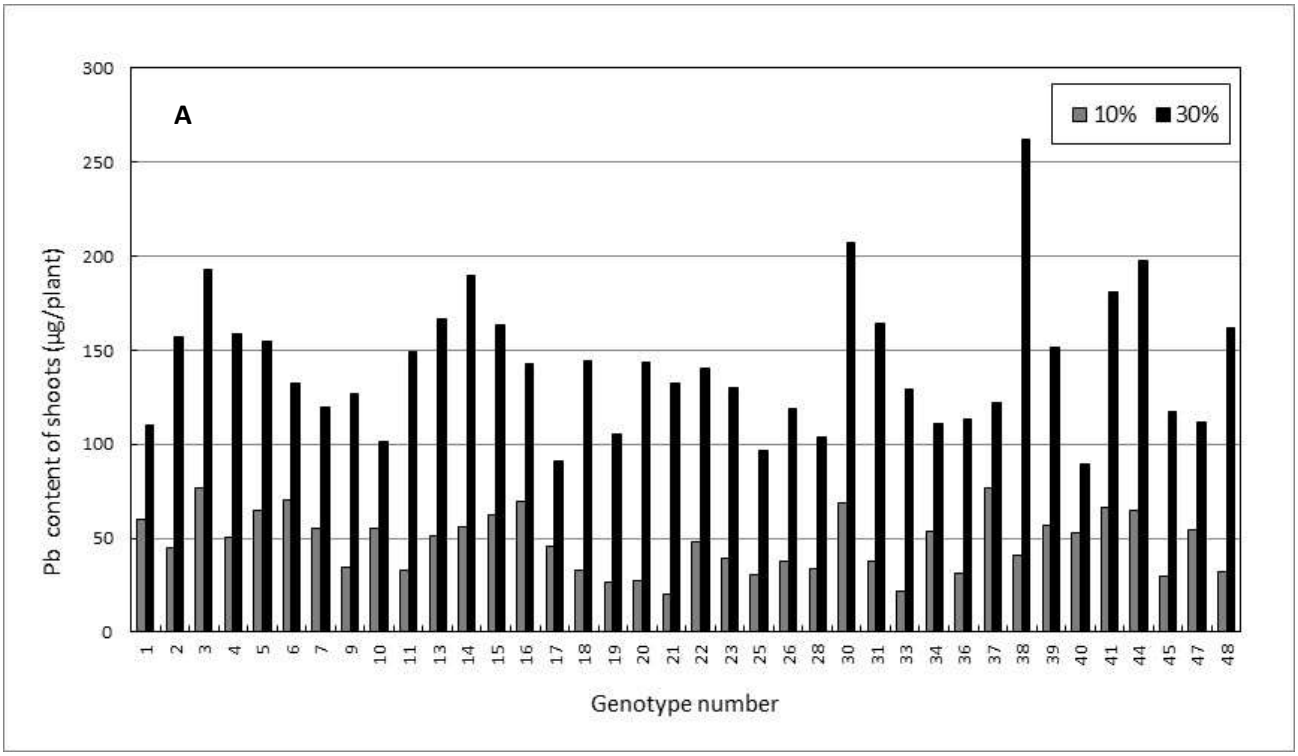

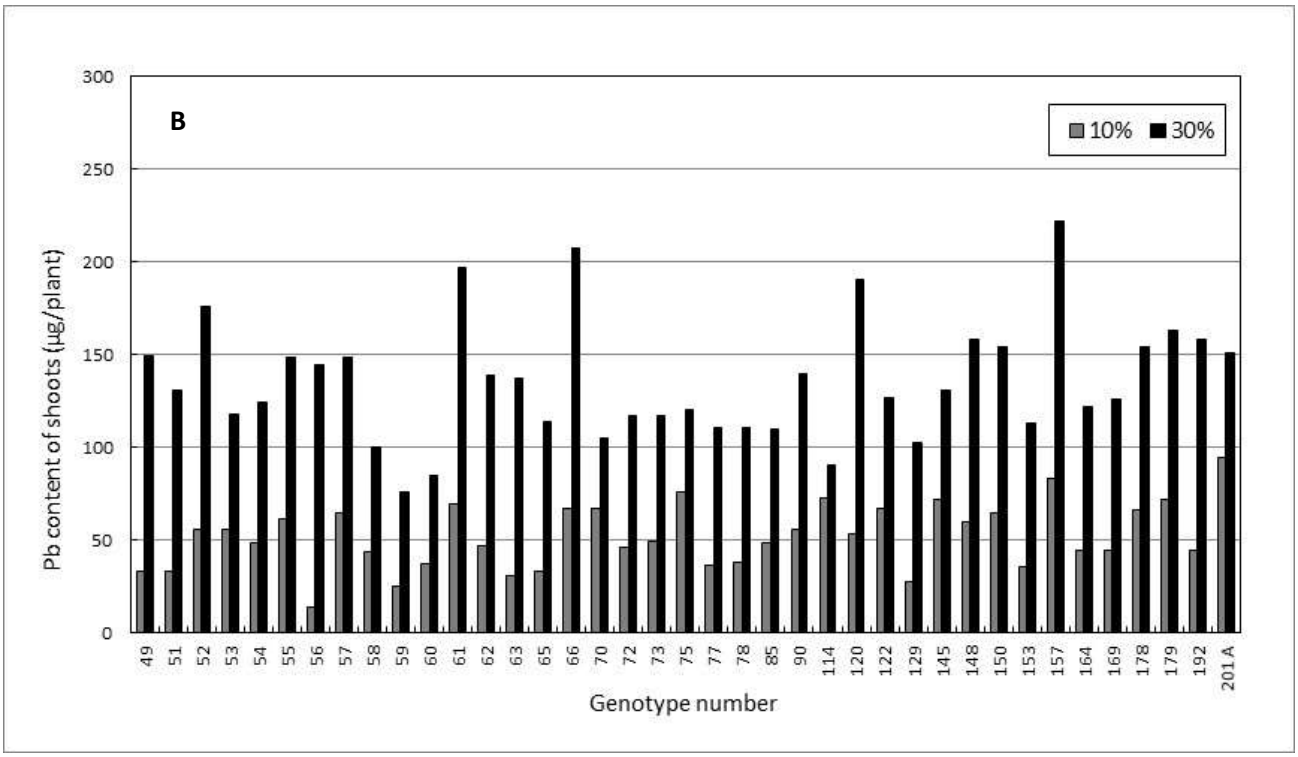

Figure 4.38 Comparison of the Pb content of the shoots, expressed as µg/plant, for 77 genotypes, harvested after 16 weeks of growth under 10% or 30% Pb treatments. Data are split for clarity into A) Genotypes 1 – 48, and B) Genotypes 49 – 201A. Mean standard deviations are 14.5 and 29.4 for the 10% and 30% Pb treatments, respectively.

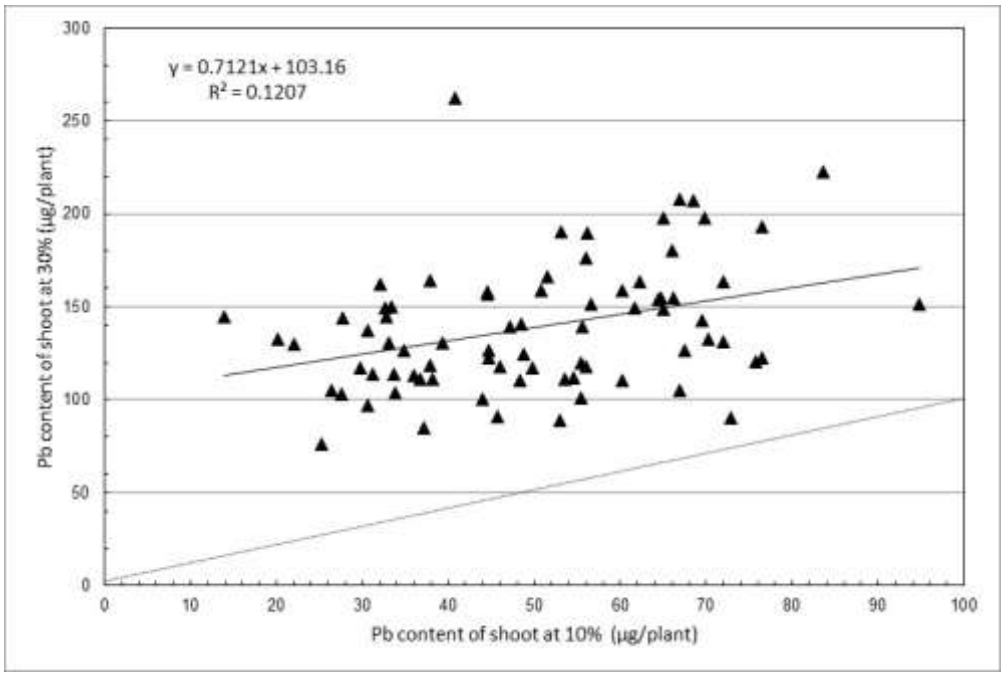

Figure 4.39 Relationship between Pb content of the shoots in the 10% and 30% Pb treatments at final harvest after 16 weeks of growth. The straight line is the linear regression for the data, whilst the dotted line is the 1:1 line (i.e. gradient = 1).

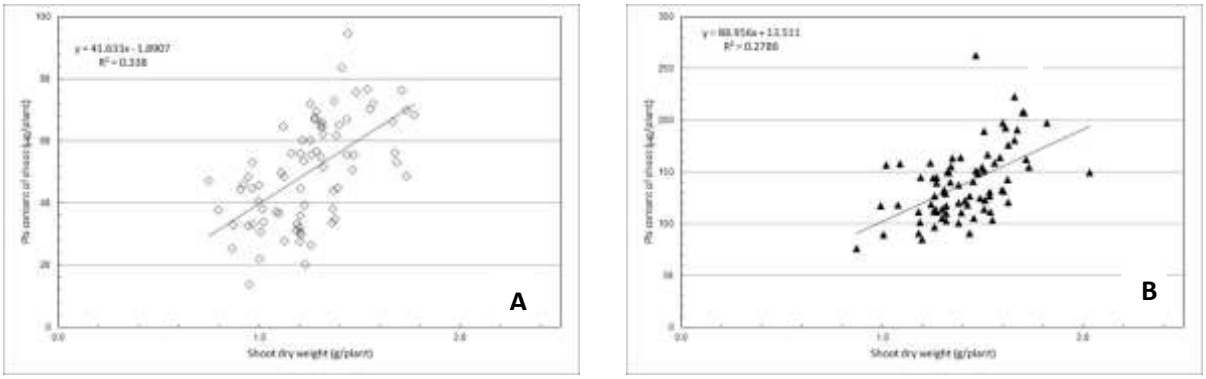

Figure 4.40 Relationship between the Pb content of the shoots and shoot dry weight at final harvest for the 77 genotypes in A) the 10% Pb, and B) 30% Pb treatments. The straight lines are the linear regressions for the data.

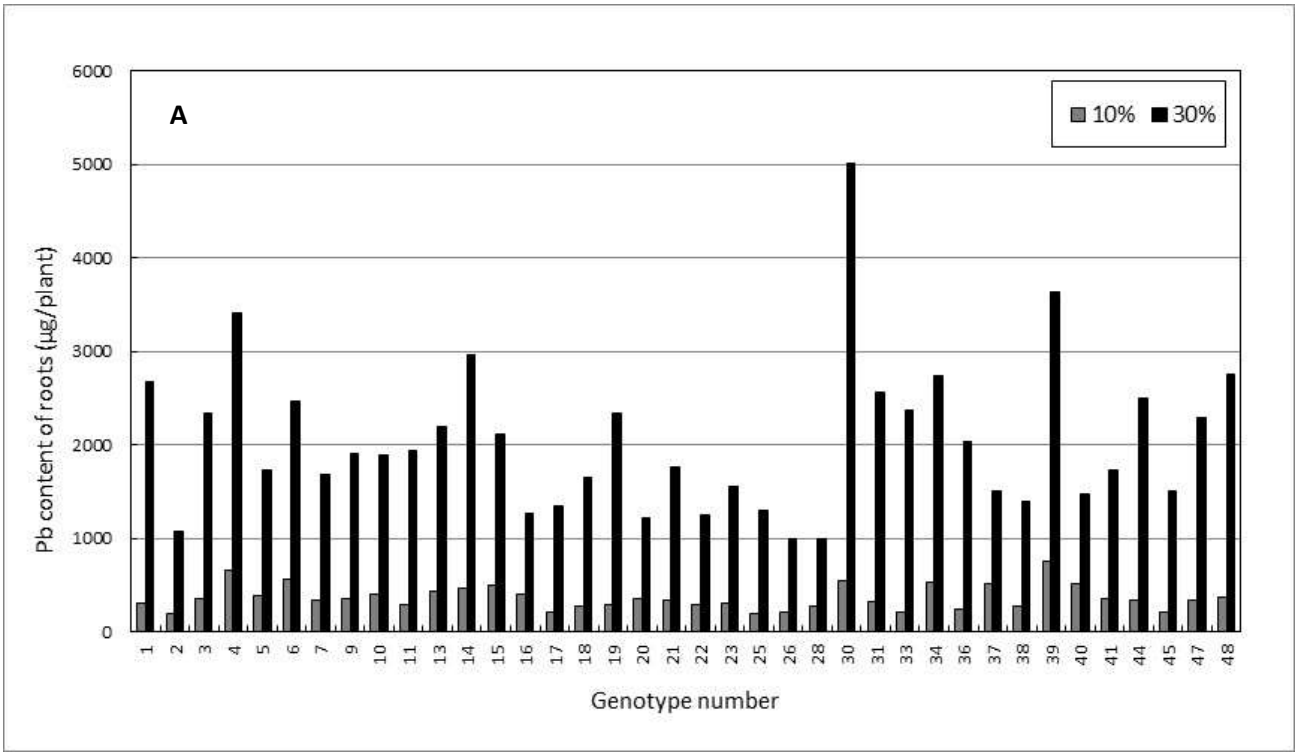

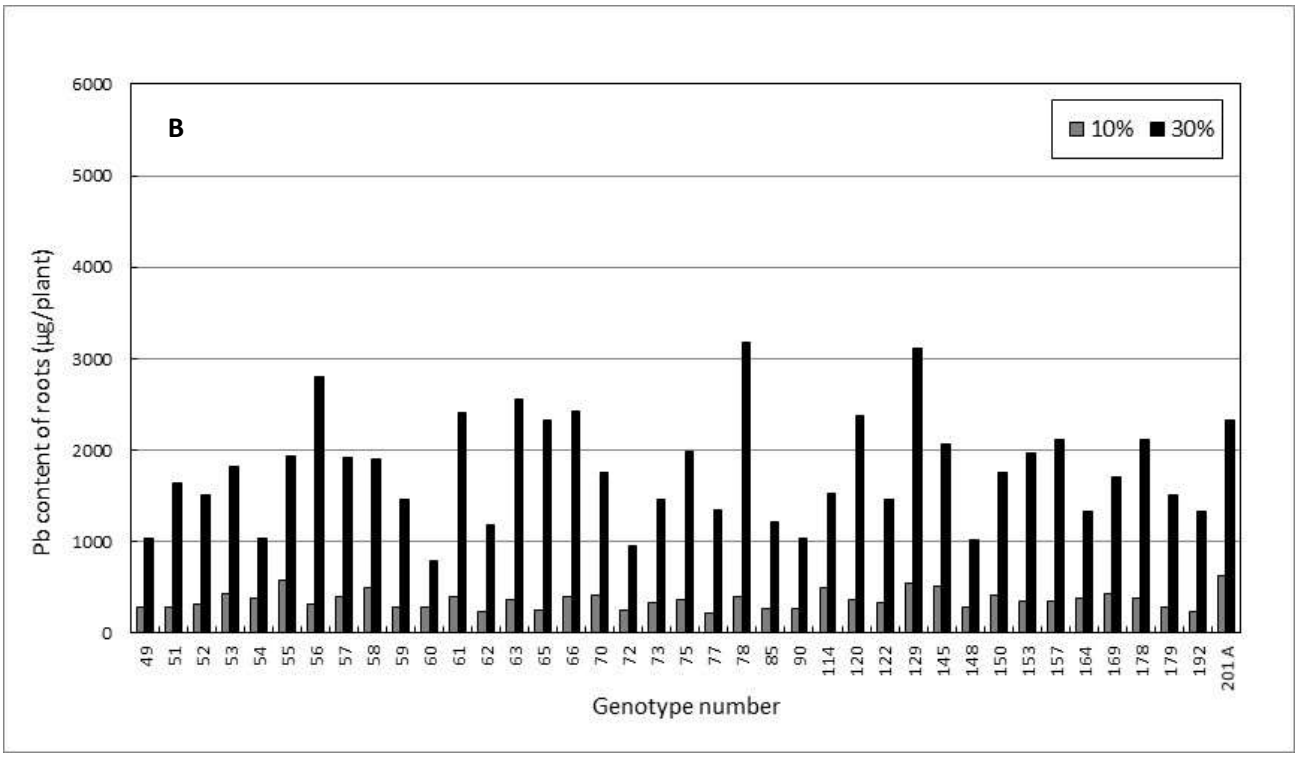

Figure 4.41 Pb content of the roots, expressed as µg/plant, for 77 genotypes, harvested after 16 weeks of growth under 10% or 30% Pb treatments. Data are split for clarity into A) Genotypes 1 – 48, and B) Genotypes 49 – 201A. Mean standard deviations are 81.6 and 399.3 for the 10% and 30% Pb treatments, respectively.

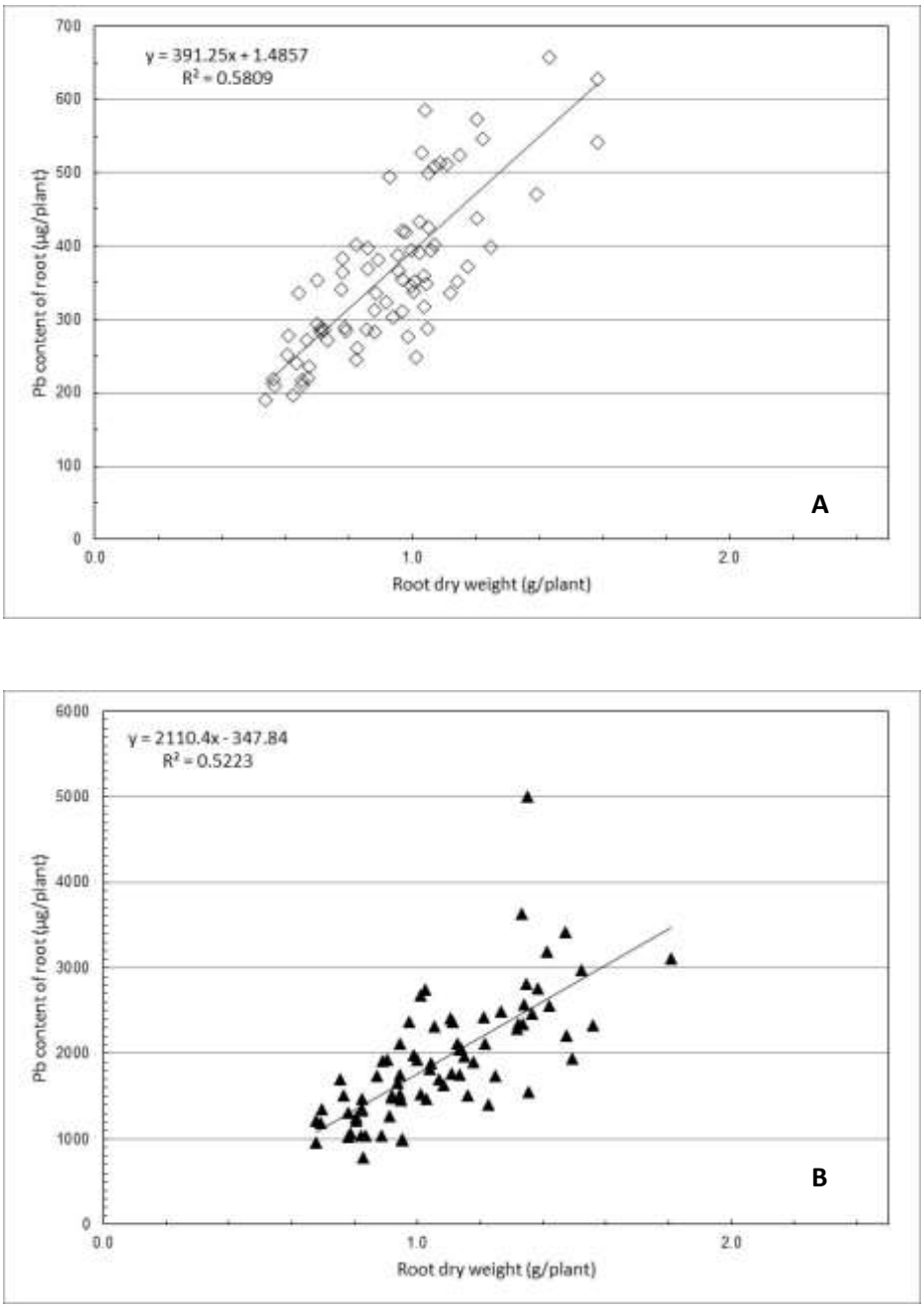

Figure 4.42 Relationship between the Pb content of the roots and root dry weight at final harvest for the 77 genotypes in A) the 10% Pb, and B) the 30% Pb treatments. The straight lines are the linear regressions for the data.

Scatter plots of the relationship between tissue concentrations of Pb in the shoots and the total Pb content of the shoots at Cut 1, after 8 weeks of growth (Figure 4.43), showed a stronger linear correlation under the 10% Pb treatment ($R^2 \sim 0.60$) compared with the 30% Pb treatment ($R^2 \sim 0.35$). By the final harvest, although shoot Pb content had increased markedly in both the 10% and 30% Pb treatments, tissue Pb concentrations in the shoots remained fairly stable within the range ~10 – 60 µg/g in the 10% treatment and between ~ 60 – 150 µg/g in the 30% treatment.

However, the correlation between the two variables increased (Figure 4.44) in the 10% treatment (R^2 ~ 0.65) and the 30% treatment (R^2 ~ 0.62).

Concentrations of Pb in root tissue varied between 250 – 500 µg/g under the 10% Pb treatment and increased to between 1,000 – 2,800 µg/g under the 30% Pb treatment, excluding one anomalous genotype. Tissue concentrations of Pb in the roots were positively correlated with the total Pb content of the root (Figure 4.45) in both the Pb treatments. The close correlation between total Pb content and tissue concentrations in the roots is evidenced by relatively high R^2 values of ~ 0.41 and ~ 0.64 in the 10% and 30% Pb treatments. In contrast with the corresponding shoot Pb relationship, the correlation in the roots was closest under the 30% Pb treatment.

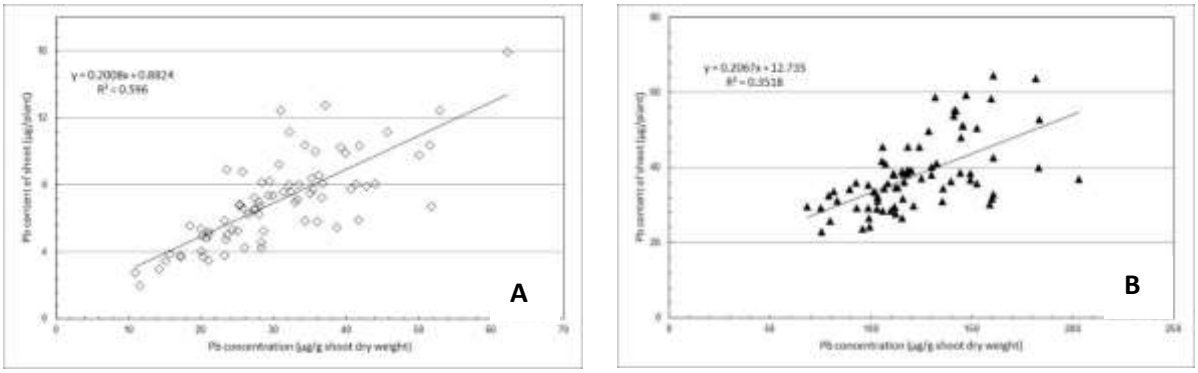

Figure 4.43. Relationship between total Pb content of the shoots and the concentration of Pb in shoot tissue of the 77 genotypes at Cut 1, after 8 weeks of growth, under A) the 10% Pb treatment, and B) the 30% Pb treatment. Straight lines are the linear regressions for the data.

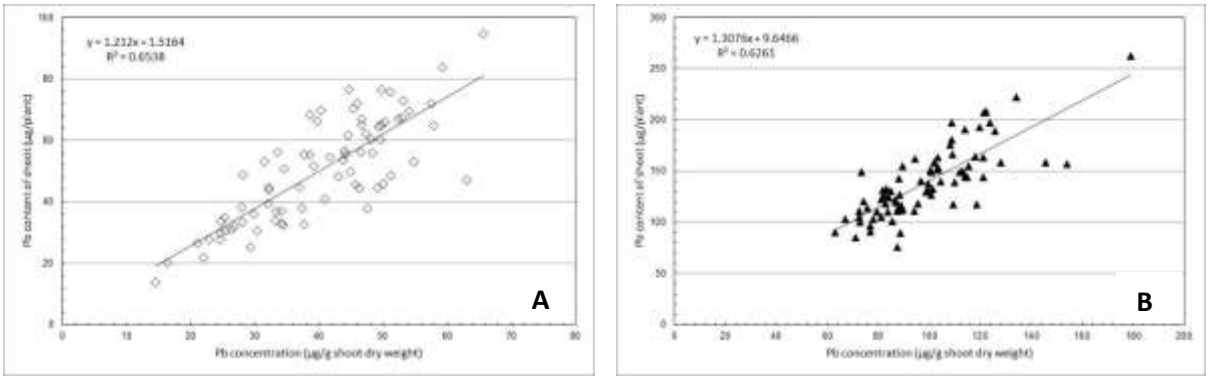

Figure 4.44 Relationship between total Pb content of the shoots and the concentration of Pb in shoot tissue of the 77 genotypes after 16 weeks of growth under A) the 10% Pb treatment, and B) the 30% Pb treatment. Straight lines are the linear regressions for the data.

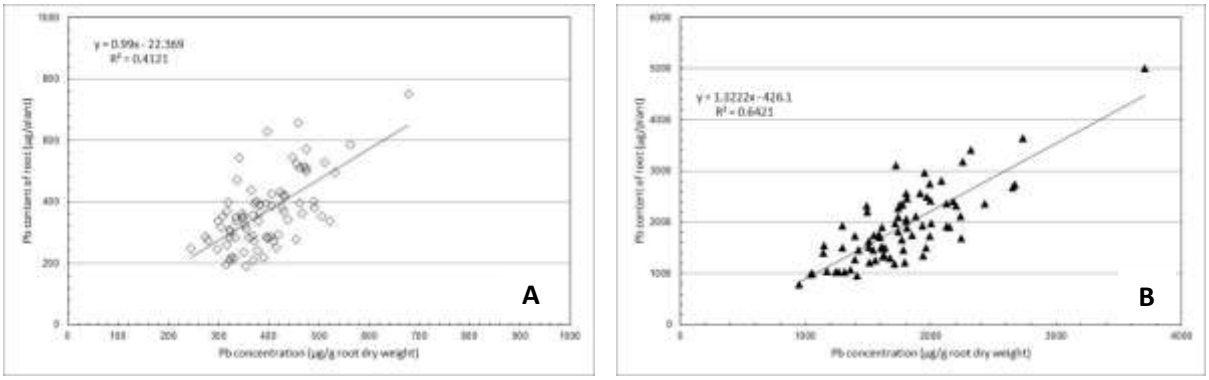

Figure 4.45 Relationship between total Pb content of the roots and the concentration of Pb in root tissue of the 77 genotypes after 16 weeks of growth under A) the 10% Pb treatment, and B) the 30% Pb treatment. Straight lines are the linear regressions for the data.

The partitioning of Pb between the shoots and roots at final harvest was similar under both the 10% (Figure 4.46) and 30% (Figure 4.47) Pb treatments. Under the 10% Pb treatment, ≥ 80% of the total Pb content was partitioned to the roots in all genotypes, and for 19 of the 77 genotypes this figure was found to be ≥ 90%. Under the 30% Pb treatment, ≥ 84% of the total Pb content was partitioned to the roots in all genotypes, whilst the figure was ≥ 90% for 70 out of the 77 genotypes. In terms of 'translocation index' (i.e. TI_{Pb} = shoot Pb content/root Pb content), none of the genotypes had a translocation index > 1 under either treatment; indeed, all TI_{Pb} were consistently << 1. Mean TI_{Pb} was 0.14 in the 10% Pb treatment, with Genotype 179 the highest TI_{Pb} of 0.25 and Genotype 56 having the lowest TI_{Pb} of 0.04. In contrast, mean TI_{Pb} in the 30% Pb treatment was 0.08, with Genotype 38 having the highest TI_{Pb} of 0.19 and Genotypes 78 and 129 having the lowest TI_{Pb} of 0.03.

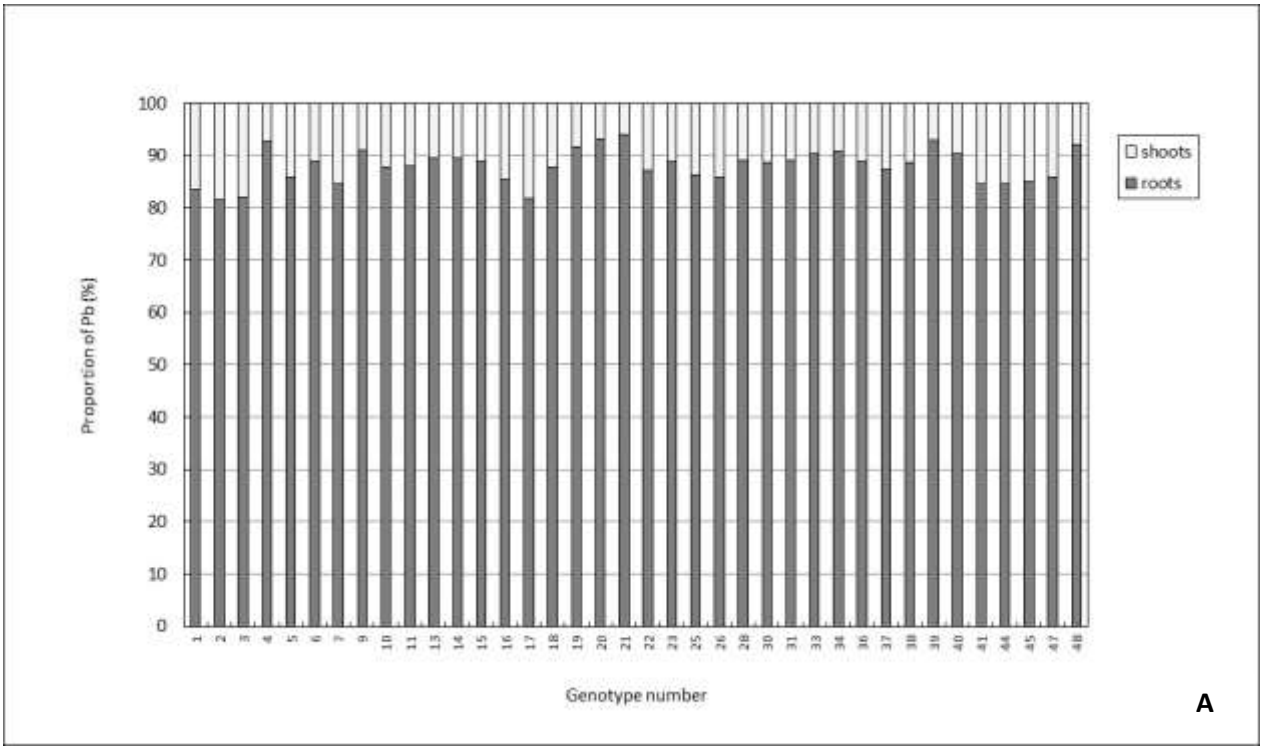

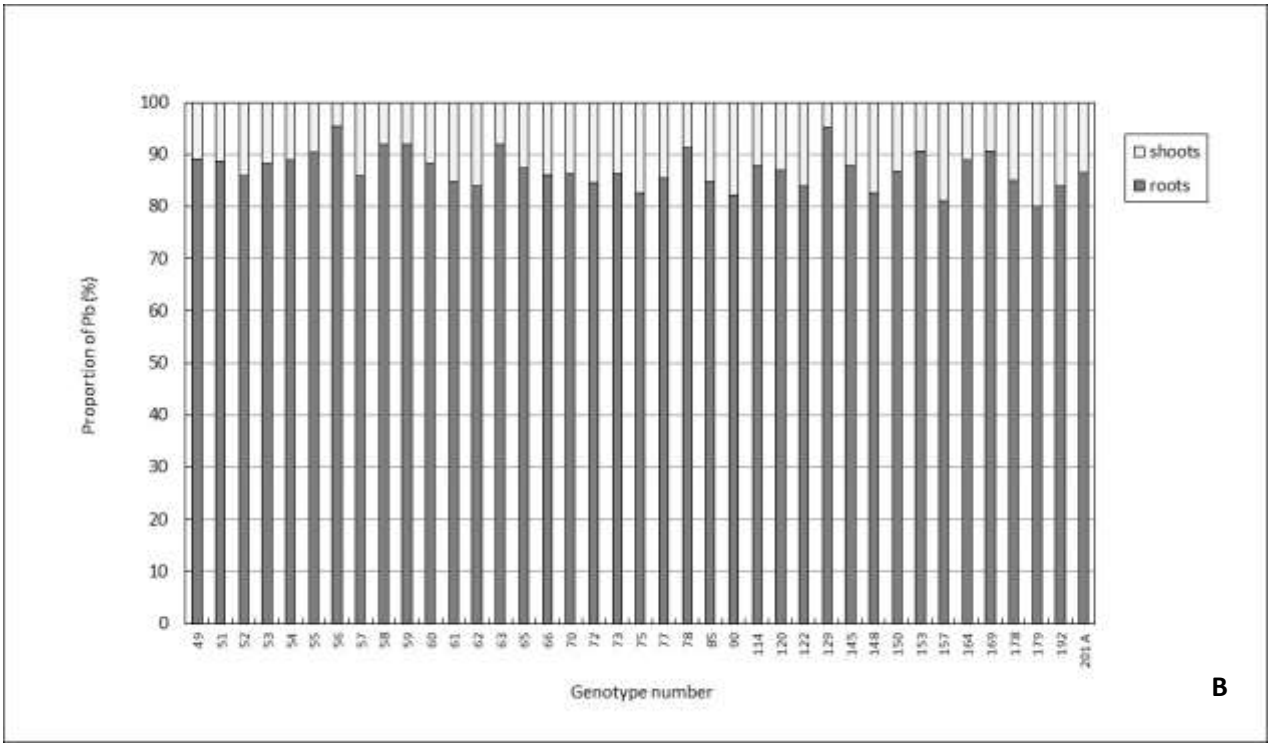

Figure 4.46 Relative partitioning of Pb by 77 genotypes between the roots and shoots, after 16 weeks of growth, under the 10% Pb treatment at final harvest. Data are split for clarity into A) Genotypes 1 – 48, and B) Genotypes 49 – 201A.

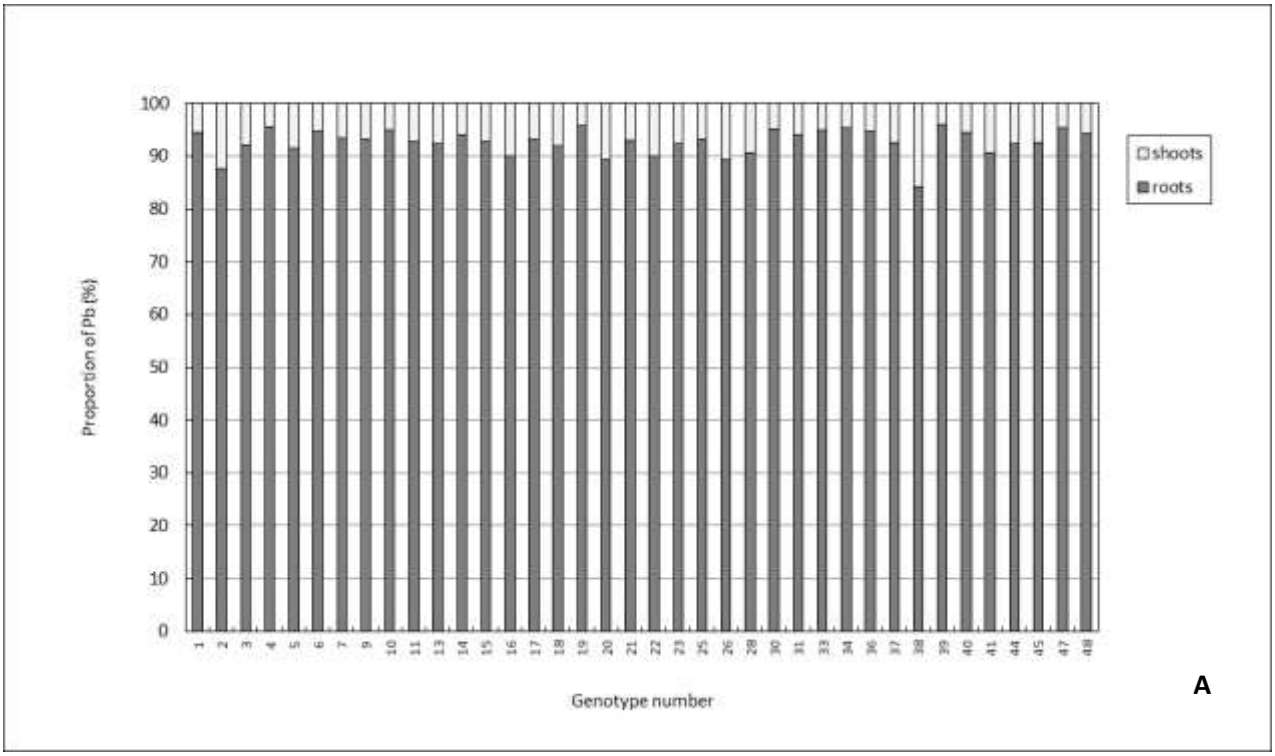

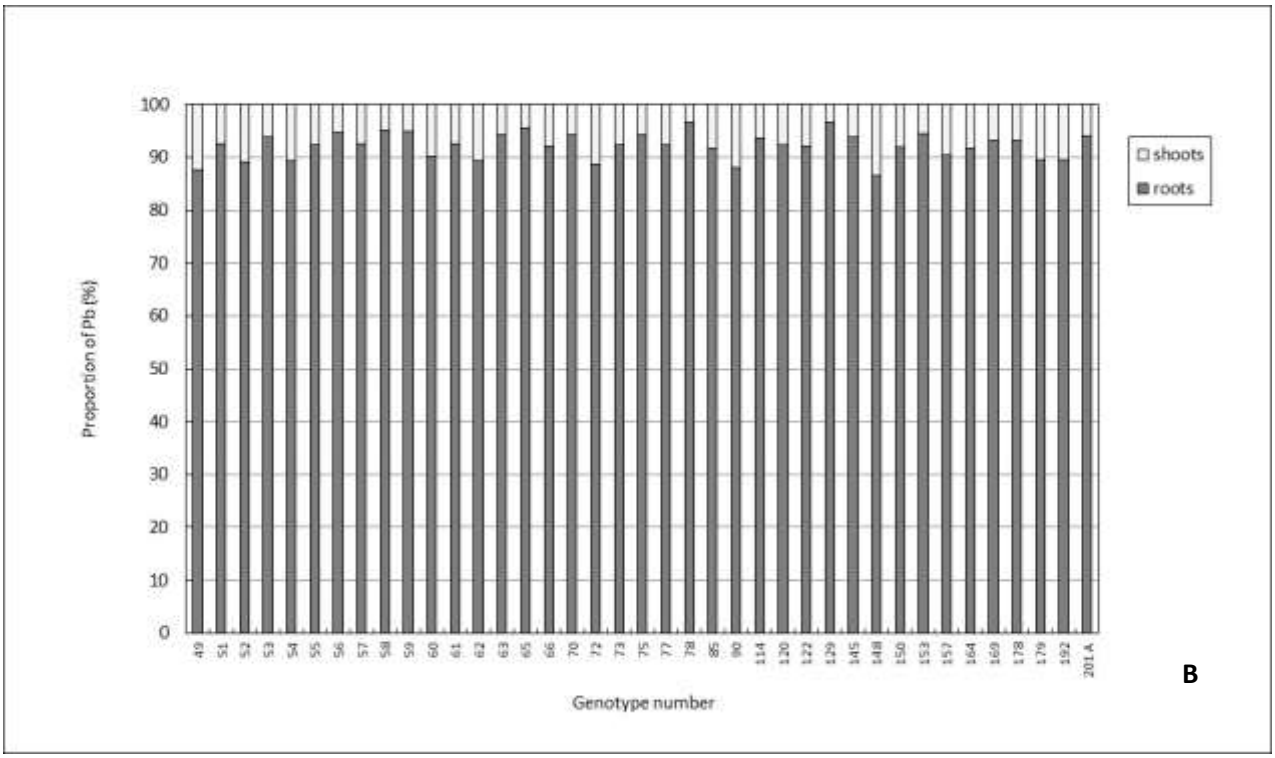

Figure 4.47 Relative partitioning of Pb by 77 genotypes between the roots and shoots, after 16 weeks of growth, under the 30% Pb treatment at final harvest. Data are split for clarity into A) Genotypes 1 – 48, and B) Genotypes 49 – 201A.

4.3 Comparison of plant growth in the control treatments

Several of the plant growth attributes measured at final harvest in the control treatments varied substantially between the replicate blocks A and B, and also between the two experiments. Mean values of the growth-related attributes across the 77 genotypes in each of the control blocks are listed in Table 4.2. The results from blocks A and B within each experiment were compared for each of these traits using two-tailed, paired t-tests. Apart from shoot dry weight and tiller number, trait values differed significantly ($p < 0.05$) between the two control blocks in the Zn experiment, and all but tiller number differed significantly in the Pb experiment.

Table 4.2 *Means for growth-related attributes measured at final harvest across the 77 genotypes in the two control treatment blocks (A and B) in the Zn and Pb experiments. Values in parentheses are standard deviations.*

	Zn experiment		**Pb experiment**	
	Control Block A	Control Block B	Control Block A	Control Block B
Shoot dry weight (g/pot)	10.42 (2.77)	10.37 (2.56)	5.75 (1.95)	4.93 (1.53)
Root dry weight (g/pot)	13.75 (7.68)	10.79 (5.86)	3.46 (1.45)	3.11 (1.26)
Total plant dry weight (g/pot)	24.17 (9.38)	21.17 (7.40)	9.21 (3.15)	8.04 (2.60)
shoot : root dry weight (g/g)	0.95 (0.43)	1.19 (0.57)	1.78 (0.48)	1.67 (0.38)
Tiller numbers	127 (35)	129 (38)	144 (47)	143 (45)

Trait values based on dry weights showed greater variation between the two control blocks compared with tiller number, in both experiments. This is illustrated by the scatter plots for total plant dry weight (Figures 4.48A and C) and tiller number (Figures 4.48B and D). The corresponding linear regressions gave $R^2 \sim 0.88$ and ~ 0.71, respectively, for tiller numbers in the Zn and Pb experiments, and $R^2 \sim 0.45$ and ~ 0.37, respectively, for total plant dry weight in the Zn and Pb experiments. Poor correlation was also observed between blocks A and B for shoot dry weight ($R^2 = 0.12$ (Zn) and 0.33 (Pb)), and shoot:root dry weight ratio ($R^2 = 0.27$ (Zn) and 0.16 (Pb)).

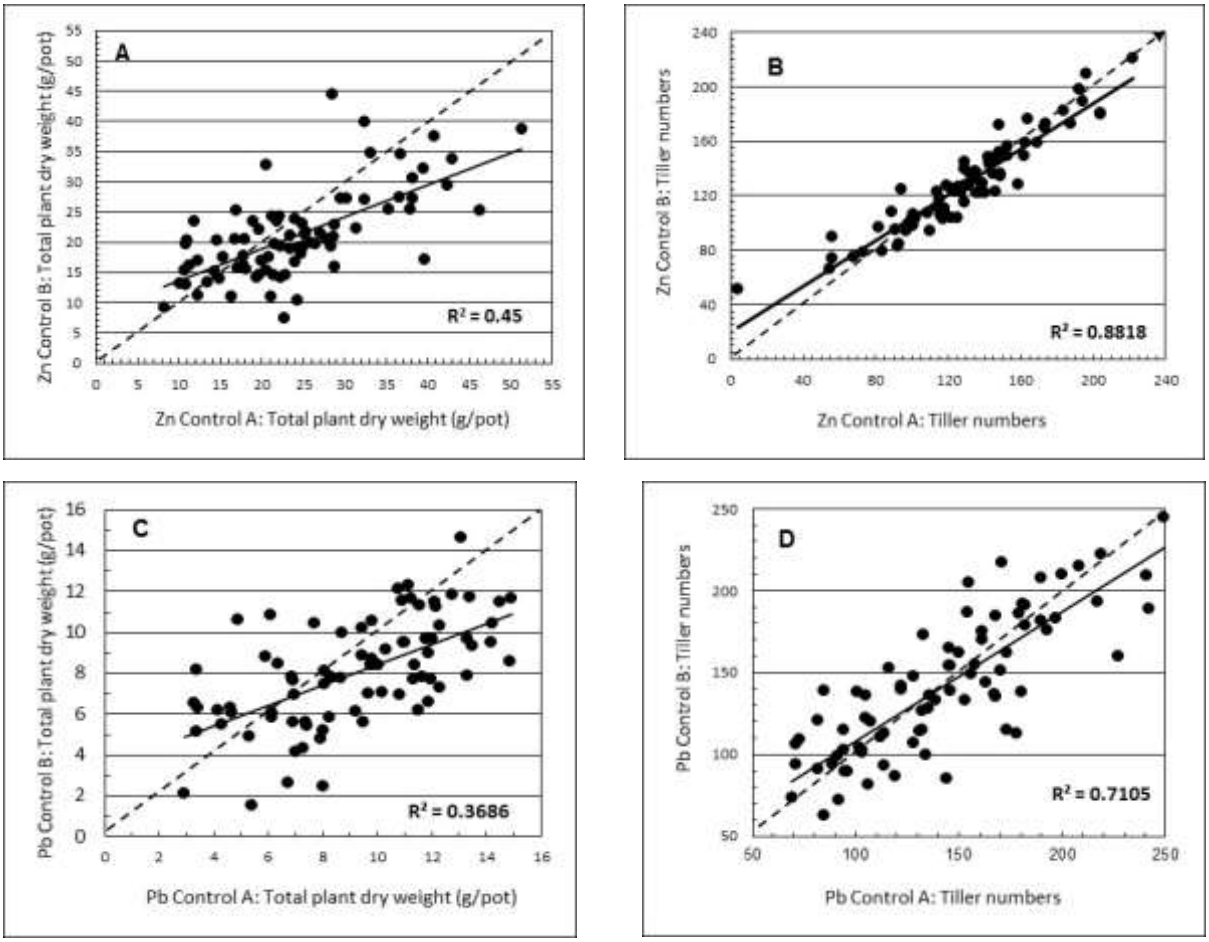

Figure 4.48 Comparisons between growth-related trait values measured at final harvest for the 77 genotypes grown in control treatment blocks A and B. A) total plant dry weight, Zn experiment, B) tiller number, Zn experiment, C) total plant dry weight, Pb experiment, and D) tiller number, Pb experiment. Straight lines and values of R^2 are for linear regressions. The dotted line is the 1:1 line (i.e. gradient = 1).

The reasons for the wide differences in dry weights between the two replicate control blocks of plants in each experiment are not immediately apparent. Neither are the reasons for the comparative uniformity of tiller numbers across blocks A and B.

The differences in trait values between the control treatments of the two experiments were greater than those observed between replicate blocks A and B within each experiment. The trait values (means of blocks A and B) were compared between each experiment, using two-tailed, paired t-tests. All the growth-related traits tested differed significantly ($p < 0.05$) between the two experiments. As observed for variation between replicate blocks A and B within each experiment, the variation between the two experiments was also higher for the dry weight traits (Figures 4.49A, B and C) compared with tiller number (Figure 4.49D).

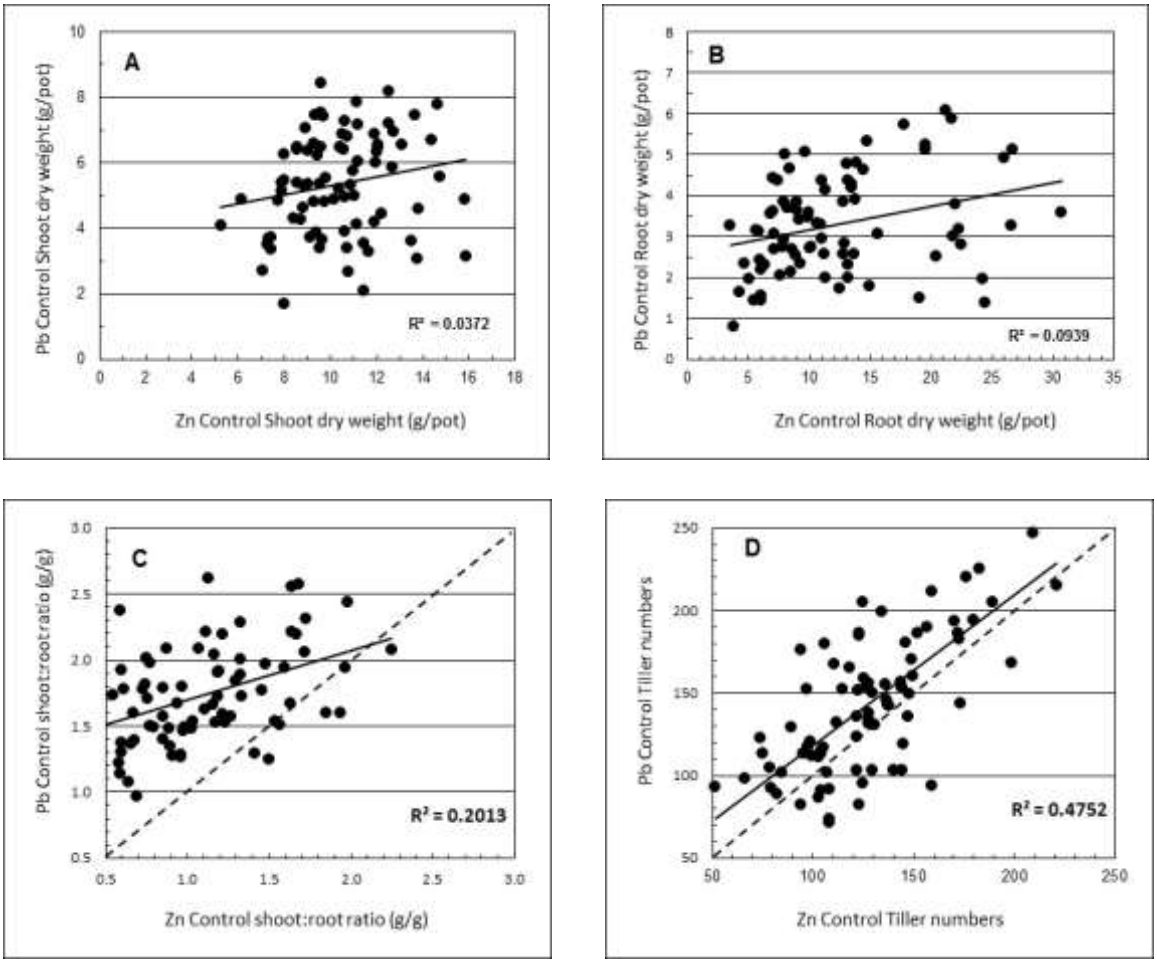

Figure 4.49 Comparisons between growth-related trait values measured at final harvest for the 77 genotypes grown in control treatments of the Zn and Pb experiments: A) shoot dry weight, B) root dry weight, C) shoot:root dry weight ratio, and D) tiller number. Trait values are means of control blocks A and B for each experiment. Straight lines and values of R^2 are for linear regressions. The dotted line is the 1:1 line (i.e. gradient = 1).

The frequency distributions for shoot and root dry weights in the control treatments (Figure 4.50) highlight the systemic differences between the two experiments. Shoot dry weights for the majority of the genotypes (58 out of 77) in the Zn experiment (Figure 4.50A) ranged between 1.5 – 2.5 g/plant, compared with 1.0 – 2.0 g/plant for the majority of genotypes (68 out of 77) in the Pb experiment (Figure 4.50B). The root dry weights show a similar pattern, with the majority of genotypes (57 out of 77) in the Zn experiment in the range of 2.0 – 4.0 g/plant (Figure 4.50C), compared with 0.6 – 1.0 g/plant for the majority of genotypes (45 out of 77) in the Pb experiment (Figure 4.50D).

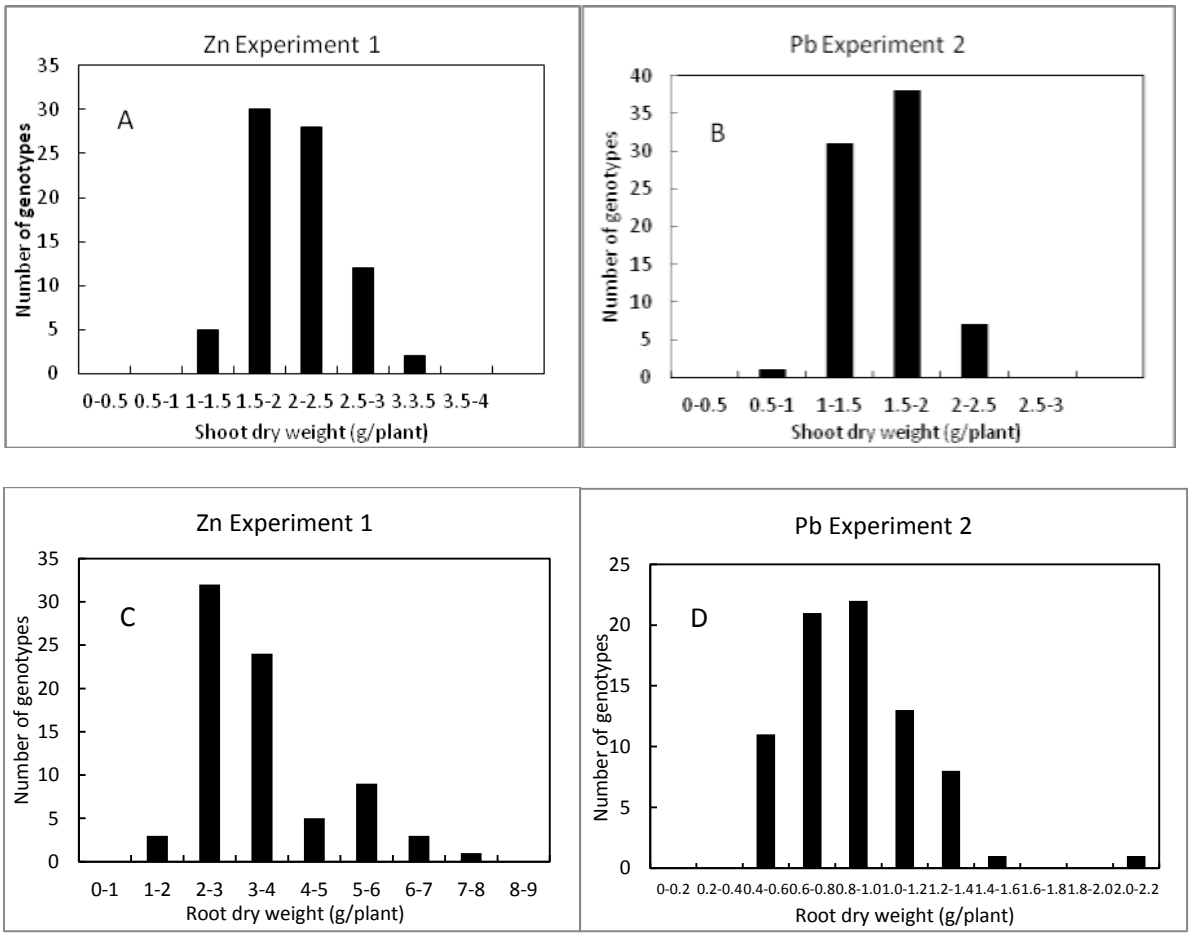

Figure 4.50 Frequency distributions for shoot dry weights (A and B) and root dry weights (C and D) of the 77 genotypes at final harvest in the control treatments of (A and C) the Zn experiment, and (B and D) the Pb experiment. Data are mean values for control treatment blocks A and B within each experiment.

The relative differences in root dry weights between the control treatments in the two experiments exceeded those for shoot dry weights. Hence, although dry weights were invariably lower for a given genotype in the Pb controls compared with the Zn controls, shoot:root dry weight ratios were almost always higher in the Pb control treatment compared with the Zn control treatment. The greater absolute and proportional partitioning of dry matter to the roots in the Zn control treatment is difficult to explain, as are most of the above differences in performance of the control plants between the two experiments. Some of the factors that may have contributed to these differences are considered below.

4.3.1 Errors in data recording

The base-line recording from the original harvest data sheets was re-checked against data in the Excel spreadsheet to ensure there were no ‘operator errors’ during data recording and input. No errors of this type were identified.

4.3.2 Environmental factors

The two experiments were conducted during the same months of successive years, referred to here as Years 1 (Zn experiment) and 2 (Pb experiment). The occurrence of significant differences in environmental conditions and weather patterns between Years 1 and 2 could account for differences in plant growth. Rainfall was discounted as a contributory factor because during both experiments the plants were grown on the same irrigated standing area (Plate 3.14) and were watered daily at regular intervals. In addition, the fertiliser application regime for both experiments was identical (Section 3.9) and no nitrate contamination was recorded in either the Castell Mine or Darren Mine tailings used in the experiments (Section 3.14). Records of total and daily average solar radiation (measured for wavelengths of between 200 – 3,000 nm using a Kipp und Zonen pyranometer) and temperature from meteorological records obtained from the on-site Plas Gogerddan Weather Station were also compared (Table 4.3), but the differences were insufficiently large to explain the divergence in growth observed between the control treatments of the two experiments.

Table 4.3 *Comparison of total monthly and average daily solar radiation (MJ/m^2) and average daily air temperature (°C) for the experimental months during Years 1 and 2.*

	Solar Radiation				**Air Temperature**	
	Year 1	Year 2	Year 1	Year 2	Year 1	Year 2
	Monthly Total *(MJ/m^2)*	Monthly Total *(MJ/m^2)*	Daily Average *($MJ/m^2/d$)*	Daily Average *($MJ/m^2/d$)*	Daily Average (^oC)	Daily Average (^oC)
June	595.6	599.8	19.9	20.0	13.6	15.1
July	468.4	487.1	15.1	15.7	15.8	15.6
August	340.0	424.5	11.0	13.7	15.6	16.1
September	273.7	307.5	9.1	10.2	13.1	13.6

4.3.3 Initial differences in plant weights

Initial tiller weights for the control plants in each experiment were compared to determine whether differences in the starting biomass between the two experiments could account for the differences in final harvest weights (Table 4.4). Total shoot fresh weights harvested from each of the two replicate blocks (A and B) of control plants at 8 and 16 weeks were also compared (Table 4.4) to identify any positional 'blocking' effect on the plants.

Table 4.4 *Comparison between the total fresh weight of tillers sown into all pots at the start of the experiments, total shoot fresh weight harvested after 8 weeks (Cut 1) and 16 weeks (final harvest), and the total root fresh weight after 16 weeks from the two replicate blocks of genotypes in the control treatment of each experiment.*

	Year 1 Zn				Year 2 Pb			
	Tiller f.wts (g)	Cut 1	Final Harvest		Tiller f.wts (g)	Cut 1	Final Harvest	
		Shoot f.wt (g)	Shoot f.wt(g)	Root f.wt(g)		Shoot f.wt(g)	Shoot f.wt(g)	Root f.wt(g)
Block A	86.34	346.89	2896.48	3243.21	106.32	231.84	1931.58	1704.19
Block B	84.26	246.73	2870.27	2835.12	111.85	205.42	1711.94	1485.68
Total	170.60	593.62	5766.75	6078.33	218.16	437.26	3643.52	3189.87

Although the initial tiller weight was higher in Year 2, shoot fresh weights were already lower after 8 weeks compared with Year 1. By the final harvest the total fresh weight of shoot and root was approximately half that of Year 1.

4.3.4 Algal contamination

In both experiments the pots were placed on saucers to minimise fertiliser wash-through and to maximise the nutrient uptake time for the plants. However, in the Pb experiment, the saucers became progressively contaminated by a thick algal growth (cf. Plates 3.15 and 4.4), probably introduced by wind dispersal. Consequently, after 8 weeks they were replaced with uncontaminated saucers. This procedure was not followed in the Zn experiment.

Plate 4.4 Pots in Pb Experiment 2 at 7 weeks, showing excessive algal contamination in the saucers.

Algal species of Chlorophyta, Cyanophyta and Chrysophyta are very efficient at nitrate uptake (Halterman and Toetz, 1984), primarily due to the presence of nitrate reductase (NR) both in the cytosol and bound to the plasma membrane (e.g. Tischner *et al*., 1989; Stöhr, 1998). Nitrate uptake by algae is also strongly influenced by light quality, with enhancement under blue light (e.g. Berges, 1997; Tischner, 2000). It is therefore possible that the lower plant growth rates in the control treatment of the Pb experiment may have been caused by nutrient shortage attributable to the presence of these high concentrations of algae during the first 8 weeks of the experiment.

4.4 QTL analysis

4.4.1 QTL from Zn Experiment 1

The results derived from MapQTL analysis of traits in Zn Experiment 1 are shown in Table 4.5, and a complete listing of all traits measured is given in Appendix 5. From an initial total of 32 traits with five K* or above, the three-step procedure reduced the number of significant QTL down to ten, all of which were located on LGs 4, 6 and 7. Six of these QTL referenced traits associated with the control treatment, and four referred to traits specific to either the 10% or 30% Zn treatments. The four QTL associated with the Zn treatments were Trait 1 ((30%) number of days survival post-sowing up), Trait 12 ((10%) final harvest tiller numbers per m^2), Trait 25 ((10%) final harvest root Zn content (ppm)), Trait 29 ((10%) final harvest proportion of total Zn in the shoot (%)). No significant QTL associated with yield, Zn uptake or utilisation efficiencies under toxic levels of Zn supply were detected.

With the exception of Trait 29C, LOD scores ranged between 3.7 and 6.95 whilst the '% variance explained' (i.e. % phenotypic variation explained) ranged between 20.4% and 51.1%. The Kruscal-Wallis test statistic associated with each of the detected QTL ranged between K***** and K*******, indicating significance levels ranging between 0.001 and < 0.0001.

The QTL data were transposed onto the new SNP-based genetic linkage map for *L. perenne*, described in Section 3.15. The map (Figure 4.51) reveals overlapping QTL, along their outer intervals, on LG4 for final harvest tiller numbers per m^2 and shoot/root dry weight ratios (Traits 12C and 23C, respectively) and overlapping QTL, along their inner intervals, on LG6 for Zn uptake efficiency and Zn efficiency ratio (Traits 36C and 38C, respectively) in the control treatment. A total of 6 QTL were mapped to LG7, with overlap of 5 QTL, namely Traits 1(30%), 12(10%), 12C, 23C and 29(10%), at genetic map distances of between ~ 35 – 65 cM. Notable

was the coincidence between QTL for traits 12(10%), 12C and 23C, two of which, as noted above, were also detected in relatively close proximity on LG4.

Table 4.5 *Results from MapQTL analysis, showing those traits in Zn Experiment 1 which have been determined as significant following all 3 test statistic parameters. The experiment treatment associated with the trait is given in parenthesis next to the trait number (C = control treatment, 10% = 10% Zn treatment, 30% = 30% Zn Treatment).*

Trait Number	Trait Description	Linkage Group	Map Position (cM)	Locus marker	KW Signif.	% variance explained	LOD	PM LOD threshold
11 (C)	Final harvest tiller numbers per plant	4	13.715	Contig11101_390	*******	31.7	**5.14**	**3.6**
		7	54.718	Contig7409_810	*******	41.4	**6.67**	**3.9**
12 (C)	Final harvest tiller numbers per m²	**4**	13.715	Contig11101_390	*******	31.4	**5.13**	**3.6**
		7	54.718	Contig7409_810	*******	40.1	**6.59**	**3.6**
23 (C)	Final harvest shoot:root dry weight ratio (g/g)	**4**	4.624	Contig41280_702	******	20.4	**3.71**	**3.5**
		7	54.718	Contig7409_810	*******	25.7	**4.53**	**3.8**
29 (C)	Final harvest proportion of total Zn in the shoot (%)	**6**	31.507	Contig34051_275	******	4	**3.8**	**3.6**
36 (C)	ZnUpE(ii)	**6**	46.092	Contig49898_259	******	38.4	**5.67**	**4.3**
38 (C)	ZnER	**6**	48.563	Contig12118_331	*****	29.1	**5.59**	**3.6**
12 (10%)	Final harvest tiller numbers per m²	**7**	54.718	Contig7409_810	*******	49.7	**6.02**	**3.8**
25 (10%)	Final harvest root Zn content (ppm)	**7**	35.423	Contig32829_1000	*******	26.3	**4.91**	**3.3**
29 (10%)	Final harvest proportion of total Zn in the shoot (%)	**7**	48.669	Contig46179_141	******	51.1	**5.42**	**4.5**
1 (30%)	Number of days survival post-sowing (max possible 118)	**7**	45.006	Contig31991_109	*******	38.5	**6.95**	**4.4**

Significance levels KW:
***=P<0.1 **=P<0.05 ***=P<0.01 ****=P<0.005 *****=P<0.001 ******=P<0.0005 *******=P<0.0001**

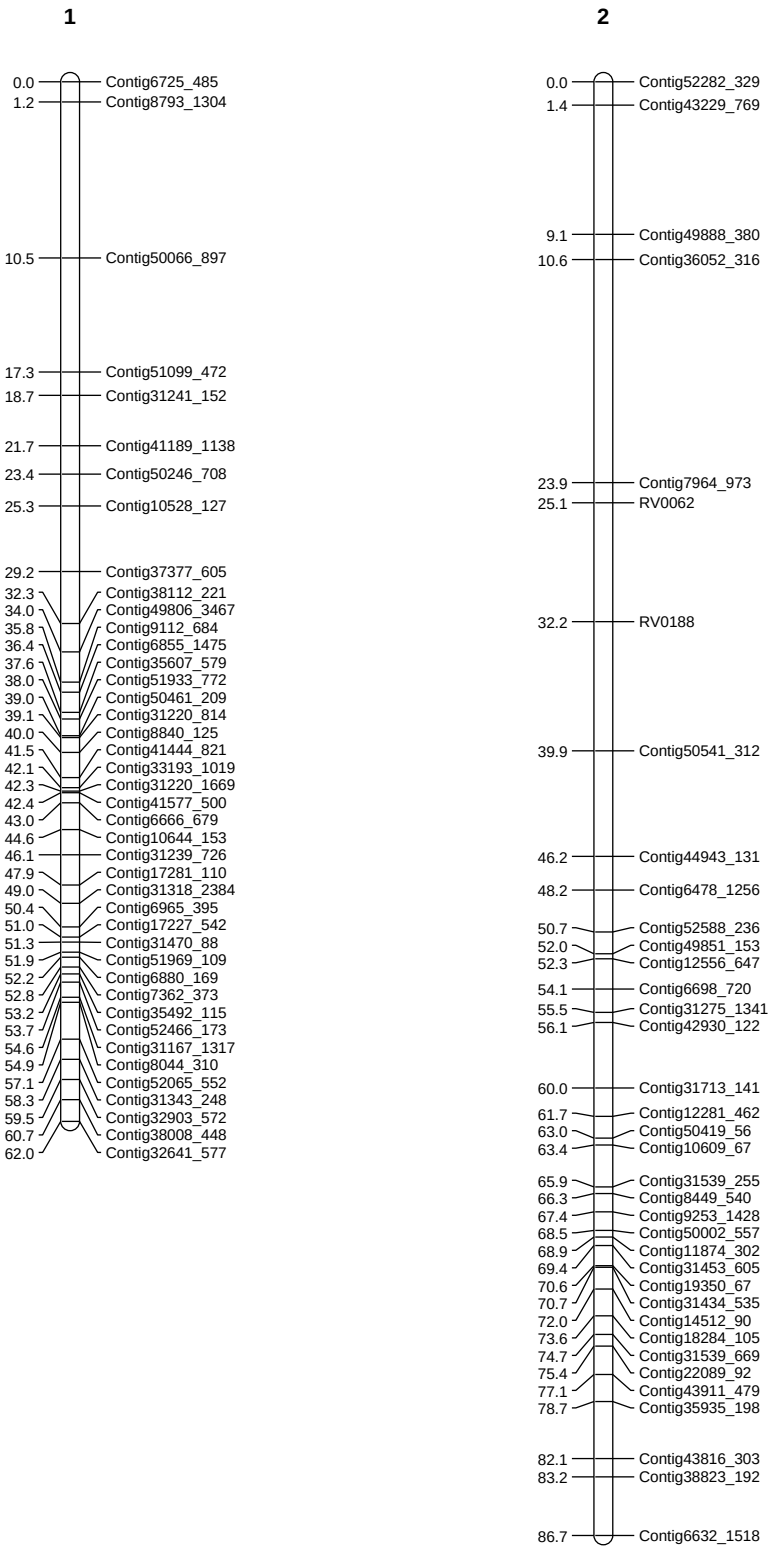

Figure 4.51 Genetic linkage diagrams showing detected QTL from Zn Experiment 1. Numbering for each QTL refers to trait number and treatment (e.g. Zn/12C = trait 12 in control treatment, Zn/12/10% = trait 12 in 10% Zn treatment). Note, that for clarity, not all contigs are shown on the linkage map.

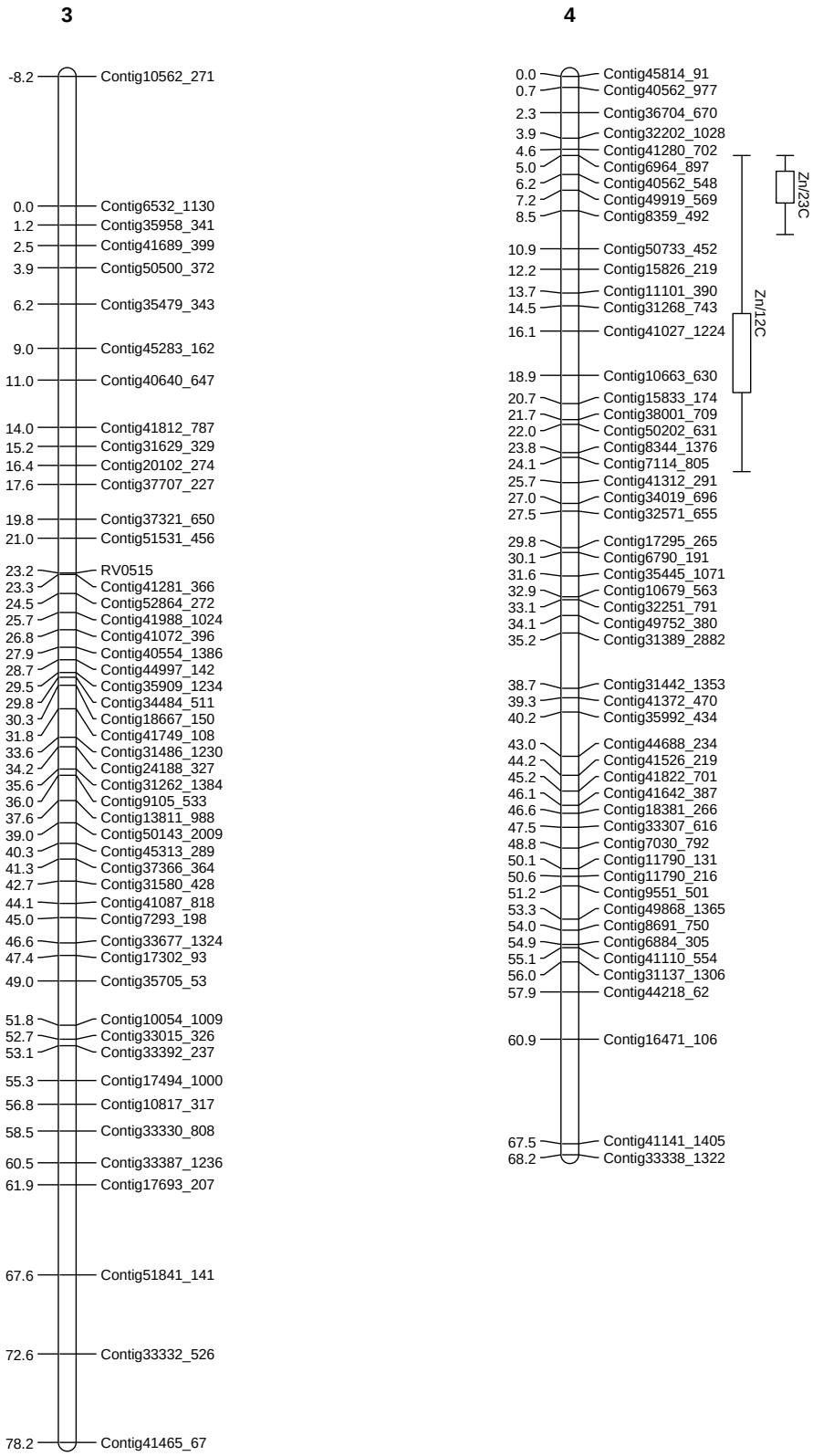

Figure 4.51 Continued.

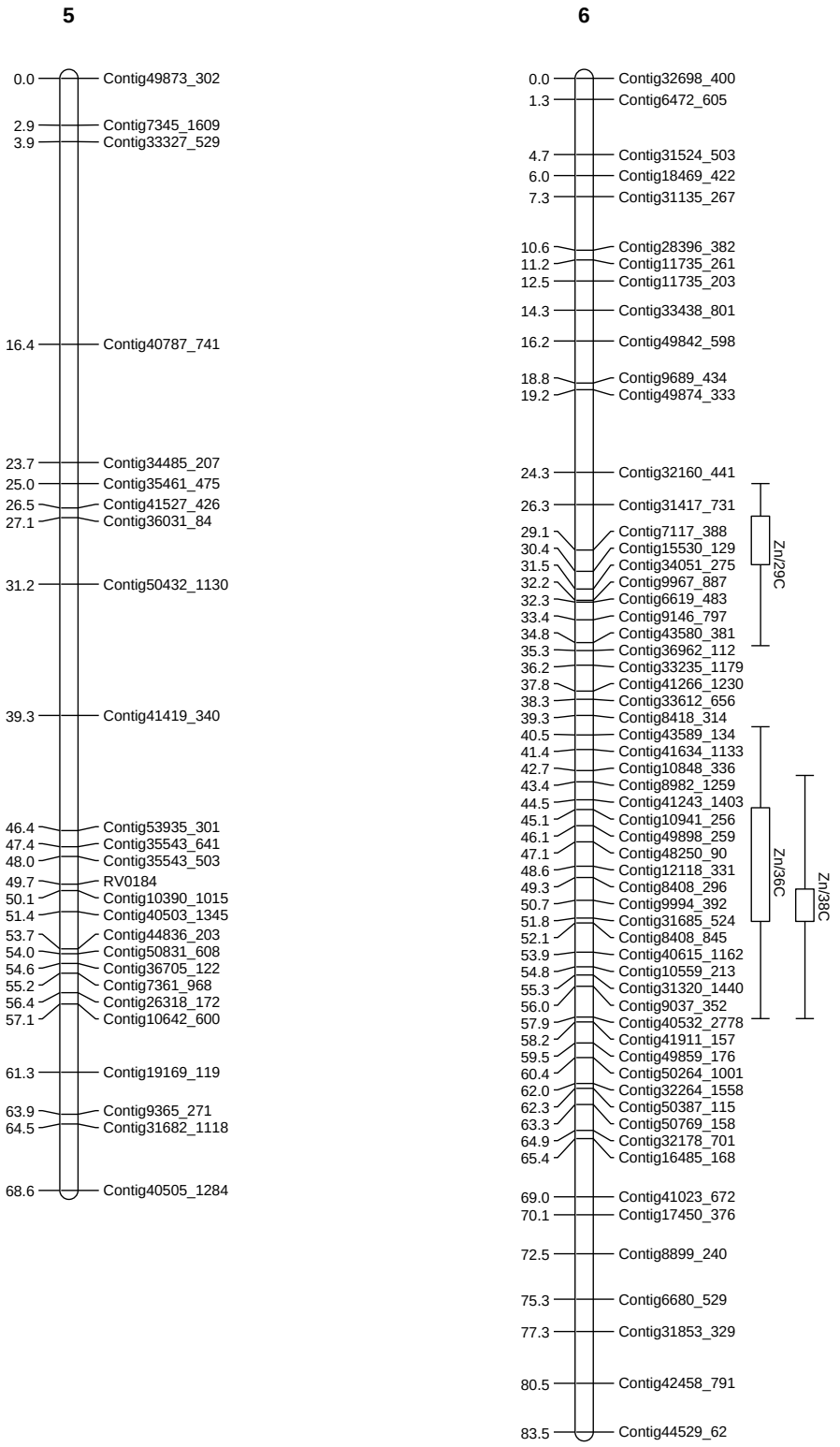

Figure 4.51 Continued.

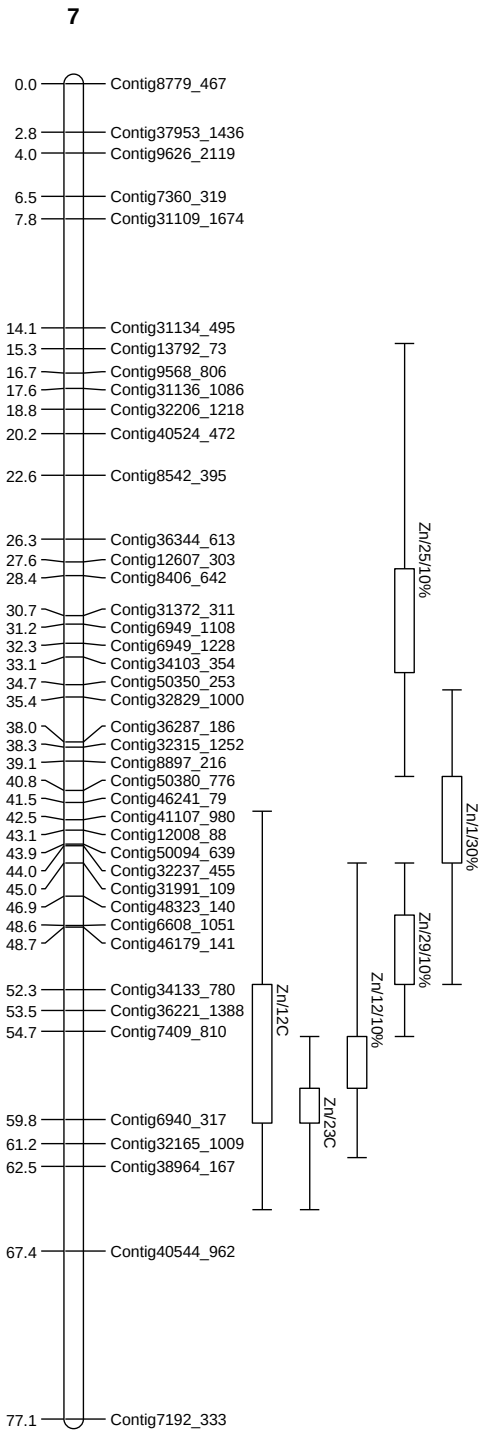

Figure 4.51 Continued.

4.4.2 QTL from Pb Experiment 2

The results derived from MapQTL analysis of traits measured in Pb Experiment 2 are shown in Table 4.6 and a complete listing of traits measured is given in Appendix 6. A far greater number of significant QTL were associated with this experiment compared with Zn Experiment 1. From the initial pool of QTL having five K* or above, the three-step procedure reduced the number of traits with one or more significant QTL down from 58 to 25, all of which were located on LGs 3, 4, 5 and 7. However, the actual number of significant QTL is lower given that several of the traits listed in Table 4.6 are biologically identical, differing numerically from each other solely in unit of measurement, generally, but not always, by a constant factor across all the genotypes. This form of duplication applied where trait values were expressed per plant, per pot or per m^2, as in the case of root dry weight (Traits 62, 63 and 64) or tiller numbers (Traits 55 and 56). Taking duplication for these traits into account, significant QTL were identified for twenty-two traits in one or more of the control, 10% or 30% Pb treatments. The traits yielding QTL were distributed across treatments as follows: five traits in the control treatment, eighteen traits in the 10% treatment and eight traits in the 30% treatment. LOD scores ranged between 3.31 and 14.11, whilst the '% variance explained' (i.e. % phenotypic variation explained) ranged between 19.7 and 65.3%. The Kruscal-Wallis test statistic associated with each of the detected QTL ranged between K***** and K********, indicating significance levels between 0.001 and < 0.0001.

Of the five traits with QTL in the control plants, two (Traits 46 and 47) only produced QTL in these plants whilst the other three traits (tiller numbers, root dry weight, shoot:root ratio) also produced QTL in both 10% and 30% Pb treatments. Of the eighteen traits with QTL in the 10% Pb treatment, twelve only produced QTL in this treatment whilst six also produced QTL in the 30% Pb treatment. Of these six traits, three also produced QTL in the control plants. Of the eight traits with QTL in the 30% treatment, only two (Traits 48 and 66) were unique to this treatment. It should be noted that two of the three traits with QTL only in the 10% and 30% Pb treatments (Traits 73 and 74) were not assessed in the control plants as they were associated with the distribution of Pb within the plant.

The highest LOD scores by far (11.0 – 14.1) were associated with the QTL for tiller numbers at final harvest (Traits 55 and 56) on LG7. Judging by the results for Trait 55, this strong QTL is almost certainly co-located in the 10% (54.7 cM) and 30% (52.3 cM) Pb treatments, and probably also in the control (46.2 cM) treatment. It is also likely to be the same QTL as that

identified on LG7 for tiller numbers in the control (54.7 cM) and 10% (54.7 cM) treatments in the Zn experiment. A second, weaker, QTL for tiller number, with LOD scores of 3 to 4 on LG3, co-located in the control (26.8 cM) and 10% (26.8 cM) Pb treatments, but was positioned differently (11.0 cM) in the 30% treatment. This QTL was not identified in the Zn experiment, although an additional QTL (LOD = 5.1) for tiller numbers was found on LG4 (13.7 cM) in the control Zn treatment.

Few QTL were identified for other growth-related traits at final harvest. Total plant dry weight (Trait 66), for example, produced a single QTL on LG7 (42.5 cM) but this was confined to the 30% treatment. As observed in the Zn experiment, no significant QTL were identified for final shoot dry weight in any of the Pb treatments. A single QTL for root dry weight (Traits 62, 63 and 64) was located on LG4 (21.7 cM) in the control treatment, but on LG7 in the 10% (52.3 cM) and 30% (44.3 cM) Pb treatments. This QTL was located close to the major QTL for tiller number on LG7 in the case of the 10% and 30% treatments.

Significant QTL were also found for shoot:root dry weight ratio (Trait 67), a measure of the partitioning of growth between shoot and root, on LG7 in the control (46.2 cM), 10% (46.9 cM) and 30% (52.3 cM) Pb treatments. This QTL was particularly strong in the 30% treatment, with an LOD of 8.9 accounting for 53% of the variance. For comparison, two QTL for shoot:root ratio were found in the Zn experiment, one on LG4 (4.6 cM) and the other on LG7 (54.7 cM), but only in the control Zn treatment.

The QTL revealed for Pb uptake, productivity and utilisation efficiencies were confined to the 10% Pb treatment. Interestingly, the single QTL for Pb uptake per plant (Traits 78 and 80) was located on LG4 (38.7 cM), but when uptake was indexed against root dry weight, (Trait 81) the single QTL was located on LG7 (52.2 cM). This co-locates with the QTL observed for root dry weight on LG7 in the 10% treatment and reflects the location of the majority of the Pb absorbed by the plants. A single relatively weak QTL for Pb productivity (Trait 79), defined as plant fresh weight gain per unit Pb absorbed, was located on LG7 (41.9 cM), whilst a stronger QTL for Pb utilisation efficiency expressed on a whole plant basis (Trait 84) was located on LG5 (49.7 cM), co-locating with the QTL observed for root dry weight on this LG.

Comparison of these results with those from the Zn experiment is hindered by the fact that significant QTL for Zn uptake, productivity or utilisation efficiencies were not found in the 10% or 30% Zn treatments. Indeed, only limited direct comparisons can be made between the two experiments in terms of QTL for metal-related traits. It is only possible with respect to

average metal concentrations in root tissue and the proportion of total metal recovery in the shoots and roots. A QTL for Zn concentration in the roots (Trait 25) was identified on LG7 (35.4 cM) in the 10% Zn treatment, whilst the single QTL for Pb concentration in the roots (Trait 69) was also located on LG7 (52.3 cM). The single QTL for the proportional recovery of Zn in the shoot (Trait 29) in the 10% Zn treatment was located on LG7 (48.7 cM). This is close to the single QTL for the proportional recovery of Pb in the shoot (Trait 73) in the 10% Pb treatment (LG7 at 46.9 cM). However, the single QTL for the same trait in the 30% Pb treatment was located on LG 5 (39.3 cM).

Transposition of the QTL data from the Pb experiment onto the new SNP-based genetic map for the *L. perenne* mapping family (Figure 4.52) highlights the strong degree of overlap between many of the QTL on LGs 3, 4, 5 and 7. For example, the QTL for Trait 56 (final harvest tiller numbers per m^2 in both the 10% and 30% Pb treatments) on LG3 were coincident at a genetic distance of between ~ 27.9 and 29.8 cM. On LG4 there was strong overlap, along their inner intervals, between 4 Pb-specific QTL, for Traits 71, 72, 78 and 80, all of which relate to Pb content and Pb uptake efficiency. These QTL were located at a genetic distance of between 38.7 and 43 cM on the LG. On LG5, two further Pb-specific QTL were identified, associated with Traits 73 and 74, which relate to total Pb content in the shoot and root in the 30% Pb treatment, respectively. These QTL were both located at a genetic distance of 39.29 cM on the LG at locus marker Contig41419_340. On LG7, a conspicuously high density cluster of overlapping QTL was identified between a genetic distance of 44.933 and 54.718 cM (inner interval). Several of these QTL are Pb-specific, namely those associated with Traits 52, 68, 69, 70, 73, 74 and 81, whilst others relate to traits associated with Pb tolerance in terms of growth (e.g. Traits 56, 64, and 67). Notable was the coincidence between QTL for Traits 67, 73, 74 (10% Pb treatment) and 56 (30% Pb treatment) on Contig31442_1353, at a genetic distance of 46.899 cM, which may provide a possible indication of pleiotropy.

Table 4.6 *Results from MapQTL analysis, showing those traits in the Pb experiment which have been determined as significant following all 3 test statistic parameters. The experimental treatment associated with the trait is given in parenthesis next to the trait number (C = control treatment, 10% = 10% Pb treatment, 30% = 30% Pb Treatment). Note that Traits 55 and 56 are essentially biologically identical as are Traits 62, 63 and 64.*

Trait Number	Trait Description	Linkage group	Map Position (cM)	Locus marker	KW signif.	% variance explained	LOD	PM LOD threshold
46 (C)	Cut 1 herbage fresh weight per pot (g)	7	31.17	Contig6949_1108	******	19.7	**3.58**	**3.4**
47 (C)	Cut 1 herbage dry weight per pot (g)	7	31.17	Contig6949_1108	*****	19.7	**3.53**	**3.5**
55 (C)	Final harvest tiller numbers per plant	3	26.75	Contig41072_396	*****	22.3	**4.01**	**3.6**
		7	46.233	Contig35555_890	*******	53.9	**11.03**	**3.7**
56 (C)	Final harvest tiller numbers per m²	7	46.233	Contig35555_890	*******	54.4	**11.09**	**3.9**
62 (C)	Final harvest root dry weight per pot (g)	4	21.694	Contig38001_709	*****	24.9	**4.18**	**3.6**
63 (C)	Final harvest root dry weight per plant (g)	4	21.694	Contig38001_709	*****	26.2	**4.39**	**3.5**
64 (C)	Final harvest root dry weight per m² (g)	4	21.694	Contig38001_709	*****	24.9	**4.18**	**3.8**
67 (C)	Final harvest shoot:root dry weight ratio (g/g)	7	45.006	Contig31991_397	*******	44.6	**5.92**	**3.9**
52 (10%)	Cut 1 shoot Pb content per plant (µg Pb)	7	45.168	Contig6858_618	******	22.2	**4.09**	**3.9**
55 (10%)	Final harvest tiller numbers per plant	3	26.75	Contig41072_396	******	22.3	**4.02**	**3.4**
		7	54.718	Contig7409_810	*******	60.5	**12.98**	**3.9**
56 (10%)	Final harvest tiller numbers per m²	3	26.75	Contig41072_396	******	23.3	**4.23**	**3.5**
		7	54.718	Contig7409_810	*******	65.3	**14.11**	**3.7**

Table 4.6 *Continued.*

Trait Number	Trait Description	Linkage group	Map Position (cM)	Locus marker	KW signif.	% variance explained	LOD	PM LOD threshold
58 (10%)	Final harvest root fresh weight per pot (g)	7	52.254	Contig34133_838	*****	36.4	**4.29**	**3.5**
62 (10%)	Final harvest root dry weight per pot (g)	7	52.254	Contig34133_838	*******	42.9	**5.97**	**3.4**
63 (10%)	Final harvest root dry weight per plant (g)	7	52.254	Contig34133_838	*******	38.7	**5.22**	**3.3**
64 (10%)	Final harvest root dry weight per m^2 (g)	7	52.254	Contig34133_838	*******	42.9	**5.97**	**3.5**
67 (10%)	Final harvest shoot:root dry weight ratio (g/g)	7	46.899	Contig48323_140	*******	47.8	**10.58**	**3.4**
68 (10%)	Final harvest shoot Pb content (ppm)	7	44.933	Contig9430_1036	*****	19.7	**3.57**	**3.4**
69 (10%)	Final harvest root Pb content (ppm)	7	52.254	Contig34133_838	*****	34.9	**4.79**	**4.6**
70 (10%)	Final harvest shoot Pb content per plant (µg Pb)	7	44.933	Contig36063_122	******	22.9	**4.24**	**3.9**
71 (10%)	Final harvest root Pb content per plant (µg Pb)	4	38.692	Contig31442_1353	*******	24.7	**4.35**	**4.1**
72 (10%)	Final harvest total Pb content per plant (µg Pb)	4	38.692	Contig31442_1353	******	23.4	**4.15**	**3.8**
73 (10%)	Final harvest proportion of total Pb in the shoot (%)	7	46.899	Contig48323_140	******	24.8	**4.64**	**3.4**
74 (10%)	Final harvest proportion of total Pb in the root (%)	7	46.899	Contig48323_140	******	24.8	**4.64**	**3.5**
78 (10%)	PbUpE(i) A	4	38.692	Contig31442_1353	******	23.4	**4.13**	**4**

Table 4.6 *Continued.*

Trait Number	Trait Description	Linkage group	Map Position (cM)	Locus marker	KW signif.	% variance explained	LOD	PM LOD threshold
79 (10%)	Pb productivity A	7	41.941	Contig49880_1051	******	17.8	**3.19**	**3.4**
80 (10%)	PbUpE(i) B	4	38.692	Contig31442_1353	******	23.4	**4.15**	**3.8**
81 (10%)	PbUpE(ii)	7	52.254	Contig34133_838	*******	37.1	**5.38**	**3.8**
82 (10%)	Pb productivity B	4	38.692	Contig31442_1353	*****	20.2	**3.68**	**3.5**
84 (10%)	PbUtE(i)	5	49.661	RV0184	*****	25.3	**4.74**	**3.6**
48 (30%)	Cut 1 shoot dry weight per plant (g)	4	34.753	Contig9278_995	*****	22.9	**4.22**	**3.5**
55 (30%)	Final harvest tiller numbers per plant	7	52.254	Contig34133_838	*******	59.2	**14.1**	**3.6**
56 (30%)	Final harvest tiller numbers per m²	3	10.979	Contig40640_647	******	23.6	**3.31**	**3.2**
		7	46.899	Contig48323_140	*******	58	**14.11**	**3.6**
58 (30%)	Final harvest root fresh weight per pot (g)	7	44.348	Contig51645_655	******	24.1	**4.45**	**3.6**
62 (30%)	Final harvest root dry weight per pot (g)	7	44.348	Contig51645_655	******	25.9	**4.83**	**3.7**
63 (30%)	Final harvest root dry weight per plant (g)	7	44.348	Contig51645_655	******	30.6	**5.87**	**3.8**
64 (30%)	Final harvest root dry weight per m² (g)	7	44.348	Contig51645_655	******	25.9	**4.83**	**3.6**

Table 4.6 *Continued*.

Trait Number	Trait Description	Linkage group	Map Position (cM)	Locus marker	KW signif.	% variance explained	LOD	PM LOD threshold
66 (30%)	Final harvest total plant dry weight per plant (g)	7	42.538	Contig41107_980	*****	23.8	**3.46**	**3.4**
67 (30%)	Final harvest shoot:root dry weight ratio (g/g)	7	52.254	Contig34133_838	*******	53	**8.91**	**3.5**
73 (30%)	Final harvest proportion of total Pb in the shoot (%)	5	39.29	Contig41419_340	*****	22.7	**4.19**	**3.9**
74 (30%)	Final harvest proportion of total Pb in the root (%)	5	39.29	Contig41419_340	*****	22.7	**4.19**	**3.7**

Significance levels KW:
***=P<0.1 **=P<0.05 ***=P<0.01 ****=P<0.005 *****=P<0.001 ******=P<0.0005 *******=P<0.0001**

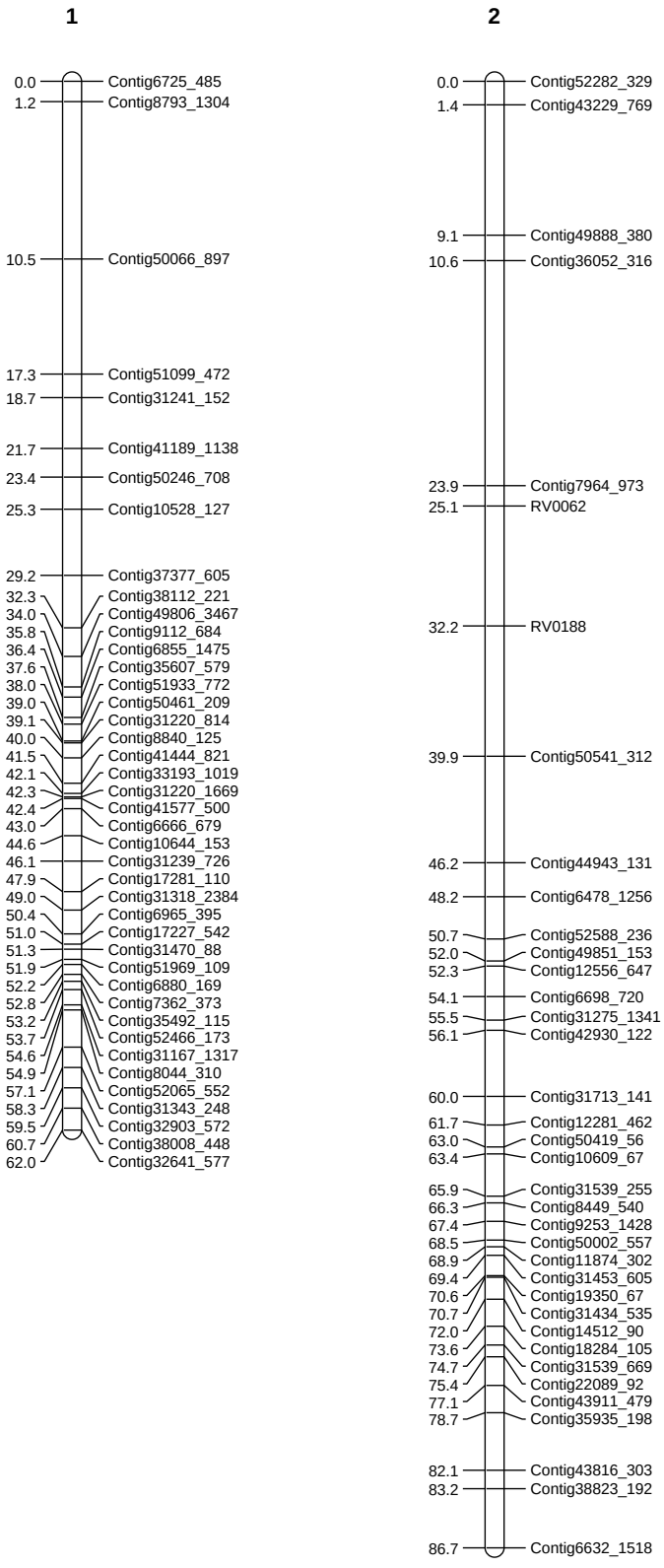

Figure 4.52 Genetic linkage diagrams showing detected QTL from Pb Experiment 1. Numbering for each QTL refers to trait number and treatment (e.g. Pb/12C = trait 12 in control treatment, Pb/12/10% = trait 12 in 10% Pb treatment). Note, that for clarity, not all contigs are shown on the linkage map.

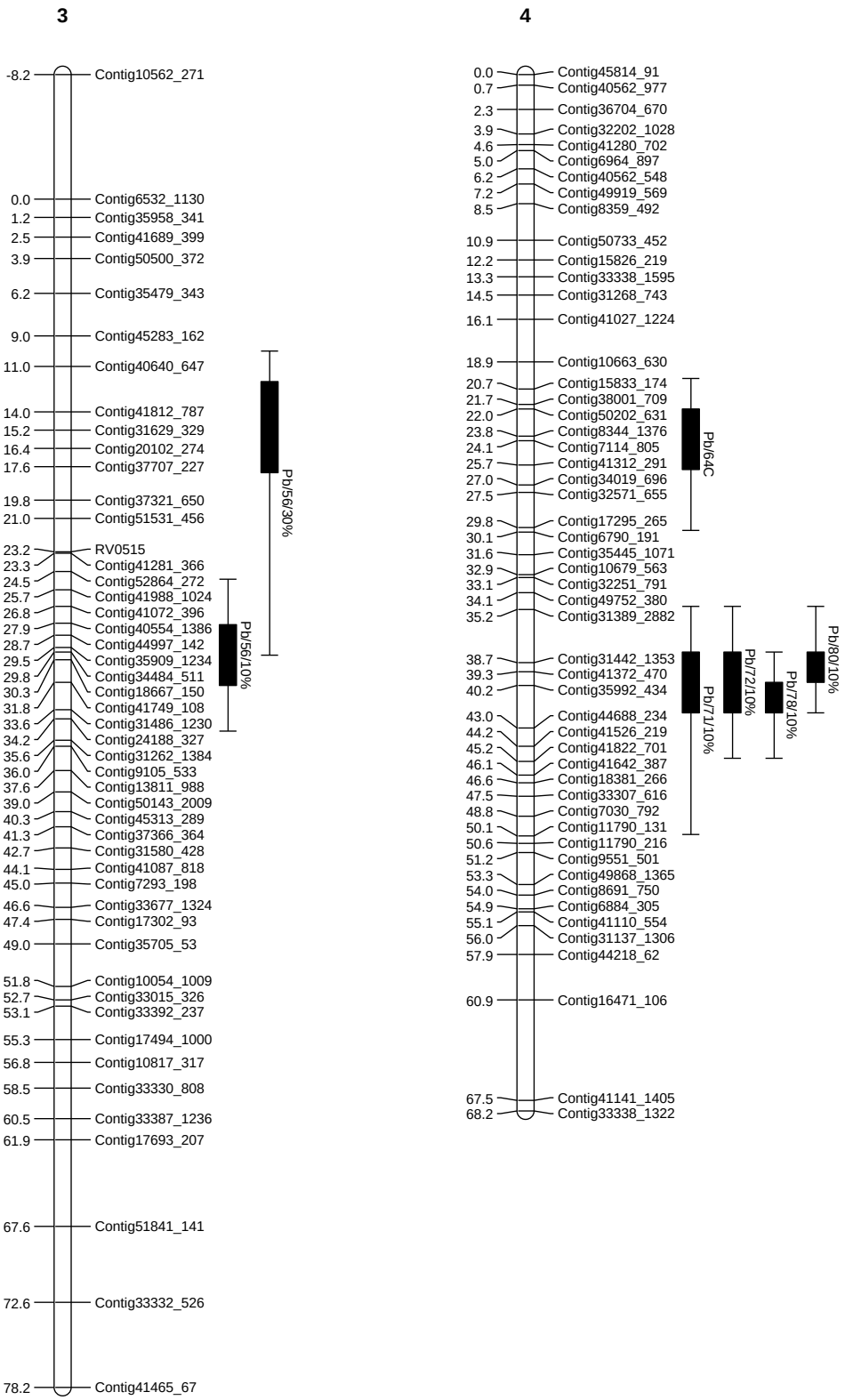

Figure 4.52 Continued.

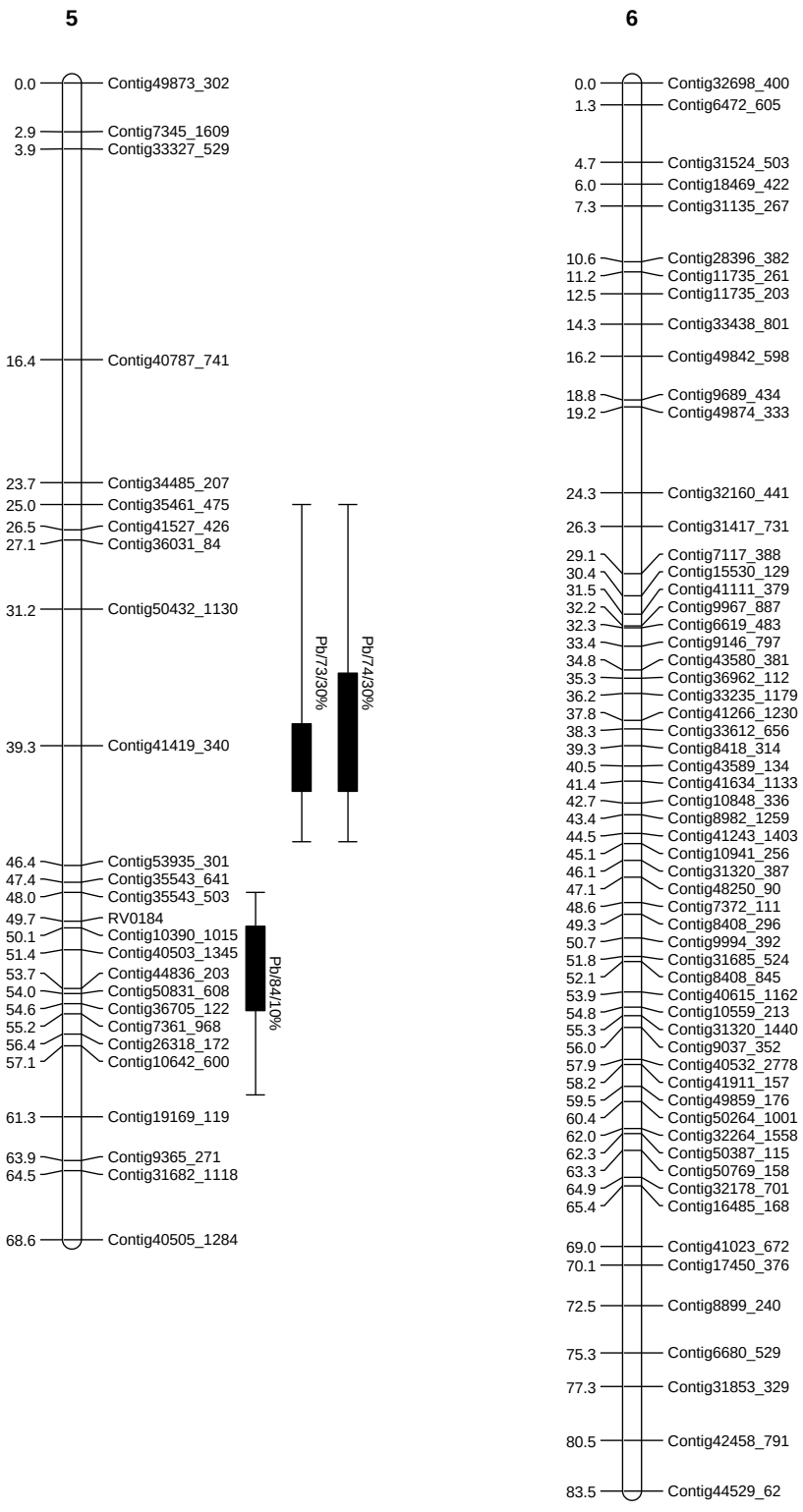

Figure 4.52 Continued.

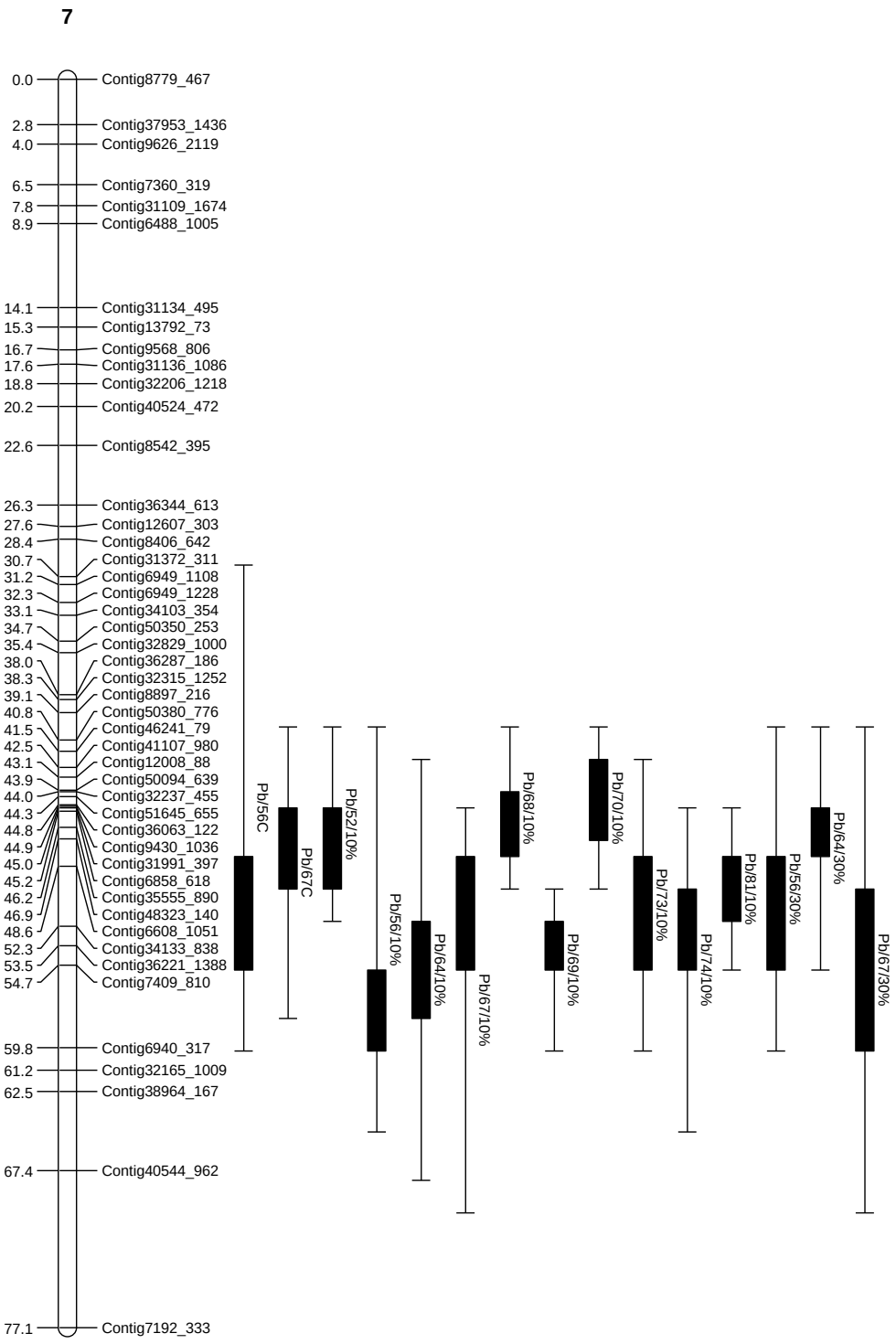

Figure 4.52 Continued.

4.5 Summary

- In Zn Experiment 1 there was a mortality rate of ~ 15% in the 10% Zn treatment which increased to ~ 40% in the 30% Zn treatment. Chlorosis was evident in both treatments.
- There was a significant decrease in shoot, root and total plant dry weights with increasing Zn substrate concentrations. There was a moderate correlation between shoot dry weight and the degree of correlation increased with increasing Zn substrate concentrations.
- The Zn content of the shoots increased with increasing Zn substrate concentrations whilst Zn content in the roots was generally higher in the 10% Zn treatment than in the 30% treatment. There was a very strong correlation between total Zn content of the root and total plant dry weight. TIs increased with increasing Zn substrate concentrations, with four genotypes having a TI of between 1 – 1.5.
- All genotypes survived to final harvest in Pb Experiment 2, with no physical evidence of chlorosis, stunted growth or die-back.
- There was a significant increase in shoot and root dry with increasing Pb substrate concentrations, and a strong correlation was observed between tiller production in the 10% and 30% Pb treatments.
- There was a marked increase in shoot and root Pb content with increasing Pb substrate concentrations, and a moderately strong correlation between root Pb content and root dry weight. A strong correlation was also observed between shoot Pb content and tissue Pb concentrations and the degree of correlation increased with exposure time. TIs were all consistently << 1, with mean TIs of 0.14 in the 10% Pb treatment and only 0.08 in the 30% Pb treatment.
- Several plant growth parameters varied between replicate Blocks A and B in each experiment and also between each experiment. In the latter case, algal contamination and concomitant nutrient reduction at the 8 week stage of Pb Experiment 2 may account for the reduced rates of plant growth in the control treatment.
- A total of 10 growth- and metal uptake-related QTL, located on LGs 4, 6 and 7, were identified from data collected during Zn Experiment 1, whilst 25 growth- and metal uptake-related QTL, located on LGs 3, 4, 5 and 7, were identified in Pb Experiment 2.

CHAPTER 5

RELATIONSHIPS BETWEEN KEY TRAITS OF POTENTIAL PRACTICAL PLANT BREEDING VALUE

5.1 Key relationships

One of the principle objectives of this research project was to identify, from within the mapping family, elite genotypes which could form the basis of new 'metal-tolerant' and 'high-metal uptake' breeding populations. The populations could be established either by polycrossing amongst the 'high' performers from this population alone, or by selecting elite individuals from this mapping family and crossing them with an elite amenity variety of *L. perenne* such as AberImp or AberSprite. This chapter investigates the correlation between key traits that are representative of growth, HM uptake efficiency and HM utilisation efficiency. HM uptake efficiency (i.e. acquisition efficiency) is a measure of the total amount of HM that each individual is able to absorb (i.e. shoot and root content), and can therefore be defined in terms of μg metal/plant. In contrast, HM utilisation efficiency (i.e. the efficiency of internal storage and tolerance) is a measure of the ratio between plant growth (g/plant) and intracellular HM sequestration, or tissue concentration, measured in mg^{-1} g^{-1}, and can therefore be defined in terms of g^2 dwt mg^{-1} metal (e.g. Humphreys and Macduff, 2000).

It was noted previously in Sections 2.3.2 and 4.1.1 that, in relation to growth, two key attributes required by plants for the phytostabilisation of contaminated substrates are a dense rooting system and the provision of high surface coverage. Thus, a high biomass production and high tiller production are important prerequisites. In Zn Experiment 1, there was a moderately high correlation between shoot dry weight and tiller production in both the 10% and 30% Zn treatment, as evidenced by relatively high R^2 values of ~ 0.4 (Figures 5.1A and 5.1B). In the 10% Zn treatment, a total of 11 genotypes, namely 4, 13, 14, 16, 19, 25, 30, 33, 77, 78 and 201A, yielded ≥ 40 tillers per plant (see Figures 4.11 and 5.1A), whilst still maintaining a relatively high dry matter production of > 1.3 g/plant, this being equivalent to the total mean shoot dry weight. Genotype 13 produced the greatest number of tillers per plant (68) and was one of the top six performers in terms of dry matter production, yielding 1.9 g/plant. In the 30% Zn treatment, a total of five genotypes, namely 1, 4, 13, 37 and 49, produced > 40 tillers per plant whilst still maintaining a relatively high dry matter production of between 1.25 and 1.6 g/plant (see Figures 4.11 and 5.1B). Once again, Genotype 13 was the best overall performer,

producing 76 tillers per plant, more than in the 10% Zn treatment, and maintaining a dry matter production of 1.4 g/plant, which was significantly greater than the total mean shoot dry weight of 0.966 g/plant.

In contrast to the Zn treatments, there was very little correlation between shoot dry weight and tiller production in either the 10% or 30% Pb treatments, as evidenced by exceedingly low R^2 values of ~ 0.02 (Figures 5.1C and 5.1D). However, in the 10% Pb treatment, a total of six individuals produced > 45 tillers per plant, namely Genotypes 4, 13, 14, 20, 78 and 201A (see Figures 4.34 and 5.1C), whilst still maintaining a relatively high dry matter production of between 1.2 and 1.7 g/plant. Genotype 78 produced the greatest number of tillers per plant (55) in the 10% Pb treatment, with a dry matter production of ~ 1.3 g/plant, slightly higher than the total mean shoot dry weight of 1.25 g/plant. In the 30% Pb treatment, a total of three individuals produced 60 or more tillers, namely Genotypes 11, 78 and 201A (see Figure 4.34), whilst yielding shoot dry weights of ≥ 1.5 g/plant. Of these, Genotype 11 was the best performer, producing 62 tillers per plant, whilst yielding a shoot dry weight of ~ 2.0 g/plant, significantly higher than the total mean shoot dry weight of 1.41 g/plant.

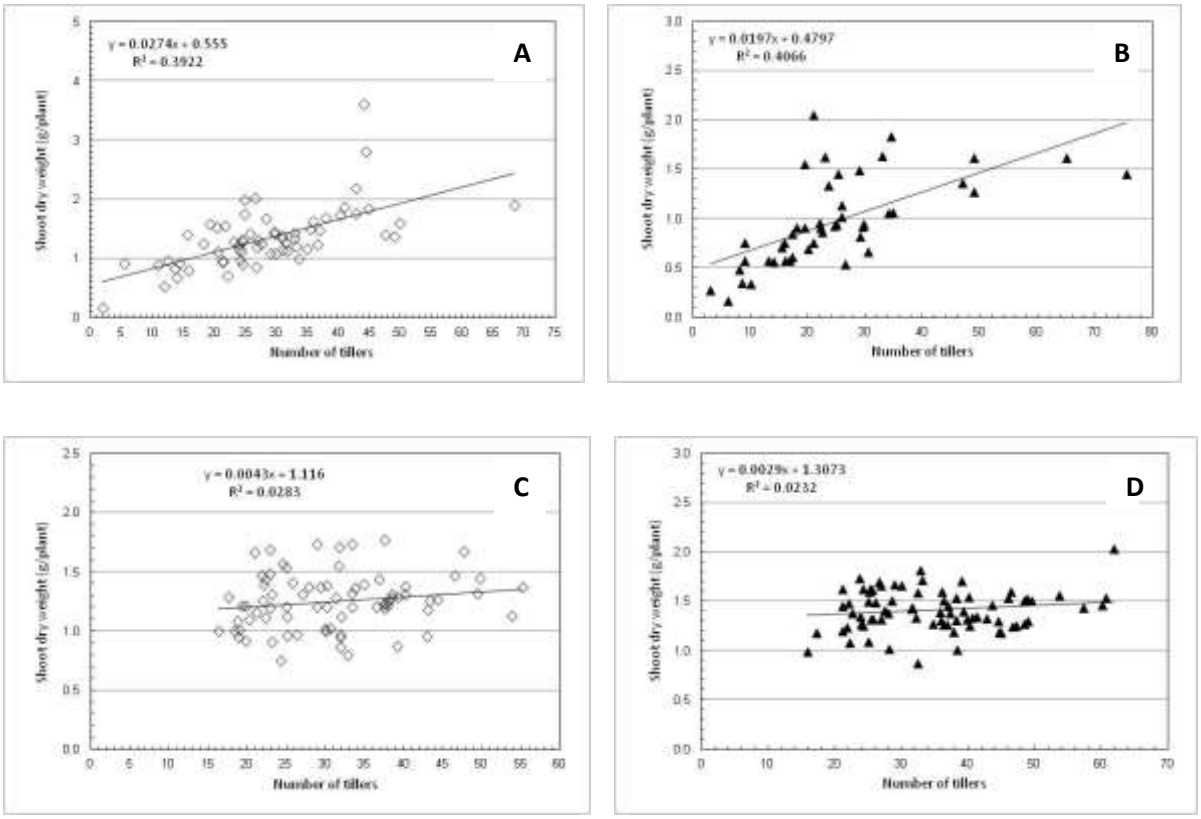

Figure 5.1 Scatter plots showing the relationship between shoot dry weight and number of tillers produced by the ≤ 77 genotypes at final harvest in A) the 10% Zn treatment, B) the 30% Zn treatment, C) the 10% Pb treatment, and D) the 30% Pb treatment. Straight lines are the linear regressions for the data.

In relation to HM uptake efficiency and HM utilisation efficiency, scatter plots of the correlation between these two parameters reveal significant variations in behaviour both within and between the Zn and Pb experiments. In the 10% Zn treatment there was only a very weak positive correlation between uptake and utilisation efficiency, as evidenced by an R^2 value of ~ 0.08, whereas in the 30% Zn treatment the degree of positive correlation had greatly increased, as evidenced by an R^2 value of ~ 0.48 (Figures 5.2A and B). In the 10% Zn treatment, Genotype 16 is of particular note since it displayed the second highest uptake efficiency coefficient (~ 26,000 µg Zn/plant) and the highest utilisation coefficient (1.36 g^2 mg^{-1} Zn). In the 30% Zn treatment, a group of three individuals, namely Genotypes 31, 49 and 57, exhibited Zn utilisation efficiency coefficients that were > 0.5 g^2 mg^{-1} Zn and Zn uptake coefficients > 13,000 µg Zn/plant, with Genotype 31 having the highest utilisation efficiency coefficient (0.56 g^2 mg^{-1} Zn) and the second highest uptake efficiency coefficient (~ 22.000 µg Zn/plant).

In contrast to the Zn treatments, both of the Pb treatments showed weak negative correlations, as evidenced by R^2 values of only ~ 0.8 in the 10% Pb treatment and ~ 0.17 in the 30% Pb treatment (Figures 5.2C and D). Although metal uptake efficiency was much lower in the Pb treatments relative to the same measure in the Zn treatments, measures of Pb utilisation efficiency were much higher than in the Zn treatments by over an order of magnitude. In the 30% Pb treatment, Genotypes 30 and 39 displayed the highest uptake efficiency (~ 5,200 µg Pb/plant and ~ 3,800 µg Pb/plant) but with nearly the smallest utilisation efficiency (~ 2.0 – 2.2 g^2 mg^{-1} Pb) of any genotype. In contrast, Genotypes 11 and 28 displayed the highest utilisation efficiency coefficients (~ 5.6 and 6.0 g^2 mg^{-1} Pb) but only relatively low uptake efficiency coefficients (~ 1,000 – 2,000 µg Pb/plant).

Other traits which were examined included metal content of either the shoots or roots as a function of tiller number, and metal uptake efficiency in the 10% treatments as a function of the same measure in the 30% treatments. Data for these trait relationships are shown in Table 5.1 and reveal only weak or very weak positive correlations, as evidenced by their relatively low R^2 values.

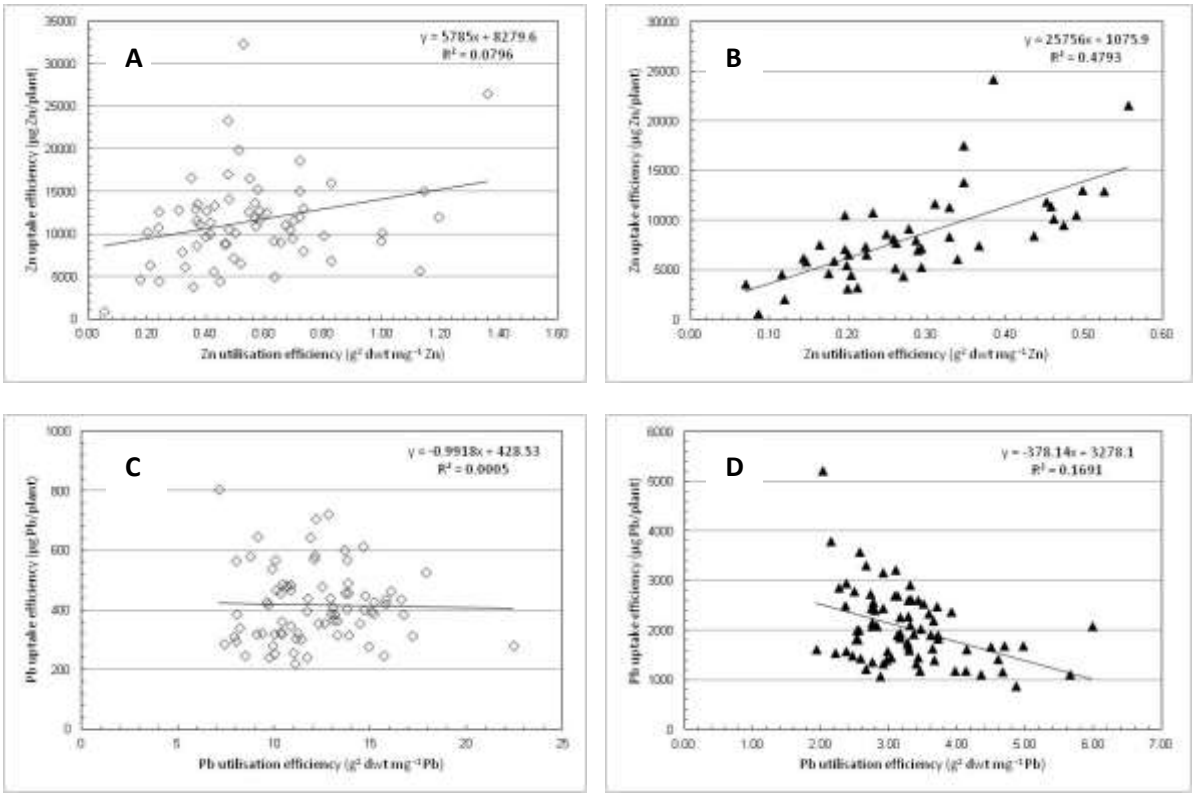

Figure 5.2 Scatter plots showing the relationships between uptake efficiency and utilisation efficiency on a whole plant basis by the ≤ 77 genotypes at final harvest in A) the 10% Zn treatment, B) the 30% Zn treatment, C) the 10% Pb treatment, and D) the 30% Pb treatment. Straight lines are the linear regressions for the data.

Table 5.1 *R^2 values for the trait relationships examined.*

Trait 1 v. Trait 2	**Zn R^2 values**		**Pb R^2 values**	
	10%	**30%**	**10%**	**30%**
Shoot dry weight (g/plant) v. number of tillers	0.39	0.41	0.03	0.02
Zn/Pb content of shoot (µg Zn/Pb/plant) v. number of tillers	0.28	0.14	0.01	0.01
Zn/Pb content of root (µg Zn/Pb/plant) v. number of tillers	0.24	0.19	0.13	0.17
Uptake efficiency (µg Zn/Pb/plant) v. utilisation efficiency (g^2 dwt mg^{-1} Zn/Pb)	0.08	0.48	0.0005 (-ve)	0.16 (-ve)
Uptake efficiency (µg Zn/Pb/plant) at 10% v. uptake efficiency (µg Zn/Pb/plant) at 30%	0.09		0.29	
Utilisation efficiency (g^2 dwt mg^{-1} Zn/Pb) at 10% v. utilisation efficiency (g^2 dwt mg^{-1} Zn/Pb) at 30%	0.02		0.0005 (-ve)	

5.2 Genotype rankings

5.2.1 Background to ranking procedure

In addition to the inter-trait correlations investigated in Section 5.1, and in order to provide a more robust analysis of genotype performance, the phenotypes for 10 representative traits, categorised as growth-related, uptake-related or utilisation efficiency traits, were ranked to identify the 'best' and 'poorest' ten performing genotypes, in the Zn and the Pb experiments. The aim of this analysis was to identify an elite group of genotypes from the 'high' performers for breeding purposes and further genetic analysis. In addition, genotypes exhibiting the highest and lowest metal uptake and tolerance could be subject to further comparative genotyping to determine the genes responsible.

The ranked traits are listed below (numbers in brackets are the trait number for each experiment respectively (Zn/Pb); see full listing in Appendices 3 and 4):

Growth-related traits

- Final harvest shoot dry weight per plant (g) (16/60)
- Final harvest root dry weight per plant (g) (19/63)
- Final harvest total plant dry weight per plant (g) (22/66)
- Final harvest tiller numbers per plant (11/55)

Uptake-related traits

- Final harvest shoot Zn/Pb content per plant (µg Zn/Pb) (26/70)
- Final harvest root Zn/Pb content per plant (µg Zn/Pb) (27/71)
- Final harvest total Zn/Pb content per plant (µg Zn/Pb) (28/72)

Utilisation efficiency traits

- Fresh weight gain/Zn/Pb uptake over experiment based on whole plant based on cut 1 and final harvest (g fwt mg^{-1} Zn/Pb) (34/79)
- Zn/Pb utilisation efficiency defined by total plant dwt at final harvest divided by the average concentration of Zn/Pb in the whole plant at final harvest (g^2 dwt mg^{-1} Zn/Pb) (39/84)
- Zn utilisation efficiency defined by shoot dwt at final harvest divided by shoot Zn concentration at final harvest (g^2 dwt mg^{-1} Zn/Pb) (40/85)

The genotypes were ranked using a 'data sorting' routine in Excel for each of the traits, and separately for the control, 10% and 30% treatments in each experiment. The ten best and the ten poorest performing genotypes for each trait are presented here.

5.2.2 Zinc tolerance and uptake

In terms of shoot and root dry matter production, Genotypes 13, 14, 16, 31 and 56 showed the highest tolerances to Zn treatment (Table 5.2). Genotypes 13, 14 and 16 were standouts in the 10% treatment, whilst 31 and 56 performed best in the 30% Zn treatment. Genotype 13 also produced the highest number of tillers in both treatments and was the only genotype in the top ten for both 10% and 30% treatments and across all four growth-related traits.

Table 5.2 *Ten best performing genotypes, ranked in descending order, for four growth-related traits measured in Zn Experiment 1 (control, 10% and 30% treatments). Bolded genotypes are discussed in the text.*

Trait 11 Tillers / plant			**Trait 16** Shoot dry weight (g/plant)			**Trait 19** Root dry weight (g/plant)			**Trait 22** Total dry weight (g/plant)		
Control	**10 %**	**30 %**	**Control**	**10 %**	**30 %**	**Control**	**10%**	**30 %**	**Control**	**10%**	**30%**
4	**13**	**13**	85	**16**	**56**	**145**	**16**	**31**	**145**	**16**	**31**
13	78	49	169	25	**31**	**14**	**14**	47	**14**	**14**	**56**
20	30	37	201A	77	22	9	**13**	**56**	169	25	49
9	19	4	48	164	48	39	4	49	201A	**13**	48
19	33	1	**145**	178	37	59	164	57	9	164	57
78	25	**14**	49	**13**	49	1	23	48	59	4	47
49	**16**	**31**	22	**14**	57	169	30	**14**	48	201A	**13**
201A	77	47	70	33	157	20	201A	**13**	1	178	37
1	4	22	25	4	60	**31**	78	59	39	78	60
36	**14**	78	61	179	**13**	58	53	6	58	77	157

The lowest shoot and root dry weights were recorded by Genotype 41 in the 10% treatment and Genotype 192 in the 30% treatment (Table 5.3). These two genotypes were also amongst the poorest with respect to tiller production.

Table 5.3 *Ten poorest performing genotypes for four growth-related traits measured in Zn Experiment 1 (control, 10% and 30% treatments). Poorest performing genotypes are at the top of the table. Bolded genotypes are discussed in the text.*

Trait 11 Tillers / plant			**Trait 16** Shoot dry weight (g/plant)			**Trait 19** Root dry weight (g/plant)			**Trait 22** Total dry weight (g/plant)		
Control	**10 %**	**30 %**	**Control**	**10 %**	**30 %**	**Control**	**10 %**	**30 %**	**Control**	**10 %**	**30 %**
75	**41**	153	**40**	**41**	**192**	**40**	**41**	**192**	**40**	**41**	**192**
150	**40**	**192**	90	72	153	72	148	26	72	72	26
73	7	85	72	148	66	54	**192**	39	54	148	153
54	72	26	38	5	26	**192**	72	65	**192**	5	66
16	150	70	26	192	85	41	150	153	38	**192**	85
41	66	120	2	66	34	157	5	28	2	150	65
53	148	66	17	26	53	28	54	23	17	7	114
17	3	129	34	7	129	2	7	85	157	18	129
72	57	53	129	18	70	62	18	114	41	**40**	70
40	192	30	15	3	19	60	**40**	150	90	26	53

The highest levels of Zn uptake were recorded by Genotypes 14 and 16 in the 10% treatment and by Genotypes 31 and 56 in the 30% treatment (Table 5.4). Genotypes 16 and 56 recovered the most Zn in the shoots, respectively, in the 10% and 30% treatments.

Table 5.4 *Ten best performing genotypes, ranked in descending order, for three uptake-related traits measured in Zn Experiment 1 (control, 10% and 30% treatments). Bolded genotypes are discussed in the text.*

Trait 26 Shoot Zn content (μg Zn/plant)			**Trait 27** Root Zn content (μg Zn/plant)			**Trait 28** Total Zn content (μg Zn/plant)		
Control	**10%**	**30%**	**Control**	**10%**	**30%**	**Control**	**10%**	**30%**
75	**16**	**56**	**14**	**14**	**31**	145	**14**	**56**
70	25	48	145	201A	**56**	**14**	**16**	**31**
85	77	22	19	**16**	60	169	201A	48
49	201A	**31**	169	78	48	48	78	60
48	178	37	9	4	49	19	4	57
1	78	157	39	49	57	58	51	49
179	164	4	48	51	51	39	49	47
201A	**56**	57	58	120	47	9	120	**14**
169	20	60	4	30	**14**	201A	164	13
59	150	150	45	164	13	1	30	4

The lowest recoveries of Zn in both the shoots and roots were by Genotypes 41 and 192, respectively, in the 10% and 30% treatments (Table 5.5).

Table 5.5 *Ten poorest performing genotypes for three uptake-related traits measured in Zn Experiment 1 (control, 10% and 30% treatments). Poorest performing genotypes are at the top of the table. Bolded genotypes are discussed in the text.*

Trait 26 Shoot Zn content (μg Zn/plant)			**Trait 27** Root Zn content (μg Zn/plant)			**Trait 28** Total Zn content (μg Zn/plant)		
Control	**10%**	**30%**	**Control**	**10%**	**30%**	**Control**	**10%**	**30%**
192	**41**	**192**	40	**41**	**192**	40	**41**	**192**
15	59	26	54	192	26	**192**	**192**	26
40	148	53	**192**	150	65	72	7	85
38	**192**	10	72	7	85	38	148	65
90	47	66	157	72	39	17	72	153
23	72	85	**41**	148	153	**41**	34	10
37	34	34	28	54	114	54	40	53
17	7	65	2	34	28	157	59	66
30	40	153	6	40	10	15	150	114
122	66	129	60	5	66	26	5	39

Averaged across the two treatments, Genotype 59 showed the highest Zn productivity (Trait 34), whilst the highest utilisation efficiencies were recorded in Genotypes 16 and 31, respectively, in the 10% and 30% treatments (Table 5.6). Genotypes 41 and 153 had the lowest utilisation efficiencies, respectively, in the 10% and 30% treatments. These two genotypes also featured amongst the lowest in terms of Zn productivity (Table 5.7).

Table 5.6 *Ten best performing genotypes, ranked in descending order, for three utilisation efficiency traits measured in Zn Experiment 1 (control, 10% and 30% treatments). Bolded genotypes are discussed in the text.*

Trait 34 Zn productivity (g fwt mg^{-1} Zn)			**Trait 39** ZnUtE(i) (g^2 dwt mg^{-1} Zn)			**Trait 40** ZnUtE(ii) (g^2 dwt mg^{-1} Zn)		
Control	**10%**	**30%**	**Control**	**10%**	**30%**	**Control**	**10%**	**30%**
192	**59**	37	145	**16**	**31**	57	**16**	49
37	33	**59**	20	13	49	164	25	**31**
7	34	22	36	25	57	169	77	13
15	153	157	**59**	**59**	37	192	164	57
34	77	9	201A	77	22	85	33	60
6	54	1	9	33	157	14	2	37
33	40	49	39	164	13	45	179	1
57	2	13	1	153	47	48	14	22
40	**192**	23	**31**	45	1	145	178	150
17	13	20	48	2	56	56	4	157

Table 5.7 *Ten poorest performing genotypes for three utilisation efficiency traits measured in Zn Experiment 1 (control, 10% and 30% treatments). Poorest performing genotypes are at the top of the table. Bolded genotypes are discussed in the text.*

Trait 34 Zn productivity (g fwt mg^{-1} Zn)			**Trait 39** ZnUtE(i) (g^2 dwt mg^{-1} Zn)			**Trait 40** ZnUtE(ii) (g^2 dwt mg^{-1} Zn)		
Control	**10%**	**30%**	**Control**	**10%**	**30%**	**Control**	**10%**	**30%**
75	7	**153**	40	**41**	**153**	40	**41**	**153**
145	14	70	72	72	192	90	72	66
14	**41**	56	18	18	66	18	5	192
169	201A	66	75	5	26	2	26	26
39	51	30	54	26	70	72	150	114
201A	26	114	2	3	129	129	3	30
18	3	120	90	148	30	26	18	19
1	18	48	150	44	114	44	11	85
120	49	19	38	11	19	150	66	70
58	63	129	157	150	78	78	148	129

5.2.3 Lead tolerance and uptake

The most tolerant genotypes in terms of shoot dry weight were Genotypes 30 and 11, respectively, in the 10% and 30% treatments (Table 5.8), whilst Genotypes 129 and 201A had the highest root dry weights across both Pb treatments. Genotype 14 also featured prominently among the top performers with respect to dry matter production across both treatments. Highest numbers of tillers were produced by Genotypes 53 and 62, respectively, in the 10% and 30% treatments. It is noteworthy that neither of these genotypes ranked in the top ten for shoot or root dry weight in either treatment.

Table 5.8 *Ten best performing genotypes, ranked in descending order, for four growth-related traits measured in Pb Experiment 2 (control, 10% and 30% treatments). Bolded genotypes are discussed in the text.*

Trait 55 Tillers / plant			**Trait 60** Shoot dry weight (g/plant)			**Trait 63** Root dry weight (g/plant)			**Trait 66** Total dry weight (g/plant)		
Control	**10 %**	**30 %**	**Control**	**10 %**	**30 %**	**Control**	**10 %**	**30 %**	**Control**	**10 %**	**30 %**
26	**53**	**62**	**26**	**30**	**11**	**26**	**201A**	**129**	**26**	**14**	**11**
78	60	33	**30**	54	61	48	**129**	**201A**	**30**	**201A**	**129**
13	39	**30**	6	61	178	**201A**	4	**14**	48	**30**	48
19	65	49	4	37	48	13	**14**	**11**	4	4	**30**
201A	72	28	7	120	**30**	78	78	13	6	37	**14**
4	**26**	85	48	**14**	66	19	**30**	4	13	**129**	4
14	13	164	37	178	120	4	6	63	39	6	**201A**
28	18	20	70	145	157	**14**	13	78	**14**	61	13
9	56	55	39	6	41	23	63	48	78	54	6
18	48	18	13	3	52	153	37	6	37	145	78

Amongst the poorest performing genotypes across the three dry matter production traits, Genotype 62 was most consistent in the 10% treatment (Table 5.9). Genotype 72 was poorest in the 30% treatment, but also featured in the bottom five performers in the 10% treatment. Neither of these two genotypes was ranked amongst the poorest in terms of tiller production.

Table 5.9 *Ten poorest performing genotypes for four growth-related traits measured in Pb Experiment 2 (control, 10% and 30% treatments). Poorest performing genotypes are at the top of the table. Bolded genotypes are discussed in the text.*

Trait 55 Tillers / plant			**Trait 60** Shoot dry weight (g/plant)			**Trait 63** Root dry weight (g/plant)			**Trait 66** Total dry weight (g/plant)		
Control	**10 %**	**30 %**	**Control**	**10 %**	**30 %**	**Control**	**10 %**	**30 %**	**Control**	**10 %**	**30 %**
45	85	5	**59**	**62**	**59**	**59**	25	20	**59**	**62**	**72**
72	28	25	51	26	45	17	77	**72**	17	26	45
22	1	38	17	**59**	40	**62**	17	**62**	51	18	2
60	164	36	22	18	2	5	**72**	17	22	**72**	**59**
17	179	16	85	2	**72**	85	18	7	85	2	17
52	148	1	1	**72**	192	22	2	45	1	25	192
164	145	11	**72**	22	17	41	**62**	25	5	17	40
16	10	65	60	11	34	1	73	148	25	192	20
75	7	90	25	56	10	192	26	2	**62**	22	**62**
59	70	78	38	192	18	25	45	22	60	77	148

The highest levels of Pb uptake to the roots were recorded by Genotypes 39 and 30, respectively, in the 10% and 30% treatments (Table 5.10). Genotype 39 was also ranked second for total Pb content in the 30% treatment. Given that most of the Pb absorbed by the plants remained in the roots rather than being translocated to the shoots, the genotype rankings were almost identical for the root (Trait 71) and total plant (Trait 72) contents of Pb. Interestingly, Genotype 39 did not feature in the top ten genotypes for shoot Pb content (Trait 70) in the 10% treatment. In contrast, Genotype 201A, the second ranking genotype for Pb content of the whole plant in the 10% treatment, was ranked first and third, respectively, for shoot and root contents of Pb.

Table 5.10 *Ten best performing genotypes, ranked in descending order, for three uptake-related traits measured in Pb Experiment 2 (10% and 30% treatments). Bolded genotypes are discussed in the text. Ranking for the control treatment is not shown as levels of Pb were below the limit of detection in these plants.*

Trait 70 Shoot Pb content (µg Pb/plant)		**Trait 71** Root Pb content (µg Pb/plant)		**Trait 72** Total Pb content (µg Pb/plant)	
10%	**30%**	**10%**	**30%**	**10%**	**30%**
201A	38	**39**	**30**	**39**	**30**
157	**157**	4	**39**	**201A**	**39**
3	66	**201A**	4	4	4
37	**30**	55	78	55	78
75	44	6	129	6	129
114	61	**30**	14	**30**	14
179	3	129	56	37	56
145	120	34	48	145	48
6	14	37	34	34	34
61	41	145	1	114	1

The lowest recoveries of Pb in the whole plant were by Genotypes 25 and 60, respectively, in the 10% and 30% treatments (Table 5.11).

Table 5.11 *Ten poorest performing genotypes for three uptake-related traits measured in Pb Experiment 2 (10% and 30% treatments). Poorest performing genotypes are at the top of the table. Bolded genotypes are discussed in the text.*

Trait 70 Shoot Pb content (µg Pb/plant)		**Trait 71** Root Pb content (µg Pb/plant)		**Trait 72** Total Pb content (µg Pb/plant)	
10%	**30%**	**10%**	**30%**	**10%**	**30%**
56	59	**25**	**60**	**25**	**60**
21	**60**	2	72	2	72
33	40	17	26	33	28
59	114	26	28	45	26
19	17	45	148	26	54
129	25	77	54	17	90
20	58	33	90	77	148
45	10	192	49	36	49
25	129	62	2	192	2
63	28	36	62	65	62

The highest Pb productivities (Trait 79) in the 10% and 30% treatments were recorded, respectively, by Genotypes 61 and 40 (Table 5.12). These two genotypes were also highly ranked for the two utilisation efficiency traits (Traits 84 and 85), although Genotype 62 was ranked first in the 30% treatment. Genotype 3 ranked first for Trait 85 in the 10% treatment, but did not feature in the top ten for Trait 84. It should be noted that the utilisation efficiency index for Trait 84 was based on the average concentration of Pb in the whole plant, compared with that of just the shoot fraction for Trait 85.

Table 5.12 *Ten best performing genotypes, ranked in descending order, for three utilisation efficiency traits measured in Pb Experiment 2 (10% and 30% treatments). Bolded genotypes are discussed in the text.*

Trait 79 Pb productivity (g fwt mg^{-1} Pb)		**Trait 84** PbUtE(i) (g^2 dwt mg^{-1} Pb)		**Trait 85** PbUtE(ii) (g^2 dwt mg^{-1} Pb)	
10%	**30%**	**10%**	**30%**	**10%**	**30%**
61	**40**	**61**	**62**	**3**	**62**
7	36	72	**40**	38	**40**
56	58	18	59	48	66
1	21	192	36	18	19
18	122	20	10	20	33
148	59	54	58	31	15
70	16	58	16	49	47
4	**61**	53	51	192	153
59	**62**	7	122	**61**	31
3	1	17	66	7	78

Genotypes 47 and 45 had the lowest Pb productivities, respectively, in the 10% and 30% treatments (Table 5.13). These two genotypes were also amongst the lowest in terms of Pb utilisation efficiency indexed to the whole plant (Trait 84). Genotype 5 was also notably poor in the 30% treatment in terms of utilisation efficiency.

Table 5.13 *Ten poorest performing genotypes for three utilisation efficiency traits measured in Pb Experiment 2 (10% and 30% treatments). Poorest performing genotypes are at the top of the table. Bolded genotypes are discussed in the text.*

Trait 79 Pb productivity (g fwt mg^{-1} Pb)		**Trait 84** PbUtE(i) (g^2 dwt mg^{-1} Pb)		**Trait 85** PbUtE(ii) (g^2 dwt mg^{-1} Pb)	
10%	**30%**	**10%**	**30%**	**10%**	**30%**
47	**45**	**47**	**5**	**66**	72
75	18	**66**	**45**	73	39
52	33	59	18	2	**5**
90	28	73	75	10	51
39	37	10	179	**45**	192
30	55	57	37	4	75
73	85	179	7	39	65
26	52	51	55	85	1
63	63	52	39	201A	77
40	6	9	60	179	4

5.2.4 Control treatment rankings

The genotype rankings for the four growth-related traits in the control treatments prompt two questions: 1) to what extent do they coincide with those in the 10% and 30% Zn and Pb treatments; and 2) how similar are the rankings in the control treatments across the two experiments?

The majority of the highest ranking genotypes in the control treatment of Zn Experiment 1 (Table 5.2) differed from those for Zn tolerance (Genotypes 13, 16, 31 and 56). For example, the top three genotypes for shoot dry weight were not among the top ten genotypes for this trait in either the 10% or 30% Zn treatments. Likewise, Genotype 145, with the highest total plant dry weight in the control treatment, was not among the top ten genotypes in either the 10% or 30% treatments. Genotypes 16 and 31 had the highest total dry weights, respectively, in the 10% and 30% treatments, but were not in the top ten genotypes for this trait in the control treatment. However, there were also some similarities between the rankings. For example, Genotype 14 was ranked second for root and total plant dry weights in both the control and 10% treatments. Likewise, Genotype 13 was ranked second for tiller number in the control treatment and first for this trait in both the 10% and 30% Zn treatments.

The results were similar in Pb Experiment 2 (Table 5.8). Genotype 26 was ranked highest for shoot, root and total dry weight in the control treatment, but did not appear amongst the top ten genotypes for any of these traits in either the 10% or 30% Pb treatments. Similarly, Genotypes 11 and 129, which ranked first and second, respectively, for total plant dry weight in the 30% Pb treatment, were not among the top ten genotypes for shoot, root or total plant dry weight in the control treatment. In contrast, Genotype 201A appeared in the top three positions for root dry weight in control, 10% and 30% Pb treatments. Furthermore, Genotype 30 ranked second, first and fifth, respectively, for shoot dry weight in the control, 10% and 30% Pb treatments.

As discussed elsewhere (see Section 4.3), the control treatment rankings for the dry matter traits differed markedly across the two experiments, but showed significant similarity for tiller numbers (Tables 5.2 and 5.8). Genotypes 145 and 26 were ranked highest for dry matter production in the control treatment of the Zn and Pb experiments, respectively. However, neither genotype featured among the top ten genotypes in the control treatment of the other experiment. The top ten control treatment genotypes in-common across the two experiments were as follows: shoot dry weight: Genotypes 48 and 70; root dry weight: Genotype 14; total plant dry weight: Genotypes 14, 39 and 48; tiller numbers: Genotypes 4, 9, 13, 19, 78 and 201A.

It is unclear why the agreement between the control treatment rankings for tiller numbers, with six out of ten genotypes in-common, was much greater than observed for the dry weight traits. However, the difference may be related to the 'forage-type x amenity-type' origins of the mapping family, in so far as amenity-type genotypes tend to be profusely tillering, whilst forage-type genotypes are characterised by high dry matter yields. The differences observed in overlap between the rankings across the two experiments suggest that G x E effects on tiller production may be inherently smaller than those on dry matter production in the mapping population used for this study.

5.2.5 Recommended genotypes for further crossing

Based on the ranking exercise, the most promising genotypes for use in further investigative or selective breeding are listed in Table 5.14. These cover Zn/Pb tolerance, above and below ground accumulation of Zn/Pb, and site stabilisation based on profuse tillering. The recommended genotypes are also tailored to conditions of 'moderate' or 'acute' site contamination based, respectively, on performance in the 10% and 30% mine-tailing treatments.

There are several notable features of the listing. Firstly, there is significant overlap between the genotypes selected for Zn and Pb, namely Genotypes 13, 14, and 201A. Secondly, several genotypes feature in two or more categories. Genotype 14, for example, is promising in terms of tolerance to contamination by Zn and Pb, and below ground accumulation of both Zn and Pb. Genotype 201A also features in listings for Zn and Pb, whilst Genotype 13 features in listings for Zn tolerance and site stabilisation. However, several genotypes are specific to either Zn (e.g. Genotypes 16, 31 and 56) or to Pb (e.g. Genotypes 11, 30, 39 and 129).

Table 5.14 *Recommended genotypes for establishing Zn- and Pb-tolerant and high uptake breeding populations using poly- or pair-crossing approaches, based on the ranking of genotypes for high performance in the two experiments. The selections are tailored to conditions of 'moderate' and 'acute' site contamination based, respectively, on performance in the 10% and 30% mine-tailing treatments. A pair of 'promising' genotypes is listed in each case. Numbers listed in parenthesis are reserve genotypes, and are generally high performers across two or more categories. The traits listed in parentheses below the desired phenotypes refer to the basis for the selections in each case.*

Phenotype	**Moderate Zn** (10% Zn tailings)	**Acute Zn** (30% Zn tailings)	**Moderate Pb** (10% Pb tailings)	**Acute Pb** (30% Pb tailings)
Tolerance (Total plant dry weight)	14, 16 (13)	31, 56 (13)	14, 201A (30, 129)	11, 129 (14, 30, 201A)
Above ground accumulation (shoot Zn/Pb content)	16, 25 (56)	48, 56 (31)	157, 201A	38, 157 (30)
Below ground accumulation (root Zn/Pb content)	14, 201A (16)	31, 56 (14)	4, 39 (30, 201A)	30, 39 (4)
Site stabilisation (tiller number)	13, 78 (14, 16)	13, 49 (14, 31)	53, 60 (26)	33, 62 (30)

It should be mentioned that genotypes which died during the Zn treatments prior to the final harvest were not considered in the ranking exercise. As noted in Section 4.1, the mortality rate in the 10% Zn treatment was ~ 15% and it increased to ~ 40% in the 30% Zn treatment. The genotypes which did not survive are listed in Table 4.1. In contrast, all genotypes survived to the final harvest under all treatments in the Pb experiment (Section 4.2).

5.3 Genotype selection in-common for Zn and Pb

One of the key objectives of this research project was to identify those genotypes that performed well in terms of growth and metal uptake in both the Zn treatments and the Pb treatments. This raises the important question of whether it is possible to select in-common for Zn and Pb. In order to address this question, results from both experiments for key traits conferring growth/tolerance and metal uptake were analysed together in the form of scatter plots. The criterion for selection was to take the top 3 genotypes plotting nearest to the 1:1 gradient line, and disregard any outliers. These genotypes could be used in future poly-crossing trials, in order to create a new elite mapping family with the potential for phytostabilisation of areas with mixed-metal contamination. As in Section 5.2, the 10% and 30% HM treatments were investigated separately to give results for 'moderate' and 'acute' contamination conditions. Figure 5.3 illustrates how the selections were made, using examples of tiller production and shoot dry weight.

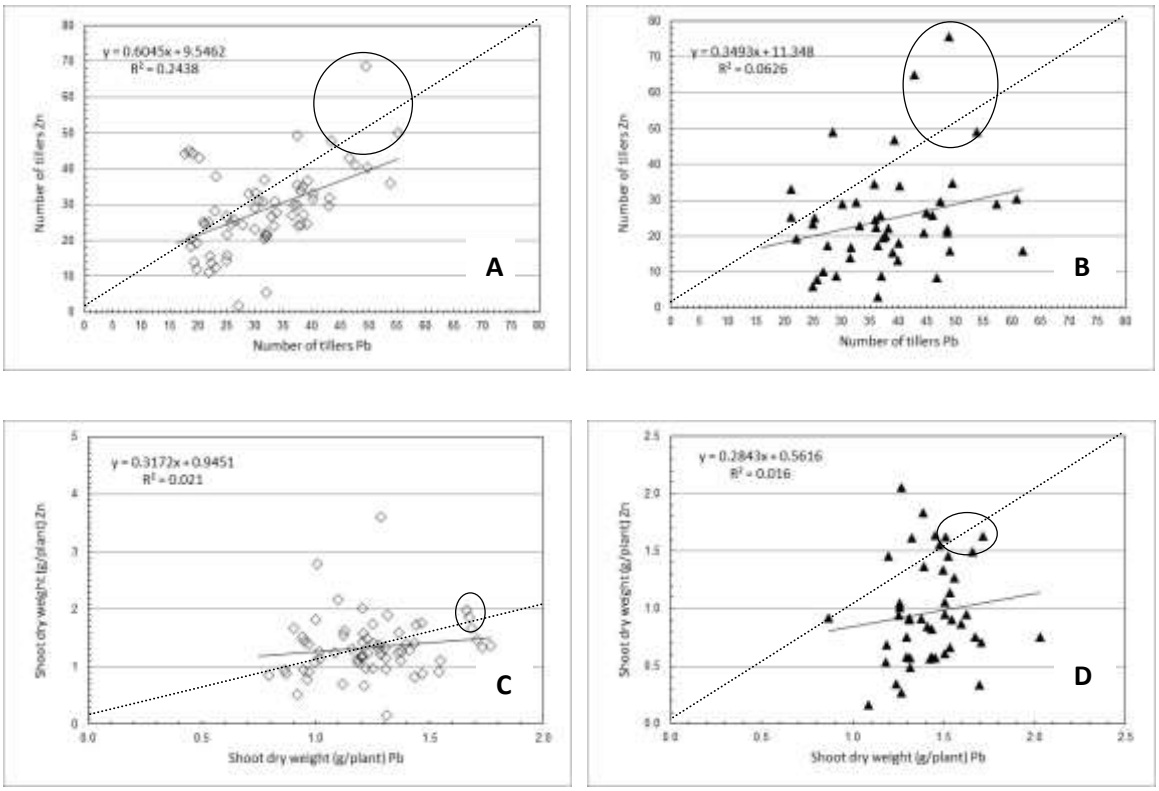

Figure 5.3 Relationship between A) tiller production in the 10% Zn treatment and tiller production in the 10% Pb treatment, B) tiller production in the 30% Zn treatment and tiller production in the 30% Pb treatment, C) shoot dry weight in the 10% Zn treatment and shoot dry weight in the 10% Pb treatment, and D) shoot dry weight in the 30% Zn treatment and shoot dry weight in the 30% Pb treatment. Straight lines are the regressions for the data and dashed lines are the 1:1 gradient line. Circles highlight the genotypes selected.

The results of this simple analysis, presented in Table 5.15, reveal that, despite very low R^2 values obtained for the trait correlations, it was still possible to select genotypes that performed well in both HM treatments. For example, in the 10% metal treatments, Genotype 4 performed well in terms of tolerance (i.e. high root and total plant dry weight) and subsurface metal uptake, whilst in the 30% metal treatments this genotype also performed well both in terms of subsurface/subaerial metal uptake and site stabilisation (tiller production). Similarly, Genotype 201A performed well in both 10% metal treatments both for tolerance and metal uptake, whilst in the 30% metal treatments Genotype 4 performed well in terms of both metal uptake and site stabilisation.

Table 5.15 *Genotypes selected for future plant breeding purposes based on their growth and metal-uptake attributes for both Zn and Pb combined.*

Phenotype	**Moderate Zn/Pb** (10% Zn/Pb tailings)		**Acute Zn/Pb** (30% mine tailings)	
	R^2	**Genotypes selected**	**R^2**	**Genotypes selected**
Tolerance (shoot dry weight)	0.02	14, 120, 178	0.02	37, 48, 157
(root dry weight)	0.17	4, 14, 201A	0.05	31, 47, 56
(total plant dry weight)	0.06	4, 30, 201A	0.02	31, 48, 56
Above ground accumulation (shoot Zn/Pb content**)**	0.001	37, 157, 201A	0.09	4, 31, 157
Below ground accumulation (root Zn/Pb content)	0.13	4, 39, 201A	0.03	4, 14, 30
Site stabilisation (tiller number)	0.24	13, 19, 78	0.06	4, 13, 49

5.4 Summary

- A ranking analysis of growth-, metal uptake- and utilisation-related traits was undertaken to identify the 'best' and 'poorest' ten performing genotypes in the Zn and Pb experiments. Four growth-related, 3 uptake-related and 3 utilisation efficiency traits were assessed. The underlying aim of this analysis was to identify those genotypes that could be used for investigative and/or selective breeding programmes.
- Genotype selections for metal tolerance, above ground metal accumulation, below ground metal accumulation and site stabilisation (tiller numbers) were identified separately both for Zn- and Pb-rich substrates.
- There was significant overlap between genotypes selected for Zn and Pb, namely Genotypes 13, 14 and 201A, and these genotypes were also high performers in two or more categories. However, several genotypes were noted as specific to either Zn (e.g. Genotypes 16, 31 and 56) or to Pb (e.g. Genotypes 11, 30, 39 and 129).
- Genotype selection in-common for Zn and Pb was also investigated using scatter plots to identify the top 3 performing genotypes in the 10% ('moderate') and 30% ('acute') HM treatments. Analysis revealed, for example, that Genotype 4 performed well in terms of tolerance and sub-surface metal uptake in the 10% HM treatments, but also performed well in terms of subsurface/subaerial and site stabilisation in the 30% HM treatments.

CHAPTER 6

COMPARISONS WITH SCREENING EXPERIMENTS FOR ZINC AND LEAD TOLERANCE IN FLOWING SOLUTION CULTURE

6.1 Screening in FSC

Screening of the mapping family used in this project has also been performed in the FSC facility in IBERS, for a range of attributes, as part of a DEFRA-commissioned research project (DEFRA LS3648) entitled 'Identification, genetic control and evaluation of traits enhancing environmental quality and bioremediation in multifunctional grassland'. These screens included growth and metal uptake over 28 days under conditions of supra-optimal concentrations in solution of Zn (Experiment 1:23:64) and toxic concentrations in solution of Pb (Experiment 1:23:66). In this chapter, the unpublished results from these two screening experiments in FSC are compared with those from the pot experiments in the current project. Such a comparison has not been made previously and is of interest for a number of reasons. Primarily, however, it provides an opportunity to compare two very different experimental systems in terms of: 1) the performance and ranking of genotypes for the traits associated with plant growth, Zn and Pb tolerance; and 2) associated QTL.

FSC is a particularly useful system for evaluating relationships between defined ionic concentrations in solution at the root surface and ion uptake and growth of plants (Wild *et al*., 1987). It also offers easy access to root systems and rapidity of batch screening. Ranking of *L. perenne* genotypes for growth and N uptake in FSC over 28 days closely matched longer term performance under field conditions (Wilkins *et al*., 1997). However, similar comparisons have not been made with respect to tolerance to toxic levels of heavy metals such as Zn and Pb. Experimental conditions in FSC do not simulate the complex chemistry (i.e. ionic speciation and fluctuating availability), physics and biology of the rhizosphere in a sand-mine tailing mixture. Intrinsically, therefore, the two experimental systems might be expected to produce somewhat different results. Such variation may also be confounded by differences between the two experimental systems in terms of length of treatment period, environmental conditions and degree of metal toxicity.

6.1.1 Growth, Zn/Pb uptake and tolerance in FSC

The two screening experiments (Experiments 1:23:64 and 1:23:66) for physiological tolerance to supra-optimal/toxic concentrations of Zn (100 µM) and Pb (25 µM) generated a large amount of trait data and revealed a number of significant relationships in terms of growth and metal uptake. The results from FSC discussed here refer only to the 77 genotypes in common with the two pot experiments of the current project, and are confined to the key traits discussed elsewhere in this thesis.

Tiller production varied widely across the mapping family (Figures 6.1A and 6.1B) and showed close correlation between control and supra-optimal/toxic treatments for both Zn ($R^2 = 0.62$) and Pb ($R^2 = 0.51$), with the majority of genotypes plotting on, or near to, the 1:1 gradient line. This agreement is reflected in the similarity between the mean numbers of tillers produced across the mapping family, at 15.3 and 15.1, respectively, for the control and supra-optimal Zn treatments; and 12.5 and 12.7, respectively, for the control and toxic Pb treatments. In the Zn screen, Genotypes 19 and 78 were the best performers, producing > 35 tillers in control and > 34 tillers in the Zn treatment, with Genotype 19 (not shown) producing > 40 tillers in control and > 47 in the Zn treatment. In the Pb experiment, Genotypes 18 and 201A were amongst the best performers, producing > 20 tillers in the control and ≥ 28 tillers in the Pb treatments, with Genotype 201A producing > 28 tillers in both the control and Pb treatments. It should be noted that the best performers in the Zn treatment performed badly in the Pb treatment and *vice-versa*.

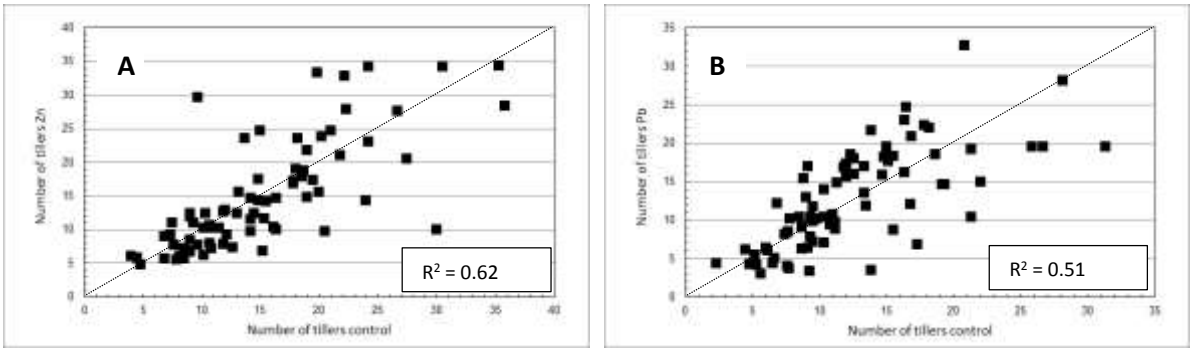

Figure 6.1 Relationships between tiller production by the 77 genotypes grown in FSC under A) supra-optimal Zn and control Zn, and B) toxic Pb and zero Pb. The dotted lines show the 1:1 line (i.e. gradient = 1).

With respect to metal tolerance, measured by total plant dry weight at final harvest (Figures 6.2A and 6.2B), control and metal treatments were closely correlated in both FSC experiments (Zn R^2

= 0.64 and Pb R^2 = 0.58). In the Pb treatment, the majority of genotypes plotted on, or near to, the 1:1 gradient line in the scatter plot for control verses toxic treatment, indicating an inconsistent effect of Pb on dry matter production across the population. In contrast, the majority of the genotypes (~ 80%) in the Zn experiment plotted below the 1:1 gradient line, indicating that dry matter production was reduced for most genotypes in the presence of a supra-optimal Zn concentration in FSC. The three best performers in the Zn experiment were Genotypes 19, 20 and 73, with total plant dry weights ≥ 1.5 g/plant. In the Pb experiment, Genotype 7, although a clear 'outlier', was the best performer with a total plant dry weight of 2.24 g/plant in the toxic Pb treatment, and considerably greater than that displayed by Genotype 52, the next best performer of all genotypes, with a total plant dry weight of 1.4 g/plant.

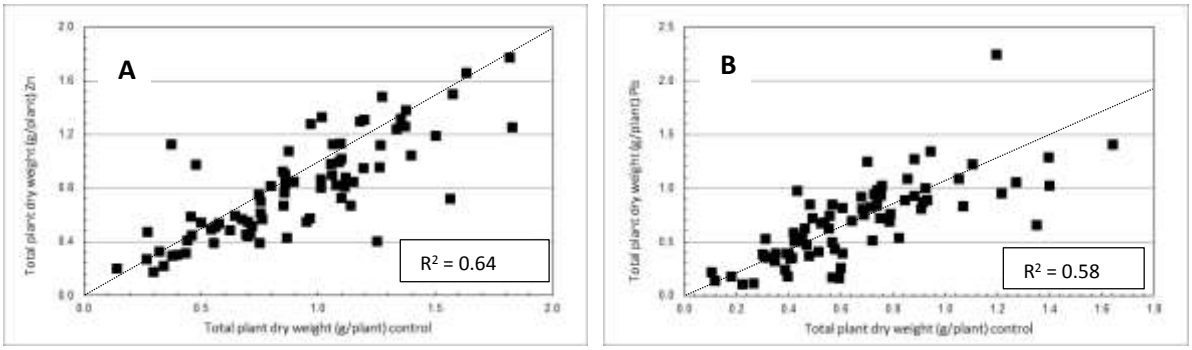

Figure 6.2 Relationships between the total plant dry weights of the 77 genotypes grown in FSC under A) supra-optimal Zn and control Zn, and B) toxic Pb and zero Pb. The dotted lines show the 1:1 line (i.e. gradient = 1).

Shoot dry weight showed a strong positive correlation with net metal uptake to the shoots after 28 days of supra-optimal/toxic treatments in both screens (Figures 6.3A and 6.3B), with R^2 = 0.92 for Zn and R^2 = 0.6 for Pb. The three best performers in the Zn experiment were Genotypes 19, 20 and 73, which displayed shoot Zn contents > 1,000 µg Zn/plant and shoot dry weights > 1.1 g/plant (Figure 6.3A). In the Pb experiment, metal content in the shoots was approximately eight times smaller, for any given shoot dry weight, than that seen in the Zn experiment. Excluding the anomalous 'outlier' Genotype 55, which accumulated > 200 µg Pb/plant, three individuals, namely Genotypes 7, 18 and 169, accumulated > 100 µg Pb/plant, whilst maintaining some of the highest shoot dry weights ranging between 0.94 – 1.7 g/plant (Figure 6.3B).

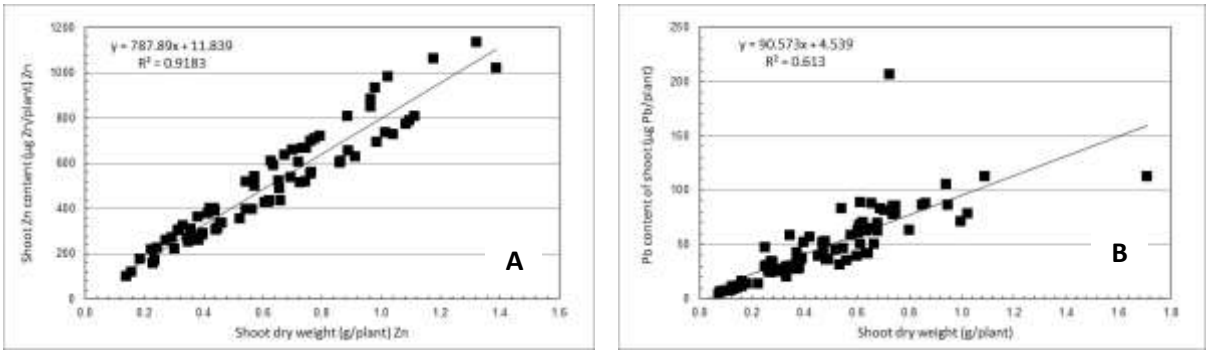

Figure 6.3 Relationship between shoot dry weight and metal uptake to the shoots of the 77 genotypes after 28 days exposure to A) supra-optimal Zn, and B) toxic Pb concentrations in FSC.

Uptake efficiency in the two FSC screens was measured as total plant (shoot + root) content of either Zn or Pb after 28 days of growth under the treatment concentrations. These values varied widely across the mapping family in both experiments (Figures 6.4A and 6.4B) and they were positively correlated with total plant dry weights, with $R^2 \sim 0.67$ in both cases. In the supra-optimal Zn treatment, Genotypes 19, 20, 47 and 73 were four of the best performers with total plant dry weights ranging between 1.47 and 1.82 g/plant, and an uptake efficiency ranging between 4,900 and 6,500 µg Zn/plant. Genotypes 3 and 61 displayed much higher uptake efficiencies of 9,365 and 8,695 µg Zn/plant, respectively, but had relatively lower total plant dry weights of 1.12 and 1.25 g/plant, respectively. In the Pb screen, Genotypes 7, 18, 52 and 66 were the best performers with total dry matter production ranging between ~ 1.24 and 2.24 g/plant, and Pb uptake efficiencies ranging between 2,400 and 4,200 µg Pb/plant.

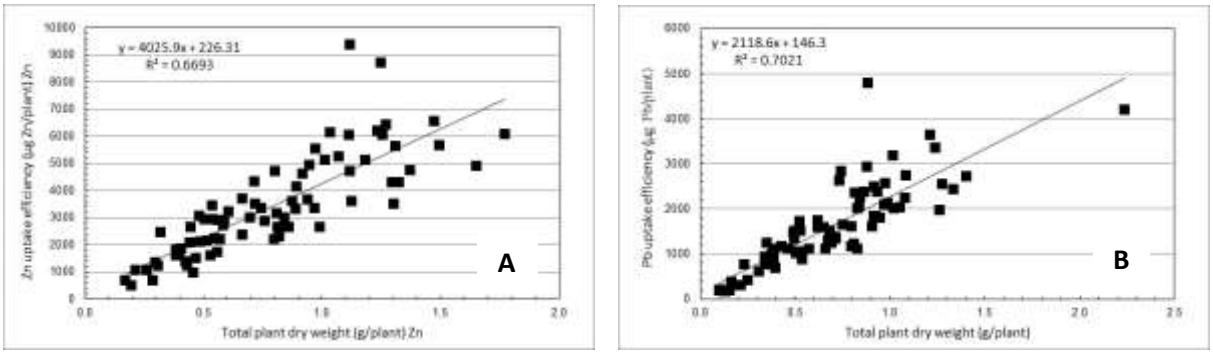

Figure 6.4 Relationships between uptake efficiencies and total plant dry weights of the 77 genotypes after 28 days exposure to A) supra-optimal Zn, and B) toxic Pb concentrations in FSC. Uptake efficiency was measured as the total plant content of Zn/Pb.

As part of the investigation of genotype performance in FSC, correlations between several other traits were assessed, the results of which are displayed in Table 6.1 in terms of R^2 values. Notable amongst these trait relationships was the relatively strong positive correlation between shoot dry weights in the control treatments and the high Zn and Pb treatments, with $R^2 = 0.65$ and $R^2 = 0.58$,

respectively. A strong positive correlation was observed between the Pb content of the roots and shoots in the toxic Pb treatment ($R^2 = 0.68$), but these same parameters were poorly correlated in the supra-optimal Zn treatment ($R^2 = 0.18$).

Table 6.1 *R^2 values for other trait relationships examined as part of the analysis of genotype performance in FSC.*

Trait 1 v. Trait 2	Zn R^2 values	Pb R^2 values
Shoot dry weight in control v. shoot dry weight in Zn/Pb (g/plant) treatments	0.65	0.58
Shoot:root dry weight ratio in control v. shoot:root dry weight ratio in Zn/Pb treatments	0.23	0.21
Zn content of the root (µg Zn/plant) in control v. Zn content of the root (µg Zn/plant) in supra-optimal Zn treatment	0.18	-
Pb content of the root (µg Pb/plant) v. Pb content of the shoot (µg Pb/plant) in toxic Pb treatment	-	0.68
Zn/Pb uptake efficiency (µg Zn/Pb/plant) v Zn/Pb utilisation efficiency (g^2 dwt mg^{-1} Zn/Pb)	0.19	0.31

6.1.2 Performance of control plants in FSC

In Section 4.3 of this thesis it was noted that several growth-related attributes measured at final harvest in the control treatments of the two pot-based experiments showed unexpected variation between the two replicate blocks in each experiment and also between the two experiments (e.g. Table 4.2). In the absence of adverse environmental factors, nitrate contamination in the mine tailings, or errors in data recording, it was concluded that algal contamination may have been responsible for the observed variations in performance (Section 4.3.4). However, in view of these observations, the results from the control treatments in the two FSC screens were compared for four key growth-related traits, namely tiller production, shoot and root dry weights and shoot:root dry weight ratios.

Scatter plots of the trait values for the 77 genotypes (Figure 6.5) showed poor correlations between the Zn and Pb screens in FSC for all four traits. Tiller numbers (Figure 6.5A) showed the strongest correlation ($R^2 = 0.29$). This compares with an R^2 value of 0.48 for the same trait in the pot experiments (Figure 4.49D). Tiller numbers for the majority of genotypes grown in FSC were higher in the control treatment of the Zn screen compared with the Pb screen. The poor correlations between the two FSC screens for shoot dry weight (Figure 6.5B, $R^2 = 0.16$) and root dry weight (Figure 6.5C, $R^2 = 0.15$), were broadly comparable with the results for these traits in the two pot

experiments (R^2 = 0.04 for shoot dry weight, R^2 = 0.09 for root dry weight). Inspection of Figure 6.5C indicates that shoot dry weights in the Zn control plants were consistently higher than those of the Pb control plants in the FSC screens. In contrast, root dry weights did not differ substantially between the control treatments in the two screens.

Shoot:root dry weight ratios (Figure 6.5D) in FSC showed the poorest correlation between the two sets of control plants (R^2 = 0.01). This compares with R^2 = 0.2 for the same trait in the pot-based experiments. Interestingly, shoot:root dry weight ratios in the pot-based experiments were consistently higher in the control plants of the Pb screen compared with the Zn screen (Figure 4.49 C), whereas the opposite was true for the screens in FSC (Figure 6.5D).

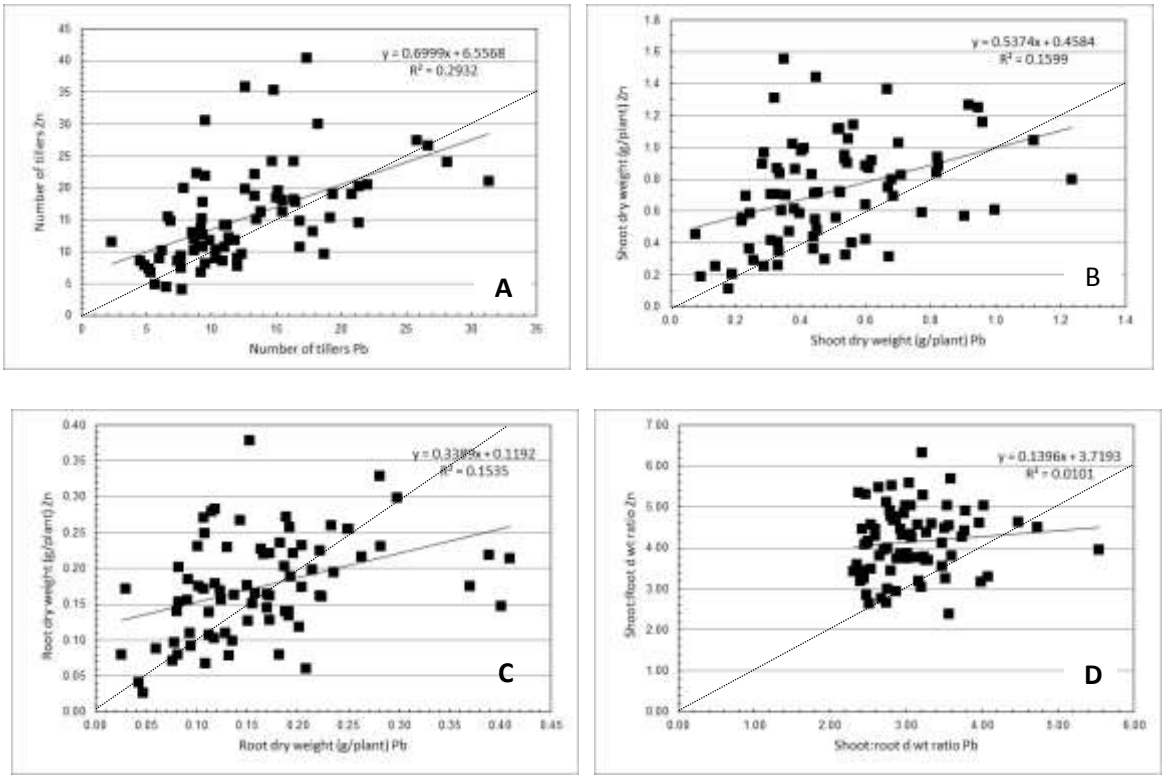

Figure 6.5 Relationship between growth-related traits in the two replicate sets of 77 control plants over two separate experiments in FSC for A) tiller production, B) shoot dry weight, C) root dry weight, and D) shoot:root ratio. Solid lines are the linear regressions for the data, whilst the dotted lines are the 1:1 lines (i.e. gradient = 1).

6.2 Comparison between genotype performance in FSC and the pot-based experiments

The performance of the 77 genotypes of *L. perenne* grown under high Zn/Pb concentrations in FSC was compared with that observed in the two pot-based experiments for a range of traits. These comprised five growth-related traits (shoot, root and total plant dry weight, shoot:root dry weight ratio and tiller production) and four metal uptake-related traits (metal content of the shoots and roots, metal uptake efficiency and metal utilisation efficiency). Linear regressions of the trait data from the two experimental systems (Table 6.2) revealed virtually no correlation between genotype performance in FSC and their performance in the pot-based experiments for any of the traits. This applied equally to Zn and Pb, and irrespective of whether the FSC data was compared against the results from the 10% or 30% mine tailing treatments in the pot experiments.

However, there were modest similarities between the results from the two experimental systems in terms of specific inter-trait relationships. For example, regression of total plant dry weight in supra-optimal/toxic treatments against the same parameter in the control treatment in FSC gave $R^2 = 0.64$ and $R^2 = 0.58$, respectively, for the Zn and Pb screens (Figure 6.2). In the pot-based 10% and 30% Zn treatments, the corresponding values were, respectively, $R^2 = 0.11$ and $R^2 = 0.14$ (see

Figure 4.9), whilst for the 10% and 30% Pb treatments values were $R^2 = 0.29$ and $R^2 = 0.28$ (see Figure 4.30). Similarly, regressions of shoot dry weight versus shoot metal content in FSC gave $R^2 \sim 0.92$ and $R^2 \sim 0.61$, respectively, for the Zn and Pb treatments (Figure 6.3). In the pot-based 10% and 30% Zn treatments, the corresponding values were $R^2 \sim 0.79$ and $R^2 \sim 0.77$, respectively (see Figure 4.15), and in the 10% and 30% Pb treatments were $R^2 \sim 0.34$ and $R^2 \sim 0.28$ (see Figure 4.40).

Table 6.2 *Coefficients of determination* **(***R^2***)** *for linear regressions of trait values for 77 genotypes of L. perenne measured in FSC and the two pot experiments performed under conditions of high Zn or Pb supply. Separate regressions were performed with data from the 10% and 30% mine tailing treatments.*

Trait correlation in FSC v. pot experiments	**Zn R^2 values**		**Pb R^2 values**	
	10%	**30%**	**10%**	**30%**
Shoot dry weight (g/plant)	0.002	0.06 (-ve)	0.002	0.0008
Root dry weight (g/plant)	0.005 (-ve)	0.005 (-ve)	0.005 (-ve)	0.005 (-ve)
Total plant dry weight (g/plant)	0.005 (-ve)	0.05 (-ve)	0.0008	0.003 (-ve)
Shoot:root ratio	0.06	0.15	0.03 (-ve)	0.008
Shoot Zn/Pb content (µg Zn/Pb/plant)	0.01 (-ve)	0.04 (-ve)	0.02	0.07
Root Zn/Pb content (µg Zn/Pb/plant)	0.003	0.05 (-ve)	0.02 (-ve)	0.006 (-ve)
Metal uptake efficiency (µg Zn/Pb/plant)	0.002	0.06 (-ve)	0.01 (-ve)	0.004 (-ve)
Metal utilisation efficiency (g^2 dwt mg^{-1} Zn/Pb)	0.04	0.005 (-ve)	0.002	0.005 (-ve)

Comparison between tiller production in FSC and the two pot-based experiments (Figure 6.6) revealed some interesting differences. In the 10% Zn pot experiment, tiller production was consistently higher for the majority of genotypes relative to the supra-optimal Zn treatment in FSC (Figure 6.6A), whereas in the 30% Zn treatment tiller production substantially declined relative to the FSC Zn treatment (Figure 6.6B). In contrast, all genotypes in the pot-based 10% and 30% Pb treatments experiment displayed consistently higher tiller production relative to the FSC Pb treatment (Figures 6.6C and D).

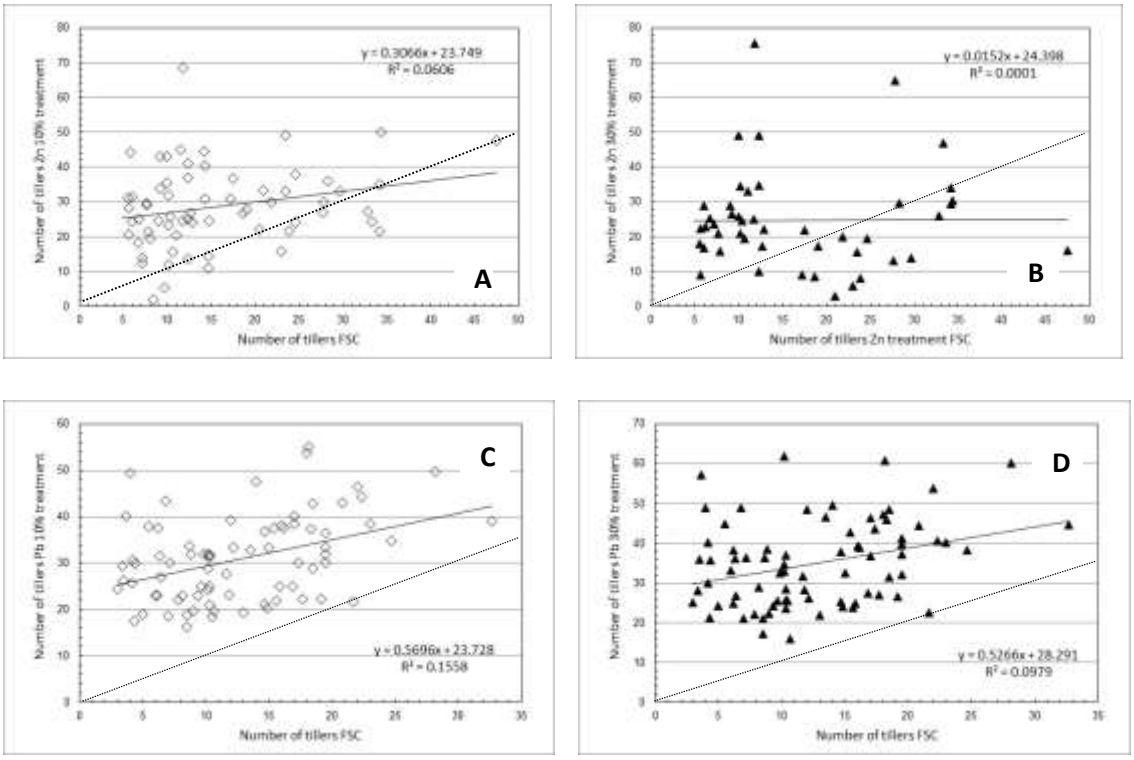

Figure 6.6 Relationship between tiller production in A) the 10% Zn pot treatment and 100 µM Zn in FSC, B) the 30% Zn pot treatment and 100 µM Zn in FSC, C) the 10% Pb pot treatment and 25 µM Pb in FSC, and D) the 30% Pb pot treatment and 25 µM Pb in FSC. Solid lines are the linear regressions for the data, whilst the dotted lines are the 1:1 lines (i.e. gradient = 1).

The reasons for the generally poor agreement between genotype performance in FSC and the two pot-based experiments across the range of traits studied in this project may well be associated with the major differences between the two experimental methods. Firstly, there was a significant difference in the duration of the experiments, with only 4 weeks of metal treatment in FSC compared to 16 weeks of metal treatment in the pot-based experiments. Secondly, there were major differences in the levels of toxic stress imposed. In FSC the concentration of Zn in solution at the start of the treatment period was only 100 µM. This compares with ~ 3,000 and 9,000 µg g^{-1} Zn (i.e. a $^{Zn}B_A$ of 1,890 and 5,670 µg g^{-1} Zn) in the 10% and 30% Zn pot experiment treatments, respectively, and only 25 µM Pb in FSC compared with ~ 1,700 and 5,100 µg g^{-1} Pb (i.e. a $^{Pb}B_A$ of 445 and 1,335 µg g^{-1} Pb) in the 10% and 30% Pb pot experiment treatments, respectively. The results from the pot experiments are certainly likely to correlate more closely with behaviour under field conditions of Zn or Pb toxicity.

A further component of the comparative analysis of the results from FSC and the pot experiments was the identification of elite genotypes for key traits. These have been identified for FSC (Section 6.1.1) and for the two pot-based experiments (Sections 5.2.2 and 5.2.3). Table 6.3 lists the top ten

performing genotypes in FSC for the four key growth-related traits and four metal uptake-related traits, together with those genotypes that also performed well in Zn Experiment 1. The agreement between the ranking produced by the two experimental systems was disappointing, with a few notable exceptions. For example, Genotype 164 was a top five performer for root, shoot and total plant Zn uptake in FSC and a top ten performer in the 10% Zn treatment (see Table 5.4). This genotype was also a top ten performer for shoot and total plant dry weight in FSC (16th in the rankings for root dry weight), and a top ten performer for shoot, root and total plant dry weight in the 10% Zn treatment (see Table 5.2). Similarly, Genotype 47 was a top five performer for tiller numbers, root and total plant dry weight in FSC, and a top ten performer in the 30% Zn treatments. This genotype was also a top three performer for root and total plant Zn uptake in FSC, and was amongst the top eight performers for the same traits in the 30% Zn treatment.

Table 6.3 *Ten best performing genotypes in FSC, ranked for four growth-related traits and four metal uptake-related traits. Genotypes amongst the top 10 performers in Pot Experiment 1 (Zn) are highlighted, those in red referring to the 10% Zn treatment, those in blue to the 30% Zn treatment, and those in green to genotypes that performed well in both treatments.*

Trait 11 Tillers/plant	**Trait 16 Shoot dry weight (g/plant)**	**Trait 19 Root dry weight (g/plant)**	**Trait 22 Total dry weight (g/plant)**	**Trait 26 Shoot Zn content (µg/plant)**	**Trait 27 Root Zn content (µg/plant)**	**Trait 28 Total Zn content (µg/plant)**	**Trait 39 Zn UtE(i) (g^2 mg^{-1} Zn)**
19	19	19	19	73	3	3	73
78	73	47	73	20	61	611	19
47	20	129	20	19	47	47	122
59	85	73	47	164	192	164	1
1	47	169	85	169	164	192	85
122	1	20	1	61	129	30	20
53	122	59	169	7	30	19	59
20	164	44	122	85	54	129	153
49	192	61	59	54	19	54	55
129	59	90	164	47	5	20	47

The corresponding comparison for Pb tolerance between FSC and Pb Experiment 2 was also disappointing (Table 6.4), with the exception of two genotypes. Firstly, Genotype 55 was a top ten performer for tiller production in FSC and also in the 30% Pb treatment (see Table 5.8). This genotype was also a top five performer for root and total plant Pb uptake, and was ranked fourth best for these traits in the 10% Pb treatments (see Table 5.10). Secondly, Genotype 66 was a top

ten performer for shoot dry weight, shoot Pb content and Pb utilisation efficiency in both FSC and the 30% Pb treatments (see Tables 5.8 and 5.12).

Table 6.4 *Ten best performing genotypes in FSC, ranked for four growth-related traits and four metal uptake-related traits. Genotypes amongst the top 10 performs in Pot Experiment 2 (Pb) are highlighted, those in red referring to the 10% Pb treatment, those in blue to the 30% Pb treatment, and those in green to genotypes that performed well in both treatments.*

Trait 55 Tillers/plant	**Trait 60 Shoot dry weight (g/plant)**	**Trait 63 Root dry weight (g/plant)**	**Trait 66 Total dry weight (g/plant)**	**Trait 70 Shoot Pb content (µg/plant)**	**Trait 71 Root Pb content (µg/plant)**	**Trait 72 Total Pb content (µg/plant)**	**Trait 84 Pb UtE(i) (g^2 mg^{-1} Pb)**
18	7	7	7	55	45	45	7
201A	18	52	52	7	7	7	164
169	52	63	18	18	77	77	18
47	164	77	66	169	169	169	52
90	66	73	164	45	55	55	66
4	169	66	169	3	3	3	10
7	77	169	77	77	192	192	23
36	201A	55	73	201A	73	73	63
5	129	45	201A	66	52	52	53
55	73	44	63	38	36	36	201A

6.3 Comparison between QTL identified in FSC and the pot-based experiments

Identification of QTL was an objective of the DEFRA-commissioned project (DEFRA LS3648). Amongst these were included QTL for 'physiological' tolerance to Zn and Pb and also for hyperaccumulation of Zn and Pb, based on trait data from the 28 day screens of the *L. perenne* mapping family in FSC. Relevant aspects of the QTL analysis in LS3648 were outlined in Section 2.5.3, with the locations of identified QTL shown on outline linkage maps for the forage and amenity alleles (see Figures 2.7 and 2.8). However, following completion of the DEFRA project, the existing genetic framework maps were significantly revised (Blackmore *et al*., 2015, 2016) through the identification of a validated set of 2,199 SNPs, spanning 1,615 contigs, of which a total of 1,161 SNPs were derived from the amenity x forage *L. perenne* mapping family used in this current project (see Section 4.4.1). Consequently, as part of this current project, the QTL derived from the screens for Zn (Experiment 1:23:64) and Pb (Experiment 1:23:66) in FSC, including control and high metal treatments, were re-mapped to the revised genetic framework maps. This was primarily to facilitate comparison with QTL identified from the two pot experiments.

The re-mapping was performed using the methodology described in Section 4.4.1. Firstly, the Kruskal-Wallis test statistic (K*) was applied and map positions and Contigs recorded. Secondly, the traits were assessed *via* interval mapping, and LOD scores were gathered for each map position. It should be noted, however, that time constraints meant that permutation tests were not performed, the LOD threshold scores were not identified and a LG map was not generated.

Following an analysis of trait data from the Zn toxicity screen in FSC using MapQTL, four growth-related traits and two metal uptake-related traits were determined as significant (Table 6.5). Likewise, four growth-related traits and one metal uptake-related trait were determined as significant, based on the trait data from the Pb toxicity screen in FSC (Table 6.5). It is notable that two of the growth-related traits for Zn (tiller numbers and shoot dry weight) yielded QTL at the same map locations on LG6 at map position 52.42 cM, although with different Contigs. In addition, one growth-related trait (shoot dry weight in control treatment) and two metal uptake-related traits (Zn uptake efficiency in control and Zn treatments) also yielded QTL at the same map locations on LG6 at map position 51.761 cM, and with the same Contigs. The QTL for the four growth-related traits derived from the Pb screen mapped to the same map positions of 52.42 cM on LG6, which was also the same map position for QTL identified for two growth-related traits (tiller numbers and shoot dry weight) in the FSC Zn treatment. The Pb-uptake efficiency trait yielded a QTL at map position 52.1 cM, which lies close to the same trait-specific QTL identified in the FSC Zn experiment.

As noted above, four growth-related traits and one metal uptake-related trait measured in the screen for Pb in FSC all yielded putative QTL on LG6. This contrasts with the QTL identified from Pb Experiment 2 (see Table 4.6 and Figure 4.53), which were located on LGs 3, 4, 5 and 7. In particular, a cluster of metal uptake-related QTL for the 10% Pb treatment were identified on LG4, whilst a very dense cluster of both growth-related and metal uptake-related QTL, for the control, 10% and 30% Pb treatments, were identified on LG7. No QTL based on Pb Experiment 2 were identified on LG6. The reasons for these differences between the two experimental systems with respect to QTL are unclear, but presumably relate in large part to the differences in the trait data discussed in Section 6.2.

QTL based on Zn Experiment 1 were located on LGs 4, 6 and 7 (see Table 4.5 and Figure 4.52). Interestingly, the QTL for tiller number was located on LG7 at map position 54.718 cM, the same position as the QTL for this trait derived from the trait values measured in FSC. Two other Zn uptake-related traits in Zn Experiment 1 yielded QTL on LG6 at map positions 46.092 and 48.563

cM. In comparison, the QTL for the same traits based on the Zn tolerance screen in FSC were located on LG6 at broadly similar map positions of 51.761 cM.

Table 6.5 *Re-mapped QTL for traits phenotyped in screens for Zn and Pb tolerance in FSC. Significance was determined by passing 2 test statistic parameters.*

Trait Number	Trait Description	Linkage Group	Map Position (cM)	Locus marker	KW Signif.	% variance explained	LOD
Zn							
147	Tiller numbers (control treatment)	**4**	14.408	Contig31268_626	****	16.6	**3.32**
		7	2.76	Contig37953_1985	****	16.4	**3.17**
148	Tiller numbers (Zn treatment)	**6**	52.42	Contig43177_374	*****	15.5	**3.11**
		7	54.718	Contig7409_810	****	17.5	**3.11**
150	Shoot dry weight (g) (control treatment)	**6**	51.761	Contig31685_524	******	23.6	**4.96**
151	Shoot dry weight (g) (Zn treatment)	**6**	52.42	Contig8408_761	******	19.3	**3.96**
162	Zn uptake efficiency (μg Zn/plant)(control treatment)	**6**	51.761	Contig31685_524	******	22.7	**4.74**
163	Zn uptake efficiency (μg Zn/plant) (Zn treatment)	**6**	51.761	Contig31685_524	******	17.7	**3.59**
Pb							
177	Tiller numbers (control treatment)	**6**	52.42	Contig8408_761	*****	16.7	**3.38**
178	Tiller numbers (Pb treatment)	**6**	52.42	Contig8408_761	*****	15.3	**3.06**
180	Shoot dry weight (g) (control treatment)	**6**	52.42	Contig8408_761	****	15.6	**3.16**
181	Shoot dry weight (g) (Pb treatment)	**6**	52.42	Contig8408_761	****	17.2	**3.48**
188	Pb uptake efficiency (μg Pb/plant) (Pb treatment)	**6**	52.1	Contig8408_845	*****	14.8	**2.96**

Significance levels KW:
***=P<0.1 **=P<0.05 ***=P<0.01 ****=P<0.005 *****=P<0.001 ******=P<0.0005 *******=P<0.0001**

6.4 Summary

- Screening of the *L. perenne* mapping family used in this research project has previously been performed in the IBERS-based FSC facility. The latter involved screens that included investigations of growth and metal uptake over 28 days under 'supra-optimal' Zn concentrations (100 µM) and 'toxic' Pb concentrations (25 µM).
- In the Zn treatment, for the majority of genotypes dry matter production was reduced. In contrast, under the Pb treatment there was an inconsistent effect of Pb on dry matter production, with the majority of genotypes plotting on, or near to, the 1:1 gradient line in a plot of control versus 'toxic' treatment.
- In both treatments a strong positive correlation was noted between shoot dry weight and net metal uptake, although the Pb content of the shoots was ~ 8 times smaller, for any given shoot dry weight, than that observed in the 'supra-optimal' Zn treatment.
- Metal uptake efficiencies, measured as total plant content of either Zn or Pb, varied widely across the mapping family, but showed a strong positive correlation with total plant dry weight.
- In the two FSC screens there was wide variation in control plant performance with respect to tiller production, shoot and root dry weights and shoot:root dry weight ratios.
- Comparison between genotype performance in FSC and the two pot experiments, for five growth-related traits and four metal uptake-related traits, revealed virtually no correlation. This has been attributed to major differences between the two experimental methods, in particular the duration of the screens and the levels of imposed toxic stress.
- The best performing genotypes in the two FSC screens were also compared with those identified in the two pot experiments, although agreement between the rankings was generally poor.
- QTL data from the FSC screens were transposed onto revised genetic framework maps to facilitate a comparison with QTL derived from the pot experiments. Within the FSC dataset, QTL for growth- and metal uptake-related traits were located on LGs 4, 6 and 7 for Zn and only on LG 6 for Pb, with a notable locus in both HM treatments on LG 6 at 52.42 cM for tiller numbers and shoot dry weight. These data contrast with the QTL derived from Pb Experiment 2 which were located on LGs 3, 4 5 and 7 with none identified on LG 6. Interestingly, the QTL for tiller numbers from Zn Experiment 1 was coincident, at map position 54.718 cM, with the QTL for this trait derived from FSC data.

CHAPTER 7

DISCUSSION

7.1 Optimisation of digestion methods

During the course of the two pot experiments undertaken during this project, it was anticipated that a total of ~ 2,900 individual samples would be generated from the Cut 1 harvest (shoots only) and the destructive final harvest (roots and shoots), each of which would require milling before digestion. In order to prepare the samples for analysis by AAS, it was necessary to devise a digestion method that not only satisfied the criteria of analytical accuracy and reproducibility, but that also facilitated the rapid throughput of large batches of samples.

A total of 11 different methods were tested for the digestion of Zn-bearing samples (Section 3.12), of which four (Test Methods 2, 4, 5 and 6) were rejected owing to the development of impurities that rendered the samples unsuitable for AAS analysis. The results from digestion and analysis of pot standards showed errors in the remaining 7 methods of between 1.87 and 15.52%, with Test Method 9 giving the most reproducible and accurate results (Table 3.5). Errors resulting from digestion and analysis of a field standard ranged between 0.6 and 8.4%, with the DGES standard oxidation method (Section 3.12) providing the most accurate results. Digestion and analysis of IAEA V-10 hay reference material, with a certified Zn concentration of 24 ppm, using each of the 7 methods, yielded concentrations ranging between 14.38 and 23.5 ppm, with Test Method 9 once again providing the most accurate analysis (Table 3.5).

Test Method 9 was adapted from an analytical method described by Husted *et al*. (2004). The latter utilised an intermediate peroxide reaction stage and allowed for the digestion of batches of up to 50 samples at one time. The adapted method was trialled without the peroxide reaction stage, and Zn recovery was found to be both accurate and reproducible. In addition, the adapted method allowed for the digestion of up to 160 samples in only one day, thereby satisfying the three critical criteria listed above. Prior to commencement of Pb Experiment 2, the method was trialled for the digestion of Pb-bearing samples and it also satisfied the three criteria (A. Brown, DGES pers comm.). A comparative analysis of the total man-hours required to digest ~ 2,900 samples using Test Method 9 and the standard DGES Method yielded times of 17.5 and 80 weeks, respectively. It is clear, therefore, that Test Method 9 provided the most rapid digestion method with a potential time saving of over 60 weeks.

7.2 Plant growth, metal uptake and translocation in Zn Experiment 1

7.2.1 Zn use and toxicity in plants

In Sections 2.1 and 2.3 it was noted that HM species such as Zn, Fe, Cu, Co and Ni are essential micronutrients that sustain plant growth and metabolism through the regulation of various biological processes, but that they become toxic to plants when supplied at high concentrations (Table 7.1). Zinc is an essential component of many critical plant enzymes such as carbonic anhydrase, alcohol dehydrogenase, SOD, aldolases, isomerases and RNA and DNA polymerases, and is implicated in protein synthesis and energy production, nucleic acid synthesis and carbohydrate and lipid metabolism (e.g. Cakmak and Marschner, 1993; Marschner, 1995; López-Millán *et al*., 2005; Hänsch and Mendel, 2009). The metal also plays an important role in the synthesis of auxin, an essential plant growth hormone (Brennan, 2005) and is also a critical prerequisite for cellular membrane integrity (Cakmak, 2000). Zinc acts to reduce the adverse effects of heat and salt stress (Peck and McDonald, 2010; Tavallali *et al*., 2010), and there is evidence that Zn is involved in the stress-induced expression of genes that

Table 7.1 *Concentration ranges (µg g^{-1}) of selected HMs in soil and crops, and shoot toxicity thresholds (from Allaway, 1968; Misra and Mani, 1991; Reichman, 2002; Mendez and Maier, 2008; Nagajyoti et al. 2010). Tissue concentrations are also shown for the experiments conducted in this study and are those measured in the 30% tailings treatments.*

Heavy metal	Range in uncontaminated soil	Range in agricultural crops	Shoot toxicity threshold	Shoot tissue concentration (this study)	Root tissue concentration (this study)
As	-	0.02-7	-	-	-
Cd	0.01-0.7	0.1-2.4	5-30	-	-
Hg	-	0.005-0.02	-	-	-
Pb	2-200	0.1-10	30-100	60-180	950-3,710
Sb	-	0.02-0.06	-	-	-
Co	1-40	0.05-0.5	-	-	-
Cr	5-3,000	0.2-1	-	-	-
Cu	2-100	4-15	2-20	-	-
Fe	7,000-55,000	140	-	-	-
Mn	100-4,000	15-100	144->2,000	-	-
Mo	0.2-5	1-100	-	-	-
Ni	10-100	1	10-100	-	-
Sr	-	0.3	-	-	-
Zn	10-300	15-200	100-400	1,890-5,680	4,820-14,250

encode for antioxidative defence enzymes such as H_2O_2-scavenging ascorbate peroxidase, catalase and glutathione reductase (Alscher *et al*., 1997).

The threshold of Zn toxicity varies widely between different plant species, as well as with the time of exposure to Zn stress and the composition of the nutrient growth medium (Tsonev and Lidon, 2012). For example, Bonnet *et al*. (2000) observed that growth retardation of *L. perenne* occurred at between 1 – 10 mM $ZnSO_4$ with a total inhibition of growth at 50 mM $ZnSO_4$ (~ 3,000 ppm Zn). By contrast, for species of *Datura* (Angel's Trumpet), growth was severely reduced after 20 days of Zn stress by only 2.5 and 5 mM $ZnSO_4$ (Vaillant *et al*., 2005), whilst in *Pisum sativum* (pea), growth was inhibited after a 1000 µM application of Zn (Doncheva *et al*., 2001). Significant reductions in root and shoot growth parameters were reported by Khudsar *et al*. (2004) in *Artemisia annua* (sweet wormwood) plants grown in soil containing Zn concentrations of 100 – 400 µg g^{-1}.

As noted in Table 2.3, the phytotoxicity of Zn in plants is manifested phenotypically by a wide range of effects. These include wilting, necrosis, a reduction in chlorophyll (Chl) content and chlorosis, and an inhibition of both root and shoot cell elongation and division (e.g. Rosen *et al*., 1977; Ren *et al*., 1993; Choi *et al*., 1996; Ebbs and Kochian, 1997; Soares *et al*., 2001; Khudsar *et al*., 2004). Rout and Das (2003) and Rout *et al*. (2003) reported that major changes were seen at a cellular level in the nuclei of root tip cells of the tropical wild grass *Echinochloa colona* at high Zn concentrations. The chromatin became highly condensed, some cortical cells became disrupted, there was dilation of the nuclear membrane, disintegration of cell organelles and the development of new cell vacuoles. In addition, the number of nucleoli increased, resulting in the synthesis of new proteins involved in Zn tolerance. The cause of chlorosis may be a function of induced Fe deficiency, as hydrated Zn^{2+} and Fe^{2+} have identical ionic radii of 0.83Å (Goldschmidt, 1963; Silva *et al*., 2014), and thus Zn may interfere with Chl synthesis either by competing with Fe for a site on a particular Chl biosynthetic enzyme (Rosen *et al*., 1977; Marshner, 1995) or through interfering with the translocation of Fe by retarding the reduction of Fe^{3+} to the favoured Fe^{2+} form by the roots (Ambler *et al*., 1970). Other research (e.g. von Wettstein *et al*., 1995) suggests that inhibition of the photosynthetic apparatus is coupled with critical changes to Chl structure, specifically the replacement of Mg^{2+} by Zn at the heart of the Chl molecule which, at toxic Zn concentrations, leads to a decrease of Chl a and Chl b and the a/b ratio (Ivanov *et al*., 2012). Finally, Zn toxicity also generates oxidative stress (e.g. López-Millán *et al*., 2005), producing ROS such as O_2^- superoxide radicals and H_2O_2

(Weckx and Clijsters, 1997), and thereby disrupting critical metabolic processes such as the antioxidant defence system (e.g. Hossain *et al*., 2015).

7.2.2 Synthesis of growth in Zn Experiment 1

During the course of Zn Experiment 1 there was a mortality rate of ~ 15% in the 10% Zn treatment, and this rate increased to ~ 40% in the 30% Zn treatment (see Table 4.1). This was an unexpected outcome since pre-experiment trials and two M.Sc. research projects (Warrender, 2005; Macro, 2005) had previously indicated that 100% survival might be achieved even in the most contaminated treatment. However, the difference in toxic effects could be attributed to the fact that these trials were conducted using tailings provenanced from different mines to those selected in this study and, in addition, the experiments were of a shorter duration (6 weeks). It is clear, therefore, that the 10% Zn treatment, equating to an absolute substrate concentration of ~ 3,000 µg g^{-1} and a $^{Zn}B_A$ of ~ 1,890 µg g^{-1}, represented a critical toxicity level, at least for some genotypes. Similarly, the 30% Zn treatment, equating to an absolute substrate Zn concentration of ~ 9,000 µg g^{-1} and a $^{Zn}B_A$ of ~ 5,670 µg g^{-1}, represented a super-critical toxicity level, fast approaching the survival threshold. These results generally compare favourably with the aforementioned studies of Bonnet *et al*. (2000), who observed that a concentration of 50 mM $ZnSO_4$ caused a cessation of growth in *L. perenne* grown under hydroponic conditions, the ~ 3,000 ppm Zn being more bioavailable in solution. However, despite the mortality, many of the genotypes survived the full term of the experiment, even in the 30% Zn treatment, although, as noted in Section 4.1, chlorosis was observed in both treatments at a very early stage, indicating a progressive reduction in Chl synthesis, caused either by a Zn-induced Fe^{2+} deficiency or Mg^{2+} substitution in the Chl molecule (Ambler *et al*., 1970; Ivanov *et al*., 2012).

As noted in Section 2.3.2, in addition to survival and longevity, other critical attributes required by plants for the phytostabilisation of HM-contaminated substrates include a rapid rate of growth, a high biomass production, dense root systems and a high rate of tiller production (Mendez and Maier, 2008; Chibuike and Obiora, 2014). With respect to plant growth during Zn Experiment 1, data presented graphically in Section 4.1.1 and summarised in Table 7.2 show that, for the majority of surviving genotypes, there was a dramatic decrease in biomass production as Zn concentration increased. This effect was observed after 8 weeks of growth (Cut 1), with only 4 individuals, namely Genotypes 16, 39, 55 and 157, having a greater shoot dry weight in the 30% Zn treatment than in the control treatment (see Figure 4.3). By final

harvest, after 16 weeks of growth, the shoot, root and total plant dry weights in the Zn treatments, relative to those in the control treatment, had declined still further, with all

Table 7.2 *Summary of the range of genotype performance in Zn Experiment 1 for five growth-related traits. Values in parentheses are the mean values for each trait.*

Trait	**Zn Treatment**		
	Control	**10%**	**30%**
Shoot dry weight (g/plant)	1.23 - 3.17 (2.1)	0.52 – 3.6 (1.34)	0.17 – 2.05 (0.97)
Root dry weight (g/plant)	0.92 – 6.13 (2.5)	0.06 – 2.41 (1.07)	0.067 – 1.62 (0.55)
Whole plant dry weight (g/plant)	1.75 - 9.01 (4.6)	0.22 – 6.01 (2.65)	0.23 – 3.45 (0.23)
Shoot : root ratio	0.47 – 1.98 (1.05)	0.43 – 2.6 (1.32)	0.54 – 4.59 (1.87)
Tiller numbers (per plant)	12 – 44 (26)	2 – 68 (29)	65 – 3 (25)

the surviving genotypes having a higher, or significantly higher, biomass production in the control treatment (see Figures 4.8 and 4.9 and Plate 7.1). Only two individuals, namely Genotypes 14 and 25, had total dry weights > 4 g/plant in the 10% Zn treatment, and only two individuals, namely Genotypes 31 and 56, had total dry weights > 3 g/plant in the 30% Zn treatment.

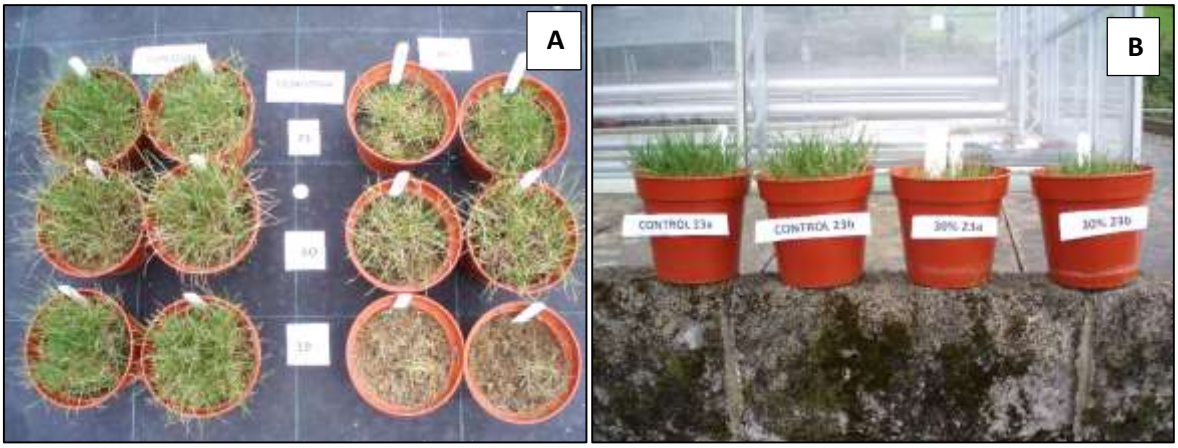

Plate 7.1 Photographs of three *L. perenne* genotypes after 16 weeks of growth, showing a significant reduction in shoot biomass in the 30% Zn treatment relative to the control treatment in A) replicate pots of genotypes 23, 60 and 19 in the control treatment on the left and in the 30% treatment on the right, and B) replicate pots of Genotype 23 in the control treatment on the left and the 30% treatment on the right.

In the case of root development, mean root dry weights were reduced to only ~ 40% and 20% of their mean control dry weights in the 10% and 30% Zn treatments, respectively, whilst a marked increase in mean shoot:root dry weight ratio with increasing Zn substrate concentration (Table 7.2) confirms published findings, discussed in Section 7.2.1, that Zn toxicity had a particularly adverse impact on root development. Only two individuals, Genotypes 14 and 16, had root dry weights > 2 g/plant in the 10% Zn treatment, and only four individuals, Genotypes

31, 47, 49 and 56 had root dry weights ≥ 1 g/plant (see Figure 4.7). This pattern of declining growth with increasing Zn concentration is shown clearly in simple plots of mean shoot, root and whole plant dry weights against treatment (Figure 7.1). These reveal an exponential decline in dry matter production, as evidenced by curves defined by regression equations of the form Ae^{-Bx}, which, it is predicted, would have continued up to lethal Zn concentrations in the range of 50% Zn by weight in the growth medium.

Interestingly, there was little variation in the mean number of tillers produced by final harvest between the three treatments (26, 29 and 25 per plant, respectively, in the control, 10% and 30% Zn treatments). Surprisingly, however, 12 genotypes produced more tillers in the 30% Zn treatment than in the 10% Zn treatment, and Genotypes 13 and 49 showed their highest rate of tiller production in the 30% treatment (see Figure 4.11).

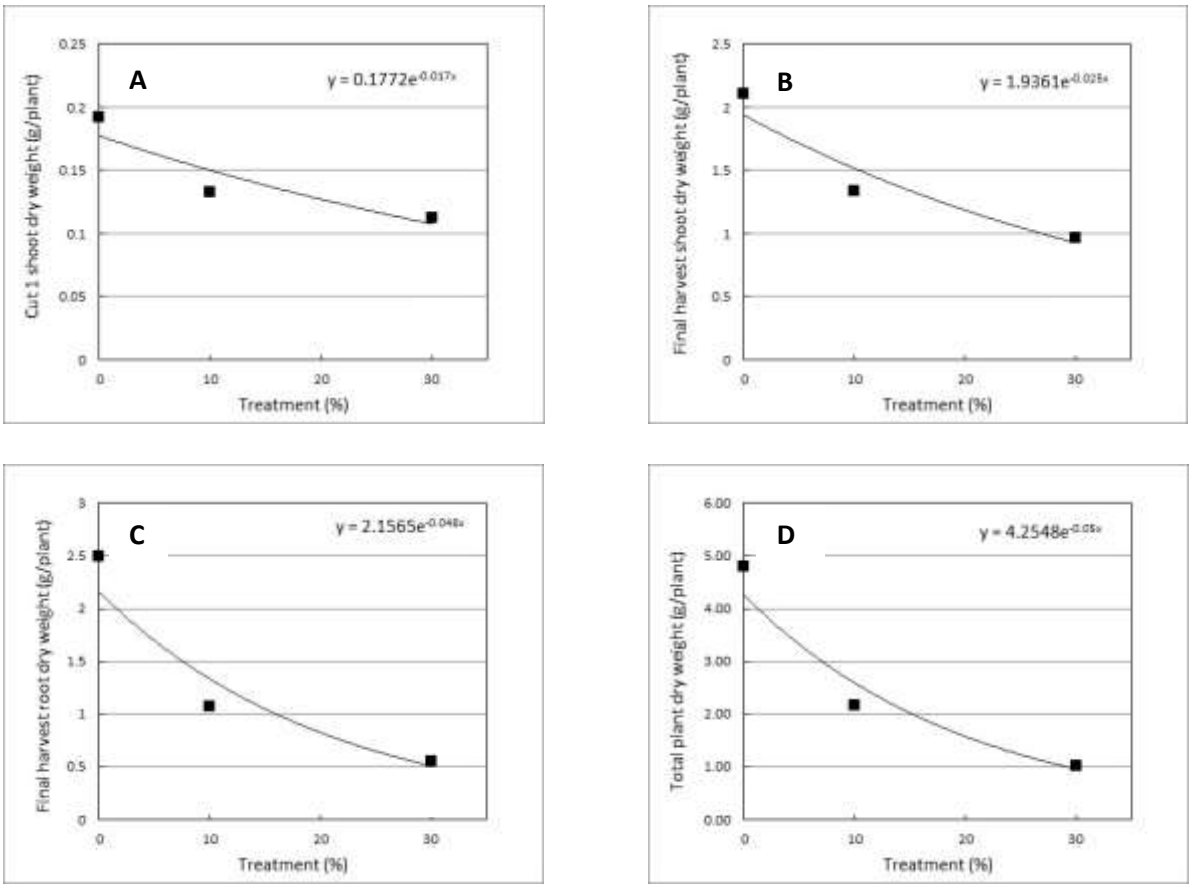

Figure 7.1 Mean dry weights of A) shoots at Cut 1, B) shoots at final harvest, C) roots at final harvest, and D) the total plant at final harvest, plotted against treatment in Zn Experiment 1.

The growth effects observed in this experiment are similar to those in previous investigations (Section 7.2.1), which have shown that a high concentration of Zn in the growing medium causes a severe and adverse impact on plant metabolism, specifically through mechanisms such as the interruption of protein and critical enzyme synthesis, the production of ROS and

disruption of the antioxidant defence system, a reduction in root and shoot cell division, and intra-cellular degradation, particularly within the nucleus. In the Zn toxicity experiment (1:23:64) conducted in FSC, and referred to in Section 6.1.1, a decrease in total plant dry matter production was noted in ~ 80% of genotypes in the supra-optimal Zn treatment, relative to the control treatment (Figure 6.2A). Similar results have also been reported widely for other plant species grown in Zn contaminated substrates. For example, Silva *et al*. (2014) reported that for rice and soybean grown in soils containing between 102 – 544 mg kg^{-1} there was a high mortality, severe chlorosis and a dramatic reduction in growth. Malik *et al*. (2011) reported on the performance of red amaranth (*Amaranthus cruentus*) cultivated in experimental soils containing 0, 200, 300 and 400 mg Zn kg^{-1}. With respect to dry matter production, there was a dramatic decline in shoot dry weights at Zn concentrations > 100 mg kg^{-1}, and a substantial decline in root dry weights at Zn concentrations > 300 mg kg^{-1} (Figure 7.2).

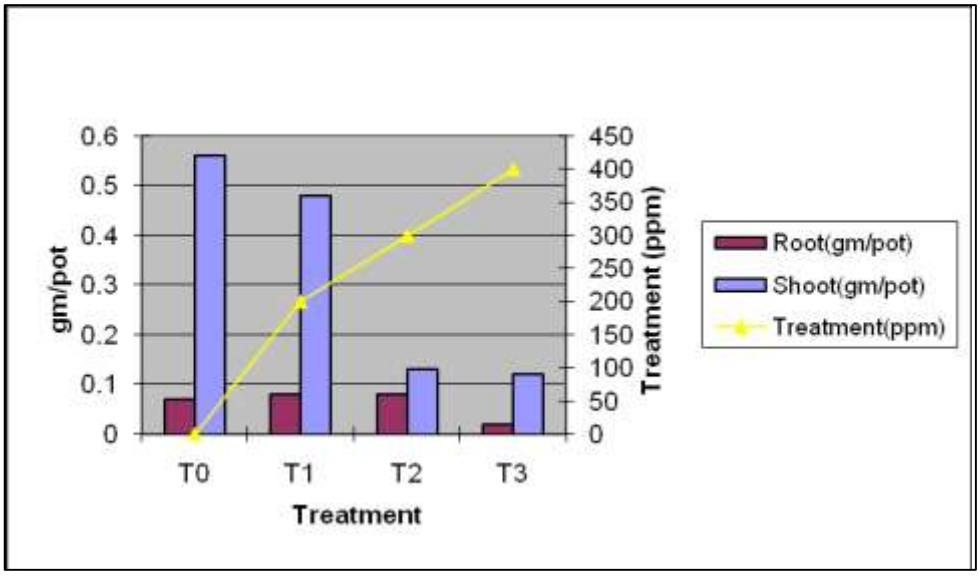

Figure 7.2 The effects of four different Zn treatments on dry matter production in red amaranth (from Malik *et al*., 2011).

Shen *et al*. (1997) conducted hydroponic-based experiments to investigate growth- and Zn-uptake responses of the hyperaccumulator species *T. caerulescens* to seven different solution Zn concentrations ranging from 1 to 1,000 mM m^{-3} (≡ 65 g m^{-3}). The results of this analysis, shown in Table 7.3, reveal that, whilst dry matter production remained stable at concentrations of up to 500 mM m^{-3}, growth of both roots and shoots showed a dramatic decline at concentrations of 1,000 mM m^{-3}. Reduction in growth was most marked in the roots, as evidenced not only by root dry weight, but also by an increase in shoot:root ratio and by a

substantial reduction in the lengths of the main roots. These changes in growth-related traits are also consistent with the results obtained from Zn Experiment 1.

Table 7.3 Dry w*eights of shoots and roots, and length of main root, in T. caerulescens exposed to seven different hydroponic-based Zn concentrations (from Shen et al., 1997).*

Zn treatment mM m^{-3}	Weight (g/plant)			Shoot/root ratio	Length of main root	
	Shoot	Root	Total		13d	20d
1	0.26	0.07	0.32	4.0	11.4	13.0
10	0.29	0.09	0.38	3.3	12.6	13.5
50	0.26	0.09	0.36	2.8	14.5	15.9
100	0.26	0.09	0.35	2.7	14.2	15.4
250	0.27	0.10	0.36	2.8	12.8	14.3
500	0.28	0.08	0.36	3.5	11.0	11.8
1000	0.16	0.03	0.19	5.7	8.3	9.3

Bonnet *et al*. (2000) investigated the effects on *L. perenne*, either infected or not infected with the endophytic fungal symbiont *Acremonium lolii*, of various treatments ranging between 0 and 50 mM $ZnSO_4$. The introduction of Zn induced toxic stress, as evidenced by a significant reduction in biomass production at between 1 and 10 mM $ZnSO_4$, a cessation of growth at 50 mM $ZnSO_4$, and a major decrease in water content (Figure 7.3A and B). These effects, which

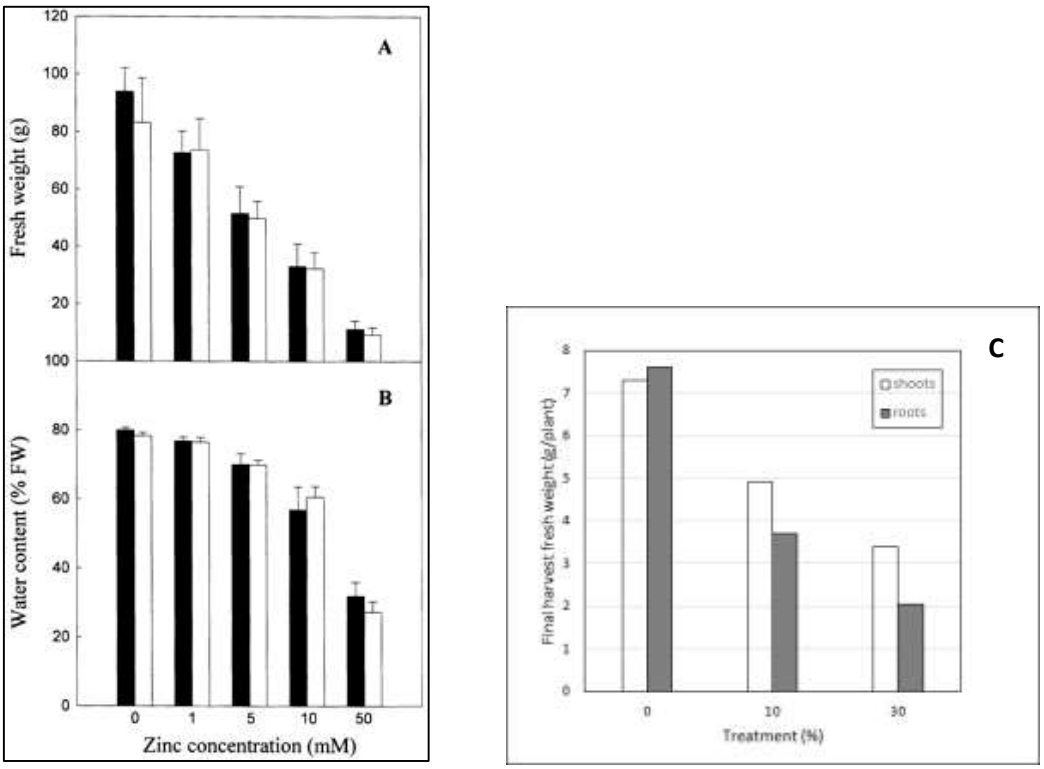

Figure 7.3 The effects of varying Zn concentrations in the culture medium (0, 1, 5, 10 and 50 mM $ZnSO_4$) on ryegrass (*L. perenne*) infected with *A. lolii* (white bars) and uninfected (black bars), showing A) plant fresh weights, B) plant water content (values are the means (s.e. < 15%) of 20 replicates; from Bonnet *et al*., 2000), and C) the reduction in fresh weights of roots and shoots, as a function of treatment, in Zn Experiment 1.

compare closely with the growth reduction recorded in Zn Experiment 1 (Figure 7.3C), were attributed to the progressive accumulation of Zn in the shoots. Indeed, data presented by Bonnet *et al*. (2000) show a strong negative correlation ($R^2 = 0.99$) between shoot dry weight and shoot tissue Zn concentrations (Figure 7.4A), and the same strong negative correlation ($R^2 > 0.99$) was observed for the same parameters in Zn Experiment 1 (Figure 7.4B).

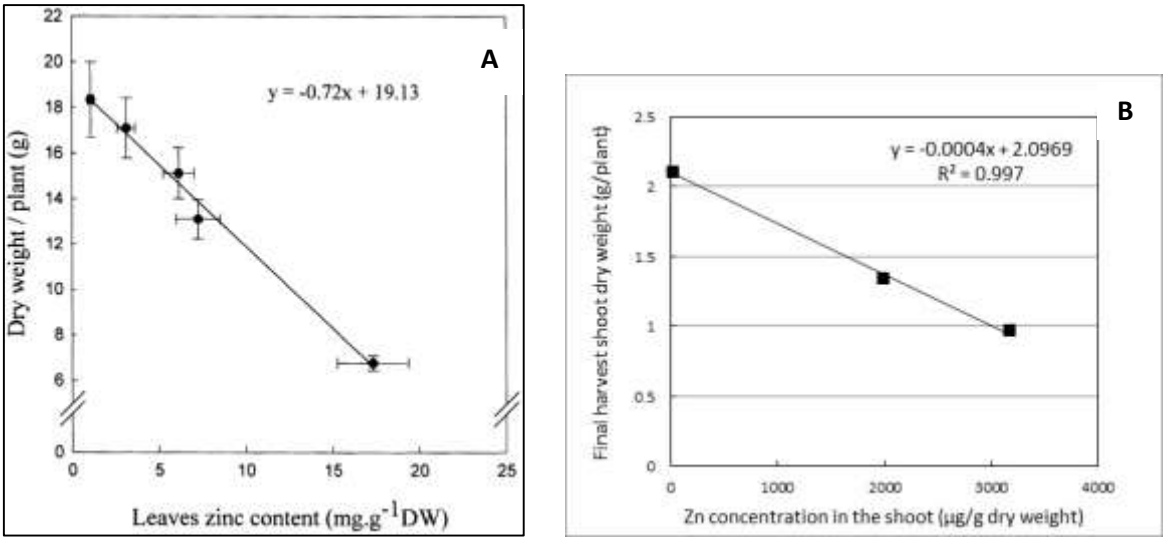

Figure 7.4 Relationship between A) plant dry weight and shoot tissue Zn concentrations in the shoots (values are the means (s.e. < 10%) of 20 replicates; from Bonnet *et al*., 2000), and B) the same parameters as recorded in Zn Experiment 1.

7.2.3 Synthesis of metal uptake and partitioning in Zn Experiment 1

In Section 2.3.2 it was noted that plants which are best suited for phytostabilisation require a high tolerance to the specific substrate contaminant and a very low translocation index (e.g. Mendez and Maier, 2008; Chibuike and Obiora, 2014), whereby metals are preferentially sequestered in the roots and not transferred to the shoots. With mortality rates of ~ 15% and 40% in the 10% and 30% zinc treatments, respectively, it is clear that whilst many genotypes in the *L. perenne* mapping family used in the current study displayed only a low tolerance to the high Zn concentrations, other genotypes displayed a high tolerance and survived the full term of the pot experiment.

The analysis of Zn uptake and partitioning in this experiment (Section 4.1.2) revealed a wide range of performance across the surviving genotypes, both in terms of absolute Zn uptake and tissue concentrations in the roots and shoots. This variation is highlighted in Table 7.4 which summarises the range of performance for six Zn uptake-related traits.

Table 7.4 *Summary of the variation in genotype performance for six Zn uptake-related traits. Values in parentheses are the mean values for each trait.*

Trait	Zn Treatment	
	10%	**30%**
Shoot content (µg Zn/plant)	270 – 8292 (2622)	313 – 9654 (3083)
Shoot tissue concentration (µg Zn g^{-1})	994 – 3572 (1988)	1,886 – 5678 (3179)
Root content (µg Zn/plant)	664 – 29334 (8887)	318 – 16305 (5319)
Root tissue concentration (µg Zn g^{-1})	4,187 – 15301 (8387)	4,823 – 14251 (9518)
Translocation index	0.11 – 1.09 (0.34)	0.28 – 1.53 (0.66)
Zn uptake efficiency (µg Zn/plant)	934 – 32429 (11468)	631 – 24169 (8402)

The highest accumulations of Zn in the root system in the 10% Zn treatment was recorded in Genotypes 4, 14, 16, 78 and 201A, each with a Zn content > 15,000 µg/plant, and with Genotype 14 containing ~ 29,000 µg/plant. In the 30% Zn treatment, only Genotype 31 had a Zn content > 15,000 µg/plant, whilst the majority of genotypes had a lower, and in some cases much lower, Zn content compared with the 10% Zn treatment. This suggests that at very high Zn substrate concentrations, which in the 30% Zn treatment equated to a $^{Zn}B_A$ of ~ 5, 700 µg g^{-1}, that at least some genotypes were adopting an avoidance strategy, rather than a tolerance strategy as in the 10% Zn treatment. With regard to the concentrations of Zn accumulated in root tissue, considered as an index of Zn tolerance, these ranged between ~ 4,000 and ~ 15,000 µg g^{-1} in both the 10% and 30% Zn treatments; the higher values probably represent a super-critical threshold concentration, above which death would occur.

In terms of accumulation of Zn in the shoots in the 10% Zn treatment, two genotypes (16 and 25) contained > 6,000 µg/plant at final harvest, whilst most of the others contained ≤ 3,000 µg/plant. Similarly, in the 30% treatment, two genotypes (48 and 56) contained > 8,000 µg/plant, whilst most of the others contained < 4,000 µg/plant. Average concentrations of Zn in shoot tissue at final harvest varied widely across the genotypes (Table 7.4) and were consistently higher in the 30% Zn treatment than in the 10% treatment. However, they were consistently lower than the average concentrations of Zn in the roots, suggesting that vacuolar compartmentation of Zn in the roots and low transfer rates to the shoots were the dominant processes. The latter is confirmed by an analysis of translocation indices across the genotypes. All genotypes showed a higher TI_{Zn} in the 30% Zn treatment relative to the 10% treatment. In the 10% Zn treatment, only Genotype 150 had a $TI_{Zn} > 1$, whilst seven individuals had a $TI_{Zn} < 0.2$, with Genotype 14 having a TI_{Zn} of ~ 0.11. In the 30% Zn treatment, four genotypes, namely

22, 26, 39 and 192, had a $TI_{Zn} \geq 1$, whilst five had $TI_{Zn} < 0.4$, with Genotypes 6 and 51 having a $TI_{Zn} \sim 0.28$.

The generally low translocation indices observed across most of the surviving genotypes, combined with their generally high Zn tolerance, as indexed by high shoot and root Zn contents and tissue Zn concentrations, satisfies the critical phytostabilisation criteria referred to above, and supports the conclusions of Arienzo *et al*. (2004), Bidar *et al*. (2007, 2009) and Padmavathiamma and Li (2009) that *L. perenne* in general, and at least certain genotypes within the mapping family, could be used for the phytostabilisation of contaminated substrates. The Zn tolerance data presented in this research project also confirm the observations of Bonnet *et al*. (2000), that *L. perenne* has a very strong capacity to self-protect against toxic Zn concentrations, both in the substrate and internally.

L. perenne also has the ability to accumulate Zn to very high tissue concentrations, both in the roots and shoots, in the latter case reflecting substrate $^{Zn}B_A$ concentrations, often with little manifestation of significant metabolic disturbance. In this context, it is important to note that, whilst tissue concentrations of only 200 µg g^{-1} are potentially phytotoxic to many plant species (e.g. Tsonev and Lidon, 2012; Khudsar *et al*., 2004), some genotypes in the 30% Zn treatment contained root and shoot tissue Zn concentrations > 5,500 µg g^{-1}, far in excess of general toxicity thresholds. As described in Section 2.1.3, a plant can be classified as a Zn hyperaccumulator if it can accumulate > 3,000 µg g^{-1} in the dry leaf tissue (e.g. Reeves and Baker, 2000). This was clearly the case for many of the *Lolium* genotypes used in the present study, both in the 10% and 30% Zn treatments (see Figures 4.19 and 4.20). However, certain other criteria, including a translocation index consistently > 1, must also be satisfied for designation as a hyperaccumulator, implying that many of the genotypes in this *L. perenne* mapping family can be categorised as belonging to the 'tolerant Zn indicator' class of plants (Baker and Walker, 1990; Mehes-Smith *et al*. 2013).

7.3 Plant growth, metal uptake and translocation in Pb Experiment 2

7.3.1 Pb toxicity in plants

In contrast to HMs such as Zn, Co, Cu and Ni, which are essential micronutrients for sustaining optimal plant growth and metabolism, other HMs such as Pb, Cd and Hg have no beneficial effects and can be very harmful to plants (Sections 2.1 and 2.3). The toxicological effects of excess Pb, some of which are listed in Table 2.3, include adverse impacts on plant morphology,

growth and photosynthetic processes (Nagajyoti *et al*., 2010). Lead toxicity is also known to inhibit seed germination and seedling growth (e.g. Morzck and Funicclli, 1982; Sudhakar *et al*., 1992). For example, Verma and Dubey (2003) reported that the presence of 1 mM Pb caused up to a 30% decrease in the germination of rice seeds and a reduction of seedling growth by up to 45%. Excess Pb also causes a rapid inhibition of root growth (Sharma and Dubey, 2005) and induces morphological changes such as radial thickening of roots and cell walls of the endodermis, lignification of the cortical parenchyma (Paivoke, 1983), as well as chlorosis (e.g. Hewilt, 1953; Burton *et al*., 1984). A considerable decrease in dry weights is generally observed under high Pb treatments (Kosobrukhov *et al*., 2004), although Wierzbicka (1998) reported that in corn seedlings an apparent increase in dry weight could be attributed to an increase in the synthesis of cell wall polysaccharides.

Key enzymes involved in Chl biosynthesis are strongly inhibited by Pb ions (Prassad and Prassad, 1987), whilst Stiborova *et al*. (1987) considered that photosynthesis is affected by the inhibiting activity of carboxylating enzymes. Pb is known to block the entry of cations, such as K, Ca, Mg, Zn, Mn, Cu and Fe^{3+}, and anions, such as NO_3^-, into the roots and thereby causes impaired uptake of some essential elements (Burzynski, 1987). Inhibition of root growth may be due to a reduction in Ca in root tips leading to a decrease in cell division or elongation (Haussling *et al*., 1988), whilst Nagajyoti *et al*. (2010) considered that the primary cause of cell growth inhibition arises from the Pb-induced oxidation of indol-3 acetic acid (IAA), the most common of the auxin class of plant growth hormones. Pb toxicity also causes water imbalance and alterations in membrane permeability (Sharma and Dubey, 2005), inhibits ATP production, and induces oxidative stress through the production of ROS including H_2O_2, the superoxide anion O_2^-, singlet oxygen $^1O_2$, and the hydroxyl radical OH^- which can result in lipid peroxidation and DNA damage (Verma and Dubey, 2003).

Plants utilise several defence strategies to cope with Pb toxicity (Pourrut *et al*., 2011). These include exclusion or a reduced uptake of Pb into the cell, and the sequestration of Pb into the vacuole as complexes. In addition, Pb may be bound by PCs, GSH and amino acids which are synthesised under exposure to high Pb concentrations (e.g. Grill *et al*., 1987), whilst the upregulation of antioxidants, such as SOD and catalase, effectively catalyses the breakdown of ROS. Lead-tolerant rice upregulates the synthesis of oxalate, a compound that precipitates Pb and thereby reduces uptake by the roots (Yang *et al*., 2000). In addition, Pb toxicity induces the synthesis of osmolytes, which play a major role in maintaining cell volume and fluid balance (Pourrut *et al*., 2011).

Lead is mainly absorbed into a plant through the roots *via* the extracellular apoplastic pathway, where it accumulates near the endodermis which acts as a partial barrier to movement between root and shoot, possibly due to negative charges that exist on root cell walls (Pourrut *et al*., 2011). Qu *et al*. (2003) studied Pb uptake by the roots of four turfgrass species grown hydroponically in solutions containing up to 450 mg L^{-1} Pb. The maximum Pb tissue concentration recorded was in the range ~ 20 mg g^{-1} root dry weight. Tall fescue (*Festuca arundinacea*) and Common fescue (*Spartina patens*) survived at 450 mg L^{-1} without displaying evidence of toxicity, whilst Centipedegrass (*Eremochloa ophiuroides*) and Buffalograss (*Buchlöe dactyloides*) deteriorated or died at this concentration. Although no shoot Pb concentration data were presented, the authors suggested that the results indicate that turfgrass plants can tolerate high Pb concentrations and absorb Pb efficiently, at least into the roots, and thus may have potential for phytoremediation.

Arienzo *et al*. (2004) studied Pb uptake to the shoots of *L. perenne* grown in soils containing up to 366 mg kg^{-1} Pb. Results showed that the plants grew healthily on all substrates and displayed no macroscopic symptoms of metal toxicity after 90 days of growth. Shoot concentrations of Pb were 0.67 and 0.98 mg kg^{-1}, which the authors concluded was 'in the range of physiologically acceptable levels'. It has been shown that Pb accumulation in the roots is generally significantly higher than in the shoots, indicating a low Pb translocation index (e.g. Cunningham *et al*., 1995; Verma and Dubey, 2003). However, Pennycress (*Thlaspi rotundifolium*) plants have been reported to accumulate Pb in the range 130 – 8,200 mg kg^{-1} shoot dry weight (Reeves and Brooks, 1983), a range far in excess of published shoot toxicity thresholds (Table 7.1), although because of its slow growth rate and small biomass, the species is not considered suitable for the phytoextraction of Pb from contaminated substrates. Finally, some cultivars of Indian Mustard (*Brassica juncea*) have been shown to accumulate up to 15 mg Pb g^{-1} in the shoot when grown in a nutrient solution containing 188 mg Pb L^{-1} (Kumar *et al*., 1995).

7.3.2 Synthesis of growth in Pb Experiment 2

In contrast to Zn Experiment 1, all of the mapping family genotypes tested survived the full length (16 weeks) of Pb Experiment 2, in both the 10% and 30% Pb treatments. Indeed, visual inspection suggested that all the genotypes were vigorous and healthy, with no obvious signs of Pb toxicity such as chlorosis or stunted growth (Plate 7.2). This suggests that both the 10%

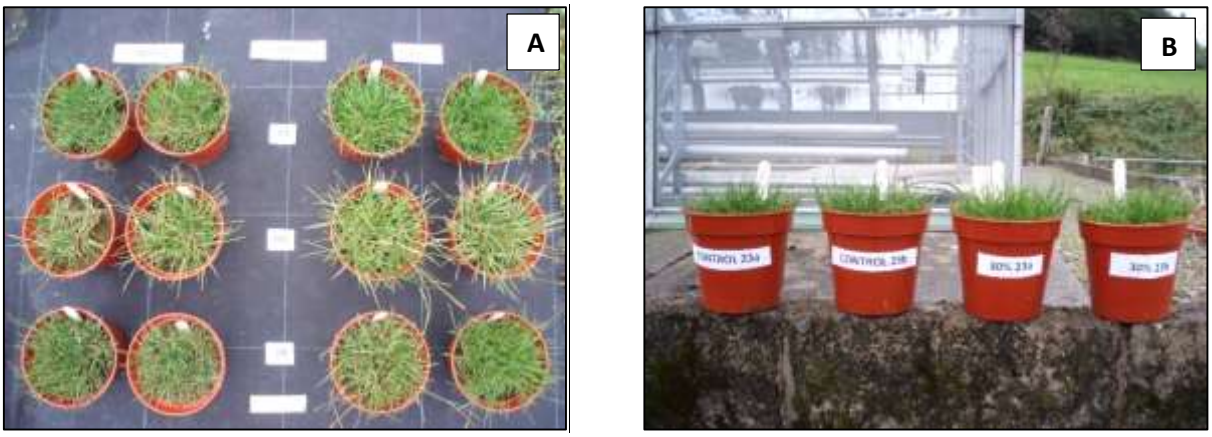

Plate 7.2 Photographs of *L. perenne* genotypes, after 16 weeks of growth, showing no visible signs of toxicity in A) replicate pots of genotypes 23, 60 and 19 in the control treatment on the left and in the 30% treatment on the right, and B) replicate pots of Genotype 23 in the control treatment on the left and the 30% treatment on the right.

Pb treatment, with an absolute substrate concentration of ~1,890 µg g^{-1} and a $^{Pb}B_A$ of ~ 445 µg g^{-1}, and the 30% Pb treatment, with an absolute substrate concentration of ~ 5,670 µg g^{-1} and a $^{Pb}B_A$ of ~ 1,335 µg g^{-1}, constituted sub-critical toxicity levels for these plants. As noted above, Arienzo *et al*. (2004) observed that substrate concentrations of only 366 µg g^{-1}, considerably less than that applied in Pb Experiment 2, did not produce any adverse impact on the growth of *L. perenne*.

As mentioned in Sections 2.3.2 and 7.2.2, in addition to survival and longevity, a rapid rate of growth, high biomass production, dense root systems, and high rates of tiller production are all critical attributes required by plants for the phyostabilisation of HM-contaminated substrates. With respect to plant growth during Pb Experiment 2, the data presented graphically in Section 4.2.1 and summarised for five growth-related traits in Table 7.5, reveal a wide variation in genotype performance, as well as substantial differences in performance compared with Zn Experiment 1 (see Table 7.3). In contrast to the exponential decline in mean biomass production with increasing HM substrate levels observed in Zn Experiment 1 (see Figure 7.1), there was a

Table 7.5 *Summary of genotype performance in Pb Experiment 2 for five growth-related traits. Values in parentheses are the mean values for each trait.*

Trait	**Pb Treatment**		
	Control	**10%**	**30%**
Shoot dry weight (g/plant)	0.42 – 1.96 (1.11)	0.75 – 1.77 (1.25)	0.87 – 2.03 (1.41)
Root dry weight (g/plant)	0.33 – 1.86 (0.69)	0.54 – 1.58 (0.93)	0.68 – 1.56 (1.07)
Whole plant dry weight (g/plant)	0.69 – 3.82 (1.8)	1.39 – 3.07 (2.18)	1.75 – 3.53 (2.48)
Shoot : root ratio	0.97 – 2.62 (1.71)	0.78 – 1.96 (1.4)	0.73 – 1.86 (1.37)
Tiller numbers (per plant)	15 – 77 (30)	16 – 54 (31)	16 – 62 (35)

linear increase in mean root, shoot, and total plant biomass production with increasing Pb substrate concentration. This was particularly evident at Cut 1 (Figure 7.5A), after 8 weeks of growth. Only Genotype 26 had a greater shoot dry weight in the control treatment compared with the 30% Pb treatment. Similarly, only Genotype 114 had a greater shoot dry weight in the 10% Pb treatment than in the 30% treatment (see Figure 4.25). This trend persisted to final harvest, after 16 weeks of growth (Figure 7.5B), with the majority of genotypes having higher shoot dry weights in the 30% Pb treatment than in either the control or 10% Pb treatments (see Figure 4.27). Indeed, only six genotypes (4, 6, 7, 26, 30 and 70) had higher shoot dry weights in the control treatment than in the 30% Pb treatment at final harvest.

A similar response to increasing Pb substrate concentration was observed for root mass. Figure 7.5C shows that mean root dry weight increased with increasing Pb substrate concentration, and at a slightly greater rate than the increase in mean shoot dry weight. This is reflected by an overall decrease in shoot:root dry weight ratio with increasing Pb substrate concentration (Table 7.5). Only Genotype 25 had a higher root dry weight in the control treatment than in either of the Pb treatments, and the majority of genotypes had higher root dry weights in the 30% Pb treatment than in the 10% treatment (see Figure 4.29). Once again, this trend contrasts markedly to the exponential decline in mean root dry weight with increasing HM substrate level observed in Zn Experiment 1 (see Figure 7.1C).

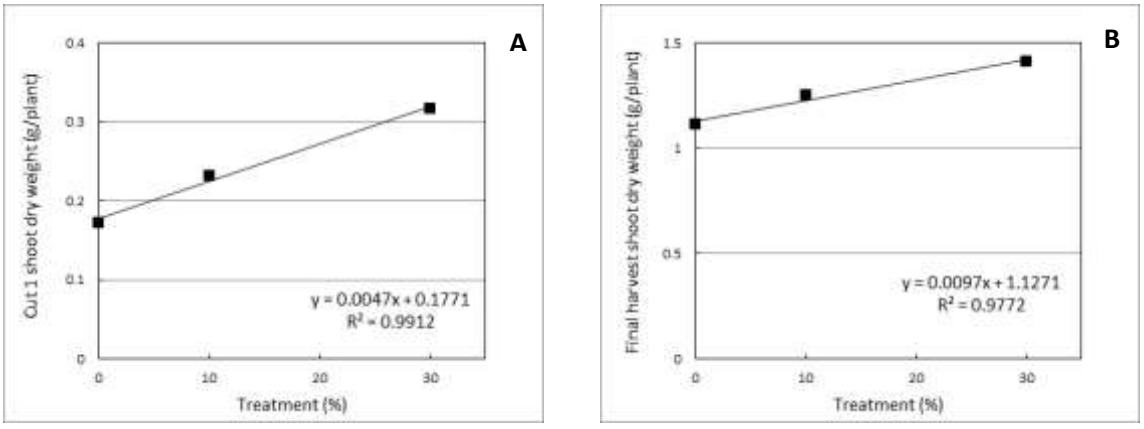

Figure 7.5 Mean dry weights of A) shoots at Cut 1, B) shoots at final harvest, C) roots at final harvest, and D) the total plant at final harvest, plotted against Pb treatment.

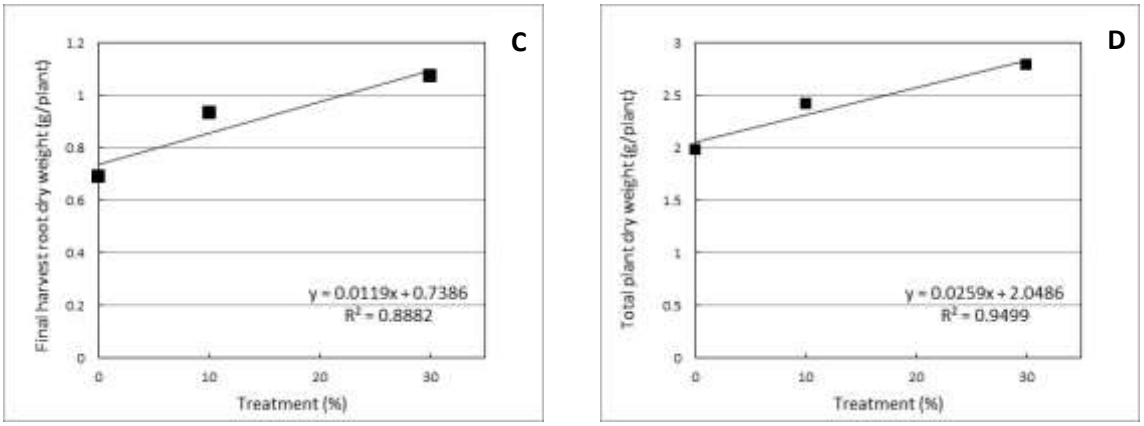

Figure 7.5 Continued.

Likewise, total plant dry weights at final harvest showed a marked increase, relative to the control treatment, of ~ 25% and ~ 40%, respectively, in the 10% and 30% Pb treatments (Figure 7.5D).

Interestingly, when compared with plant dry weights, tiller numbers increased relatively modestly with increasing Pb substrate concentration, as evidenced by means of 30, 31 and 35 tillers per plant, in the control, 10% and 30% Pb treatments, respectively. However, there was significant variation amongst genotypes in this respect, with 64 out of the 77 genotypes producing more tillers in the 30% Pb treatment than in the 10% Pb treatment.

The positive growth responses to increasing levels of Pb in the substrate observed in this experiment were unexpected, given the very different trends observed in response to increasing HM concentrations in Zn Experiment 1 and the responses to Pb toxicity commonly reported in the literature. As noted in Section 7.3.1, the primary manifestation of Pb toxicity is the rapid inhibition of root growth (Fahr *et al*., 2013); indeed, a significant reduction in root dry mass has been reported in many plant species, including *Oryza sativa* (Verma and Dubey, 2003), *Zea mays* (Koshevnikov *et al*., 2009), *Pisum sativum* (Malecka *et al*., 2009), *Sedum alfredii* (Gupta *et al*., 2010) and *Triticum aestivum* (Kaur *et al*., 2013), and in total dry biomass for *L. perenne* (Arienzo *et al*., 2004). Jelea *et al*. (2015) reported that for *L. perenne* cultured hydroponically under five Pb different treatments (0, 0.05, 0.1, 0.5 and 1 g $PbNO_3$ L^{-1}) there was a significant reduction in root and shoot dry weight. Root dry weight decreased from 0.024 g/plant in the control treatment to 0.009 g/plant in the 1g $PbNO_3$ treatment, whilst for the same treatments shoot dry weight decreased from 0.05 g/plant to 0.035 g/plant.

In contrast, in the Pb toxicity experiment (1:23:66) conducted in FSC at IBERS with the same *L. perenne* mapping family as used in the current project, discussed in Section 6.1.1, the high Pb treatment induced little or no adverse impact on growth relative to the control treatment (see Figure 6.2B). Increases in performance in response to increasing Pb concentrations, as indexed by root growth, shoot and root dry weight, have also been recorded with other plant species. For example, Qu *et al*. (2003) grew Saltmeadow cordgrass (*Spartina patens*) hydroponically in Pb concentrations of between 0 and 450 mg L^{-1}. These authors reported that, at a concentration of 50 mg L^{-1}, the plants appeared darker green and healthier and also developed substantial new roots. Even at a Pb concentration of 450 mg L^{-1}, the plants showed no sign of chlorosis, withering or root deterioration and still developed new roots and shoots. Similar morphological characteristics were observed during Pb Experiment 2. McComb *et al*. (2012) reported on the short-term effects of Pb on the growth-related performance of coffeeweed (*Sesbania exaltata* Raf.) grown under hydroponic conditions. The shoot dry weight results from that study (Figure 7.6) showed that shoot biomass increased with time of exposure to Pb, across all treatments. Furthermore, on day 12 of the experiment the shoot dry weight of plants exposed to 15 µM Pb exceeded that of the control plants.

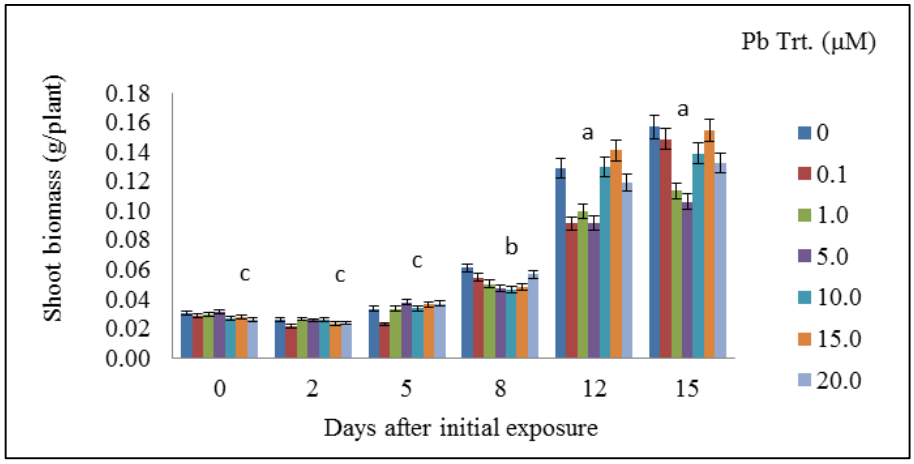

Figure 7.6 Shoot biomass (g dry weight/plant) of *S.exaltata* exposed to different Pb concentrations (µM) and growth periods (from McComb *et al*., 2012).

Similar trends were observed for root biomass (Figure 7.7); root dry weights increased over time at all Pb concentrations, with those in the 15 and 20 µM treatments either the same or exceeding those in the control treatment.

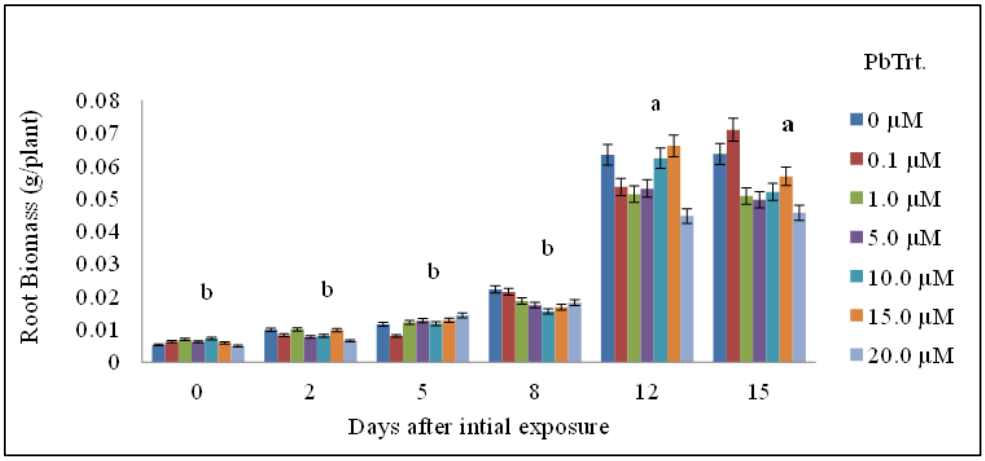

Figure 7.7 Root biomass (g dry weight/plant) of *S. exaltata* exposed to different Pb concentrations (µM) and growth periods (from McComb *et al*., 2012).

Finally, Cao *et al*. (2016) reported the results of a pot-based experiment using *L. perenne* cultured in soils containing Pb concentrations of 0, 200, 300, 500 and 1,000 mg kg^{-1}. Interestingly, the uninoculated control plants showed an increase in biomass production up to substrate concentrations of 300 mg kg^{-1} for shoot fresh weight, and 500 mg kg^{-1} for root fresh weight and tiller numbers, after which all growth parameters gradually declined (Figure 7.8).

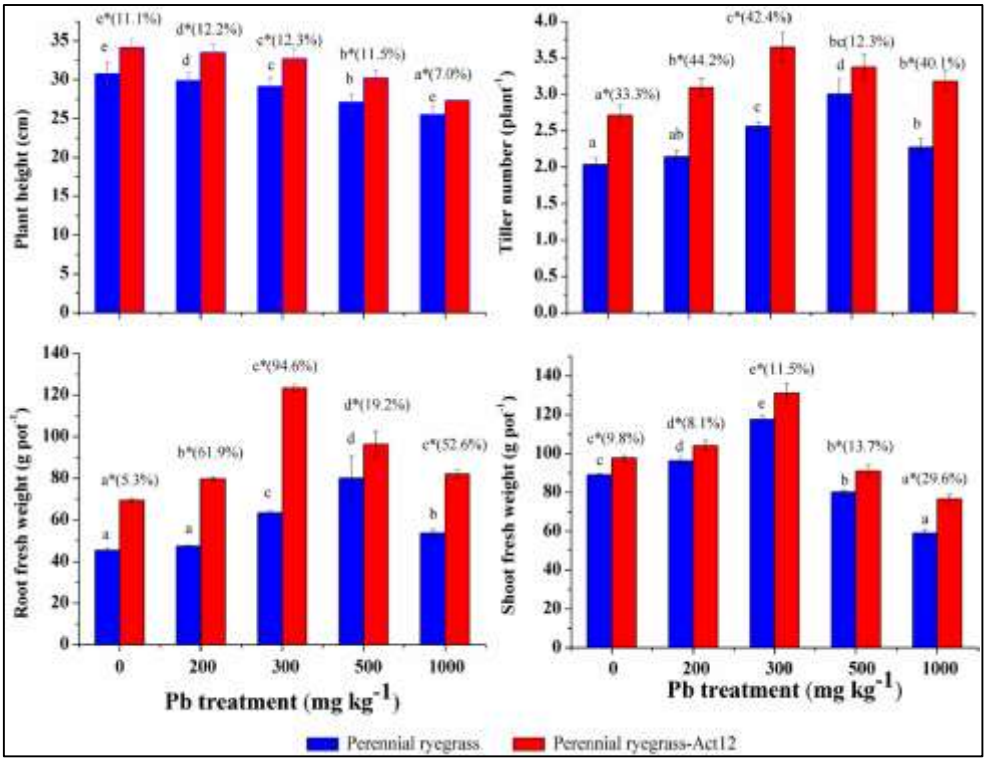

Figure 7.8 Growth parameters (plant height, tiller number, root fresh weight and shoot fresh weight) of *L. perenn*e after 60 days of growth in Pb-treated soil inoculated with or without *Streptomyces pactum*Act12 (from Cao *et al*., 2016).

In the current study, as discussed below in Section 7.3.3, substantial accumulation of Pb was recorded in the roots (~ 1,000 – 5,000 µg/plant) and, to a lesser extent, in the shoots (~ 75 –

260 µg/plant) of all the genotypes exposed to the 30% Pb treatment. Furthermore, the average concentrations of Pb in the root (1,000 – 2,800 µg g^{-1}) and shoot (~ 60 – 150 µg g^{-1}) tissue exceeded reported toxicity thresholds (see Table 7.1). The absence of any negative effects of Pb treatment on growth therefore remains puzzling. One possible explanation may be that advocated by Wierzbicka (1998), who attributed an increase in the dry weight of corn seedlings exposed to Pb to an increase in the synthesis of cell wall polysaccharides. However, in the absence of cellular analysis in the present study, this explanation remains conjecture only. In conclusion, the lack of any obvious phytotoxic effects of Pb, such as chlorosis, inhibition of root growth and high rates of mortality, in this experiment suggests that substrate Pb concentrations in both the 10% and 30% treatments in Pb Experiment 2 were sub-critical in terms of toxicity for all the genotypes tested in the *L. perenne* mapping family, at least over the 16 week time span of this experiment.

7.3.3 Synthesis of metal uptake and partitioning in Pb Experiment 2

The critical attributes required for phytostabilisation include a high tolerance to the specific substrate contaminant, both in terms of growth and metal uptake, and a very low translocation index (see Section 2.3.2). Analysis of Pb uptake and partitioning in Pb Experiment 2 (Section 4.2.2) revealed, as for Zn Experiment 1, wide variation in performance amongst the 77 genotypes tested. This applied both to the quantities of Pb absorbed per plant and to concentrations of Pb in the roots and shoots, as summarised in Table 7.6.

Table 7.6 *Summary of the variation in genotype performance for six Pb uptake-related traits. Values in parentheses are the mean values for each trait.*

Trait	Pb Treatment	
	10%	30%
Shoot content (µg Pb/plant)	13.86 – 94.73 (50.11)	75.99 – 262.54 (138.84)
Shoot tissue concentration (µg Pb g^{-1})	21.98 – 65.69 (40.09)	63.03 – 179.14 (98.8)
Root content (µg Pb/plant)	190.62 – 750.35 (366.41)	787.42 – 5009.59 (1909.8)
Root tissue concentration (µg Pb g^{-1})	274.22 – 678.44 (392.72)	949.85 – 3708.06 (1766.68)
Translocation index	0.04 – 0.25 (0.14)	0.03 – 0.19 (0.08)
Pb uptake efficiency (µg Pb/plant)	221.21 – 708.39 (416.52)	872.33 – 5216.68 (2048.64)

With regard to the accumulation of Pb in the roots, only three genotypes (4, 39 and 201A) contained more than 600 µg/plant at final harvest in the 10% Pb treatment, with Genotype 39 containing the most Pb at ~ 750 µg g^{-1}. The Pb content of the roots in the 30% Pb treatment

showed a much greater range, with five genotypes (4, 30, 39, 78 and 129) containing over 3,000 µg/plant and Genotype 30 containing the most Pb at ~ 5,000 µg/plant. The concentration of Pb in root tissue, an index of Pb tolerance, varied three-fold across the 77 genotypes in both Pb treatments, but was generally far higher in the 30% Pb treatment, ranging up to ~ 3,700 µg g^{-1}. As might be expected, the Pb content of the roots was reasonably positively correlated with the average Pb concentration in root tissue (see Figure 4.45), with R^2 values of ~ 0.41 and ~ 0.64, respectively, in the 10% and 30% Pb treatments. Given that all the genotypes appeared healthy and vigorous at final harvest it is likely that the root Pb contents and tissue concentrations were at sub-critical toxicity levels and that some form of Pb compartmentation in the roots was being successfully maintained.

Shoot Pb content was very low in all genotypes after 16 weeks exposure to the Pb treatments, indicating only limited translocation of Pb from the roots. Indeed, the maximum shoot content of Pb recorded in both Pb treatments was much lower than the minimum value, for the same parameter, recorded in Zn Experiment 1. In the 10% Pb treatment, only nine genotypes contained more than 70 µg/plant, with Genotypes 157 and 201A containing the most Pb at > 94 and > 83 µg/plant, respectively. Although the Pb content of the shoots was generally higher in the 30% Pb treatment, only four genotypes contained > 200 µg/plant, with Genotype 38 displaying the highest Pb content at > 262 µg/plant. As observed for Pb in the roots, the total content of Pb in the shoots was linearly correlated with the average tissue concentrations of Pb in the shoots, with R^2 values of ~ 0.65 and ~ 0.63, respectively, in the 10% and 30% Pb treatments (see Figure 4.44). Concentrations of Pb in the shoots were consistently higher in the 30% Pb treatment (63 – 180 µg g^{-1}) compared with the 10% Pb treatment (22 – 66 µg g^{-1}), and frequently exceeded published shoot toxicity thresholds of 30 – 100 µg Pb g^{-1} (Table 7.1).

As shown in Table 7.6, tissue Pb concentrations were far higher in the roots than in the shoots, often by a factor of ten, indicating that compartmentation and storage of Pb in the roots, as well as very low Pb transfer rates to the shoots, were the dominant processes. This is confirmed by an analysis of translocation indices across the genotypes. As noted in Section 4.2.2, under the 10% Pb treatment, 19 of the 77 genotypes partitioned ≥ 90% of the total plant Pb content in the roots, whilst in the 30% Pb treatment this increased to 70 of the 77 genotypes. In the 10% Pb treatment, seven genotypes had a $TI_{Pb} < 0.1$, whilst in the 30% Pb treatment 58 genotypes had a $TI_{Pb} < 0.1$. A reduction in mean TI_{Pb} with increasing Pb concentration indicates that root Pb storage mechanisms become progressively more important in maintaining optimal plant homeostasis.

Given that the growth media used in this experiment contained $^{Pb}B_A$ of ~ 445 (10% Pb treatment) and 1,335 µg Pb g^{-1} (30% Pb treatment), the low translocation indices observed across all genotypes, together with the generally high Pb tolerance, as indexed by relatively high root contents and tissue concentrations of Pb, suggest that *L. perenne* can be categorised in the 'tolerant Pb excluder' class of plants (Baker and Walker, 1990; Mehes-Smith *et al*., 2013). The results are also consistent with the conclusions of other authors (e.g. Arienzo *et al*., 2004; Bidar *et al*., 2007, 2009) that *L. perenne* in general could be used for the phytostabilisation of Pb contaminated substrates. The top performing genotypes within the mapping family trialled in Pb Experiment 2 certainly show potential for this purpose.

It is clear from the foregoing discussion that the root system of *L. perenne*, as with many other species, play a critical role in protecting the plant from the adverse impacts of Pb-contaminated substrates. Several defence strategies have been adopted by plants involving, for example, extracellular precipitation and the formation of mechanical barriers such as the deposition of callose (e.g. Bacic *et al*., 2009). In most plants, however, 90 – 96% of the total plant Pb is stored in the roots (Wierzbicka and Antosiewicz, 1993; Kumar *et al*., 1995). The results of Pb Experiment 2 are consistent with this range, and support the view that the accumulation potential of the roots makes *L. perenne* highly suited for phytoremediation (Fahr *et al*., 2013). Lead can be stored in root cell walls (e.g. Malecka *et al*., 2009) which are able to bind divalent metal ions such as Pb and which become most effective in the presence of an increasing polysaccharide content. The root cell vacuole is ultimately one of the primary sites for Pb sequestration (e.g. Sharma and Dubey, 2005; Clemens, 2006). Lead that has entered the cytoplasm can be chelated by PCs, for example, and transported across the tonoplast and into the vacuole *via* HM transporters such as ATPases (e.g. Talke *et al*., 2006; Morel *et al*., 2009).

The quantities of Pb that can be absorbed and stored in the roots vary greatly both within and between species. Concentrations of Pb in root tissue in Pb Experiment 2 ranged between 274 – 678 and 949 – 3,708 µg g^{-1}, respectively, in the 10% and 30% Pb treatments. In the pot-based experiment of Cao *et al*. (2016), the roots of *L. perenne* control plants growing in soil with a Pb concentration of 1,000 mg kg^{-1} (a value broadly comparable with the bioavailable Pb fraction in the 30% Pb treatment) contained only 133.51 mg kg^{-1}, significantly less than the concentrations observed in Pb Experiment 2 (Table 7.6). Interestingly, Cao *et al*. (2016) reported that the shoots of *L. perenne* contained 21.88 µg g^{-1} in the 1,000 mg kg^{-1} Pb treatment, a value that is consistent with the results from Pb Experiment 2. Qu *et al*. (2003) reported on Pb uptake by the roots of four turfgrass species grown hydroponically in solutions containing

Pb at concentrations between 0 – 450 mg L^{-1}. In contrast to the results of Pb Experiment 2, there was a quadratic relationship between Pb accumulation in the roots and the concentration of Pb in solution in the turfgrass experiment, with root tissue Pb concentrations reaching > 20,700 µg g^{-1} at 415 mg Pb L^{-1} in Centipedegrass (*Eremochloa ophiuroides*), and > 21,500 µg g^{-1} at 345 mg Pb L^{-1} in Buffalograss (*Buchlöe dactyloides*). Such studies indicate substantial differences between species with respect to Pb uptake, with some species, including several turfgrasses and known Pb accumulators/hyperaccumulators such as *Thlaspi caerulescens* and other members of the Brassicaceae, having enhanced biophysical and biochemical adaptations to Pb tolerance.

7.3.4 Comparative analysis, experiment limitations and opportunities

The foregoing discussion has focussed primarily on behavioural variations within each experiment. However, the experimental data have also revealed fundamental differences in behaviour and performance between each experiment, particularly in terms of parameters such as survival, growth of shoot, root and whole plant, and metal uptake. This section briefly addresses those differences with a focus on experiment limitations and causal hypotheses for the observed variations, as well as opportunities for further bioremedial applications of the *L. perenne* mapping family.

With regard to survivability, whilst all genotypes survived to final harvest in each of the Pb treatments, there was significant mortality in the two Zn treatment amounting to ~ 15% in the 10% Zn treatment and ~ 40% in the 30% Zn treatment (see Table 4.1). These data, together with the healthy appearance of all genotypes, suggests that substrate concentrations in the two Pb treatments were below a critical threshold and that significantly higher Pb concentrations, possibly of up to 50% by weight of tailings (equivalent to an absolute substrate Pb concentration of ~ 9,450 µg g^{-1} and a $^{Pb}B_A$ of ~ 2,225 µg g^{-1}), may have elicited a toxic response in the plants. Alternatively, the duration of the experiment could have been increased to 20 weeks. In contrast, and as noted in Section 7.2.2, the 10% and 30% Zn treatments represented, respectively, critical and super-critical toxicity levels for some genotypes. The data suggest that a 5% Zn treatment, equating to an absolute substrate Zn concentration of ~ 1,500 µg g^{-1} and a $^{Zn}B_A$ of ~ 945 µg g^{-1} may have induced limited toxic stress but yielded 100% survival amongst the genotypes, an outcome that would have also enhanced QTL detection, a factor discussed in more detail in Section 7.4. As suggested in the case of Pb, a longer experiment duration at this reduced level of toxicity may have been appropriate.

In relation to growth, experiment data revealed significant differences in performance depending on HM species. In particular, whilst mean shoot, root and total plant dry weights decreased exponentially with increasing substrate Zn concentration, the same growth parameters showed a linear increase with increasing Pb substrate concentrations (see Figures 7.1 and 7.5). The roots especially showed a significant decline in mean dry weight to only ~ 23% of their mean control dry weight in the 30% Zn treatment. These data confirm that whilst Zn is an essential micronutrient, at super-critical concentrations the same metal induces a significant impact on root development, an interruption in photosynthetic process as evidenced by chlorosis, and oxidative stress (e.g. Rout and Das, 2003; von Wettstein *et al*., 1995; López-Millán *et al*., 2005). The linear increase in growth parameters, which was most marked in the roots under the Pb treatments, once again strongly suggests that substrate Pb concentrations were significantly below critical toxicity thresholds. The increases in mean growth parameters may be variously attributed to a radial thickening of the roots and endodermal cell walls, and an increase in cell wall polysaccharide synthesis (e.g. Paivoke, 1983; Wierzbicka, 1998).

With regard to metal uptake, shoot and root Zn content and shoot and root tissue Zn concentrations were substantially higher in Zn Experiment 1 than for the same parameters recorded in Pb Experiment 2 (see Tables 7.4 and 7.6). This reflects a fundamental difference both in the plants' requirements of these two HMs and in storage mechanisms. In the case of Zn, as an essential micronutrient, certain of the *L. perenne* genotypes were able to translocate Zn to shoot tissue concentrations far in excess of substrate Zn concentrations and with TIs of up to 1.53 in the 30% Zn treatment, thereby enabling the plants to be classified as 'tolerant Zn indicators'. In contrast, as a non-essential/toxic HM, Pb sequestration to the shoots was minimal whilst in the roots, tissue Pb concentrations were substantially lower than the substrate Pb concentration and only slightly higher than bioavailable substrate Pb concentrations. In addition, TIs were generally very low in the Pb treatments, with a mean of only 0.08 in the 30% Pb treatment. These observations suggest that, in contrast to the Zn treatments, root vacuole sequestration of Pb was the dominant process (e.g. Clemens, 2006), thereby allowing the plants to be classified as 'tolerant Pb excluders'.

The overall success of the two pot experiments in highlighting differential performance of *L. perenne* genotypes grown in Zn- and Pb-contaminated substrates suggests that the mapping family may provide a suitable platform for further investigations into their phytostabilisation potential in the presence of high concentrations of other essential and non-essential/toxic HMs. Within the former class of HMs, Cu, Mn, Fe, Ni and Co are metals which are required by plants

in very small quantities but, like Zn, become toxic if taken up in excess of the plant's optimal requirements. Interestingly, some of these metal species are relevant at a local level, having been exploited historically in Wales (Bevins *et al*., 2010) and now contribute a significant metal load to local ecosystems. For example, Cu was extracted from several mines in the CWO, as well as from syn-volcanic veins associated with the Snowdon Volcanic Group in northern Snowdonia, exhalative deposits at Parys Mountain on Anglesey, and the Coed-y-Brenin porphyry-style mineral deposit in central Snowdonia. Lower Cambrian syn-sedimentary exhalative Mn deposits were extensively worked around the Harlech Dome in North Wales, whilst sedimentary ironstones were widely exploited in the Upper Carboniferous (Westphalian) 'Coal Measures' of South Wales.

Copper is produced commercially through the processing of primary sulphide minerals such as chalcopyrite ($CuFeS_2$), chalcocite (Cu_2S), covellite (CuS), and bornite (Cu_5FeS_4) (Friedrich *et al*., 1986). The metal plays an important role in photosynthesis, CO_2 assimilation and ATP synthesis (e.g. Mahmood and Islam, 2006), and is an essential component of enzymes such as SOD and ascorbate oxidase, which are involved in the regulation of potentially harmful superoxide radicals. However, exposure to excess Cu induces oxidative stress and the production of ROS (Stadtman and Oliver, 1991), inhibits growth (e.g. Ouzounidou, 1994), and adversely affects seed germination and seedling root systems when accompanied by Cd (e.g. Neelima and Reddy, 2002).

Nickel is extracted from minerals such pentlandite ($(NiFe)S_8$), Ni-bearing limonite ($(FeNi)O(OH)$), and garnierite ($(NiMg)_3Si_2O_5(OH)_4$) (Davis, 2000). The metal is a constituent of several important enzymes such as urease, which metabolises urea N into available ammonia, and SOD (Nagajyoti *et al*., 2010). In excess concentrations, Ni inhibits seed germination, retards shoot and root growth, affects nutrient absorption and water uptake, impairs plant metabolism, photosynthesis and transpiration, and induces Fe deficiency that causes chlorosis and necrosis (Rahman *et al*., 2005; Gajewska *et al*., 2006; Ahmad and Ashraf, 2011).

Manganese occurs principally in the form of pyrolusite (MnO_2), braunite ($(Mn^{2+}Mn^{3+}{}_6)[O_8]SiO_4$), psilomelane ($(BaH_2O)_2Mn_5O_{10}$) and, to a lesser extent, rhodochrosite ($MnCO_3$) (Bevins, 1994; Bevins *et al*., 2010). The metal is a major contributor to various biological systems in plants, including photosynthesis, respiration and nitrogen assimilation. Manganese is also involved in pollen germination, pollen tube growth, root cell elongation and in conferring resistance to root pathogens. (Millaleo *et al*., 2010). It is a cofactor in over 35

enzymes in plants, including Mn-SOD, and is involved in metabolic processes such as IAA activation (Burnell, 1988). However, high concentrations of Mn are extremely toxic to plants, causing a reduction in photosynthesis and Chl a and b content, and the generation of ROS. A decrease in growth rate and chlorosis has been reported for *L. perenne* (Mora *et al*., 2009).

The main ores of cobalt include cobaltite (CoAsS) and safflorite ($CoAs_2$), as well as their weathering products such as erythrite ($Co_3(AsO_4)_2.H_2O$), although the main commercial source is as a by-product of copper and zinc refining (Davis, 2000). Cobalt is an essential component of several enzymes and coenzymes such as vitamin B_{12} and cobamide, which play a role in root nodule N fixation. The metal retards leaf senescence, increases drought resistance and inhibits ethylene biosynthesis. Morphological effects of excess Co include leaf fall, inhibition of greening, premature leaf closure and reduced shoot growth and biomass production (Li *et al*., 2009). At an intracellular level, excess Co inhibits photosynthetic activity and RNA synthesis, and retards karyokinesis and cytokinesis (Palit *et al*., 1994).

Iron, whose principal source is from oxides such as magnetite (Fe_3O_4) and hematite (Fe_2O_3) (Liu, 2015), is an essential plant micronutrient which plays an important role in the electron transport chains of photosynthesis and respiration, and facilitates chloroplast development and Chl biosynthesis (Connolly and Guerinot, 2002; Nagajyoti *et al*., 2010) . It is also a constituent of cytochrome, catalase, peroxidase and SOD (Marschner, 1995). Excess Fe causes morphological effects such as inhibition of root growth and a reduction in yield, as well as inducing the production of free OH^- radicals that impair cellular structure, and damage cell membranes, DNA, lipids and proteins (Kuswantoro, 2014).

Amongst the 'non-essential/toxic' class of HMs, Cd is highly phytotoxic (Table 2.3). The most important source of cadmium is the mineral greenockite (CdS), which is nearly always closely associated with sphalerite (ZnS). As a consequence, Cd is mainly obtained as a by-product of Zn refining (Cobb, 2008). The metal induces adverse morphological effects such as chlorosis, growth inhibition and finally death (Benavides *et al*., 2005; Guo *et al*., 2008) and its presence affects the uptake, transport and use of water, Ca, Mg, P and K (Das *et al*., 1997) and reduces nitrate absorption and translocation by inhibiting nitrate reductase activity in the shoots (Hernandez *et al*., 1996). The presence of Cd reduces ATPase activity at the root cell membrane, inhibits Chl biosynthesis and reduces the activity of enzymes that control CO_2 fixation (De Filippis and Ziegler, 1993; Fodor *et al*., 1995). Cadmium also causes oxidative

stress, either by inducing oxygen free radical production or by decreasing enzymatic and non-enzymatic antioxidants (e.g. Sandalio *et al*., 2001; Cho and Seo, 2004).

The main source of mercury (Hg) is the primary sulphide cinnabar (HgS), from which the familiar liquid metal is obtained by heating in air and condensing the resultant vapour (Rytuba, 2003). The divalent form of mercury (Hg^{2+}) has a strong phytotoxic effect at an intracellular level (Azavedo and Rodriguez, 2012), triggering the production of ROS, and affecting the antioxidant defence system by interfering with the modulation of GSH, SOD and glutathione reductase (e.g. Ortega-Villasante *et al*., 2005; Israr *et al*., 2006). Exposure to Hg reduces photosynthesis, Chl synthesis, transpiration rates and water uptake, and causes the loss of K, Mg and Mn and the accumulation of Fe (Boening, 2000). Even low doses of Hg are known to be mutagenic and genotoxic, resulting in chromosomal aberrations and spindle alterations (Patra *et al*., 2004).

Nearly all chromium (Cr) is obtained from the Fe-Cr oxide mineral chromite ($FeCr_2O_4$) and, in its hexavalent Cr(VI) form, is highly toxic to plants (Gu and Wills, 1988). It is taken up by carriers of essential ions such as SO_4^{2-} and Fe and causes a range of toxic effects including a reduction in seed germination, in root and shoot/leaf growth, and in yield (Shanker *et al*., 2005; Dotaniya *et al*., 2014). There is a direct impact on enzyme functionality, with a reported decrease in the activity of enzymes related to starch and N metabolism, whilst other adverse physiological effects include a decrease in Chl synthesis, structural changes to chloroplasts leading to inhibition of photosynthesis, oxidative damage to membrane lipids, and the generation of ROS (Singh *et al*., 2013). Uptake of macronutrients such as N, P and K decreases and a decrease in Fe, Ca and Mg uptake has been noted in *L. perenne* (Vernay *et al*., 2007). In addition, Cr(VI) is genotoxic, affecting chromosome morphology and causing damage to DNA (Oliveira, 2012).

The experimental work carried out as part of this research project has shown that many genotypes in the *L. perenne* mapping family possess a strong tolerance to high substrate concentrations of both Zn and Pb, and in particular to the former. In addition, it is important to note that for both HMs, and in particular for Zn, tissue metal concentrations recorded in some genotypes were greater than published shoot toxicity thresholds (Table 7.1). Plant performance, both in regard to growth and metal uptake, also confirms the results of previous investigations which have shown that the species has a high potential for the phytostabilisation of Zn- and Pb-contaminated soils. However, in light of the severe toxicological impacts of other essential and

non-essential HMs, briefly reviewed above, it is possible that the *L. perenne* mapping family may have a further role to play in research into tolerance to other HMs. Since only limited data has been published hitherto, preliminary screening experiments, initially carried out in FSC, and using a range of supra-optimal but sub-lethal HM concentrations to determine metal-specific toxicity thresholds, could provide a rapid insight into growth, metal uptake capacity and tolerance characteristics when cultured in the presence of a wide range of different HMs. For those metals towards which *L. perenne* might show a strong degree of tolerance, further pot-based experiments could be undertaken to fully assess any trait-related impacts and to identify those genotypes which are tolerant to a specific HM. The results of such experiments may provide positive confirmation that *L. perenne* could also have good potential for the phytoremediation of soils, not only contaminated by Zn and Pb, but by a wide range other metal species.

7.4 Synthesis of QTL analysis and the identification of candidate genes

The genetic basis of HM-tolerance in plants was briefly addressed in Section 2.4.2. It has been proposed that genetic adaptations may have occurred at the earliest stages of terrestrial colonisation, during Upper Palaeozoic times, and have since continued over many millions of years to the present-day (Wild, 1978; Ernst, 2000). It is believed that different grass species diverged from a common ancestor between about 65 – 55 Ma, at the start of the Cenozoic Era, with the subsequent appearance of the subfamily Pooideae (Figure 7.9), to which *L. perenne* belongs, between 58 – 42 Ma during the Eocene Epoch (Gaut, 2000; Sandve *et al*., 2008).

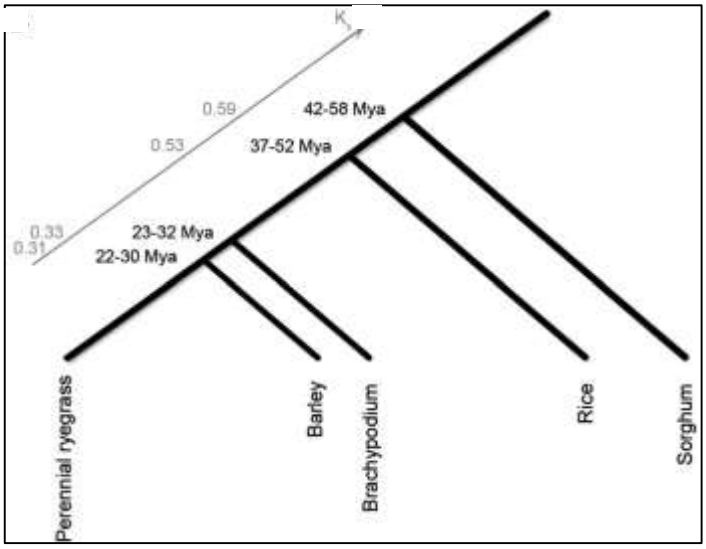

Figure 7.9 Schematic diagram showing Pooideae divergence times of perennial ryegrass from barley, Brachypodium, rice, and sorghum, respectively, estimated at 22 to 30, 23 to 32, 37 to 52, and 42 to 58 Ma (from Pfeifer *et al*., 2013).

Studies suggest that after the divergence from Brachypodium, but before the barley – ryegrass split, a core Pooideae ancestor with seven chromosomes evolved from a 12 chromosome ancestor ~ 30 – 22 Ma, during the Oligocene Epoch, after which its genome size greatly increased (Kellog and Bennetzen, 2004; Catalán *et al*., 2012). These structural genetic changes may have been induced by genomic stress triggered by earlier environmental changes, in particular a rapid global cooling event at the Eocene – Oligocene boundary, approximately 34 Ma (Zachos *et al*., 2001; Liu *et al*., 2009; Sandve and Fjellheim, 2000; King, 2006). Such evolutionary trends, which probably have involved a range of events at genome level including diploidisation, and whole-genome or segmental duplications (Salse *et al*., 2009), would most certainly have gone hand-in-hand with contemporaneous gene-based adaptations to metal tolerance in plants. In addition, the close evolutionary relationship between members of the grass family, spanning many millions of years, has resulted in a high degree of genomic synteny and macro-colinearity (Pfeifer *et al*., 2013), in particular between perennial ryegrass and barley, which share the same number of chromosomes, as well as between perennial ryegrass, Brachypodium and rice.

Although the genetic basis of adaptive traits is still a matter of debate amongst evolutionary biologists, it is believed that metal tolerance in plants evolved through the progressive adaptation of various metal homeostasis processes such as metal uptake, chelation, translocation and storage (e.g. Pollard *et al*., 2002; Clemens, 2006). Nevertheless, many questions remain to be answered; for example, how many genes are involved in metal tolerance, how large is their phenotypic effect, and are they involved in any form of pleiotropism (e.g. tolerance to different metals and the control of different phenotypic traits)?

As outlined in Section 2.4.2, QTL mapping provides a powerful tool for investigations of genetic architecture and the identification of chromosomal regions and, in particular, candidate genes that control HM tolerance. Therefore, in order to investigate the putative locations of candidate genes for Zn and Pb tolerance in *L. perenne*, the trait data collated during the two pot experiments were subjected to a comprehensive QTL analysis (Section 4.4.1) that employed the Kruskal-Wallis statistical test to determine 'significant' traits, interval mapping to determine a 'QTL likelihood map' and LOD score, and a permutation test to determine LOD thresholds for each trait. The results of this analysis for Zn (Section 4.4.2) revealed the presence of 10 growth- and Zn uptake-related QTL on LGs 4, 6 and 7, with LOD scores ranging between 3.7 and 6.95 and '% phenotypic variance explained' ranging between 20.4 and 51.1%. The results for Pb (Section 4.4.3) revealed 22 growth- and Pb uptake-related QTL in LGs 3, 4, 5

and 7, with LOD scores ranging between 3.31 and 14.11 and '% phenotypic variance explained' ranging between 19.7 and 65.3%.

QTL output may be subject to the so-called 'Beavis effect' which predicts that, in experiments using progeny sizes of only ~ 100 genotypes, there is a reduction in QTL detection power as well as an inflation in the estimates of overall genetic effects (Beavis, 1994; Kearsey and Farquahar, 1998; Xu, 2003). According to these authors, recommended optimal progeny sizes are ~ 400 for any given experiment. The relatively high mortality in the 10% and 30% Zn treatments, respectively, 12 and 31 genotypes, and the fact that only 77 genotypes were used in total in each experiment, makes it likely that the 'Beavis effect' applied to the QTL data generated in this study. Nevertheless, the linkage maps with the transposed QTL derived from the two experiments (see Figures 4.52 and 4.53) yielded useful results. For example, in the absence of published QTL for Zn- or Pb-related traits in *L. perenne*, they provide an opportunity to comment on the underlying genetic basis of metal tolerance in this economically important species.

L. perenne is the most widely sown perennial forage grass in the temperate regions of both hemispheres and is of agricultural importance because it is fast growing, has a high nutritional value and a good recovery under a grazing regime (e.g. Hubbard, 1984). In addition, the species has recognised phytostabilising potential for the bioremediation of contaminated substrates (Arienzo *et al*., 2004; Bidar *et al*., 2007, 2009). Although significant genetic improvement of this species has been achieved for agronomic traits through phenotypic selection, progress could be accelerated by using genetic marker-assisted selection (Abberton *et al*., 2008). This also applies to breeding for phytoremediation. The identification of genes that confer metal tolerance and control metal uptake, transport and storage, would also be useful in this context. However, there is very little published information on the genetic basis of metal tolerance in *L. perenne*. Data derived from Pb Experiment 2 yielded growth- and Pb uptake-related QTL that formed a particularly dense cluster on LG7, with a further close association of Pb uptake-related QTL on LG4, for the 10% Pb treatment, and on LG5 for the 30% Pb treatment (see Figure 4.53). Data from Zn Experiment 1 also yielded growth- and Zn-related QTL which formed a closely-associated assemblage on LG7 (see Figure 4.52). These results strongly suggest that a gene which controls aspects of both growth- and metal-uptake may be present on chromosome 7, whilst polygenetic control for Pb uptake is indicated by the presence of QTL on LGs 4 and 5. In respect of growth, Pauly *et al*. (2012) reported that, for three connected populations of *L. perenne*, marker 'OSW', located at map position 17.2 cM on LG7, had many growth-related

QTL located nearby and that this region co-localised with published QTL for fresh weight, leaf length, plant height and heading dates. However, in contrast, Anhalt *et al*. (2009) reported that in an in-bred F2 *L. perenne* population, QTL for biomass traits were located on all LGs, indicating polygenetic control. In addition, the presence on LG7 of QTL for tillering, an index of biomass production, which has been identified by Thorogood (pers comm.), is confirmed by the QTL analysis presented in Sections 4.4.2 and 4.4.3.

Studies of other plant species, in particular *T. caerulescens* and *A. halleri*, the latter being an emerging model species for the molecular characterisation of metal tolerance and hyperaccumulation, have yielded important information. Willems *et al*. (2007) used QTL analysis to investigate the genetic architecture of Zn tolerance in *A. halleri*. Three QTL were identified on LGs 3, 4 and 6, each region co-localising, respectively, with MTP1-A, MTP1-B and HMA4, three genes that are well known to be involved in metal homeostasis in plants. Genes MTP1-A and MTP1-B (Metal Tolerance Protein-Vacuolar Transporters) are cation diffusion facilitators which are known to influence Zn homeostasis in *A. halleri* (e.g. Dräger *et al*., 2004). HMA genes, which are P_{1B}-type heavy metal transporting ATPases, are known to play a crucial role in the transport of metal ions and have been identified in all living organisms. A total of 8 HMA genes have been identified in Arabidopsis, and genomic analysis indicates that they fall into two discrete groups, namely HMA1-4 for the transport of Zn, Co, Cd and Pb, and HMA5-8 for the transport of Cu and Ag (Courbot *et al*., 2007). HMA4 is of particular importance because it is known to encode a Zn-Cd-Pb pump that ensures effective translocation of metal to the shoot (e.g. Hanikenne *et al*., 2008). Further confirmation of the role of HMA4 was provided by Frérot *et al*. (2010), who identified HMA4 at QTL Zn AcLP-1/Zn AcHo-1 on LG3 in *A. halleri* and noted that it showed a strong expression under high external Zn concentrations. In *T. caerulescens*, which has an 88% DNA identity in genomic coding regions with *A. thaliana* (Peer *et al*. 2003), Assunçao *et al*. (2006) identified 2 QTL, with substantial LOD scores, for root Zn accumulation, on LGs 3 and 5. With only a small segregating population (71 individuals), other QTL may not have been generated due to the Beavis effect. However, studies indicate that the gene underlying the QTL on LG3 has an orthologue on LG5 of Arabidopsis, which is a region where there are three known genes that are involved in metal homeostasis.

Although numerous QTL for growth- and Zn/Pb-related traits have been identified in this project, with strong assemblages on LGs 4, 5 and 7 for Pb and on LGs 6 and 7 for Zn, in the

absence of a definitive genetic map for *L. perenne*, it has not been possible to directly link these QTL to any underlying genes. However, the aforementioned close synteny and macro-colinearity between rice and Brachypodium, shown in Figure 7.10, offers an indirect method for relating the contig-based QTL identified during this research to candidate genes. Figure 7.10B shows that complete genome conservation only exists between rice chromosome Os2 and perennial ryegrass LG6. Chromosome LG1 is represented by an insertion of Os10 between two distinct segments of Os5, whilst for LG3, which is mainly represented by Os1, an additional fragment of Os4 was identified that is also present on LG2 and LG4. Chromosome LG2 is composed of two distinct segments of Os4 and Os7, whilst LG7 is represented by an insertion of Os6 between two distinct segments of Os8. In contrast, LG4 and LG5 show evidence of large-scale genomic re-structuring, being represented by Os3, Os4, Os10 and Os11, and by Os3, Os9 and Os12, respectively.

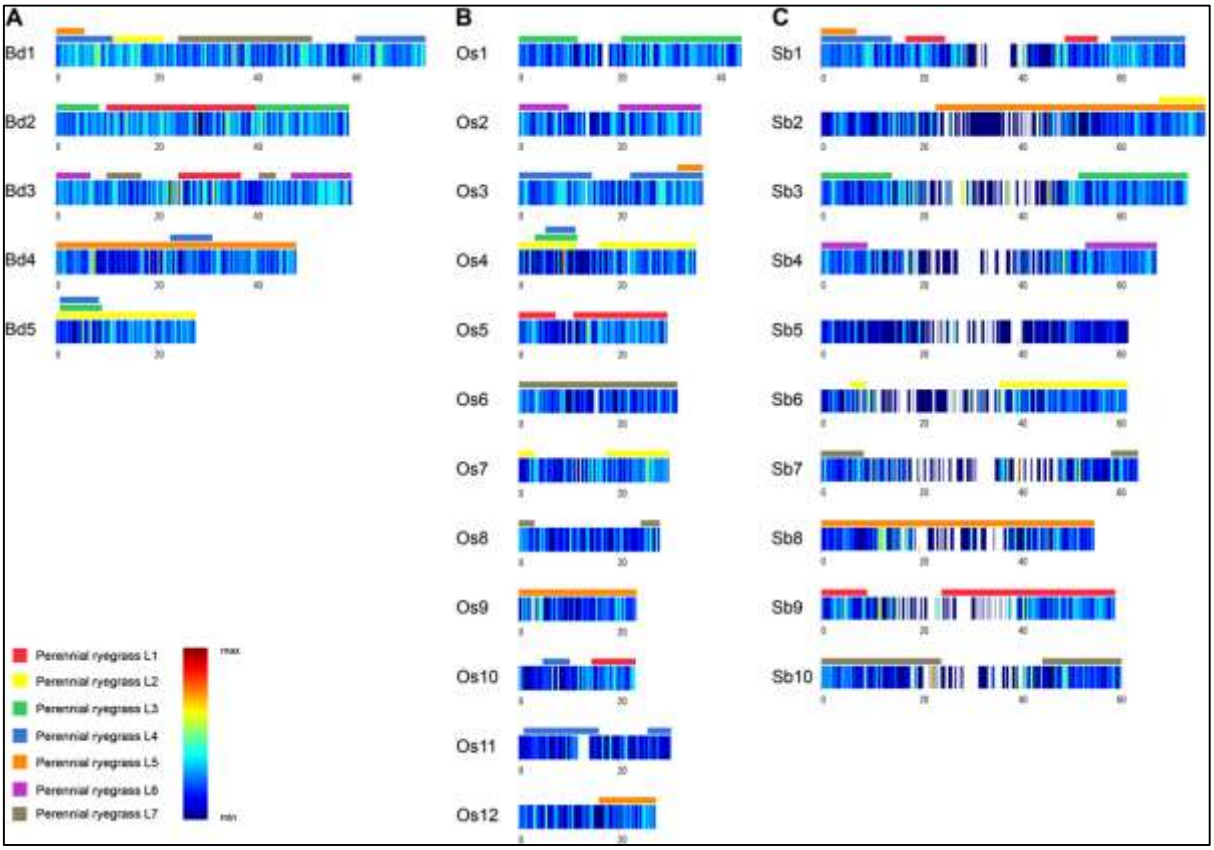

Figure 7.10 Syntenic relationships between perennial ryegrass and A) Brachypodium (Bd), B) rice (Os) and, C) sorghum (Sb). Heat maps represent entire syntenic chromosomes of Brachypodium, rice, and sorghum. Coloured bars visualise that part of the chromosome that was defined as syntenic to perennial ryegrass *via* the barley bridge. The colour of the heat maps illustrates the density of perennial ryegrass marker sequences matching the Brachypodium, rice, and sorghum genomes (from Pfeifer *et al*., 2013).

With regard to the relationship between *L. perenne* and *B. distachyon*, high resolution genetic maps reveal that LG1 is represented by an insertion of a segment of Bd3 between two distinct segments of Bd2, whilst LG2 is represented by segments of Bd1 and Bd5. There is a highly conserved synteny between LG4 and Bd1, LG5 and Bd4, and LG6 and Bd3. Linkage group 7 is represented by an insertion of a segment of Bd3 between segments of Bd1. These relationships are illustrated in Figure 7.11.

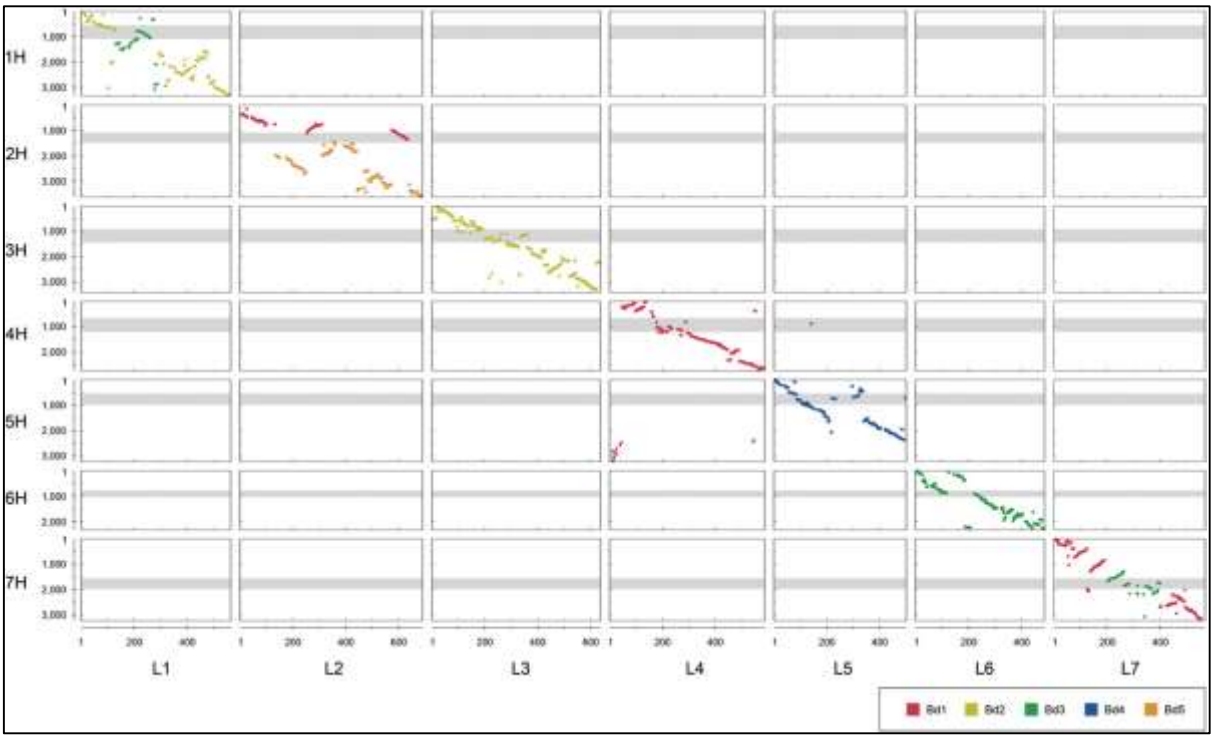

Figure 7.11 Microsyntenic relationships between perennial ryegrass, barley and Brachypodium. Each dot represents a Brachypodium gene, colour coded according to its chromosomal origin, that was anchored in both the perennial ryegrass and the barley GenomeZipper (from Pfeifer *et al*., 2013).

Although complete genome sequences have been established both for rice (International Rice Genome Sequencing Project, 2005) and Brachypodium (International Brachypodium Initiative, 2010), it was decided to use the latter species in the search for candidate genes conferring HM tolerance in *L. perenne*. In addition to the putative presence of HMA, MTP1 and Nramp genes, the role of the ZIP family of HM (Zn, Cd, Fe and Mn) transporter genes, first identified in plants (Guerinot, 2000), has been the subject of much interest. Liu and Chu (2015) identified 96 *bdbZIP* genes that were distributed unevenly on each chromosome of *B. distachyon* (Figure 7.12). Although ~ 80% of the genes were suppressed by the presence of Cu, Zn, Mn and Cd, many others were up-regulated, suggesting an important role in metal tolerance.

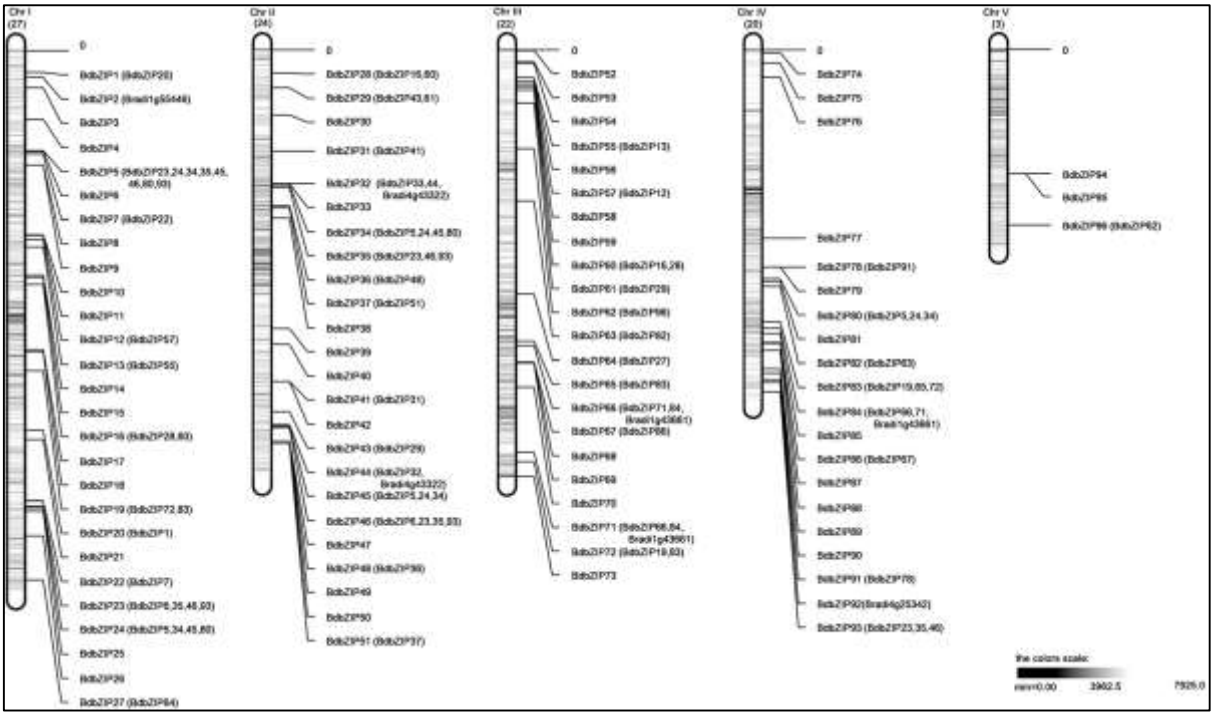

Figure 7.12 Chromosomal locations and regional duplication of 96 bZIP genes identified in *B. distachyon* (from Liu and Chu, 2015).

Three different bioinformatic-based approaches were trialled in an effort to identify candidate genes for HM tolerance in the *L. perenne* mapping family. The first of these utilised the gene Basic Local Alignment Search Tool (BLAST) on an on-line genetic resource database (Gramene, 2016) to co-localise the contigs identified from the QTL analysis (Sections 4.4.2 and 4.4.3) with *B. distachyon* genes, and to interrogate the database to confirm gene function. A preliminary assessment using this 'forward genetics' approach revealed a complex 'one-to-many' relationship, further analysis of which lay outside the scope of this research project.

A second 'forward genetics' approach utilised IBERS' in-house Lolium GenomeZipper database (Thorogood, pers comm.) to match the QTL in Tables 4.5 and 4.6 with their corresponding genes in *B. distachyon* and to identify gene function (Tables 7.7 and 7.8). For those QTL identified for traits from Zn Experiment 1, the QTL on LGs 4, 6 and 7 co-located to genes on Bd1, Bd3, and Bds 1 and 3, respectively (Table 7.7), confirming the aforementioned close syntenic relationship between these chromosomes. Although no HM-specific genes were identified, and whilst some of the genes shown in Table 7.7 are involved in the regulation of intracellular energy production (galactosidase and citrate synthase), others have been shown to play a role in the stress defence systems of plants. For example, it has been shown that ferritins (e.g. 1g44090) play a significant role in the defence machinery against oxidative stress and that ferritin synthesis is required for a proper maintenance of cellular redox status (Ravet *et al*.,

2009; Briat *et al*., 2010). Vesicle associated membrane proteins (VAMPs) (1g05030) are known to block programmed cell death (PCD) downstream of an oxidative burst and have been shown to prevent H_2O_2-induced apoptosis in Arabidopsis. One function of PCD is to remove sub-lethally stressed cells and a key role of ROS has been implicated in PCD through the failure to maintain cell membrane integrity, the latter being a major cause of cell death during oxidative stress (Levine *et al*., 2001). LITAF (lipopolysaccharide-induced tumor necrosis factor-alpha factor) (3g44320) domain proteins are hypothesised to form a compact Zn^{2+} binding structure, localised in the cell membrane, and it has been proposed that they play a role in cellular immune responses (He *et al*., 2011).

For those QTL identified for traits from Pb Experiment 2, QTL on LGs 3, 4, 5 and 7 co-located to genes on Bd 2, Bd1, Bd 4, and Bds 1 and 3, respectively (Table 7.8), once again confirming the aforementioned close syntenic relationship between these chromosomes. The only mismatch was for the QTL for Trait 71 (contig 31442), which co-localised to Bds 3 and 4. Although no HM-related genes were identified, the genes shown in Table 7.8 all play an important role in a wide variety of processes in plants. For example, nucleolar GTP (guanosine triphosphate)-binding protein (1g46650) regulates many cellular processes such as cell growth and differentiation, plant signalling, nuclear protein import, vesicle transport and vesicle formation (e.g. Terryn *et al*., 1993; Yang and Meinke, 2000; Assmam, 2002). ATP synthase (e.g. 2g17290) is a critical enzyme that creates the energy storage molecule adenosine triphosphate (ATP). The enzyme is integrated into the thylakoid membrane of the chloroplast, where it takes part in the light-dependent reactions of photosynthesis (e.g. McCarty *et al*., 2000). Phosphoenolpyruvate (PEP) carboxylase (e.g. 1g39167) catalyses the addition of bicarbonate (HCO_3^-) to PEP to form oxaloacetate and inorganic phosphorus. The reaction is used for carbon fixation, CO_2 and water exchange and to regulate metabolic flux through the energy-generating citric acid cycle, and thereby is important for amino acid biosynthesis (Cousins et al., 2007). B-S glucosidase activity (e.g. 1g10890) is fundamental in many biological pathways in plants, including carbohydrate metabolism, the degradation of structural polysaccharides, host-pathogen interactions and cellular signalling. The enzyme also stimulates the release of pathogen-defending compounds and activates phytohormones such as auxin (Carpita and Gibeaut, 1993; Leah *et al*., 1995).

Table 7.7 *Relationship between trait-related QTL from Zn Experiment 1 and their associated genes and gene functions in B. distachyon.*

TRAIT	LG	Contig	Bradi	Function
11(C) Final harvest tiller numbers per plant	4	11101	1g09940	Expressed protein
	7	7409	1g3330	Protein of unknown function (DUF579)
23(C) Final harvest shoot:dry weight ratio (g/g)	4	41280	1g05030	Vesicle associated membrane protein
29(C) Final harvest proportion of total Zn in shoot (%)	6	34051	3g57840	Emp24/gp25L/p24 family/GOLD family
36(C) ZnUpE(ii)	6	49898	3g44320	LITAF-domain-containing protein, putative, expressed
38(C) ZnER	6	12118	3g06930	Citrate synthase, putative, expressed
25(10%) Final harvest root Zn content (ppm)	7	32829	1g44090	Ferritin/ribonucleotide reductase-like family protein
			1g55420	Ferritin/ribonucleotide reductase-like family protein
29(10%) Final harvest proportion of Zn in shoot (%)	7	46179	1g37450	Beta galactosidase 1
			3g08180	Beta galactosidase 1

Table 7.*8* *Relationship between trait-related QTL from Pb Experiment 2 and their associated genes and gene functions in B. distachyon.*

TRAIT	LG	Contig	Bradi	Function
46(C) Cut 1 herbage (g)	7	6949	1g46650	Nucleolar GTP-binding protein
			3g32120	Unclassified
55(C) Final harvest tiller numbers per plant	3	41072	2g17290	ATP synthase alpha/beta family protein
			2g13090	ATP synthase subunit beta
			2g20977	ATP synthase subunit beta
			2g46790	ATP synthase alpha/beta family protein
	7	35555	1g39167	Phosphoenolpyruvate carboxylase 2
			3g09210	Phosphoenolpyruvate carboxylase 3
62(C) Final harvest root dry weight per pot (g)	4	38001	1g10890	B-S glucosidase 44
			1g10917	B-S glucosidase 44
			1g10930	B-S glucosidase 44
			1g10940	B-S glucosidase 44
			1g19270	B-S glucosidase 44

Table 7.8 *Continued.*

67(C) Final harvest shoot:root dry weight ratio (g/g)	7	31991	1g41797	Protein of unknown function (DUF3411)
52(10%) Cut 1 shoot Pb content per plant (µg Pb)	7	6858	1g30160	Leucine-rich receptor-like protein, kinase family protein
			1g37960	Protein kinase family protein with leucine-rich repeat domain
			1g69097	Protein kinase family protein with leucine-rich repeat domain
			3g08647	Protein kinase family protein with leucine-rich repeat domain
			3g08660	Protein kinase family protein with leucine-rich repeat domain
			3g16740	Protein kinase family protein with leucine-rich repeat domain
			3g16790	Protein kinase family protein with leucine-rich repeat domain
			3g35137	HAESA-like 1
55(10%) Final harvest tiller numbers per plant	3	41072	2g13090	ATP synthase subunit beta
			2g17290	ATP synthase alpha/beta family protein
			2g20977	ATP synthase subunit beta
			2g46790	ATP synthase alpha/beta family protein
	7	7409	1g3330	Protein of unknown function (DUF579)
58(10%) Final harvest root fresh weight per pot (g)	7	34133	1g35730	NAD(P)-binding Rossmann-fold superfamily protein
			1g35736	NAD(P)-binding Rossmann-fold superfamily protein
			1g35742	NAD(P)-binding Rossmann-fold superfamily protein
			1g47300	Cinnamoyl coa reductase 1
			3g19670	Cinnamoyl coa reductase 1
67(10%) Final harvest shoot:root dry weight ratio (g/g)	7	48323	1g38340	CBL-interacting protein kinase 12
68(10%) Final harvest shoot Pb content (ppm)	7	9430	1g35780	Pheophytinase
70(10%) Final harvest shoot Pb content per plant (µg)	7	36063	3g13250	Expressed protein
71(10%) Final harvest root Pb content per plant (µg)	4	31442	3g45600	Transmembrane 9 superfamily member, putative, expressed
			4g23990	Transmembrane 9 superfamily member, putative, expressed
			4g41270	Transmembrane 9 superfamily member, putative, expressed
79(10%) Pb productivity A	7	49880	3g55730	Signal transduction histidine kinase, hybrid type, ethylene sensor
			3g56550	Signal transduction histidine kinase, hybrid type, ethylene sensor
			3g57807	Signal transduction histidine kinase, hybrid type, ethylene sensor
48(30%) Cut 1 shoot dry weight (g)	4	9278	1g44810	GATA-type zinc finger transcription factor family protein
			1g67100	GATA-type zinc finger transcription factor family protein
56(30%) Final harvest tiller numbers per m^2	3	40640	2g00650	1-deoxy-D-xylulose 5-phosphate reductoisomerase
58(30%) Final harvest root fresh weight per pot (g)	7	51645	3g13690	RNA-binding (RRM/RBD/RNP motifs) family protein
66(30%) Final harvest total plant dry weight per plant (g)	7	41107	3g19810	Alpha-soluble NSF attachment protein 2
73(30%) Final harvest proportion of total Pb in shoot	5	41419	4g35990	Expressed protein

Leucine-rich repeat receptor kinases (LRR-RKs) (e.g. 1g301600) comprise the largest subfamily of transmembrane receptor-like kinases in plants. They regulate a wide range of defence- and development-related processes including cell proliferation and growth, abscission, hormone perception, host-specific and non-host-specific defence responses and wounding response (Li and Chory, 1997; Torri, 2004; Zan *et al*., 2013). NAD(P)-binding Rossmann-fold superfamily proteins (e.g. 1g35730) play a critical role in amino acid, carbohydrate and hormone metabolism and participate in various developmental process such as hormone biosynthesis or catabolism, as well as redox sensory mechanisms (Kavanagh *et al*., 2008; Moummou *et al*., 2012).

Cinnamoyl CoA reductase (e.g. 1g47300) catalyses the first specific committed step in the synthesis of lignin monomers and thereby provides mechanical strength and aids in water conduction through the vascular tissue of plants (Lacombe *et al*., 1997). Calcineurin B-like (CBL) proteins (1g38340) and CBL-interacting protein kinases (CIPK) mediate plant responses to a variety of external stresses, for example drought and salt tolerance, and stimulate plant development through auxin transport (Tripathi *et al*., 2009; Tai *et al*., 2016). Pheophytinase (pheophytin pheophorbide hydrolase) (1g35780) is an important component of the Chl breakdown machinery of senescent leaves and shoots (Schelbert *et al*., 2009; Cheng and Gaun, 2014). Histidine kinases (e.g. 3g55730) are involved in a range of functions including hormone (e.g. ethylene and cytokinin) signalling, osmosensing, cold perception, and the regulation of salt sensitivity and pathogen resistance (Gamble *et al*., 1998; Nongpuir *et al*., 2012). GATA-type zinc finder transcription family proteins (e.g. 1g44810) exert important biological functions in plants by interacting with RNA, DNA or chromatin, influencing plant growth and development, and controlling phytohormone response and abiotic and biotic stress responses (Li *et al*., 2013). The enzyme 1-deoxy-D-xylulose 5-phosphate reductoisomerase (2g00650) forms part of the metabolic pathway from methylerythritol phosphate to isoprenoids, the latter representing one of the oldest known organic compounds, having been identified in the 3.1 Ga Fig Tree shale deposit in South Africa (Lehninger, 1970). The emission of isoprene is used to combat various abiotic stresses (e.g. heat stress) and is also known to confer resistance to ROS (Proteau, 2004; Sharkey *et al*., 2007; Vickers et al., 2009). Alpha-soluble NSF attachment proteins (α-SNAP) (3g19810) are required for vesicle transport between the endoplasmic reticulum and the Golgi apparatus. The correct targeting of proteins to the vacuole or other organelles requires the formation of a SNAP receptor (SNARE) protein complex which delivers

its cargo protein to the target compartment, at which point dissociation of the complex requires α-SNAP (Surpin and Raikhel, 2004).

The third method that was trialled in the search for candidate genes conferring HM tolerance involved a 'reverse genetics' approach. The aforementioned in-house database was interrogated for the locations of all HM-specific genes in *B. distachyon*, which were then co-localised to contigs in the Lolium GenomeZipper database. A total of 229 HM-specific genes were identified in the Brachypodium GenomeZipper database (Appendix 7), which included members that code for ABC transporters, Nramp transporters, bZIP proteins, SOD, Cd/Zn-transporting ATPase and a wide range of non-specific metal cation transporters. These were co-localised to their corresponding contigs in the Lolium GenomeZipper database. They were found to be distributed across all linkage groups in *L. perenne*, confirming a strong polygenetic control of metal tolerance. Twenty contigs were located on LG1, 17 on LG2, 26 on LG3, 46 on LG4, 27 on LG5, 28 on LG6 and 39 on LG7. Only 26 *B. distachyon* genes did not co-localise to a contig in the Lolium GenomeZipper database. The distribution of the HM-specific genes across the seven *L. perenne* linkage groups, and their spatial relationship to the QTL identified during this research project, are shown on Figure 7.13.

Three key points have emerged from this investigation. First, without exception, all the HM-specific genes and linkage groups identified in *B. distachyon* mapped to their corresponding linkage groups in *L. perenne* (i.e. Bd1 mapped to LGs 4 and 7, Bd2 to LG3, Bd3 to LGs 6 and 7, Bd4 to LG5, and Bd5 to LG2). This once again confirms the highly conserved synteny between the *L. perenne* and *B. distachyon* genomes (e.g. Pfeifer *et al*., 2013; Figure 7.11). Second, Figure 7.13 illustrates that many HM-specific genes either occur on LGs with no identified QTL (e.g. LGs 1 and 2; Figures 7.13A and B), or are located at specific locations on LGs that have no corresponding QTL. Whilst the reasons for this are unclear, it may be attributed to the 'Beavis effect', discussed above, whereby the relatively low population sizes, particularly in Zn Experiment 1 which had only 65 and 46 surviving genotypes in the 10% and 30% Zn treatments, respectively, after 16 weeks of growth, may have resulted in a reduction in QTL detection power.

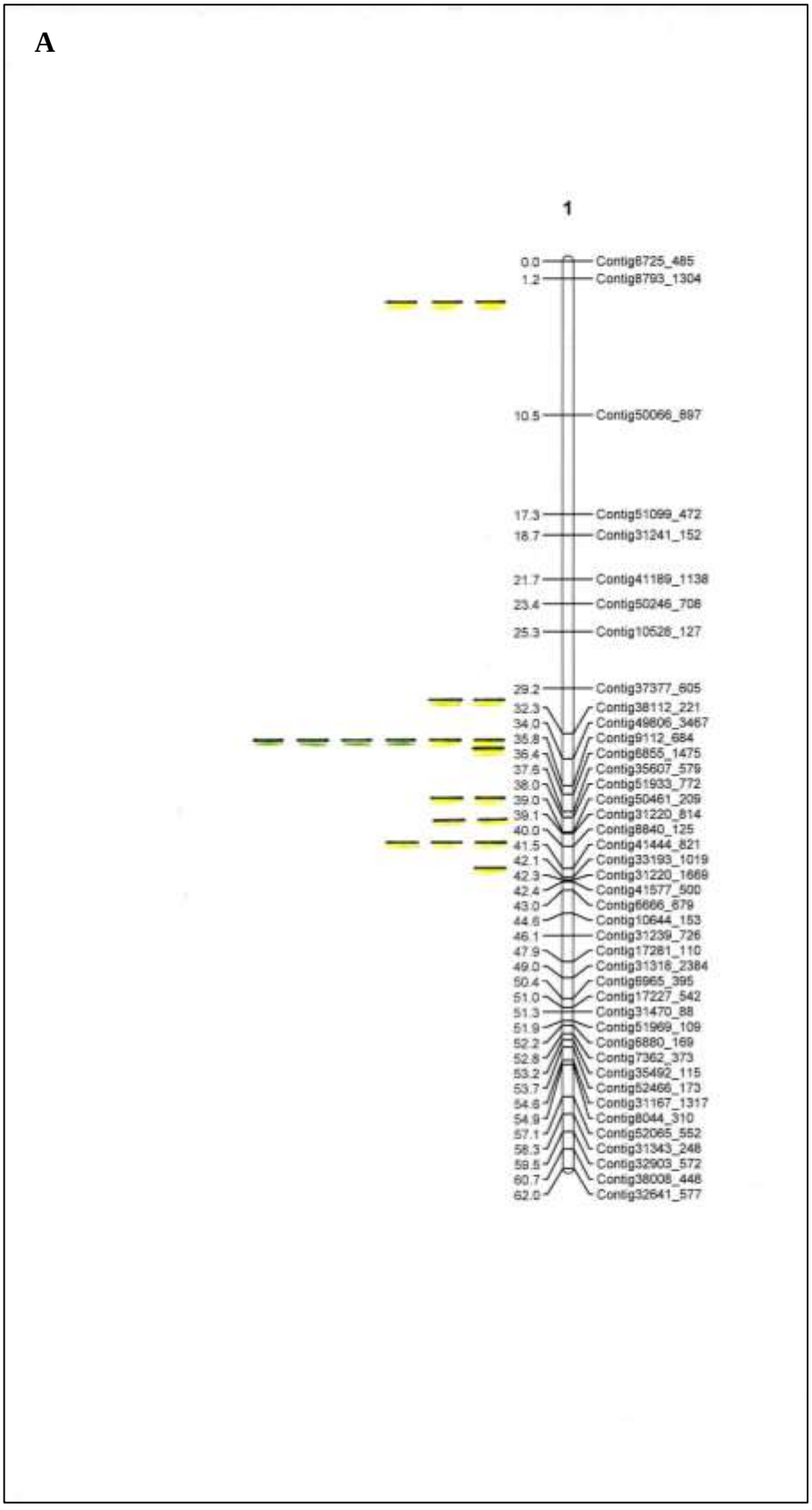

Figure 7.13 Composite genetic linkage maps, showing transposed QTL derived from Zn Experiment 1 and Pb Experiment 2 mapped to HM-specific genes identified from the Brachypodium GenomeZipper. The HM-specific genes are colour coded according to the respective Brachypodium chromosome on which they are located, as shown in Figure 7.11. Numbers refer to the *L. perenne* linkage group.

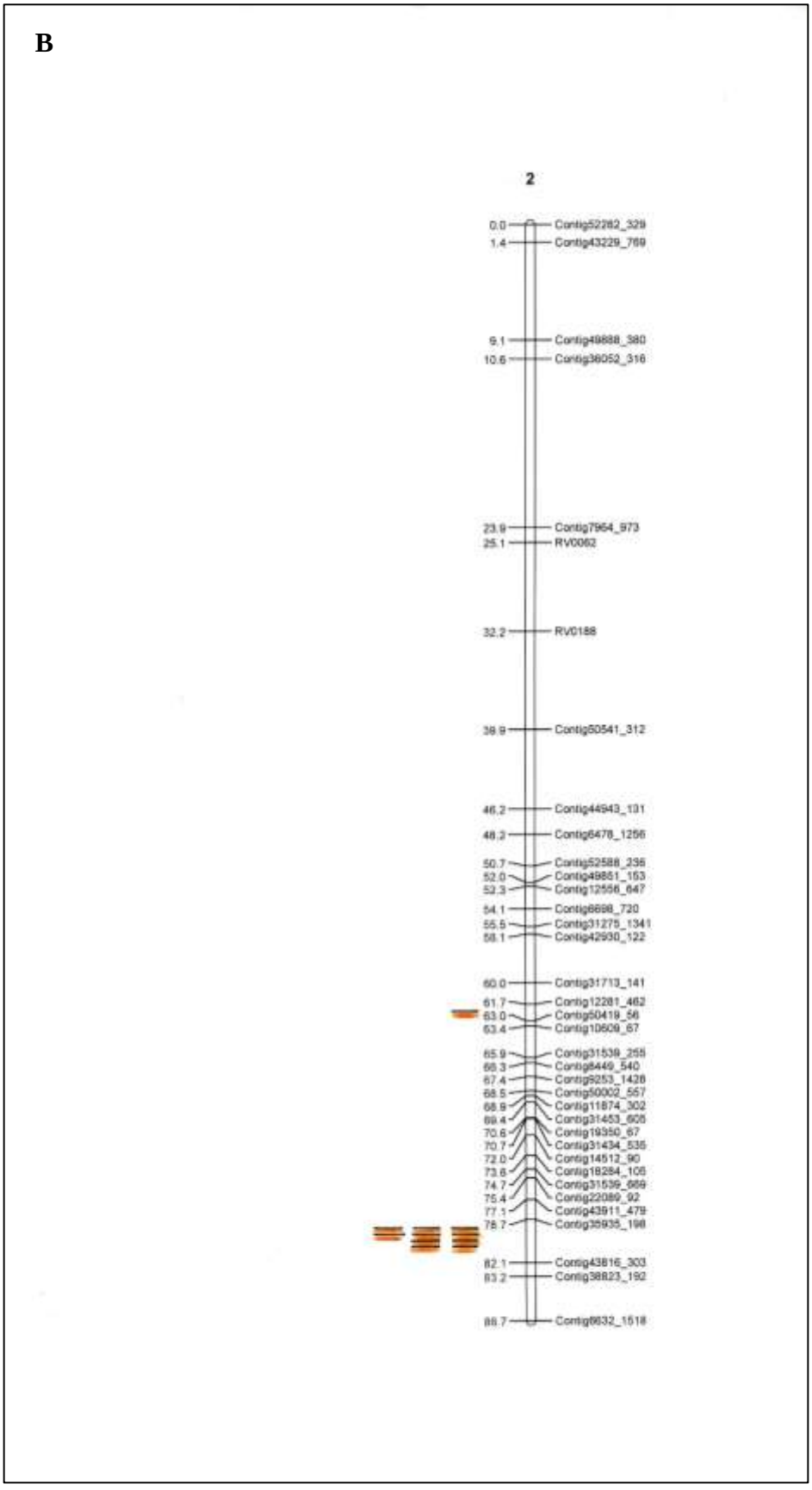

Figure 7.13 Continued.

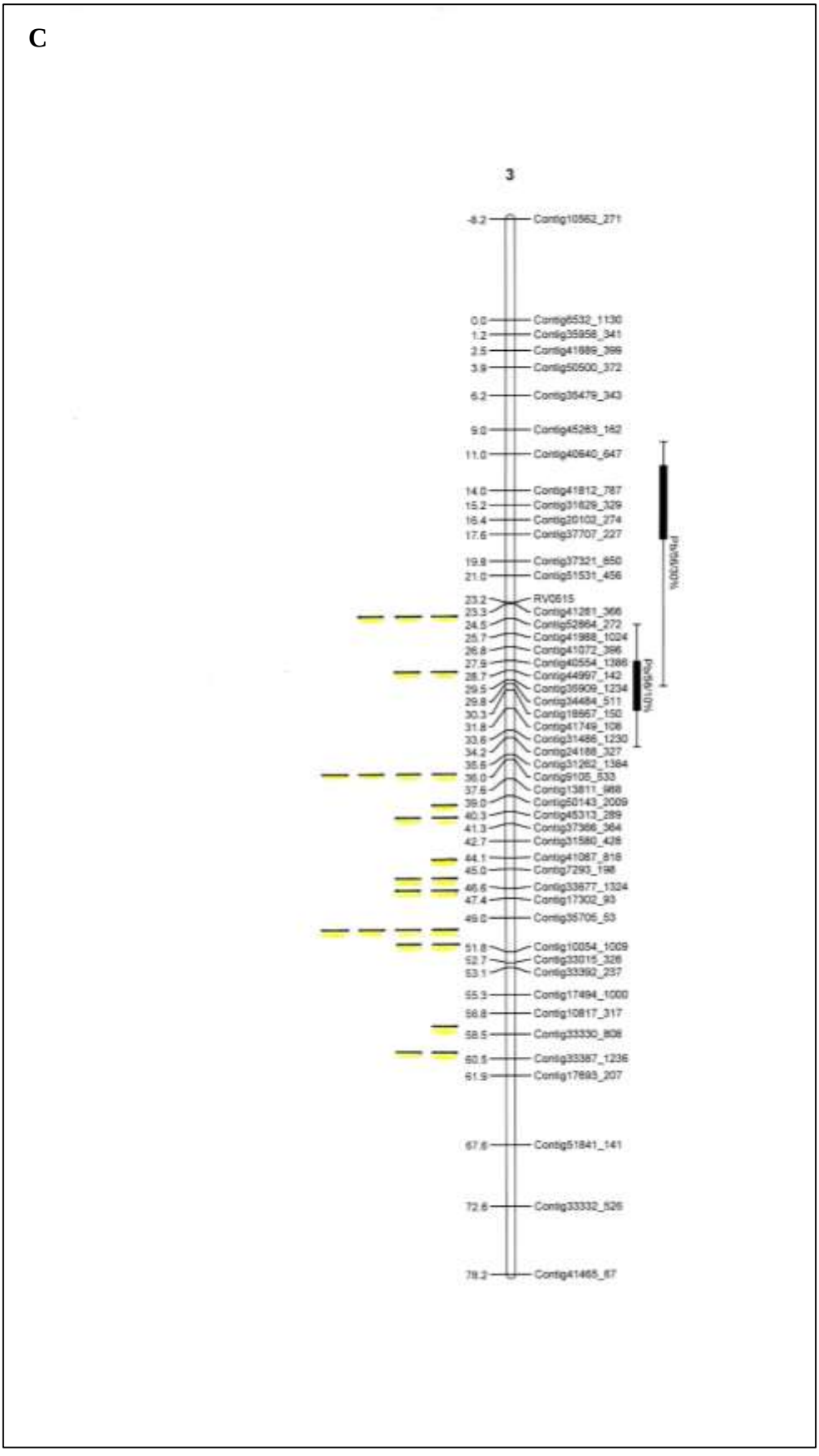

Figure 7.13 Continued.

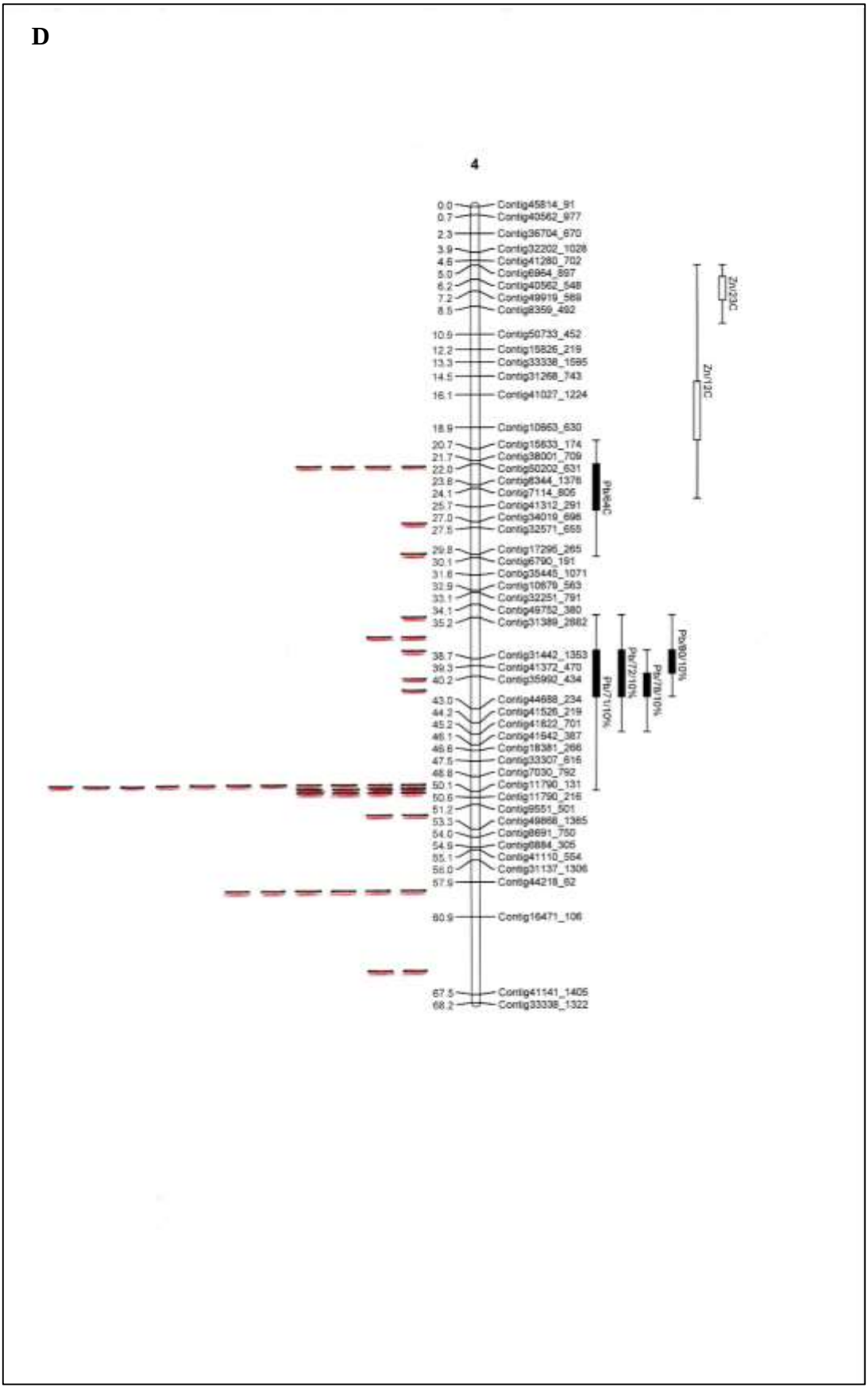

Figure 7.13 Continued.

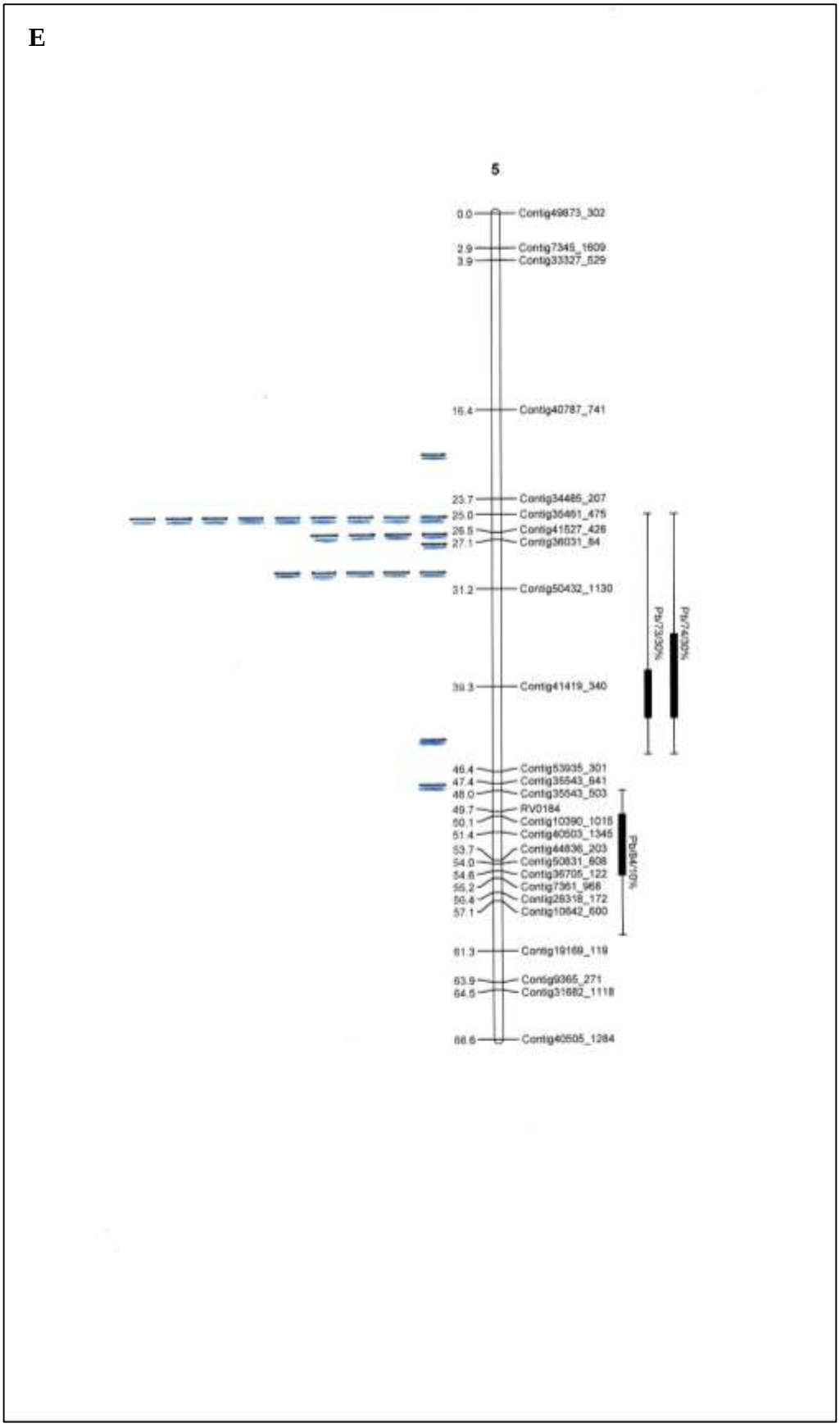

Figure 7.13 Continued.

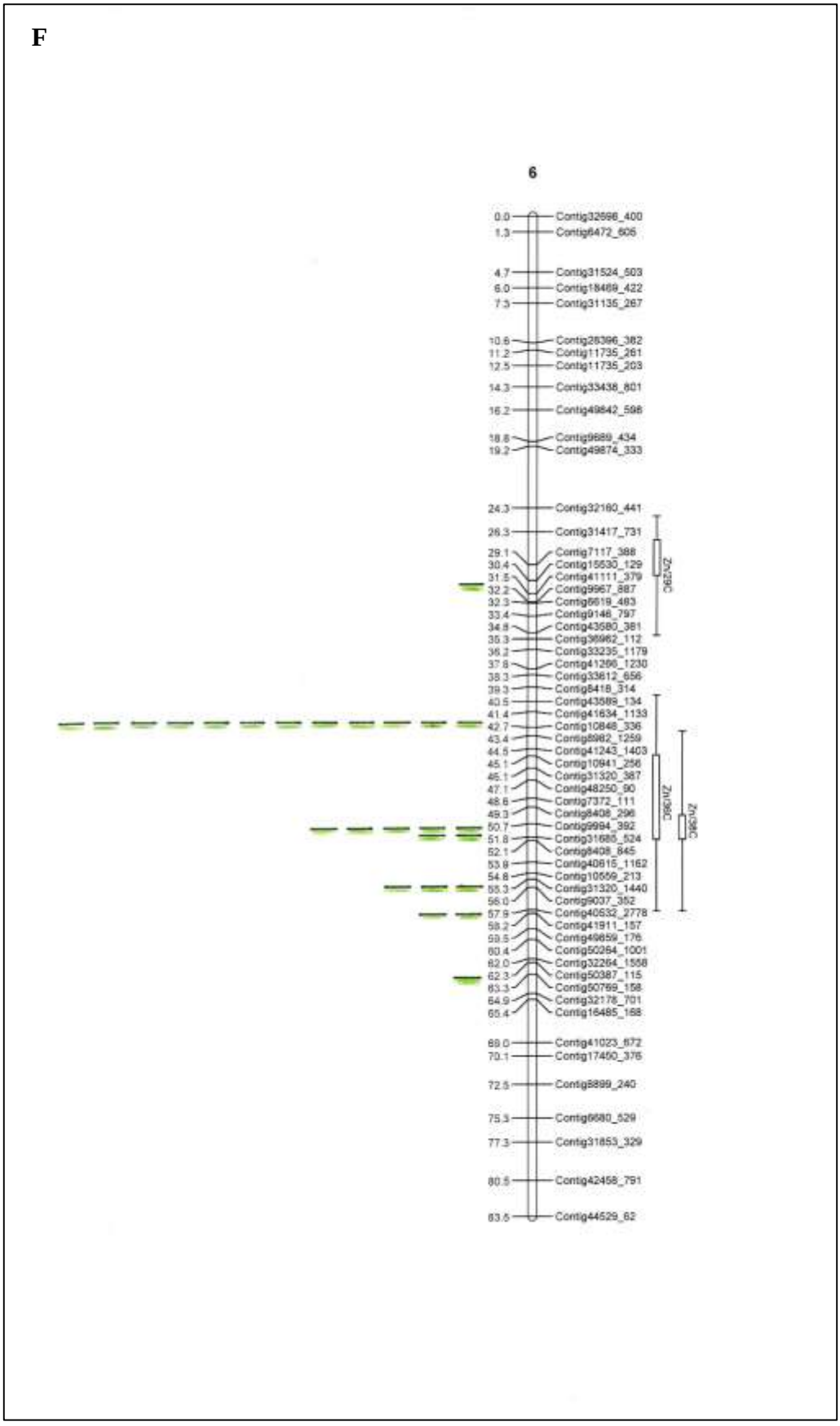

Figure 7.13 Continued.

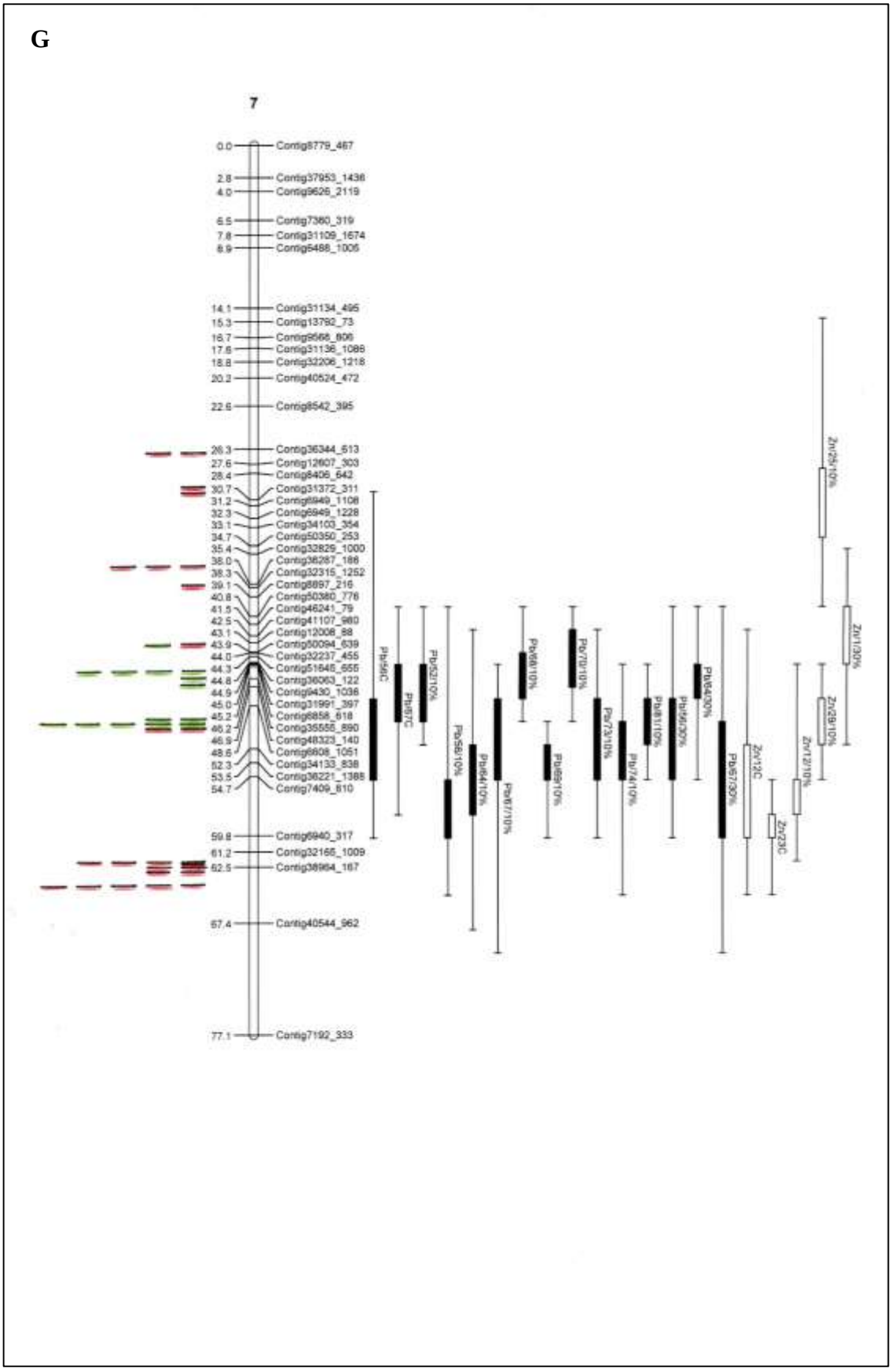

Figure 7.13 Continued.

Third, Figure 7.13 is a preliminary attempt to map HM-specific genes derived from the Brachypodium GenomeZipper to corresponding QTL identified from an analysis of the trait data gathered during Zn Experiment 1 and Pb Experiment 2. Of special note is an assemblage of HM-related genes that occur on LG7 at a genetic distance of between 26.5 – 63.3 cM (Figure 7.13G). As well as containing growth-related QTL, this region also contains many Zn and Pb uptake-related QTL, for example those for root and shoot metal content, and Pb uptake efficiency. The majority of the genes co-locate within the outer intervals of the QTL and many of these co-locate within the inner intervals, in particular between 43.5 – 46.5 cM. Similarly, a cluster of genes on LG6 co-locates to two Zn uptake-related QTL between 42.1 – 58.3 cM, whilst a single gene co-localises within the outer interval of a QTL for shoot Zn content at 30.8 cM (Figure 7.13F). On LG5, a cluster of genes co-locates within the outer intervals of two QTL for total root Pb content and total shoot Pb content at a genetic distance of between 25.3 – 28.5 cM (Figure 7.13E), whilst on LG4, a series of genes co-locates to QTL for root Pb content, total Pb content and Pb uptake efficiency (Figure 7.13D). Finally, although the majority of genes shown on LG3 have no corresponding QTL, a set of two genes co-locate to the inner interval of a QTL for tiller numbers in the 10% Pb treatment, and a further three genes co-localise to the outer interval of a QTL for tiller numbers in the 30% Pb treatment (Figure 7.13C). The results of this investigation provide evidence that many of the QTL are underlain by genes that are responsible for HM transport, and the presence of such genes on at least three LGs strongly suggests that the control of HM transport is polygenic. In addition, the co-localisation of metal transporting genes with QTL for both HM- and growth-related traits suggests a possible pleiotropic relationship.

A final point for discussion relates to the identification of HM-related QTL in other species of grass that are phylogenetically related to *L. perenne*. Although *B. distachyon* is noted as a model grass species, little work has been published on the genetic control of HM uptake and tolerance. In contrast, and as noted in Section 2.4.2, considerable work has focussed on identifying QTL for HM tolerance and uptake in Common wheat (*T. aestivum*) and rice (*O. sativa*). For example, in the case of the latter species, Norton *et al*. (2009) identified QTL for grain Zn content on Os6, 7 and 10, and for grain Pb content on Os1, 4, 6 and 12. They also identified QTL for leaf Zn content on Os 1, 2 and 6 and for leaf Pb content on Os7. Garcia-Oliveira *et al*. (2009) reported a major QTL for grain Zn content on Os8, whilst Anurahda *et al*. (2012) identified QTL for grain Fe content that were co-located with QTL for grain Zn content on Os7 and Os12. Nawaz *et al*. (2015) identified QTL for grain Zn content on Os1, 3, 8, 9 and 11, whilst Huang

et al. (2015) reported a QTL for grain Zn content on Os9 and three cases of QTL co-localisation for Pb/Cd on Os5, Zn/Pb on Os7 and Pb/Se on Os9. Based on the aforementioned close syntenic relationship between rice and perennial ryegrass (Figure 7.10), these investigations indicate the putative presence of genes conferring Pb tolerance and uptake on LGs 5 and 7, for which uptake-related QTL were identified, and also on LGs 1, 2 and 3, for which no uptake-related QTL were identified. In the case of Zn uptake, the investigations indicate the presence of uptake-related genes on LGs 4, 6 and 7, for which metal-related QTL were identified, as well as on LGs 1, 2, 3 and 5, for which no QTL were identified. Although inconclusive, these studies also suggest a strong polygenetic control of Zn and Pb tolerance and uptake. One potentially rewarding avenue for further investigation could be to utilise both the conserved syntenic and gene co-linearity relationships between perennial ryegrass and rice to establish whether there is co-localisation between the QTL identified in this study and the map positions of metal-related QTL in published research.

7.5 Genotypes for further study and strategies for plant breeding

As discussed in detail in Chapter 5, one of the principal objectives of this research project was to identify, from within the mapping family, those genotypes which had superior performance in terms of growth and/or metal uptake. Table 7.9 shows the genotypes identified in Sections 5.2.5 and 5.3 that could be taken forward for possible future breeding programmes, through either poly- or pair-crossing (see Tables 5.14 and 5.15), to produce either a Zn- or Pb- tolerant, or a Zn- and Pb-tolerant population. The table shows that the promising genotypes are a representative mix of the different phenotypes (i.e. amenity, forage or intermediate types) represented within the population (see Plate 7.3).

Table 7.9 *Recommended genotypes for further investigation, as identified in the ranking procedures described in Chapter 5 (see Tables 5.14 and 5.15), scored for their phenotype.*

Genotype	Amenity	Forage	Intermediate
4	*		
11	*		
13			*
14	*		
16		*	
19	*		
25		*	
26			*
30		*	
31		*	
33			*
37			*
38	*		
39			*
47	*		
48		*	
49		*	
53			*
56		*	
60		*	
62		*	
78			*
120			*
129	*		
157		*	
178		*	
201A	*		
Total	8	11	8

Flowering time, or heading date (defined as the first date that three emerging flower heads are visible on the plant), is relatively variable across the population. Heading date is measured by plant breeders sequentially from Day 1 being the 1st of May, Day 30 being the 30th of May, Day 31 being the 1st of June, and so on. In this population of *L. perenne*, heading dates for individual genotypes range from between ~ day 55 to ~ day 75 (Thorogood, pers comm.). This range would need consideration in order for any potential cross to be successful. For example, to reduce the range of heading dates, it would be possible to delay flowering in the early-heading forage-types by maintaining them during the spring months in temperature-controlled 'cold rooms'.

Plate 7.3 Examples of the phenotypic variation displayed by the mapping population. At the time of scoring, A) amenity-types (e.g. Genotype 201A) were not flowering, B) intermediate-types (e.g. Genotype 13) had few emerging heads, and C) forage-types (e.g. Genotype 16) were in full flower (in the example shown here, plant C had 27 flowers).

The selected genotypes could then be placed in an isolation chamber (Plate 7.4). To prevent contamination, these chambers are sealed and have automatic irrigation systems and fans which circulate filtered, pollen-free air. The plants would be maintained in isolation for ~ 2 months before the process of harvesting seed would begin. Alternatively, a pair-cross approach could be used (Plate 7.5), whereby the flowering heads of the two individual plants of interest are sealed within a breathable bag for ~ 2 months. To maximise potential seed yield from a pair-cross, the heading dates should be within a few days of each other, whereas a poly-cross can have up to fourteen days variation in heading date amongst the population. However, the closer together the heading dates, the better the chance of pollination (Lovatt, pers comm.). The intention would be ultimately to create a new, metal-tolerant variety, which could then be subjected to rigorous Distinctness, Uniformity and Stability (DUS) testing, though this would take many years of seed multiplication and field trials.

Plate 7.4 A) Isolation chambers at IBERS, and B) genotypes of Italian ryegrass (*Lolium multiflorum*) in the process of being poly-crossed. The plants are maintained in isolation houses for ~ 2 months before the process of seed harvesting commences.

Plate 7.5 Pair-crossing of genotypes of Italian ryegrass (*Lolium multiflorum*) at IBERS.

In all the examples listed in Table 7.10, the heading dates for the pair-crosses suggested are a close match, if the reserve genotype (given in parentheses) is considered in order to obtain the closest flowering times and therefore the best chance of seed production. A similar approach can be adopted with regards to the genotypes selected 'in-common', for Zn and Pb, based on

Table 7.10 *Recommended genotypes for establishing Zn- and Pb-tolerant and high uptake breeding populations using poly- or pair-crossing approaches, based on the ranking of genotypes for high performance in the two experiments detailed in Chapter 5 (Table 5.14). Numbers listed in parenthesis are reserve genotypes. The corresponding heading date for each genotype is shown in the adjacent column.*

	Moderate Zn (10% Zn tailings)	**Heading date**	**Acute Zn** (30% Zn tailings)	**Heading date**	**Moderate Pb** (10% Pb tailings)	**Heading date**	**Acute Pb** (30%Pb tailings)	**Heading date**
Tolerance (Total plant dry weight)	14, 16 (13)	**70, 62 (64)**	31, 56 (13)	**61, 64 (64)**	14, 201A (30, 129)	**71, 75 (70, 71)**	11, 129 (14, 30, 201A)	**71, 71 (71, 71, 75)**
Above ground accumulation (shoot Zn/Pb content)	16, 25 (56)	**62, 62 (64)**	48, 56 (31)	**64, 64 (61)**	157, 201A	**70, 75**	38, 157 (30)	**66, 70 (71)**
Below ground accumulation (root Zn/Pb content)	14, 201A (16)	**71, 75 (62)**	31, 56 (14)	**61, 64 (71)**	4, 39 (30, 201A)	**63, 62 (71, 75)**	30, 39 (4)	**71, 62 (63)**
Site stabilisation (tiller number)	13, 78 (14, 16)	**64, 67 (71, 62)**	13, 49 (14, 31)	**64, 63 (71, 61)**	53, 60 (26)	**70, 63 (57)**	33, 62 (30)	**67, 59 (71)**

their growth and metal uptake attributes (Table 7.11). In all cases, two of the three suggested genotypes have heading dates within a few days of each other. Hence, selection for pair-crossing would be based on consideration of these dates. With the exception of Genotypes 26 and 178, both with heading dates of Day 57, the suggested genotypes for generating seed *via* a poly-cross all have heading dates which lie within the 14 day 'optimum' range.

Table 7.11 *Genotypes selected for future plant breeding purposes, based on their growth and metal-uptake attributes for both Zn and Pb combined, as detailed in Chapter 5 (Table 5.15), with corresponding heading dates for each genotype shown in the adjacent column.*

Phenotype	**Moderate Zn/Pb** (10% Zn/Pb tailings)		**Acute Zn/Pb** (30% mine tailings)	
	Genotypes selected	**Heading dates**	**Genotypes selected**	**Heading dates**
Tolerance (shoot dry weight)	14, 120, 178	**71, 63, 57**	37, 48, 157	**66, 64, 70**
(root dry weight)	4, 14, 201A	**63, 71, 75**	31, 47, 56	**61, 66, 64**
(total plant dry weight)	4, 30, 201A	**63, 71, 75**	31, 48, 56	**61, 64, 64**
Above ground accumulation (shoot Zn/Pb content)	37, 157, 201A	**66, 70, 75**	4, 31, 157	**63, 61, 70**
Below ground accumulation (root Zn/Pb content)	4, 39, 201A	**63, 62, 75**	4, 14, 30	**63, 71, 71**
Site stabilisation (tiller number)	13, 19, 78	**64, 68, 67**	4, 13, 49	**63, 64, 63**

L. perenne (variety unspecified) has recently been used with success in experimental mine remediation studies (e.g. Hutchings and Leij, 2016), in which seeds were sown into pots of Zn- and Pb-contaminated mine tailings (Zn ~ 1,900 ppm and Pb ~ 18,500 ppm) mixed with a biochar amendment, and with growth measured after 4 weeks. In all cases, the plants with the greatest biomass were those grown with the soil amendment added (Plate 7.6), with the most dramatic improvement in performance being noted in root growth and density. Given the specific criteria for Zn and Pb tolerance in the current project, it would be informative to test whether the performance of genotypes selected in this study is enhanced by the addition of this soil amendment. This could form part of a breeding program to develop high-performing, metal-tolerant varieties. With their enhanced growth and tolerance, these plants would have an

increased site stabilisation potential and, in combination with a biochar soil amendment, could be field trialled at selected mines in the CWO.

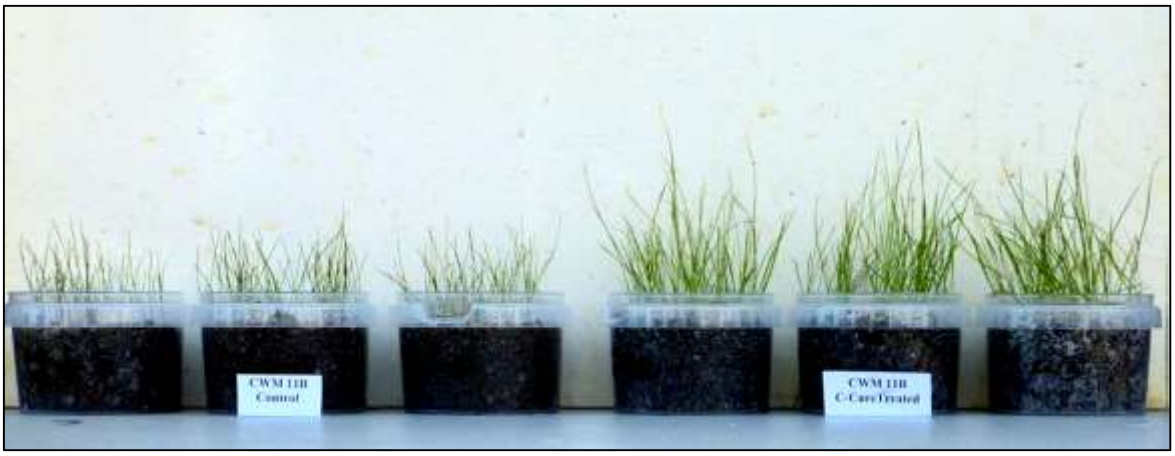

Plate 7.6 *L. perenne* after 27 days growth in containers filled with untreated Pb- and Zn-rich tailings (control – 3 pots on the left) and tailings with biochar amendment (3 pots on the right). From Hutchings and Leij. (2016).

7.6 Agronomic considerations

As discussed in Section 7.2.3 there was wide variation in genotype performance for uptake-related traits in Zn Experiment 1. In particular, shoot metal content ranged between 270 – 8,292 µg/plant in the 10% treatment, with a mean of 2,622 µg/plant, and between 313 – 9,654 µg/plant in the 30% treatment, with a mean of 3,083 µg/plant (Table 7.4). Maximum root metal content was typically much higher, ranging between 664 – 29,334 µg/plant in the 10% treatment, with a mean of 8,887 µg/plant, and between 318 – 16,305 µg/plant in the 30% treatment, with a mean of 5,319 µg/plant. Given the substrate Zn concentrations of 3,000 µg g^{-1} in the 'moderate' 10% treatment and 9,000 µg g^{-1} in the 'acute' 30% treatment, the results of this experiment suggest that *L. perenne* may be categorised within the 'tolerant metal indicator' class of plants with respect to Zn (Baker and Walker, 1990).

Although there was also wide variation in genotype performance for uptake-related traits in Pb Experiment 2, the Pb accumulated in the shoots and roots was generally much lower than the Zn accumulation observed in the Zn experiment. Hence, shoot Pb content ranged between 14 – 95 µg/plant in the 10% treatment, with a mean of 50 µg/plant, and between 76 – 263 µg/plant in the 30% treatment, with a mean of 139 µg/plant (Table 7.6). The Pb content of the roots was always much higher compared with the shoots, ranging between 191 – 750 µg/plant in the 10% treatment, with a mean of 366 µg/plant, and between 787 – 5,010 µg/plant in the 30% treatment, with a mean of 1,910 µg/plant. In view of the substrate Pb concentrations of 1,690 µg g^{-1} in the

'moderate' 10% treatment and 5,070 µg g^{-1} in the 'acute' 30% treatment, the results of this experiment suggest that *L. perenne* may be categorised within the 'tolerant metal excluder' class of plants with respect to Pb (Baker and Walker, 1990).

The consequences of such high levels of metal content for sustainable forage production by *L. perenne* on contaminated sites are difficult to assess. This is partly because data on deficiency and toxicity levels of HMs in perennial forage species are relatively scarce (Gupta *et al.*, 2001), particularly under field conditions. Furthermore, quoted critical tissue concentrations may depend on factors such as analytical technique, duration of exposure, plant growth stage and the presence or absence of other heavy metal species in the substrate. Chapman (1966) summarised the Zn content of plant leaves as deficient (< 20 – 25 ppm in dry matter), sufficient but not excessive (25 – 150 ppm) and excessive (> 400 ppm). According to Mayland *et al.* (2007), Zn levels in pasture plants range from 10 – 70 mg kg^{-1}, most commonly between 10-30 mg kg^{-1}; cattle grazing forage containing 15 – 20 mg Zn kg^{-1} made greater live weight gains when supplementary Zn was added to their diet. The uncertainty extends to the long-term agronomic effects of high Pb levels on forage productivity (e.g. Gough *et al.*, 1979), although lead poisoning of horses and cattle following ingestion of forage containing high levels of Pb has been documented in several countries (e.g. Foulds *et al*., 2014). Relatively speaking, Zn is less toxic to grazing animals compared with Pb, although toxicity resulting from intake of high Zn feed has also been demonstrated (see Gough *et al.*, 1979). If either grazing, hay or silage production is to be developed as part of a contaminated site management plan, the most suitable *L. perenne* genotypes for evaluating will be those showing high tolerance to Zn/Pb in combination with the lowest accumulation of these metals in the shoot.

This research, as well as other published studies of metal tolerance in *L. perenne*, have confirmed that the species is highly suited for the phytostabilisation of Zn and Pb contaminated substrates. It is therefore informative to 'scale-up' the experimental data to assess the quantitative implications of field-based phytoremediation applications. It should be noted that the derived values are based on the results of short-term experiments of 16 weeks duration, representing approximately half the annual growing season. Using the average quantities of Zn and Pb absorbed 'per pot' across the 77 mapping family genotypes, it is possible to roughly estimate the quantities accumulated per hectare by a perennial ryegrass sward (Table 7.12). The estimates for Zn stored in root and shoot compartments are, respectively, 16.5 kg ha^{-1} and 4.7 kg ha^{-1}, for a Zn concentration of 3,000 µg g^{-1} in the substrate (10% treatment). Interestingly, the corresponding values for the 30% treatment (9,000 µg Zn g^{-1} in the substrate) are

substantially lower, at 6.4 kg ha^{-1} and 3.66 kg ha^{-1}, respectively, in root and shoot. In contrast, storage of Pb in the sward increases with increasing substrate concentration of HM. The quantities of Pb accumulated in root and shoot tissues are estimated to be 1 kg ha^{-1} and 0.14 kg ha^{-1}, respectively, for a substrate concentration of 1,690 µg Pb g^{-1}; increasing to 5.3 kg ha^{-1} and 0.4 kg ha^{-1}, respectively, for a substrate concentration of 5,070 µg Pb g^{-1}.

Table 7.12 *Estimated quantities of Zn and Pb potentially stored in the shoot and root compartments of perennial ryegrass swards grown in mine tailings mixed with sand over 16 weeks. Values are the mean of ≤ 77 genotypes and are expressed as kg* ha^{-1}.

Treatment	Zn (kg ha^{-1})		Pb (kg ha^{-1})	
	Shoot	Root	Shoot	Root
Control	0.14	0.18	-	-
10%	4.72	16.5	0.14	1.02
30%	3.66	6.40	0.39	5.35

Similar estimates were based on the results for the top three genotypes in terms of accumulation of Zn/Pb in the shoots and roots (Table 7.13). With respect to the accumulation of Zn in the shoot, Genotype 201A showed a two-fold increase over the mean genotype value in the 10% treatment, whilst Genotype 23 showed almost a three-fold increase over the mean value in the 30% treatment. In terms of Pb accumulated in the shoot, Genotype 201A also showed a near two-fold increase over the mean value in the 10% treatment, whilst Genotype 13 showed a near two-fold increase over the mean value in the 30% treatment.

Table 7.13 *The top three genotypes for shoot and root accumulation in the 10% and 30% tailings treatments for Zn and Pb, or, 'maximum-efficiency genotypes'.*

	Zn				Pb			
	Shoot		Root		Shoot		Root	
Treatment	**Genotype**	**kg ha^{-1}**	**Genotype**	**kg ha^{-1}**	**Genotype**	**kg ha^{-1}**	**Genotype**	**kg ha^{-1}**
10%	201A	9.2	14	83.0	201A	0.26	39	2.1
	20	9.1	201A	48.9	157	0.23	4	1.8
	14	8.7	4	40.9	3	0.21	201A	1.7
30%	23	9.7	60	21.4	38	0.67	30	14.2
	48	9.5	51	20.2	157	0.62	39	10.3
	60	7.9	57	16.7	66	0.58	4	9.6

It is also informative to consider the phytostabilisation efficiency of *L. perenne*. For example, assuming an 'acute' substrate Zn concentration of ~ 10,000 ppm, a tailings density of ~ 2.5 g cm^{-3}, and a tailings depth of 1 m, the total amount of stabilised Zn could equate to 250 t ha^{-1}. In the case of an 'acute' substrate Pb concentration of ~ 6,000 ppm, a tailings density of ~ 2.5 g cm^{-3} and a tailings depth of 1 m, the total amount of stabilised Pb could equate to 150 t ha^{-1}.

7.7 Summary

- Digestion Test Method 9, adapted from Husted *et al*. (2004), facilitated both a high level of analytical accuracy and reproducibility, as well as providing a potential time saving of over 60 weeks across the duration of this research project.
- Zinc is in the class of essential plant nutrients that sustain growth and metabolism, but becomes highly phytotoxic at high concentrations. Although there was little variation in mean tiller production across the three Zn treatments, mean growth parameters reduced exponentially with increasing Zn substrate concentrations. All genotypes showed a higher TI_{Zn} in the 30% Zn treatment than in the 10% Zn treatment, with four genotypes having a $TI_{Zn} \geq 1$. Results indicate that many of the mapping family genotypes can be categorised in the 'tolerant Zn indicator' class of plants.
- Pb is in the non-essential class of HMs and is very harmful to plants. Although there was very little variation in mean tiller production across the three Pb treatments, there was a marked linear increase in mean growth parameters with increasing Pb substrate concentrations. Root tissue Pb concentrations were much higher than in the shoots indicating only limited metal translocation, the latter being confirmed by very low TIs in both Pb treatments. Data indicate that *L. perenne* can be categorised in the 'tolerant Pb excluder' class of plants.
- Based on parameters such as survival, growth, metal uptake and translocation, significant differences in performance were observed between the two pot experiments. These variations in performance probably reflect the 'essential micronutrient' status of Zn and the non-essential/toxic nature of Pb. Higher Pb substrate concentrations, possibly up to 50% by weight of tailings, or a longer exposure time at 30% Pb concentrations, may have elicited a deleterious response, whilst lower Zn substrate concentrations, possibly of only 5% by weight of tailings, may have yielded 100% survival amongst the genotypes. An increase in survival rates in Zn Experiment 1 would have enhanced QTL detection.

- Plants require several other essential micronutrient HM species, including Cu, Mn and Fe, all of which have been extensively exploited in Wales and now pose a local contamination issue. The success of the two pot experiments suggests that the *L. perenne* mapping family may provide a suitable platform for further investigations into their phytostabilisation potential both for essential micronutrient HMs as well as for non-essential/toxic HM species such as Cr, Hg and Cd.
- A close synteny and macro-colinearity exists between *L. perenne* and *B. distachyon*. This facilitated a 'forward genetics' approach that utilised an in-house Lolium genome zipper database to match identified QTL with their corresponding genes, of known function, in *B. distachyon*. Although no HM-specific genes were identified, some have been shown to play a role in stress defence systems.
- A 'reverse genetics' approach attempted to co-localise HM-specific genes in *B. distachyon* to contigs in the Lolium genome zipper database. Genes, often closely spaced, were identified on LGs 3, 4, 5, 6 and 7 in regions that co-locate within the intervals of identified QTL for HM transport and/or growth. Data suggest both polygenic and pleiotropic relationships.
- Genotypes have been identified from a ranking analysis which, through either poly- or pair-crossing produce either Zn- or Pb-tolerant populations as well as Zn- and Pb-tolerant populations.
- From an agronomic standpoint, if either grazing or silage/hay production is developed as part of contaminated site management plan, then the most suitable genotypes will be those with a Zn and/or Pb tolerance combined with the lowest TIs. Data confirm the phytostabilisation potential of many genotypes in the *L. perenne* mapping family, and analysis indicates their potential to stabilise 250 t Zn ha^{-1} and 150 t Pb ha^{-1} at 'acute' HM concentrations.

CHAPTER 8

CONCLUSIONS AND RECOMMENDATIONS

8.1 Context

The aim of this study was to characterise the tolerance of perennial ryegrass (*L. perenne*) to high levels of Zn and Pb using a morphologically diverse mapping family, and to identify associated QTL, potential candidate genes and elite genotypes for use in selective breeding for enhanced tolerance to HMs and phytoremediatory applications.

The anthropogenic exploitation of metals has resulted in widespread HM contamination on all continents, with the exception of Antarctica, and an associated decline in ecosystem health and resilience. In the CWO, one of many mining districts in the British Isles and the source of material used in this project, the extraction and processing of Pb-, Zn-, and Cu-rich ores, which reached a zenith during the 19th Century, has caused widespread HM contamination. Acid mine drainage, tailings and spoil all act as point sources of HM emission that has led to contamination of watercourses, including main rivers and their tributaries, and to long-term HM residency in agriculturally valuable land on adjacent floodplains. These environmental impacts have focussed attention on the urgent need for mine remediation programmes throughout the CWO.

Phytoremediation of contaminated areas is a technique which utilises plants that are adapted to growing on HM-rich substrates through the development, at a biomolecular and genetic level, of either avoidance or tolerance strategies. The use of such plants offers a very low cost alternative to other high cost, heavy engineering-based remedial methods.

Perennial ryegrass is not only an important agricultural crop in temperate latitudes, but is also a recognised phytostabilising species, possessing certain key attributes including: 1) a high metal tolerance; 2) a dense rooting system; 3) a high growth rate enabling rapid ground surface coverage; and 4) a very low translocation index, minimising the potential for HMs to enter the food chain through livestock grazing. Collectively, these attributes substantially enhance the potential value of perennial ryegrass for the bioremediation of HM contaminated soils.

Much of the experimental work in this study was concerned with the measurement of traits associated with growth, metal uptake and partitioning across 77 genotypes belonging to an amenity x forage type mapping family that were grown on substrates contaminated with different concentrations of either Zn or Pb. This involved sourcing dominantly monometallic

Zn- or Pb-rich tailings from mines in the CWO. A monometallic composition was desirable to avoid any potential inter-metal synergistic or antagonistic effects, although this could not be fully achieved in practice, given the HM impurities inherent in mine tailings. Zn-rich tailings, with a concentration of ~ 30,500 µg Zn g^{-1} and a $^{Zn}B_A$ of ~ 18,900 µg g^{-1}, were provenanced from Castell Mine, whilst Pb-rich tailings, with a concentration of 18,900 µg Pb g^{-1} and a $^{Pb}B_A$ of ~ 4,450 µg g^{-1}, were provenanced from Darren Mine. Two pot-based experiments, carried out in successive years, used sand as the growing medium in the control treatment, together with two metal treatments which used mixtures of sand and Zn- and Pb-rich tailings to generate concentrations of 10% (~ 3,000 µg Zn g^{-1} and ~ 1,890 µg Pb g^{-1}) and 30% (~ 9,000 µg Zn g^{-1} and ~ 5,070 µg Pb g^{-1}) by weight. A Cut 1 shoot harvest was undertaken after 8 weeks of growth and a final destructive harvest was carried out after 16 weeks of growth.

Approximately 2,900 herbage samples were generated during the two pot experiments, all of which required milling and acid digestion prior to HM analysis by AAS. In view of various constraints, a digestion method was required that was both accurate and time-efficient to process these samples. Eleven different digestion methods were trialled, leading to the development of a new method, that not only yielded excellent levels of recovery and analytical accuracy, but that produced an estimated time saving of over 60 weeks relative to the standard method available within the hosting department (DGES method).

8.2. Summary of metal tolerance

8.2.1. Zinc tolerance

Mortality rates in Zn Experiment 1 amongst the 77 genotypes were 15% and 40%, respectively, in the 10% and 30% Zn treatments. This suggests that substrate Zn concentrations were above critical toxicity thresholds for some, but not all, genotypes. Symptoms of Zn toxicity varied widely in severity across the mapping family, with morphological effects such as chlorosis and wilting observed at a very early stage in the experiment. Tolerance indices, based on growth parameters, were consistently < 1. This was also observed in the supra-optimal Zn experiment conducted in FSC. Mean dry matter production declined exponentially as Zn substrate concentration increased, and this reduction was particularly severe in respect of root dry weight, confirming the adverse impact of high Zn concentrations on root development. Concentrations of Zn in shoot and root tissues varied widely across the genotypes. Zinc content of the shoot in the 10% treatment ranged between ~ 300 – 8,000 µg/plant across the population, with a mean value of ~ 2,600 µg/plant. In the 30% treatment, values for Zn content of the shoot ranged

between ~ 300 – 9,000 µg/plant, with a mean value of ~ 3,000 µg/plant. Zinc contents in the root tissue were also highly variable, such that in the 10% treatment, Zn content ranged between ~ 700 – 30,000 µg/plant, with a mean value of ~ 9,000 µg/plant, whilst in the 30% treatment, Zn content ranged between ~ 300 – 16,000 µg/plant, with a mean value of ~ 5,000 µg/plant. Taken as a whole, the results indicated that many genotypes in the mapping family fall within the 'tolerant Zn-indicator class' of plants, confirming their potential for being used in phytostabilisation programmes.

8.2.2. Lead tolerance

All 77 genotypes survived for the full treatment period of 16 weeks in Pb Experiment 2, with no visible signs of Pb toxicity in either the 10% or 30% Pb treatments. This suggests that substrate $^{Pb}B_A$ concentrations were at sub-critical levels. Tolerance indices, based on growth parameters, were > 1 for the majority of genotypes in both Pb treatments. Mean shoot, root, whole plant dry matter production and tillering increased linearly as Pb concentrations increased. Lead content of the shoot in the 10% treatment ranged between ~ 15 – 90 µg/plant, with a mean value of ~ 50 µg/plant, which increased in the 30% treatment to ~ 80 – 250 µg/plant, with a mean value of ~ 140 µg/plant. Lead content in the roots in the 10% treatment ranged between ~ 200 – 750 µg/plant, with a mean value of ~ 360 µg/plant, and this range increased in the 30% treatment to ~ 800 – 5,000 µg/plant, with a mean value of ~ 2,000 µg/plant. Although concentrations of Pb in shoot and root tissue varied widely across the genotypes, TI_{Pb} were consistently << 1, with over 80% of the total Pb content of the plant being stored in the roots. This suggests that these genotypes can be categorised within the 'tolerant Pb-excluder' class of plants, thereby confirming their potential use for the phytostabilisation of contaminated soils.

8.3 Genetic basis of metal tolerance

8.3.1 QTL for Zn and Pb tolerance

Each pot experiment generated 43 data sets of trait values for the 77 mapping family genotypes, in each of the three treatments (control, 10% and 30%). These data sets were subjected to a stringent QTL analysis comprising three components, namely a standard Kruskal-Wallis test statistic, interval mapping and a permutation test. Twenty-two significant QTL were identified from the data sets in Pb Experiment 2. A dense cluster of 15 growth- and metal uptake-related QTL were identified on LG7, many with overlapping inner intervals, whilst a cluster of 4

overlapping uptake-related QTL were identified on LG4, and two overlapping uptake-related QTL were identified on LG5.

Fewer QTL, 10 in total, were identified from the data sets in Zn Experiment 1, probably due to the high genotype mortality observed in this experiment and the associated 'Beavis effect'. Nevertheless, a cluster of 6 growth- and uptake-related QTL were identified on LG7, some with overlapping inner intervals, and 3 uptake-related QTL on LG6.

The QTL identified in this study showed little correlation with those identified from trait data generated by short-term screens, of 28 days' duration, for growth under supra-optimal Zn or toxic Pb supplies in FSC. Interestingly, however, QTL for Traits Zn/12C, Pb/55/10%, and Pb/56/10% (tiller numbers) from the pot experiments were coincident, at map location 54.718 cM on LG7, with the QTL for Trait 148 (tiller numbers) from the FSC supra-optimal Zn treatment. The QTL identified in this study suggest the presence of tolerance-conferring genes on LG4 and, in particular, on LG7.

8.3.2 Underlying candidate genes for HM tolerance

A 'forward genetics' approach was used in an effort to identify candidate genes underlying the QTL. This approach involved mapping the QTL *via* their contig numbers to their corresponding contigs and underlying genes, of known function, in Brachypodium. This approach confirmed the close synteny between *L. perenne* and *B. distachyon* and suggests that some underlying genes may play a role in the stress defence system. A 'reverse genetics' approach was based on identifying 229 HM-specific genes in the Brachypodium GenomeZipper database and relating them back to their inferred position on the *L. perenne* LG maps. This approach also confirmed a highly conserved synteny and suggests that many of the QTL discovered in this project may be underlain by genes that are responsible for HM transport. The presence of these genes on at least three LGs indicates that HM transport is polygenic, whilst the co-localisation of candidate metal transporting genes with QTL for both HM- and growth-related traits suggests a possible pleiotropic relationship. Further investigations, based on the close synteny between *O. sativa* and *L. perenne*, may provide further insights into the presence of underlying candidate genes.

8.4 Experiment limitations

The two experiments carried during this study generated a large volume of growth-, metal-uptake and QTL data, that collectively represent a significant contribution to existing published material specifically relating to *L. perenne*. However, the high mortality in the Zn treatments

and the contrasting low levels of toxic stress observed in the Pb treatments indicate that different substrate HM concentrations and/or different experiment durations might have been appropriate. In the case of the Zn experiment, the 10% Zn treatment is viewed as a critical concentration and suggests that a 5% treatment may have yielded 100% survival, allowing for higher resolution of growth and metal uptake parameters as well as an increase in QTL detection. In the case of the Pb experiment, a higher substrate metal concentration, possibly up to 50% by weight of tailings, or a longer experiment duration in the 10% and 30% treatments, may have induced a toxicological effect. Finally, although the use of a greater number of *L. perenne* genotypes may have resulted in a higher rate of QTL detection, the 77 genotypes used in the study represented a maximum number in terms of, for example, experiment feasibility, sample processing capability and analysis.

8.5 Selective breeding for HM tolerance

Genotype performance in the two pot experiments were ranked for 10 representative growth-related, uptake-related and metal utilisation efficiency traits. This enabled an elite group of genotypes to be identified. These will form the basis of site-stabilising Zn- and/or Pb-tolerant breeding populations. Ranking on the basis of performance in the short-term screens in FSC showed only limited similarity with the ranking order derived from the pot experiments. The highly ranked genotypes identified in the two pot experiments will be used in further poly- or pair-crossing breeding approaches to develop experimental breeding populations exhibiting high metal-tolerance. Subject to further trialling, these populations could ultimately form a basis for the implementation of full-scale, field-based phytostabilisation programmes.

Finally, whilst Zn and Pb are categorised, respectively, as an essential metal micronutrient and a non-essential/toxic metal, several other HMs in both classes (e.g. Cu, Mn, Fe, Cd) are highly toxic to plants at even quite low substrate concentrations. Many sites of former and currently active mineral exploitation occur in the temperate zones of both hemispheres. It is in these latter areas, such as the UK, mainland Europe, Asia, N. Africa, N. and S. America, Australia and New Zealand that *L. perenne* now flourishes. The results of this Zn- and Pb-based study have confirmed the phytostabilisation potential of *L. perenne* in general, and strongly suggest that the amenity x forage mapping family of *L. perenne* would provide a suitable platform for investigating the potential use of this plant in the bioremediation of sites contaminated with other HM species.

BIBLIOGRAPHY

ABBERTON, M.T., MARSHALL, A.H., HUMPHREYS, M.W., MACDUFF, J.H., COLLINS, R.P. & MARLEY, C.L. 2008. Genetic improvement of forage species to reduce the environmental impact of temperate livestock grazing. *Advances in Agronomy*, **98**, 311-355.

ABUMAIZAR, R.J. & SMITH, E.H. 1999. Heavy metal contaminant removal by soil washing. *Journal of Hazardous Materials*, **70**, 71-86.

AHMAD, M.S. & ASHRAF, M. 2011. Essential roles and hazardous effects of nickel in plants. *Reviews of Environmental Contamination and Toxicology*, **214**, 125-167.

AJAZ HAJA MOHIDEENA, R., THIRUMALAI ARASUC, V., NARAYANANB, K.R. & ZAHIR HUSSAIND, M.I. 2010. Bioremediation of heavy metal contaminated soil by the exigobacterium and accumulation of Cd, Ni, Zn and Cu from soil environment. *International Journal of Biological Technology*, **1**, 94-101.

ALLAWAY, W.H. 1968. Agronomic control over the environmental cycling of trace elements. *Advances in Agronomy*, **20**, 235-274.

ALPASLAN, B. & YUKSELEN, M.A. 2002. Remediation of lead contaminated soils by stabilization/solidification. *Water, Air and Soil Pollution*, **133**, 253-263.

ALSCHER, R.G., DONAHUE, J.L. & CRAMER, C.L. 1997. Reactive oxygen species and antioxidants: relationships in green cells. *Physiologia Plantarum*, **100**, 224-233.

AMBLER, J.E., BROWN, J.C. & GAUCH, H.G. 1970. Effect of zinc on translocation of iron in soybean plants. *Plant Physiology*, **46**, 320-323.

ANHALT, U.C.M., HESLOP-HARRISON, J., PIEPHO, H., BYRNE, S. & BARTH, S. 2009. Quantitative trait loci mapping for biomass yield traits in a Lolium inbred line derived F2 population. *Euphytica*, **170**, 99-107.

ANURADHA, K., AGARWAL, S., RAO, K.V., VIRAKTAMATH, B.C. & SARLA, N. 2012. Mapping QTLs and candidate genes for iron and zinc concentrations in unpolished rice of Madhukar x Swarna RILs. *Gene*, **508**, 233-240.

ARIENZO, M., ADAMO, P. & COZZOLINO, V. 2004. The potential of *Lolium perenne* for revegetation of contaminated soil from a metallurgical site. *Science of the Total Environment*, **319**, 13-25.

ARMSTEAD, I.P., TURNER, L.B., KING, I.P., CAIRNS, A.J. & HUMPHREYS, M.O. 2002. Comparison and integration of genetic maps generated from F-2 and BC1-type mapping populations in perennial ryegrass. *Plant Breeding*, **121**, 501-507.

ARMSTEAD, I.P., TURNER, L.B., MARSHALL, A.H., HUMPHREYS, M.O., KING, I.P. & THOROGOOD, D. 2008. Identifying genetic components controlling fertility in the outcrossing grass species perennial ryegrass (*Lolium perenne*) by quantitative trait loci analysis and comparative genetics. *New Phytologist*, **178**, 559-571.

ASSMAM, S.M. 2002. Heterotrimeric and unconventional GTP binding proteins in plant cell signalling. *The Plant Cell*, **14**, 355-373.

ASSUNÇÃNO, A., PIEPER, B., VROMANS, J., LINDHOUT, P., AARTS, M. & SCHAT, H. 2006. Construction of a genetic linkage map of *Thlaspi caerulescens* and quantitative trait loci analysis of zinc accumulation. *New Phytolologist*, **170**, 21-32.

AZEVEDO, R. & RODRIGUEZ, E. 2012. Phytoxicity of mercury in plants: a review. *Journal of Botany*, doi:10.1155/2012/848614.

BACIC, A., FINCHER, G. B, & STONE, B.A. 2009. *Chemistry, Biochemistry, and Biology of 1-3 Beta Glucans and Related Polysaccharides*. San Diego, CA: Elsevier Science.

BAKER, A.J.M. & BROOKS, R.R. 1989. Terrestrial higher plants which hyperaccumulate metallic elements: a review of their distribution, ecology and phytochemistry, *Biorecovery*, **1**, 81-126.

BAKER, A. J. M. & WALKER, P. L. 1990. Ecophysiology of metal uptake by tolerant plants: Heavy metal uptake by tolerant plants. In: **SHAW, A.J. (ed.)** *Evolutionary Aspects*. CRC, Boca Raton, 155-177.

BÁLINT, A. F., KOVACS, G., BÖRNER, A., GALIBA, G. & SUTKA, J. 2003. Substitution analysis of seedling stage copper tolerance in wheat. *Acta Agronimica Hungarica*, **51**, 397-404.

BALL, T.K. & NUTT, M.J.C. 1976. Preliminary mineral reconnaissance of Central Wales. *Report of the Institute of Geological Science*, No. 75/14.

BASEL CONVENTION. 2009.
http://www.ihpa.info/docs/library/reports/Pops/June2009/SBC_LogoGEOMELTMainSheet_190109_Prov.pdf

BEAUMONT, P.B. 1973. The ancient pigment mines of Southern Africa. *South African Journal of Science*, **69**, 140-146.

BEAVIS, W. D. 1994. The power and deceit of QTL experiments: lessons from comparative QTL studies. In: **TRADE, A.S. (ed.)** *Proceedings of the 49th Annual Corn and Sorghum Industry Research Conference*, ASTA, Chicago, 250-266.

BEGONIA, M.T., BEGONIA, G.B., IGHOAVODHA, M. & GILLIARD, D. 2005. Lead accumulation by Tall Fescue (*Festuca arundinacea* Schreb.) grown on a lead-contaminated soil. *International Journal of Environmental Research and Public Health*, **2**, 228-233.

BENAVIDES, P., GALLEGO, S.M. & TOMARO, M.L. 2005. Cadmium toxicity in plants. *Brazilian Journal of Plant Physiology*, **17**, 21-34.

BERGES, J. 1997. Miniview: algal nitrate reductases. *European Journal of Phycology*, **32**, 3-8.

BERTI, W.W.R. & CUNNINGHAM, S.D. 2000. Phytostabilization of metals. In: **RASKIN, I. & ENSLEY, B.D. (eds)** *Phytoremediation of Toxic metals – Using Plants to Clean Up the Environment*. John Wiley & Sons, New York, 71-88.

BEVINS, R.E. 1994. *A Mineralogy of Wales*. National Museum of Wales, Geological Series No. 16, Cardiff, 145pp.

BEVINS, R.E. & MASON, J.S. 1997. *Cwmystwyth Mine*. Welsh Metallophyte and Metallogenic Evaluation Project. Countryside Council for Wales. Science Report No.56.

BEVINS, R.E., YOUNG, B., MASON, J.S., MANNING, D.A.C. & SYMES, R.F. 2010. *Mineralisation in Great Britain*. Geological Conservation Review Series, No. **36**, Joint Nature Conservation Committee, Peterborough, 598pp.

BICK, D.E. 1976. *The Old Metal Mines of Mid Wales. Part 3 Cardiganshire – North of Goginan*. The Pound House, Newent, 72pp.

BICK, D.E. 1992. *The Old Metal Mines of Mid Wales. Parts 1&2 Cardiganshire – South of Goginan*. Revised Edition. The Pound House, Newent, 104pp.

BIDAR, G., GARÇON, G., PRUVOT, C., DEWAELE, D., CAZIER, F., DOUAY, F. & SHIRALI, P. 2007. Behaviour of *Trifolium repens* and *Lolium perenne* growing in a heavy metal contaminated field: plant metal concentrations and phytotoxicity. *Environmental Pollution*, **147**, 546-553.

BIDAR, G., PRUVOT, C., GARÇON. G., VERDIN, A., SHIRALI, P. & DOUAY, F. 2009. Seasonal and annual variation of metal uptake, bioaccumulation and toxicity in *Trifolium repens* and *Lolium perenne* growing in a metal-contaminated field. *Environmental Science and Pollution Research International*, **16**, 42-53.

BLACKMORE, T., THOMAS, I., McMAHON, R., POWELL, W. & HEGARTY, M. 2015. Genetic-geographic correlation revealed across a broad European ecotypic sample of perennial ryegrass (*Lolium perenne*) using array-based SNP genotyping. *Theoretical Applied Genetics*, **128**, 1917-1932.

BLACKMORE, T., THOROGOOD, D., McMAHON, R., POWELL, W. & HEGARTY, M. 2016. Germplasm dynamics: the role of ecotypic diversity in shaping the patterns of genetic variation in *Lolium perenne*. *Scientific Reports*, **6**, 22603; doi:10.1038/srep22603.

BLAYLOCK, M.J., SALT, D.E. & DUSHENKOV, S. 1997. Enhanced accumulation of Pb in Indian mustard by soil-applied chelating agents. *Environmental Science and Technology*, **31**, 860-865.

BODDI, B., ORAVECZ, A.R. & LEHOCZKI, E. 1995. Effect of cadmium on organization and photoreduction of protochlorophyllide in dark-grown leaves and etioplast inner membrane preparations of wheat. *Photosynthetica*, **31**, 411-420.

BOENING, D. W. 2000. Ecological effects, transport, and fate of mercury: a general review. *Chemosphere*, **40**, 1335-1351.

BONNET, M., CAMARES, O. & VEISSEIRE, P. 2000. Effects of zinc and influence of *Acremonium lolii* on growth parameters, chlorophyll *a* fluorescence and antioxidant enzyme activities of ryegrass (*Lolium perenne* L. *cv* Apollo). *Journal of Experimental Botany*, **51**, 945-953.

BORROW, G.H. 1862. *Wild Wales*. John Murray Publisher, 543pp.

BOYD, R.S. 2012. Plant defence using toxic inorganic ions: Conceptual models of the defensive enhancement and joint effects hypotheses. *Plant Science*, **195**, 88-95.

BOYD, R.S. & JAFFRÉ, T. 2001. Phytoenrichment of soil Ni concentration by *Serbetia acuminata* in New Caledonia and the concept of elemental allelopathy. *South African Journal of Science*, **97**, 535-538.

BOYD, R.S. & MARTENS, S.M. 1992. The raison d'être for metal hyperaccumulation by plants. In: **NAKER, A.J.M., PROCTOR, J. & REEVES, R.D. (eds)** *The Vegetation of Ultramafic (Serpentine) Soils*, Intercept Limited, Andover, 279-289.

BRADLEY, S.B. & COX, J.J. 1990. The significance of the floodplain to the cycling of metals in the river Derwent catchment, UK. *Science of the Total Environment*, **97/98**, 441-454.

BRENNAN, R.F. 2005. *Zinc application and its availability to plants*. Unpublished Ph. D. thesis, Murdoch University.

BRIAT, J-F., RAVET, K., ARNAUD, N., DUC, C., BOUCHEREZ, J., TOURAINE, B., CELLIER, F. & GAYMARD, F. 2010. New insights into ferritin synthesis and function highlight a link between iron homeostasis and oxidative stress in plants. *Annals of Botany*, **105**, 811-822.

BROADHURST, C., CHANEY, R., ANGLE, J., MAUGEL, T., ERBE, E. & MURPHY, C. 2004. Simultaneous hyperaccumulation of nickel, manganese, and calcium in Alyssum leaf trichomes. *Environmental Science and Technology*, **38**, 5797-5802.

BURNELL, J. 1988. The biochemistry of manganese in plants. In: **GRAHAM, R.D., HANNAM, R.J. & UREN, N.J. (eds)** *Manganese in soils and plants*. Kluwer Academic Publishers, Dordrecht, The Netherlands, 125-137.

BURT, R., WAITE, P. & BURNLEY, R. 1986. *The Mines of Cardiganshire, The Mineral Statistics of the United Kingdom 1845-1913,* Vol. **7**, University of Exeter Press in association with the Northern Mines Research Society, Exeter, 167pp.

BURT, R., WAITE, P. & BURNLEY, R. 1990. *The Mines of Shropshire and Montgomeryshire with Cheshire and Staffordshire, The Mineral Statistics of the United Kingdom 1845-1913,* Vol. **9**, University of Exeter Press in association with the Northern Mines Research Society, Exeter, 104pp.

BURTON, K.W., MORGAN, E. & ROIG, A. 1984. The influence of heavy metals on the growth of sitka-spruce in South Wales forests. II Greenhouse experiments. *Plant and Soil*, **78**, 271-282.

BURZYNSKI, M. 1987. The influence of lead and cadmium on the absorption and distribution of potassium, calcium, magnesium and iron in cucumber seedlings. *Acta Physiologiae Plantarum*, **9**, 229-238.

CAKMAK, I. 2000. Possible roles of zinc in protecting plant cells from damage by reactive oxygen species. *New Phytologist*, **146**, 185-205.

CAKMAK, I. & MARSCHNER, H. 1993. Effect of zinc nutritional status on superoxide radical and hydrogen peroxide scavenging enzymes in bean leaves. In: **BARROW, N.J. (ed.)** *Plant nutrition - from genetic engineering field practice*. Kluwer, The Netherlands, 133-137.

CAO, S., WANG, W., ZHAO, Y., YANG, S., WANG, F., ZHANG, J. & SUN, Y. 2016. Enhancement of lead phytoremediation by perennial ryegrass (*Lolium perenne* L.) using agent of *Streptomyces pactum* Act12**.** *Journal of Petroleum & Environmental Biotechnology*, **7**, 269-276.

CARPENTER, K.E. 1924. A study of the fauna of rivers polluted by lead mining in the Aberystwyth district of Cardiganshire. *Annals of Applied Biology,* **11**, 1-23.

CARPITA, N.C. & GIBEAUT, D.M. 1993. Structural models of primary cell walls in flowering plants: consistency of molecular structure with the physical properties of the walls during growth. *The Plant Journal*, **3**, 1-30.

CATALÁN, P., MÜLLER, J., HASTEROK, R., JENKINS, G., MUR, L.A.J., LANGDON, T., BETEKHTIN, A., SIWINSKA, D., PIMENTAL, M. & LÓPEZ-ALVAREZ, D. 2012. Evolution and taxonomic split of the model grass *Brachypodium distachyon*. *Annals of Botany*, **109**, 385-405.

CAVE, R. & HAINS, B.A. 1986. *Geology of the country between Aberystwyth and Machynlleth*. Memoir of the British Geological Survey. Sheet 163 (England and Wales).

CAVE, R.R., ANDREWS, J.E., JICKELLS, T. & COOMBES, E.G. 2005. A review of sediment contamination by trace metals in the Humber catchment and estuary, and the implications for future estuary water quality. *Estuarine, Coastal and Shelf Science*, **62**, 547-557.

CHAFFAI, R. & KOYAMA, H. 2011. Heavy metal tolerance in *Arabidopsis thaliana. Advances in Biological Research*, **60**, 1-49.

CHANEY, R.L., MALIK, M. & LI, Y.M. 1997. Phytoremediation of soil metals. *Current Opinion in Biotechnology*, **8**, 279-284.

CHAPMAN, H. D. 1966. Zinc. In: **CHAPMAN, H.D. (ed.)** *Diagnostic criteria for plants and soil*. University of California, Division of Agricultural Science, 484-499.

CHENG, Y. & CAUN, J. 2014. Involvement of pheophytinase in ethylene-mediated chlorphyll degradation in the peel of harvested 'Yali' pear. *Journal of Plant Growth Regulation*, **33**, 364-372.

CHO, U. & SEO, N. 2004. Oxidative stress in *Arabidopsis thaliana* exposed to cadmium is due to hydrogen peroxide accumulation. *Plant Science*, **168**, 113-120.

CHOI, J., PAK, C. & LEE, C.W. 1996. Micronutrient toxicity in French marigold. *Journal of Plant Nutrition*, **19**, 901-916.

CLARKSON, D.T. & LUTTGE, U. 1989. Mineral nutrition: divalent cations, transport and compartmentation. *Progress in Botany*, **51**, 93-112.

CLEAL, C.J. & THOMAS, B.A. 2005. *Palaeozoic Palaeobotany of Great Britain*. Geological Conservation Review Series, JNCC, Chapman & Hall, 295pp.

CLEMENS, S. 2006. Toxic metal accumulation, responses to exposure and mechanisms of tolerance in plants. *Biochimie*, **88**, 1707-1719.

CLEMENS, S., BLOSS, T., VESS, C., NEUMANN, D., NIES, D.H. & ZUR NIEDEN, U. 2002. A transporter in the endoplasmic reticulum of Schizosaccharomyces pombe cells mediates zinc storage and differentially affects transition metal tolerance. *Journal of Biological Chemistry*, **277**, 18215-18221.

CLEMENT, C.R., HOPPER, M.J., CANAWAY, R.J. & JONES, L.H.P. 1974. A system for measuring the uptake of ions by plants from solutions of controlled composition. *Journal of Experimental Botany*, **25**, 81-99.

CLEMENT, C.R., HOPPER, M.J. & JONES, L.H.P. 1978. The uptake of nitrate by *Lolium perenne* from flowing nutrient solution. I. Effect of NO_3^- concentration. *Journal of Experimental Botany*, **29**, 453-464.

COBB, A, 2008. *Cadmium*. Marshall Cavendish Corporation, New York, 32pp.

COBBETT, C. & GOLDBROUGH, P. 2002. Phytochelatins and metallothioneins: roles in heavy metal detoxification and homeostasis. *Annual Review of Plant Biology*, **53**, 159-182.

COLZI, I., DOUMETT, S., DEL BUBBA, M., FORNAINI, J., ARNETOLI, R. & GONNELLI, C. 2011. On the role of the cell wall in the phenomenon of copper tolerance in *Silene paradoxa* L. *Environmental and Experimental Botany*, **72**, 77-83.

COURBOT, M., WILLEMS, G., MOTTE, P., ARVIDSSON, S., ROOSENS, N., SAUMITO-LAPRADE, P. & VERBRUGGEN, N. 2007. A major quantitative trait locus for cadmium tolerance in *Arabidopsis halleri* colocalizes with HMA4, a gene encoding a heavy metal ATPase1. *Plant Physiology*, **144**, 1052-1065.

COUSINS, A.B., BAROLI, I., BADGER, M.R., IVAKOV, A., LEA, P.J., LEEGOOD, R.C. & von CAEMMERER, S. 2007. The role of phosphoenolpyruvate carboxylase during C_4 photosynthetic isotope exchange and stomatal conductance. *Plant Physiology*, **145**, 1006-1017.

CUNNINGHAM, S.D., BERTI, W.R. & HUANG, J.W. 1995. Phytoremediation of contaminated soils. *Trends in Biotechnology*, **13**, 393-397.

DAS, P., SAMANTARAY, S. & ROUT, G.R. 1997. Studies on cadmium toxicity in plants: a review. *Environmental Pollution*, **98**, 29-36.

DAVIES, J.R., FLETCHER, C.J.N., WATERS, R.A., WILSON, D., WOODHALL, D.G. & ZALASIEWICZ. 1997. *Geology of the country around Llanilar and Rhayader*. Memoir of the British Geological Survey, Sheets 178 and 179 (England and Wales).

DAVIES, R.D. & BECKETT, P.H.T. 1978. Upper critical levels of toxic elements in plants. II. Critical levels of Cu in young barley, wheat, rape, lettuce and rye grass and of Ni and Zn in young barley and rye grass. *New Phytologist*, **80**, 23-32.

DAVIS, J.R. 2000. *Nickel, cobalt and their alloys*. ASM Speciality Handbook, ASM International, USA, 422pp.

De FILIPPIS, L.F. & ZIEGLER, H. 1993. Effect of sublethal concentrations of zinc, cadmium and mercury on the photosynthetic carbon reduction cycle of Euglena. *Journal of Plant Physiology*, **142**, 167-172.

DENIAU, A. X., PIEPER, B., TEN BOOKUM, W.M., LINDHOUT, P., AARTS, M.G.M. & SCHAT, H. 2006. QTL analysis of cadmium and zinc accumulation in the heavy metal hyperaccumulator *Thlaspi caerulescens*. *Theoretical Applied Genetics*, **113**, 907-920.

DONCHEVA, S., STOYANOVA, Z. & VELIKOVA, V. 2001. Influence of succinate on zinc toxicity of pea plants. *Journal of Plant Nutrition*, **24**, 789-804.

DOTANIYA, M.L., MEENA, M.L. & DAS, H. 2014. Chromium toxicity on seed germination, root elongation and coleoptile growth of pigeon pea (*Cajanus cajan*). *Legume Research*, **37**, 227-229.

DRÄGER, D.B., DESBROSSES-FONROUGE, C., KRACH, A.N. & CHARDONNENNS, R.C. 2004. Two genes encoding *Arabidopsis halleri* MTP1 metal transport proteins co-segregate with zinc tolerance and account for high MTP1 transcript levels. *Plant Journal*, **39**, 425-439.

DRESLER, S., HANAKA, A., BEDNAREK, W. & MAKSYMIEC, W. 2014. Accumulation of low-molecular-weight organic acids in roots and leaf segments of *Zea mays* plants treated with cadmium and copper. *Acta Physiologiae Plantarum*, **35**, 1565-1575.

DUMSDAY, J.L., SMITH, K.F., FORSTER, J.W. & JONES, E.S. 2003. SSR-based genetic linkage analysis of resistance to crown rust (*Puccinia coronata* f. sp. *lolii*) in perennial ryegrass (*Lolium perenne*). *Plant Pathology*, **52**, 628-637.

DUNHAM, K., BEER, K.E., ELLIS, R.A., GALLAGHER, M.J., NUTT, M.J.C. & WEBB, B.C. 1978. United Kingdom. In: **BOWIE, H.V.U., KVALHEIM, A. & HASLAM, H.M. (eds)** *Mineral*

Deposits of Europe, Volume I, Northwest Europe. Institute of Mining and Metallurgy and the Mineralogical Society, London, 263-317.

EBBS, S.D. & KOCHIAN, L.V. 1997. Toxicity of zinc and copper to *Brassica* species: implications for phytoremediation. *Journal of Environmental Quality*, **26**, 776-781.

ENVIRONMENT AGENCY WALES. 2002. Metal Mine Strategy for Wales.

ENVIRONMENT AGENCY. 2008a. *Identification and prioritisation of abandoned non-coal mines*. SC030136/14. Collaborative project with DEFRA, Welsh Assembly Government, Department of Communities and Local Government. Draft.

ENVIRONMENT AGENCY. 2008b. *Assessment of Metal-Mining-Contaminated River sediments in England and Wales*. Science Report: SC030136/SR4, 55pp.

ERNST, W.H.O. 1994. Bioavailability of heavy metals and decontamination of soils by plants. In: **ANTSRØM, M. & BJØRKLAND, A. (eds)** *Mobility and forms of metals in acid sulphate soils – implications for stream water chemistry*. 3rd International Symposium on Environmental Geochemistry, Krakow. Book of Abstracts, 110.

ERNST, W.H.O. 2000. Evolution and ecophysiology of metallophytes in Africa and Europe. In: **BRECKLE, S.W., SCHWEIZER, B. & ARNDT, U. (eds)** *Results of worldwide ecological studies*. Stuttgart, G. Heimbach, 23-35.

ERNST, W. H. O. 2006. Evolution of metal tolerance in higher plants. *Forest, Snow and Landscape Research*, **80**, 251-274.

EVANGELOU, M.W.H., EBEL, M. & SCHAEFFER, A. 2007. Chelate assisted phytoextraction of heavy metals from soil. Effect, mechanism, toxicity and fate of chelating agents. *Chemosphere*, **68**, 989-1003.

FAHR, M., LAPLAZE, M., BENDAOU, N., EL MZIBRI, M., BOGUSZ, D. & SMOUNI, A. 2013. Effect of lead on root growth. *Frontiers in Plant Science*, **4**, 1-7.

FARAGO, M.E. & COLE, M.M. 1988. Nickel and plants. In: **SIGEL, H. & SIGEL, A. (eds)** *Metal ions in biological systems*, Vol. 23, Nickel and its role in biology. Marcel Dekker, New York, 47-90.

FITCHES, W.R. 1972. Polyphase deformation structures in the Welsh Caledonides near Aberystwyth. *Geological Magazine*, **109**, 149-155.

FITCHES, W.R. 1992. Ponterwyd Quarry. In: **TREAGUES, J.E. (ed.)** *Caledonian Structures in Britain South of the Midland Valley*. Joint Nature Conservation Committee, Chapman and Hall, 137-139.

FLETCHER, C.J.N., SWAINBANK, I.G. & COLEMAN, T.B. 1993. Metallogenic evolution in Wales: constraints from lead isotope modelling. *Journal of the Geological Society of London*, **150**, 77-82.

FODOR. F. 2002. Physiological responses of vascular plants to heavy metals. In: **PRASAD, M.N.V. & STRZALKA, K. (eds)** *Physiology and Biochemistry of Metal Toxicity and Tolerance in Plants*, Kluwer Academic, Dortrech, 149-177.

FODOR, A., SZABO, A. & ERDEI, L. 1995. The effects of cadmium on the fluidity and H^+-ATPase activity of plasma membrane from sunflower and wheat roots. *Journal of Plant Physiology*, **14**, 787-792.

FOULDS, S.A., BREWER, P.A., MACKLIN, M.G., HARESIGN, W., BETSON, R.E. & RASSNER, S.M.E. 2014. Flood-related contamination in catchments affected by historical metal mining: An unexpected and emerging hazard of climate change. *Science of the Total Environment*, **476**, 165-180.

FRÉROT, H., FAUCON, M-P., WILLEMS, G., GODÉL, C., COURSEAUX, A., DARRAC, A., VERBRUGGEN, N. & SAUMITOU-LAPRADE, P. 2010. Genetic architecture of zinc hyperaccumulation in *Arabidopsis halleri*: the essential role of QTL x environment interactions. *New Phytologist*, **187**, 355-367.

FRIEDRICH, G.H., GENKIN, A.D., NALDRETT, A.J., RIDGE, J.D., SILLITOE, R.H. & VOKES, F.M. 1986. *Geology and Metallogeny of Copper Deposits*. Special publication No. 4 of the Society for Geology Applied to Minerals. Springer-Verlag, Berlin, 582pp.

FUGE, R., LAIDLAW, I.M.S., PERKINS, W.T. & ROGERS, K.P. 1991. The influence of acidic mine and spoil drainage on water quality in the Mid-Wales area. *Environmental Geochemistry and Health*, **13**, 70-75.

FUGE, R., PEARCE, F.M., PEARCE, N.J.G. & PERKINS, W.T. 1993. Geochemistry of Cd in the secondary environment near abandoned metalliferous mines, Wales. *Applied Geochemistry*, Supplementary Issue No. 2, 29-35.

GAJEWSKA, E., SKLODOWSKA, M., SLABA, M. & MAZUR, J. 2006. Effect of nickel on antioxidative enzymes activities, proline and chlorophyll contents in wheat shoots. *Biologia Plantarum*, **50**, 653-659.

GALL, J.E. & RAJAKARUNA, N. 2013. The physiology, functional genomics, and applied ecology of heavy metal-tolerant *Brassicaceae*. In: **LANG, M. (ed.)** *Brassicaceae*. Nova Science Publishers, 121-148.

GAMBLE, R.L., COONFIELD, M.L. & SCHALLER, E.G. 1998. Histidine kinase activity of the ETRI ethylene receptor from Arabidopsis. *Proceedings of the National Academy of Science, USA*, **95**, 7825-7829

GANEVA, G., LANDJEVA, S. & MERAKCHIJSKA, M. 2003. Effects of chromosome substitutions on copper toxicity tolerance in wheat seedlings. *Biologia Plantarum*, **47**, 621-623.

GARBISU, C. & ALKORTA, I. 1997. Bioremediation: principles and future. *Journal of Clean Technology, Environmental Toxicology and Occupational Medicine*. **6**, 351-366.

GARBISU, C. & ALKORTA, I. 2007. Basic concepts on heavy metal soil bioremediation. *The European Journal of Mineral Processing and Environmental Protection*, **3**, 58-66.

GARBISU, C., LLAMA, M.J. & SERRA, J.L. 1997. Effect of heavy metals on chromate reduction by *Bacillus subtilis*. *Journal of General and Applied Microbiology*, **43**, 369-371.

GARBISU, C., ALKORTA, I., LLAMA, M.J. & SERRA, J.L. 1998. Aerobic chromate reduction by *Bacillus subtilis*. *Biodegradation*, **9**, 133-141.

GARCIA-OLIVEIRA, A.L., TAN, L., FU, Y. & SUN, C. 2009. Genetic identification of quantitative trait loci for contents of mineral nutrients in rice grains. *Journal of Plant Biology*, **51**, 84-92.

GAUT, B.S. 2002. Evolutionary dynamics of grass genomes. *New Phytologist*, **154**, 15-28

GECHEV, T.S., VAN BREUSEGEM, F., STONE, J.M., DENEV, I. & LALOI, C. 2006. Reactive oxygen species as signals that modulate plant stress responses and programmed cell death. *BioEssays*, **28**, 1091-1101.

GOLDSCHMIDT, V. 1962. *Geochemistry*. Clarendon press, Oxford.

GONZALEZ-OREJA, J.A., ROZAS, M.A., ALKORTA, I. & GARBISU, C. 2008. Dendroremediation of heavy metal polluted soils. *Reviews on Environmental Health*, **23**, 223-234.

GOUGH, L.P., SHACKLETTE, H.T. & CASE, A. A. 1979. Element concentrations toxic to plants, animals, and man. U.S. Geological Survey Bulletin 1466. iii + 80 pp. Washington. U.S. Government Printing Office, Stock No. 024–001–03201–5.

GRAMENE. 2016. Gramene: A comparative resource for plants. http://gramen.org/

GRILL, E., WINNACKER, E.L. & ZENK, M.H. 1987. Phytochelatins, a class of heavy-metal-binding peptides of plants are functionally analogous to metallothioneins. *Proceedings of the National Academy of Science USA*, **84**, 439-443.

GRIMSHAW, D.L., LEWIN, J. & FUGE, R. 1976. Seasonal and short-term variations in the concentrations and supply of dissolved zinc to polluted aquatic environments. *Environmental Pollution*, **11**, 1-7.

GU, F. & WILLS, B.A. 1988. Chromite – mineralogy and processing. *Minerals Engineering*, **1**, 235-240.

GUERINOT, M.L. 2000. The ZIP family of metal transporters. *Biochimica et Biophysica Acta – Biomembranes*, **1465**, 190-198.

GUO, J., DAI, X., XU, W. & MA, M. 2008. Over expressing GSHI and AsPCSI simultaneously increases the tolerance and accumulation of cadmium and arsenic in *Arabidopsis thaliana*. *Chemosphere*, **72**, 1020-1026.

GUPTA, D. K., HUANG, H. G., YANG, X. E., RAZAFINDRABE, B. H. N. & INOUHE, M. 2010. The detoxification of lead in *Sedum alfredii* H. is not related to glutathione. *Journal of Hazardous Materials*, **177**, 437-444.

GUPTA, U.C., MONTEIRO, F.A. & WERNER, J.C. 2001. Micronutrients in grassland production. In: International Grassland Congress, 19, São Pedro, Proceedings. São Pedro, SBZ, 149-156.

GUSTIN, J. L., LOUREIRO, M. E., KIM, D., NA, G., TIKHONOVA, M. & SALT, D. E. 2009. MTP1-dependent Zn sequestration into shoot vacuoles suggests dual roles in Zn tolerance and accumulation in Zn hyperaccumulating plants. *Plant Journal*, **57**, 1116-1127.

HALL, G.W. 1988. *The gold mines of Merioneth*. Griffin Publications, 99pp.

HALL, J. L. & WILLIAMS, L. 2003. Transition metal transporters in plants. *Journal of Experimental Botany*, **54**, 2601-2613.

HALTERMAN, S.G. & TOETZ, D.W. 1984. Kinetics of nitrate uptake by freshwater algae. *Hydrobiologia*, **114**, 209-214.

HANIKENNE, M., TALKE I.N., HAYDON, M.J., LANZ, C., NOLTE, A., MOTTE, P., KROYMANN, J., WEIGEL, D. & KRÄMER, U. 2008. Evolution of metal hyperaccumulation required cis-regulatory changes and triplication of HMA4. *Nature*, **453**, 391-396.

HÄNSCH, R. & MENDEL, R.R. 2009. Physiological functions of mineral micronutrients (Cu, Zn, Mn, Fe, Ni, Mo, B, Cl). *Current Opinion in Plant Biology*, **12**, 259-266.

HARTER, R.D. 1983. Effect of soil pH on adsorption of lead, copper, zinc and nickel. *Soil Science Society of America Journal*, **47**, 47-51.

HATCH, D.J., HOPPER, M.J. & DHANOA, M.S. 1986. Measurement of ammonium ions in flowing solution culture and diurnal variation in uptake in *Lolium perenne*. *Journal of Experimental Botany*, **37**, 589-96.

HAUSSLING, M., JORNS, C.A., LEHMBECKER, G., HECHT-BUCHOLZ, C. & MARSCHNER, H. 1988. Ion and water uptake in relation to root development of Norway Spruce (*Picea abies* (L.) Karst). *Journal of Plant Physiology*, **133**, 486-491.

HAWKES, J.S. 1997. Heavy metals. *Journal of Chemical Education*, **74**, 1369-1374.

HE, S., TAN, G., HUANG, K., REN, J. & ZHANG, X. 2011. The LSD1-interacting protein GILP is a LITAF domain protein that negatively regulates hypersensitive cell death in Arabidopsis. *PloS ONE* 6(4):e18750.doi:10.371/journal.pone.0018750.

HERNANDEZ, L.E., CARPENA-RUIZ, R. & GARATE, A. 1996. Alterations in the mineral nutrition of pea seedlings exposed to cadmium. *Journal of Plant Nutrition*, **19**, 1581-1598.

HEWITT, E.J. 1953. Metal inter-relationships in plant nutrition. *Journal of Experimental Botany*, **4**, 59-64.

HEWITT, E.J. 1966. *Sand and water culture methods used in the study of plant nutrition*. Technical Communication No. 22 (Revised 2nd Edition). Commonwealth Agricultural Bureaux, 547pp.

HOSSAIN, M. A. & FUJITA, M. 2010. Evidence for a role of exogenous glycinebetaine and proline in antioxidant defense and methylglyoxal detoxification systems in mung bean seedlings under salt stress. *Physiology and Molecular Biology of Plants*, **16**, 19-29.

HOSSAIN, M. A., PIYATIDA, P., TEIXAIRA da SILVA, J.A. & FUJITA, M. 2012. Molecular mechanism of heavy metal toxicity and tolerance in plants: central role of glutathione in detoxification of reactive oxygen species and methylglyoxal and in heavy metal chelation. *Journal of Botany*, **2012**, 1-37.

HSU, Y. T. & KAO, C.H. 2004. Cadmium toxicity is reduced by nitric oxide in rice leaves. *Plant Growth Regulation*, **42**, 227-238.

HU, Y., GE, Y., ZHANG, C., JU, T. & CHENG, W. 2009. Cadmium toxicity and translocation in rice seedlings are reduced by hydrogen peroxide pretreatment. *Plant Growth Regulation*, **59**, 51-61.

HUANG, Y., SUN, C., MIN, J., CHEN, Y., TONG, C. & BAO, J. 2015. Association mapping of quantitative trait loci for mineral element contents in whole grain rice (*Oryza sativa* L.). *Journal of Agricultural and Food Chemistry*, **63**, 10885-10892.

HUBBARD, C.E. 1984. *Grasses: a guide to their structure, identification, uses and distribution in the British Isles*. Penguin Books, Middlesex, England, 3rd Edition, 476pp.

HUDSON-EDWARDS, K.A., MACKLIN, M.G., CURTIS, C.D. & VAUGHAN, D.J. 1996. Processes of formation and distribution of Pb-, Zn-, Cd- and Cu-bearing minerals in the Tyne Basin, North East England: implications for metal-contaminated river systems. *Environmental Science and Technology*, **30**, 72-80.

HUGHES, S.J.S. 1979. The decline of mining at Cwmystwyth. *Journal of the Ceredigion Antiquarian Society*, 419-438.

HUGHES, S.J.S. 1981. *The Cwmystwyth Mines*. British Mining – Monograph of the Northern Mine Research Society, No. **17**, Northern Mine Research Society, Sheffield, 78pp.

HUGHES, S.J.S. 1989. Bwlchglas Mine. *U.K. Journal of Mines and Minerals*, **7**, 20-28.

HUGHES, S.J.S. 1990. *The Darren Mines*. British Mining – Monograph of the Northern Mine Research Society, No. **40**, Northern Mine Research Society, Sheffield, 153pp.

HUMPHREYS, M.O. & MACDUFF, J.H. 2000. Mapping genes affecting NUE components and understanding the physiological and molecular basis of genetic differences in NUE. *Proceedings of COST 814 workshop on N-use efficiency,* 218-235.

HUSTED, S., MIKKELSEN, B.F., JENSEN, J. & NIELSEN, N.E. 2004. Elemental fingerprint analysis of barley (*Hordeum vulgare*) using inductively coupled plasma mass spectrometry, isotope-ratio mass spectrometry and multivariate statistics. *Analytical and Bioanalytical Chemistry*, **378**, 171-182.

HUTCHINGS, T. & LEIJ, F.D. 2016. The potential of the C-Cure solutions remediation technique to establish vegetation on mine spoils at Cwmystwyth to reduce soil erosion and improve water quality. *Report to Natural Resources Wales*.

INTERNATIONAL BRACHYPODIUM INITIATIVE. 2010. Genome sequencing and analysis of the model grass *Brachypodium distachyon*. *Nature*, **463**, 763-768.

INTERNATIONAL RICE GENOME SEQUENCING PROJECT. 2005. The map-based sequence of the rice genome. *Nature*, **436**, 793-800.

ISHIBASHI, Y., CERVATES, C. & SILVER, S. 1990. Chromium reduction in *Pseudomonas putida*. *Applied and Environmental Microbiology*, **56**, 2268-2270.

ISHIKAWA, S., ABE, T., KURAMATA, M., YAMAGUCHI, M., ANDO, T., YAMAMOTO, T. & YANO, M. 2010. A major quantitative trait locus for increasing cadmium-specific concentration in rice grain is located on the short arm of chromosome 7. *Journal of Experimental Botany*, **61**, 923-934.

ISRAR, M., SAHI, S., DATTA, R. & SARKAR, D. 2006. Bioaccumulation and physiological effects of mercury in *Sesbania drummonii*. *Chemosphere*, **65**, 591-598.

IVANOV, Y.V., SAVOCHIN, Y.V. & KUZNETSOV, V.V. 2012. Scots pine as a model plant for studying the mechanisms of conifers adaptation to heavy metal action: 2. Functioning of antioxidant enzymes in pine seedlings under chronic zinc action. *Russian Journal of Plant Physiology*, **59**, 50-58.

IXER, R.A. & BUDD, P. 1998. The mineralogy of Bronze Age copper ores from the British Isles; implications for the composition of early metalwork. *Oxford Journal of Archaeology*, **17**, 15-41.

JABEEN, R., AHMAD, A. & IQBAL, M. 2009. Phytoremediation of heavy metals: physiological and molecular mechanisms. *Botanical Reviews*, **75**, 339-364.

JAMES, D.M.D. 2011. Turbidite pathways, pore-fluid pressures and productivity in the Central Wales Orefield. *Journal of the Geological Society of London*, **168**, 1107-1120.

JARVIS, S.C., JONES, L.H.P. & CLEMENT, C.R. 1977. Uptake and transport of lead by perennial ryegrass from flowing solution culture with a controlled concentration of lead. *Plant and Soil*, **46**, 371-379.

JARZEMBOWSKI, E.A., SIVETER, D.J., PALMER, D. & SELDEN, P.A. 2010. *Fossil Arthropods of Great Britain*. Geological Conservation Review Series, JNCC, Peterborough, 294pp.

JELEA, S-G., JELEA, M. & JELEA, O-C. 2015. Phytotoxicity of lead on *Lolium perenne* L. and *Lactuca saliva* var. *capita* L: effects of germination and growth. *Bulletin of University of Agricultural Sciences and Veterinary Medicine Cluj-Napoca*, **72**, 1-7.

JENKINS, D.A., JOHNSON, D.B. & FREEMAN, C. 2000. Mynydd Parys Cu-Pb-Zn mines: mineralogy, microbiology and acid mine drainage. In: **COTTER-HOWELLS, A., CAMPBELL, B., VALSAMI-JONES, D. & BATCHELDER, E. (eds)** *Environmental mineralogy: Microbial interactions, anthropogenic influences, contaminated land and waste management*. Mineralogical Society Series, **9**. Mineralogical Society, London, 161-179.

JONES, E., MAHONEY, N.L., HAYWARD, M.D., ARMSTEAD, I.P., JONES, J.G., HUMPHREYS, M.O., KING, I.P., KISHIDA, T., YAMADA, T. & BALFOURIER, F. 2002. An enhanced molecular marker based genetic map of perennial ryegrass (*Lolium perenne*) reveals comparative relationships with other Poaceae genomes. *Genome*, **45**, 282-295.

JONES, L.H.P., CLEMENT, C.R. & HOPPER, M.J. 1973. Lead uptake from solution by perennial ryegrass and its transport from roots to shoots. *Plant and Soil*, **38**, 403-414.

JONES, N., OUGHAM, H. & THOMAS, H. 1997. Markers and mapping: we are all geneticists now. *New Phytologist*, **137**, 165-177.

JONES, O.T. 1922. *Lead and Zinc. The mining district of North Cardiganshire and West Montgomeryshire*. Special Report on the Mineral Resources of Great Britain, Memoir of the Geological Survey of Great Britain, **20**, HMSO, London.

KAUR, G., SINGH, H.P., BATISH, D. R. & KOHLI, R.K. 2013. Lead (Pb)-induced biochemical and ultra-structural changes in wheat (*Triticum aestivum*) roots. *Protoplasma*, **1**, 53-62.

KAVANAGH, K.L., JÖRNVALL, H., PERSSON, B. & OPPERMANN, U. 2008. The SDR superfamily: functional and structural diversity within a family of metabolic and regulatory enzymes. *Cellular and Molecular Life Sciences*, **65**, 3895-3906.

KEARSEY, M. J. & FARQUHAR, A.G. 1998. QTL analysis in plants: Where are we now? *Heredity*, **80**, 137-142.

KELLOGG, E.A. & BENNETZEN, J.L. 2004. The evolution of nuclear genome structure in seed plants. *American Journal of Botany*, **91**, 1709-1725.

KHUDSAR, T., MAHMOODUZZAFAR, T., IQBAL, M. & SAIRAM, R.K. 2004. Zinc-induced changes in morpho-physiological and biochemical parameters in *Artemisia annua*. *Biologia Plantarum*, **48**, 255-260.

KING, C. 2006. Paleogene and Neogene: uplift and cooling climate. In: **BRENCHLEY, P.J. & RAWSON, P.F. (eds)** *The Geology of England and Wales*. The Geological Society, London, 395-428

KING, J., THOMAS, A., JAMES, C., KING, I. & ARMSTEAD, I. 2013. A DArT marker genetic map of perennial ryegrass (*Lolium perenne* L.) integrated with detailed comparative mapping information; comparison with existing DArT marker genetic maps of *Lolium perenne*, *L. multiflorum* and *Festuca pratensis*. *BMC Genomics*, **14**, 437-444.

KOSAMBI, D.D. 1944. The estimation of map distances from recombination values. *Annals of Eugenics*, **12**.

KOSHEVNIKOVA, A.D., SEREGIN, I.V., BYSTROVA, E.I., BELYAEVA, A.I., KATAEVA, M.N. & IVANOV, V. 2009. The effects of lead, nickel and strontium nitrates on cell division and elongation in maize roots. *Russian Journal of Plant Physiology*, **56**, 242-250.

KOSOBRUKHOV, A., KNYZEVA, I. & MUDRIK, V. 2004. *Plantago major* plants responses to increased content of lead in soil: growth and photosynthesis. *Plant Growth Regulation*, **42**, 145-151.

KOYAMA, H., KAWAMURA, A., KIHARA, T., HARA, T., TAKITA, E. & SHIBATA, D. 2000. Overexpression of mitochondrial citrate synthase in *Arabidopsis thaliana* improved growth on a phosphorus-limited soil. *Plant and Cell Physiology*, **41**, 1030-1037.

KRÄMER, U. 2005. MTP1 mops up excess zinc in Arabidopsis cells. *Trends in Plant Science*, **10**, 313-315.

KRUCKEBERG, A.R. & RABINOWITZ, D. 1985. Biological aspects of endemism in higher plants. A*nnual Review of Ecology and Systematics*, **16**, 447-479.

KRUCKBERG, A.R. & REEVES, R.D. 1995. Nickel accumulation by serpentine species of *Streptanthus* (Brassicaceae): field and greenhouse studies. *Madroño*, **42**, 458-469.

KUMAR, N.P.B.A., DUSHENKOV, V., MOTTO, H. & RASKIN, I. 1995. Phytoextraction: the use of plants to remove heavy metals from soils. *Environmental Science & Technology*, **29**, 1232-1238.

KUMPIENE, J., LAGERVIST, A. & MAURICE, C. 2007. Stabilization of Pb- and Cu-contaminated soil using coal fly ash and peat. *Environmental Pollution*, **145**, 365-373.

KUSWANTORO, H. 2014. Relative growth rate of six soybean genotypes under iron toxicity conditions. *International Journal of Biology*, **6**, 11-17.

LACOMBE, E., HAWKINS, S., VAN DOORSSELAERE, J., PIQUEMAL, J., GOFFNER, D., POEYDOMENGE, O., BOUDET, A.M. & GRIMA-PETTENATI, J. 1997. Cinnamoyl COA reductase, the first committed enzyme of the lignin branch biosynthetic pathway: cloning, expression and phylogenetic relationships. *Plant Journal*, **11**, 42-441.

LANGEDAL, M. 1997. Dispersion of tailings in the Knabeåna – Kvina drainage basin Norway, 2: Mobility of Cu and Mo in tailings-derived fluvial sediments. *Journal of Geochemical Exploration*, **58**, 173-183.

LEAH, R., KIGEL, J., SVENDSEN, Ib. & MUNDY, J. 1995. Biochemical and molecular characterization of a barley seed β-glucosidase. *The Journal of Biological Chemistry*, **270**, 15789-15797.

LEHNINGER, A.L. 1970. *Biochemistry*. Worth Publishers Inc, New York. 833pp.

LELAND, J. 1906. *The Itinerary in Wales of John Leland in or about the years 1536-1539*. Extracted from his mss. Imprint London, George Bell & Sons.

LEVINE, A., BELENGHI, B., DAMARI-WEISLER, A. & GRANOT, D. 2001. Vesicle-associate Membrane Protein of Arabidopsis suppresses Bax-induce apoptosis in yeast downstream of oxidative burst. *The Journal of Biological Chemistry*, **276**, 46284-46289.

LEWIN, J. & MACKLIN, M.G. 1987. Metal mining and floodplain sedimentation in Britain. In: **GARDINER, V. (ed.)** *International Geomorphology 1986 Part I*. John Wiley and Sons, Chichester, 1009-1027.

LEWIN, J., BRADLEY, S.B. & MACKLIN, M.G. 1983. Historical valley alluviation in mid-Wales. *Geological Journal*, **18,** 331-350.

LEWIN, J., DAVIES, B.E. & WOLFENDEN, P.J. 1977. Interactions between channel change and historic mining sediment. In: **GREGORY, K.J. (ed.)** *River Channel Changes.* John Wiley & Sons, 353-367.

LEWIS, A. 1990. Underground exploration of the Great Orme copper mines. In: **CREW, P. & CREW, S. (eds)** *Plas Tanybwlch Occasional Paper*, **No. 1**, Snowdonia National Park Centre, Blaenau Ffestiniog, 5-10.

LI, X. & THORNTON, I. 1993. Multi-element contamination of soils and plants in old mining areas, U.K. *Applied Geochemistry*. Supplementary Issue No. 2, 51-56.

LI, H.F., GRAY, C., MICO, C., ZHAO, F.J. & McGRATH, S.P. 2009. Phytotoxicity and bioavailability of cobalt to plants in a range of soils. *Chemosphere*, **75**, 979-986.

LI, J. & CHORY, J. 1997. A putative leucine-rich repeat receptor kinase involved in brassinosteroid signal transduction. *Cell*, **90**, 929-938.

LI, W-T., HE, M., WANG, J. & WANG, Y-P. 2013. Zinc-finger proteins (ZFP) in plants – a review. *Plant Omics Journal*, **6**, 474-480.

LIU, L. 2015. *Iron ore: mineralogy, processing and environmental sustainability*. Woodhead Publishing, Elsevier, 631pp.

LIU, C. P., SHEN, Z. G, & LI, X. D. 2007. Accumulation and detoxification of cadmium in *Brassica pekinensis* and *B. chinensis*. *Biologia Plantarum*, **51**, 116-120.

LIU, Z., PAGANI, M., ZINNIKER, D., DECONTO, R., HUBER, M., BRINKHUIS, H., SHAH, S.R., LECKIE, R.M. & PEARSON, A. 2009. Global cooling during the Eocene-Oligocene climate transition. *Science*, **323**, 1187-1190.

LIU, X. & CHU, Z. 2015. Genome-wide evolutionary characterization and analysis of bZIP transcription factors and expression profiles in response to multiple abiotic stresses in *Brachypodium distachyon*. *BMC Genomics*, **16**, 227-242.

LÓPEZ-MILLÁN, A.F., ELLIS, D.R. & GRUSAK, M.A. 2005. Effect of zinc and manganese supply on the activities of superoxide dismutase and carbonic anhydrase in *Medicago truncatula* wild type and *raz* mutant plants. *Plant Science*, **168**, 1015-1022.

LUO, Y. & RIMMER, D.L. 1995. Zinc-copper interaction affecting plant growth on a metal-contaminated soil. *Environmental Pollution*, **88**, 79-83.

LUO, C., SHEN, Z. & LI, X. 2005. Enhanced phytoextraction of Cu, Pb, Zn and Cd with EDTA and EDDS. *Chemosphere*, **59**, 1-11.

MACKLIN, M.G. 1996. Fluxes and storage of sediment-associated heavy metals in floodplain systems: Assessment and river basin management issues at a time of rapid environmental change. In: **ANDERSON, M.G., WALLING, D.E. & BATES, P.D. (eds)** *Floodplain Processes.* John Wiley & Sons, 441-460.

MACKLIN, M.G. & LEWIN, J. 1986. Terraced fills of Pleistocene and Holocene age in the Rheidol Valley, Wales. *Journal of Quaternary Science,* **1**, 21-34.

MACKLIN, M.G., BREWER, P.A., COULTHARD, T.J., TURNER, J.N., BIRD, G. & HUDSON-EDWARDS, K.A. 2002. The chemical and physical impacts of recent mine tailings dam failures on river systems: key issues for sustainable catchment management in former and present mining areas. In*: Proceedings of a seminar on proposed EU directive on mining waste*. Office of the Deputy Prime Minister, London, 18-24.

MACKLIN, M.G., RUMSBY, B.T. & NEWSON, M.D. 1992. Historical floods and vertical accretion of fine-grained alluvium in the Lower Tyne valley, North East England. In: **BILLI, P., HEY, R.D., THORNE, C.R. & TACCONI, P. (eds)** *Dynamics of gravel-bed rivers*. John Wiley & Sons, Chichester, 573-589.

MACNAIR, M.R. 1993. The genetics of metal tolerance in vascular plants. *New Phytologist*, **124**, 541-559.

MACNICOL, R.G. & BECKETT, P.H.T. 1985. Critical tissue concentrations of potentially toxic elements. *Plant and Soil*, **85**, 107-130.

MACRO, A. 2005. *Genotypic variation within adapted ecotypes of Lolium perenne for tolerance and phytoremediation potential to contaminated mine spoil.* Unpublished M.Sc. thesis, University of Wales.

MAESTRI, D., MARMIROLI, M., VISIOLI, G. & MARMIROLI, N. 2010. Metal tolerance and hyperaccumulation: Cost and trade-offs between traits and environment. *Environmental and Experimental Botany*, **68**, 1-13.

MAGNUSON, M.L., KELTY, C.A. & KELTY, K.C. 2001. Trace metal loading on water-borne soil and dust particles characterized through the use of Split-flow thin-cell fractionation. *Analytical Chemistry*, **73**, 3492-3496.

MAHMOOD, T. & ISLAM, K.R. 2006. Response of rice seedlings to copper toxicity and acidity. *Journal of Plant Nutrition*, **29**, 943-957.

MALECKA, A., PIECHALAK, A. & TOMASZEWSKA, B. 2009. Reactive oxygen species production and antioxidative defense system in pea root tissues treated with lead ions: the whole roots level. *Acta Physiologia Plantarum*, **31**, 1053-1063.

MALIK, N.J., CHAMON, A.S., MONDOL, M.N., ELAHI, S.F. & FAIZ, S.M.A. 2011. Effects of different levels of zinc on growth and yield of red amaranth (*Amaranthus* sp.) and rice (*Oryza sativa*, variety BR49). *Journal of the Bangladesh Association of Young Researchers*, **1**, 79-91.

MANNING, W. 1959. *The future of non-ferrous mining in GB and Ireland*. Institute of Mining and Metallurgy, London.

MARQUES, A.P.G.C., RANGEL, A.O.S.S. & CASTRO, P.M.L. 2009. Remediation of heavy metal contaminated soils: phytoremediation as a potentially promising clean-up technology. *Critical Reviews in Environmental Science and Technology*, **39**, 622-654.

MARSCHNER, H. 1995. *Mineral nutrition of higher plants*. 2nd edition. Academic Press, Toronto.

MASON, J.S. 1994. *Regional parageneses for the Central Wales Orefield*. Unpublished M.Phil. thesis, University of Wales.

MASON, J. S. 1997. Regional polyphase and polymetallic vein mineralisation in the Caledonides of the Central Wales Orefield. *Transactions of the Institution of Mining and Metallurgy of London*, Section B: *Applied Earth Science,* **106**, 135-143.

MAYLAND, H.F., CHEEKE, P.R., MAJAK, W. & GOFF, J.P. 2007. Forage-induced animal disorders. In: **BARNES, R.F., NELSON, C.F., MOORE. K.J. & COLLINS, M. (eds)** *Forages: The Science of Grassland Agriculture* (6th edition). Blackwell Publishing, Ames, IA, USA, 687-707.

MAYOWA, N. M. & MILLER, T. E. 1991. The genetics of tolerance to high mineral concentrations in the Tribe Triticeae - a review and update. *Euphytica*, **57**, 175-185.

McCARTY, R.E., EVRON, Y. & JOHNSON, E.A. 2000. The chloroplast ATP synthase: a rotary enzyme? *Plant Biology*, **51**, 83-109.

McCOMB, J., HENTZ, S., MILLER, G., BEGONIA, M. & BEGONIA G. 2012. Effects of lead on plant growth, lead accumulation and phytochelatin contents of hydroponically-grown *Sesbania exaltata*. *World Environment*, **2**, 38-43.

MEERS, E., TACK, F.M.G., VAN SLYCKEN, S., RUTTENS, A., Du LAING, G., VANGRONSVELD, J. & VERLOO, M.G. 2008. Chemically assisted phytoextraction: a review of potential soil amendments for increasing plant uptake of heavy metals. *International Journal of Phytoremediation*, **10**, 390-414.

McGRATH, S.P. & ZAO, F-J. 2003. Phytoextraction of metals and metalloids from contaminated soils. *Current Opinion in Biotechnology*, **14**, 277-282.

MEHES-SMITH, M., NKONGOLO, K. & CHOLEWA, E. 2013. Coping mechanisms of plants to metal contaminated soil. In: **SILVER, S. & YOUNG, S. (eds)** *Environmental Change and Sustainability*, Intech, 53-90.

MENDEZ, M.O. & MAIER, R.M. 2008. Phytostabilization of mine tailings in arid and semiarid environments – an emerging remediation technology. *Environmental Health Perspectives*, **116**, 278-283.

MERRINGTON, G. & ALLOWAY, B.J. 1994. The transfer and fate of Cd, Cu, Pb and Zn from two historic metalliferous mine sites in the U.K. *Applied Geochemistry*, **9**, 677-687.

McGRATH, S.P. & ZHAO, F. 2003. Phytoextraction of metals and metalloids from contaminated soils. *Current Opinion in Biotechnology*, **14**, 277-282.

MGANGA, N., MANOKO, M. L. K. & RULANGARANGA, Z. K. 2011. Classification of plants according to their heavy metal content around North Mara gold mine, Tanzania: Implication for phytoremediation. *Tanzania Journal of Science*, **37**, 109-119.

MIGHALL, T. & CHAMBERS, F.M. 1993. The environmental impact of prehistoric mining at Copa Hill, Cwmystwyth, Wales. *The Holocene*, **3/3**, 260-264.

MILLALEO, R., REYES-DIAZ, M., IVANOV, A.G., MORA, M.L. & ALBERDI, M. 2010. Manganese as an essential and toxic element for plants: transport, accumulation and resistance mechanisms. *Journal of Soil Science and Plant Nutrition*, **10**, 470-481.

MILLER, G., BEGONIA, G.B., BEGONIA, M.T., NTONI, J. & HUNDLEY, O. 2008. Assessment of the efficacy of chelate-assisted phytoextraction of lead by Coffeeweed (*Sesbania exaltata* Raf.). *International Journal of Environmental Research and Public Health*, **5**, 428-435.

MISRA, S.G. & MANI. 1991. *Soil pollution*. Ashish Publishing House, Punjabi Bagh.

MORA, M., ROSAS, A., RIBERA, A. & RENGEL, R. 2009. Differential tolerance to Mn toxicity in perennial ryegrass genotypes; involvement of antioxidative enzymes and root exudation of carboxylates. *Plant and Soil*, **320**, 79-89.

MOREL, M., CROUZET, J., GRAVOT, A., AUROY, P., LEONHARDT, N. & VAVASSEUR, A. 2009. AtHMA3, a P1B-ATPase allowing Cd/Zn/Co/Pb vacuolar storage in *Arabidopsis*. *Plant Physiology*, **149**, 894904.

MOUMMOU, H., KALLBERG, Y., TONFACK, L.B., PERSSON, B. & van der REST, B. 2012. The plant short-chain dehydrogenase (SDR) superfamily: genome-wide inventory and diversification patterns. *BMC Genomics*, **12**, 219.

MORZCK, E. & FUNICCLLI, N.A. 1982. Effect of lead and on germination of *Spartina alterniflora* Losiel seeds at various salinities. *Environmental Experimental Botany*, **22**, 23-32.

NAGAJYOTI, P.C., LEE, K.D. & SREEKANTH, T.V.M. 2010. Heavy metals, occurrence and toxicity for plants: a review. *Environmental Chemistry Letters*, **8**, 199-216.

NAWAZ, Z., KAKAR, K.U., LI, X-b., LI, S., ZHANG, B., SHOU, H-x. & SHU, Q-y. 2015. Genome wide association mapping of quantitative trait loci (QTLs) for contents of eight elements in brown rice (*Oryza sativa* L.). *Journal of Agricultural and Food Chemistry*, **63**, 8008-8016.

NEELIMA, P. & REDDY, K.J. 2002. Interaction of copper and cadmium with seedlings growth and biochemical responses in *Solanum melongena*. *Environmental Pollution Technology*, **1**, 285-290.

NEUMANN, D., ZUR NIEDEN, O., SCHWEIGER, W., LEOPOLD, I. & LICHTENBERGER, O. 1997. Heavy metal tolerance of *Minuartia verna*. *Journal of Plant Physiology*, **151**, 101-108.

NONGPIUR, R., SONI, P., KARAN, R., SINGLA-PAREEK, S.L. & PAREEK, A. 2012. Histidine kinases in plants. *Plant Signaling & Behaviour*, **7**, 1230-1237.

NORTON, G.J., DEACON, C.M., XIONG, L., HUANG, S., MEHARY, A.A. & PRICE, A.H. 2009. Genetic mapping of the rice ionome in leaves and grain: identification of QTL for 17 elements including arsenic, cadmium, iron and selenium. *Plant and Soil*, doi:10.1007/s 1104-009-0141-8.

NORVELL, W.A. 1984. Comparison of chelating agents as extractants for metals in diverse soil materials. *Soil Science Society of America Journal*, **48**, 1285-1292.

OLIVEIRA, H. 2012. Chromium as an environmental pollutant: insights on induced plant toxicity. *Journal of Botany*, doi:10.1155/2012/375843.

ORTEGA-VILLASANTE, C., RELLÁN-ÁLVAREZ, R., del CAMPO, F.F., CARPENA-RUIZ, R.O. & HERNÁNDEZ, L.E. 2005. Cellular damage induced by cadmium and mercury in *Medicago sativa*. *Journal of Experimental Botany*, **56**, 2239-2251.

OUZOUNIDOU, G. 1994. Change in chlorophyll fluorescence as a result of copper treatment: dose response relations in Silene and Thlaspi. *Photosynthetica*, **29**, 455-462.

PADMAVATHIAMMA, P. & LI, L. 2009. Phytostabilization – a sustainable remediation technique for zinc in soils. *Water, Air and Soil Pollution; Focus*, **9**, 253-260.

PAIVOKE, H. 1983. The short term effect of zinc on growth anatomy and acid phosphate activity of pea seedlings. *Annals of Botany*, **20**, 307-309

PAL, R. & RAI, J. P. N. 2010. Phytochelatins: peptides involved in heavy metal detoxification. *Applied Biochemistry and Biotechnology*, **160**, 945-963.

PALMITER, R. 1998.The elusive function of metallothioneins. *Proceedings of the National Academy of Science of the United States of America*, **95**, 8428-8430.

PATRA, M., BHOWMIK, N., BANDOPADHYAY, B. & SHARMA, A. 2004. Comparison of mercury, lead and arsenic with respect to genotoxic effects on plant systems and the development of genetic tolerance. *Environmental and Experimental Botany*, **52**, 199-223.

PAULY, L., FLAJOULOT, S., GARON, J.G., JULIER, B., BÉGUIER, V. & BARRE, P. 2012. Detection of favourable alleles for plant height and crown rust tolerance in three connected populations of perennial ryegrass (*Lolium perenne* L.) *Theoretical Applied Genetics*, doi:10.1007/s00122-011-1775-5.

PECK, A.W. & McDONALD, G.K. 2010. Adequate zinc nutrition alleviates the adverse effects of heat stress in bread wheat. *Plant and Soil*, **337**, 355-374.

PEER, W.A., MAMOUDIAN, M., LAHNER, B., REEVES, R.D., MURPHY, A.S. & SALT, D, E. 2003. Identifying model metal hyperaccumulating plants: germplasm analysis of 20 Brassicaceae accessions from a wide geographical area. *New Phytologist*, **159**, 421-430.

PFEIFER, M., MARTIS, M., ASP, T., MAYER, K.F.X., LÜBBERSTEDT, T., BYRNE, S., FREI, U. & STUDER, B. 2013. The perennial ryegrass GenomeZipper: targeted use of genome resources for comparative grass genomics. *Plant Physiology*, **161**, 571-582

PHILLIPS, W.J. 1972. Hydraulic fracturing and mineralisation. *Journal of the Geological Society of London*, **128**, 337-359.

PILONS-SMITS, E. 2005. Phytoremediation. *Annual Review of Plant Biology*, **56**, 15-39.

PINTO, A.P., SIMÕES, I. & MOTA, A.M. 2008. Cadmium impact on root exudates of sorghum and maize plants: a speciation study. *Journal of Plant Nutrition*, **31**, 1746-1755.

PIRRIE, D., POWER, M.R., WHEELER, P.D., CUNDY, A., BRIDGES C. & DAVEY, G. 2002. Geochemical signature of historical mining: Fowey Estuary, Cornwall, UK. *Journal of Geochemical Exploration*, **76**, 31-43.

POSCHENRIEDER, C. & BARCELÓ. J. 2004. Water relations in heavy metal stressed plants. In: **PRASAD, M.N.V. (ed.)** *Heavy Metal Stress in Plants*. Springer, Berlin, 249-270.

POURRUT, B., SHAHID, M., DUMAT, C., WINTERTON, P. & PINELLI, E. 2011. Lead uptake, toxicity and detoxification in plants. *Reviews of Environmental Contamination and Toxicology*, **213**, 113-136.

PRASSAD, D.D.K. & PRASSAD, A.R.K. 1987. Altered δ-aminolae vulinic acid metabolism by lead and mercury in germinating seedlings of Bajra (*Pennisetum typhoideum*). *Journal of Plant Physiology*, **127**, 241-249.

PROTEAU, P.J. 2004. 1-deoxy-D-xylulose-5-phosphate reductoisomerase: an overview. *Bioorganic Chemistry*, **32**, 483-493.

QU, R.L., LI, D., DU, R. & QU, R. 2003. Lead uptake by roots of four turfgrass species in hydroponic cultures. *Horticultural Science*, **38**, 623-626.

RAHMAN, H., SABREEN, S., ALAM, S. & KAWAI. 2005. Effects of nickel on growth and composition of metal micronutrients in barley plants grown in nutrient solution. *Journal of Plant Nutrition*, **28**, 393-404.

RAJAKARUNA, N., TOMPKINS, K.M. & PAVICEVIC, P.G. 2006. Phytoremediation: an affordable green technology for the clean-up of metal contaminated sites in Sri Lanka. *Ceylon Journal of Science*, **35**, 25-39.

RAKESH SHARMA, M.S. & RAJU, N.S. 2013. Correlation of heavy metal contamination with soil properties of industrial areas of Mysore, Karnataka, India, by cluster analysis. *International Research Journal of Environment Sciences*, **2**, 22-27.

RASKIN, I., KUMAR, P.B.A.N., DUSHENKOV, S. & SALT, D.E. 1994. Bioconcentration of heavy metals by plants. *Current Opinion in Biotechnology*, **5**, 285-290.

RASCIO, N. & NAVARI-IZZO, F. 2011. Heavy metal hyperaccumulating plants: how and why do they do it? And what makes them so interesting. *Plant Science*, **180**, 169-181.

RAUGH, B.L., BASTEN, C. & BUCKLER, E.S. 2002. Quantitative trait loci analysis of growth response to varying nitrogen sources in *Arabidopsis thaliana*. *Theoretical Applied Genetics*, **104**, 743-750.

RAVET, K., TOURAINE, B., BOUCHEREZ, J., BRIAT, J-F., GAYMARD, F. & CELLIER F. 2009. Ferritins control interaction between iron homeostasis and oxidative stress in Arabidopsis. *The Plant Journal*, **57**, 400-412.

RAYBOULD, J.G. 1973. *Studies in the variations in paragenetic sequence and zoning in the mineral veins of Cardiganshire and Montgomeryshire*. Unpublished Ph.D. thesis, University of Wales.

RAYBOULD, J.G. 1974. Ore textures, paragenesis and zoning in the lead-zinc veins of Mid-Wales. *Transactions of the Institution of Mining and Metallurgy*. Section B: *Applied Earth Science*, **83**, B111-B120.

REEVES, R.D. & BAKER, A.J.M. 2000. Metal-accumulating plants. In: **RASKIN, I. & ENSLEY, B.D. (eds)** *Phytoremediation of Toxic Metals: Using Plants to Clean Up the Environment.* Wiley, New York, 193-229.

REEVES, R.D. & BROOKS, R.R. 1983. European species of *Thlaspi* L. (Cruciferae) as indicators of nickel and zinc. *Journal of Geochemical Exploration*, **18**, 275-283.

REN, F., LIU, T., LIU, H. & HU, B. 1993. Influence of zinc on the growth, distribution of elements, and metabolism of one-year old American ginseng plants. *Journal of Plant Nutrition*, **16**, 393-405.

RIVERS POLLUTION COMMISSION. (1868). 1874. *Fifth report of the commissioners appointed in* 1868 *to inquire into the best means of preventing the pollution of rivers*.

ROSEN, J.A., PIKE, C.S. & GOLDEN, M.L. 1977. Zinc, iron and chlorophyll metabolism in zinc-toxic corn. *Plant Physiology*, **59**, 1085-1087.

ROUT, G.R., SANGHAMITRA, S. & DAS, P. 2000. Effects of chromium and nickel on germination and growth in tolerant and non-tolerant populations of *Echinochloa colona* (L). *Chemosphere*, **40**, 855-859.

ROUT, J.A. & DAS, P. 2003. Effect of metal toxicity on plant growth and metabolism: I Zinc. *Agronomie*, **23**, 3-11.

RYTUBA, J.J. 2003. Mercury from mineral deposits and potential environmental impact. *Environmental Geology*, **43**, 326-338.

SALSE, J., BOLOT, S., THROUDE, M., JOUFFE, V., PIEGU, B., QURAISHI, U.M., CALCAGNO, T., COOKE, R., DELSENY, M. & FEUILLET, C. 2008. Identification and characterization of shared duplications between rice and wheat provide new insight into grass genome evolution. *The Plant Cell*, **20**, 11-24.

SALIN, M. L. 1988. Toxic oxygen species and protective systems of the chloroplast. *Physiologia Plantarum*, **72**, 681-689.

SALT, D.E., PRINCE, R.C., PICKERING, I.J. & RASKIN, I. 1995. Mechanisms of cadmium mobility and accumulation in Indian mustard. *Plant Physiology*, **109**, 1427-1433.

SALT, D.E., SMITH, R.D. & RASKIN, I. 1998. Phytoremediation. *Annual Review of Plant Biology*, **49**, 643-668.

SALT, D., PRINCE, R.C., BAKER, A., RASKIN, I. & PICKERING, I. 1999. Zinc ligands in the metal hyperaccumulator *Thlaspi caerulescens* as determined using X-ray absorption spectroscopy. *Environmental Science and Technology*, **33**, 713-717.

SANDALIO, L.M., DALURZO, H.C., GOMEZ, M., ROMERO-PUERTAS, M.C. & del RÍO, L.A. 2001. Cadmium-induced changes in the growth and oxidative metabolism of pea plants. *Journal of Experimental Botany*, **52**, 2115-2126.

SANDVE, S.R. & FJELLHEIM, S. 2010. Did gene family expansions during the Eocene-Oligocene boundary climate cooling play a role in Pooideae adaptation to cool climates? *Molecular Ecology*, **19**, 2075-2088.

SANDVE S.R., RUDI, H., ASP, T. & ROGNLI, O.A. 2008. Tracking the evolution of a cold stress associated gene family in cold tolerant grasses. *Evolutionary Biology*, **8**, 245.

SANTOS, F., HERNÁNDEZ-ALLICA, J., BECERRIL, J., AMARAL, D., SOBRINHO, N., MAZUR, N. & GARBISU, C. 2006. Chelate-induced phytoextraction of metal polluted soils with *Brachiaria decumbens. Chemosphere*, **65**, 43-50.

SCHELBERT, S., AUBRY, S., BURLA, B., KESSLER, F., KRUPINSKA, K. & HÖRTENSTEINER, S. 2009. Pheophytin pheophorbide hydrolase (pheophytinase) is involved in chlorophyll breakdown during leaf senescence in Arabidopsis. *The Plant Cell*, **21**, 767-785.

SCHNELLMAN, G.A. & SCOTT, B. 1970. Lead-zinc mining areas of Great Britain. **In**: *Proceedings of the Ninth Commonwealth Mining and Metallurgy Congress 1969*, **2**, 325-356.

SHANKER, A.K., CERVANTES, C., LOZA-TAVERA, H. & AVODAINAYAGAM, S. 2005. Chromium toxicity in plants. *Environment International*, **31**, 739-753.

SHARKEY, T.D., POSSELL, M., COJOCARIU, C.I., VELIKOVA, V.B., LAOTHAWONKIKUL, J., RYAN, A., MULLINEAUZ, P.M. & HEWITT, N.C. 2009. Isoprene synthesis protects transgenic plants from oxidative stress. *Plant, Cell & Environment*, **32**, 520-531.

SHARMA, P. & DUBEY, R.S. 2005. Lead toxicity in plants. *Brazilian Journal of Plant Physiology*, **17**, 35-52.

SHAW, I. 2000. *The Oxford History of Ancient Egypt*. Oxford University Press, New York.

SHEN, Z.G., ZHAO, F.J. & McGRATH S.P. 1997. Uptake and transport of zinc in the hyperaccumulator *Thlaspi caerulescens* and the non-hyperaccumulator *Thlaspi ochroleucum*. *Plant, Cell & Environment*, **20**, 898-906.

SILVA, M.L.S., VITTI, G.C. & TREVIZAM, A.R. 2014. Heavy metal toxicity in rice and soybean plants cultivated in contaminated soil. *Revista Ceres*, **61**, 248-254.

SINGH, H.P., MAHAJAN, P., KAUR, S., BATISH, D.R. & KOHLI, R.K. 2013. Chromium toxicity and tolerance in plants. *Environmental Chemistry Letters*, **11**, 229-254.

SOARES, C. R. F. S., GRAZZIOTI, P.H., SIQUEIRA, J.O., De CARVALHO, J.G. & MOREIRA, F.M.S. 2001.Toxidez de zinco no crescimento e nutriçã o de *Eucalyptus maculata* e *Eucalyptus urophylla* em solução nutritiva. *Pesquisa Agropecuária Brasileira*, **36**, 339-348.

SOLANKI, R. & DHANKHAR, R. 2011. Biochemical changes and adaptive strategies of plants under heavy metal stress. *Biologia*, **66**, 195-204.

SOUSSSANA, J-F., MINCHIN, F.R., MACDUFF, J.H., RAISTRICK, N., ABBERTON, M.T. & MICHAELSON-YATES, T.P.T. 2002. A simple model of feed-back regulation for nitrate uptake and N_2 fixation in contrasting phenotypes of white clover. *Annals of Botany*, **90**, 139-147.

STADTMAN, E.R. & OLIVER, C.N. 1991. Metal-catalyzed oxidation of proteins. Physiological consequences. *Journal of Biological Chemistry*, **266**, 2005-2008.

STIBOROVA, M., PITRICHOVA, M. & BREZINOVA, A. 1987. Effect of heavy metal ions in growth and biochemical characteristic of photosynthesis of barley and maize seedlings. *Biologia Plantarum*, **29**, 453-467.

STÖHR, C. 1998. Plasma membrane-bound nitrate reductase in algae and higher plants. In: **ASARD, A., BÉRCZI, A. & CAUBERGS, R.J. (eds)** *Plasma membrane redox systems and their role in biological stress and disease*. Springer, Netherlands, 103-119.

STRAUSS, S.Y. & BOYD, R.S. 2011. Herbivory and other cross-kingdom interactions on harsh soils. In: **HARRISON, S.H. & RAJAKARUNA, N. (eds)** *Serpentine: the evolution and ecology of a model system*. University of California Press, Berkeley, 181-199.

SUDHAKAR, C., SYMALABAI, L. & VEERANJAVEYULER, K. 1992. Lead tolerance of certain legume species grown on lead tailings. *Agriculture, Ecosystems and Environment*, **41**, 253-261.

SURPIN, M. & RAIKHEL, N. 2004. Traffic jams affect plant development and signal transduction. *Nature Reviews of Molecular Cell Biology*, **5**, 100-109.

SWAIN, C.H., BREWER, P.A., MACKLIN, M.G. & SIMKIN, J. 2005. *The ecological, geomorphological and geochemical controls on river shingle health development on the Afon Rheidol and Afon Ystwyth, Ceredigion.* CCW Contract Report No. RE0492, Countryside Council for Wales, Bangor.

SWAINBANK, I.G., COLMAN, T.B., FLETCHER, C.J. & MASON, J.S. 1992. Multiple sources for lead mineralization in the Caledonian terrane of Wales. In: **FOSTER, R.P. (ed.)** *Mineral deposit modelling in relation crustal reservoirs of the ore-forming elements*. Institution of Mining and Metallurgy Conference abstracts, Nottingham, April 22-23, 1992, Institution of Mining and Metallurgy, London.

TALKE, I.N., HANIKENNE, M. & KRAMER, U. 2006. Zinc-dependent global transcriptional control, transcriptional deregulation, and higher gene copy number for genes in metal homeostasis of the hyperaccumulator *Arabidopsis halleri*. *Plant Physiology*, **142**, 148-167.

TANHAN, P., POKETHITIYOOK, P., KRUATRACHUE, M., CHAIYARAT, R. & UPATHAM, M. 2011. Effects of soil amendments and EDTA on lead uptake by *Chromolaena odorata*: greenhouse and field trial experiments. *International Journal of Phytoremediation*, **13**, 897-911.

TAVALLALI, V.M., RAHEMI, M., ESHGHI, S., KHOLDEBARIN, B. & RAMEZANIAN, Z. A. 2010. Zinc alleviates salt stress and increases antioxidant enzyme activity in the leaves of pistachio (*Pistacia vera* L. 'Badami') seedlings. *Turkish Journal of Agriculture and Forestry*, **34**, 349-359.

TERRYN, N., VAN MONTAGU, M. & INZÉ, D. 1993. GTP-binding proteins in plants. *Plant Molecular Biology*, **22**, 143-152.

TEZUKA, K., MIYADATE, H., KATOU, K., KODAMA, I., MATSUMOTO, S., KAWAMOTO, T., MASAKI, S., SATOH., H, YAMAGUCHI, M., SAKURAI, K., TAKAHASHI, H., SATOH-NAGASAWA, N., WATANABE, A., FUJIMURA, T. & AKAGI, H. 2010. A single recessive gene controls cadmium translocation in the cadmium hyperaccumulating rice cultivar Cho-Ko-Koku. *Theoretical Applied Genetics*, **120**, 1175-1182.

TIMBERLAKE. S. 1988. Bronze Age mining at Cwmystwyth: the radiocarbon dates. *Archaeology in Wales*, **28**, 50.

TISCHNER, R. 2000. Nitrate uptake and reduction in higher and lower plants. *Plant, Cell & Environment*, **23**, 1005-1024.

TISCHNER, R., WARD, M.R. & HUFFAKER, R.C. 1989. Evidence for a plasma membrane-bound nitrate reductase involved in nitrate uptake of *Chlorella sorokiniana*. *Planta*, **178**, 19-24.

TORRI, K. U. 2004. Leucine-rich repeat receptor kinases in plants: structure, function and signal transduction pathways. *International Review of Cytology*, **234**, 1-46.

TRIPATHI, V., PARASURAMAN, B., LAXMI, A. & CHATTOPADHYAYI, D. 2009. CIPK, a CBL-interacting protein kinase is required for development and salt tolerance in plants. *The Plant Journal*, doi: 10.1111/j.1365-313X.2009.03812.x

TSONEV, T. & LIDON, J.C.L. 2012. Zinc in plants – An overview. *Emirates Journal of Food and Agriculture*, **24**, 322-333.

UENO, D., KOYAMA, E., KONO, I., ANDO, T., YANO, M., & MA, J. F. 2009. Identification of a novel major quantitative trait locus controlling distribution of Cd between roots and shoots in rice. *Plant and Cell Physiology*, **50**, 2223-2233.

VAILLANT, N., MONNET, F., HITMI, A., SALLANON, H. & COUDRET, A. 2005. Comparative study of responses in four *Datura* species to a zinc stress. *Chemosphere*, **59**, 1005-1013.

VAN der ENT, A., BAKER, A.J.M., REEVES, R.D., POLLARD, A.J. & SCHAT, H. 2012. Hyperaccumulators of metal and metalloid trace elements; Facts or fiction. *Plant and Soil*, **267**, 1-16.

VAN OOIJEN, J.W., BOER, M.P., JANSEN, R.C. & MALIEPAARD, C. 2002. Map QTL® 4.0, software for the calculation of QTL positions on genetic maps. Wageningen, The Netherlands: Plant Research International.

VERBRUGGEN, N., HERMANS, C. & SCHAT, H. 2009. Molecular mechanisms of hyperaccumulation in plants. *New Phytologist*, **181**, 759-776.

VERMA, S. & DUBEY, R.S. 2003. Lead toxicity induces lipid peroxidation and alters the activities of antioxidant enzymes in growing rice plants. *Plant Science*, **164**, 645-655.

VERNAY, P., GAUTHIER-MOUSSARD, C. & HITMI, A. 2007. Interaction of bioaccumulation of heavy metal chromium with water relation, mineral nutrition and photosynthesis in developed leaves of *Lolium perenne* L. *Chemosphere*, **68**, 1563-1575.

VIRKUTYTE, J., SILLAPÄÄ, M. & LATOSTENMAA, P. 2002. Electrokinetic soil remediation – critical overview. *The Science of the Total Environment*, **289**, 97-121.

VON WETTSTEIN, D., GOUGH, S. & KANNANGARA. 1995. Chlorophyll biosynthesis. *The Plant Cell*, **7**, 1039-1057.

WANG, A.S., ANGLE, J.S., CHANEY, R.L., DELORME, T.A. & REEVES, R.D. 2006. Soil pH effects on uptake of Cd and Zn by *Thlaspi caerulescens*. *Plant and Soil*, **281**, 325-337.

WARRENDER, R. 2005. *The phytoextraction potential of Lolium perenne for the remediation of heavy-metal contaminated mine spoil, with particular reference to genotypic variation in tolerance within a mapping family*. Unpublished M.Sc. thesis, University of Wales.

WECKX, J.E.J. & CLIJSTERS, H.M.M. 1997. Zn phytotoxicity induces oxidative stress in primary leaves of *Phaseolus vulgaris*. *Plant Physiology and Biochemistry*, **35**, 405-410.

WEST, G.A. 1970. *Copper: its mining and use by the aboriginies of the Lake Superior region*. Greenwood Press, Westport, Connecticut.

WESTGATE, R. 2000. *Experimental studies of weathering processes in waste from metalliferous mines in the Central Wales Orefield*. Unpublished M.Sc. thesis, University of Wales.

WHITE, C., SHARMAN, A.K. & GADD, G.M. 2011. An integrated microbial process for the bioremediation of soil contaminated with toxic metals. *Nature Biotechnology*, **16**, 572-575.

WIERZBICKA, M. 1998. Lead in the apoplast of *Allium cepa* L. root tips – ultra structural studies. *Plant Science*, **133**, 105-119.

WIERZBICKA, M. & ANTONSIEWICZ. 1993. How lead can easily enter the food chain – a study of plant roots. *Science of the Total Environment: Supplementary*, **1**, 423-429.

WILD, A., JONES, L. H. P. & MACDUFF, J. H. 1987. Uptake of mineral nutrients and crop growth: the use of flowing nutrient solutions. *Advances in Agronomy*, **41,** 171-219.

WILD, H. 1978. The vegetation of heavy metal and other toxic soils. In: **WERGER, M.J.A. (ed.)** *Biogeography and ecology of Southern Africa*. The Hague, Junk, 1301-1332

WILKINS, P.W., MACDUFF, J.H., RAISTRICK, N. & COLLISON, M. 1997. Varietal differences in perennial ryegrass for nitrogen use efficiency in leaf growth following defoliation: performance in

flowing solution culture and its relationship to yield under simulated grazing in the field. *Euphytica*, **98**, 109-119.

WILLEMS, G., DRÄGER, D. B., COURBOT, M., GODÉ, C., VERBRUGGEN, N. & SAUMITOU-LAPRADE, P. 2007. The genetic basis of zinc tolerance in the metallophyte *Arabidopsis halleri ssp. halleri* (Brassicaceae): An analysis of quantitative trait loci. *Genetics*, **176**, 659-674.

WILSON, M.J. & BELL, N. 1996. Acid deposition and heavy metal mobilisation. *Applied Geochemistry*, **11**, 133-137.

WONG, H., SAKAMOTO, T., UMEMURA, K. & SHIMAMATO, K. 2004. Down-regulation of metallothionein, a reactive oxygen species scavenger, by the small GTPase OsRac1 in rice. *Plant Physiology*, **135**, 1447-1456.

XU, S. 2003. Theoretical basis of the Beavis effect. *Genetics*, **165**, 2259-2268.

YANG, Y.Y., JUNG, J.Y., SONG, W.Y., SUH, H.S. & LEE, Y. 2000. Identification of rice varieties with high tolerance or sensitivity to lead and characterisation of the mechanism of tolerance. *Plant Physiology*, **124**, 1019-1026.

YANG, X.E., LONG, X.X., YE, H.B., HE, Z.L., CALVERT, D.V. & STOFFELLA, P.J. 2004. Cadmium tolerance and hyperaccumulation in a new Zn-hyperaccumulator. *Plant and Soil*, **259**, 181-189.

YONG, C. & MA, L. Q. 2002. Metal tolerance, accumulation, and detoxification in plants with emphasis on arsenic in terrestrial plants. In: *Biogeochemistry of Environmentally Important Trace Elements*. *American Chemical Society*, 95-114.

ZACHOS, J., PAGANI, M., SLOAN, L., THOMAS, E. & BILLUPS, K. 2001. Trends, rhythms, and aberrations in global climate 65 Ma to present. *Science*, **292**, 686-693

ZAN, Y., JI, Y., ZHANG, Y., YANG, S., SONG, Y. & WANG, J. 2013. Genome-wide identification, characterization and expression analysis of *populus* leucine-rich receptor-like kinase genes. *BMC Genomics*, **14**, 318.

ZENK, M. H. 1996. Heavy metal detoxification in higher plants - a review. *Gene*, **179**, 21-30.

ZHAO, S., JIN, L. & DUO, L. 2013. The use of a biodegradable chelator for enhanced phytoextraction of heavy metals by *Festuca arundinacea* for municipal solid waste compost and associated heavy metal leaching. *Bioresource Technology*, **129**, 249-255.